Summer 7-14-2022

Discovering Novel Polyextremotolerant Fungi, and Determining their Ecological Role Within the Biological Soil Crust Consortium

Erin Carr
University of Nebraska-Lincoln, erin.creasey@huskers.unl.edu

DISCOVERING NOVEL POLYEXTREMOTOLERANT FUNGI, AND DETERMINING THEIR ECOLOGICAL ROLE WITHIN THE BIOLOGICAL SOIL CRUST CONSORTIUM

by

Erin C. Carr

A DISSERTATION

Presented to the Faculty of

The Graduate College at the University of Nebraska

In Partial Fulfillment of Requirements

For the Degree of Doctor of Philosophy

Major: Biological Sciences

(Genetics, Cellular, and Molecular Biology)

Under the Supervision of Professors Wayne R. Riekhof & Steven D. Harris

Lincoln, Nebraska

June, 2022

DISCOVERING NOVEL POLYEXTREMOTOLERANT FUNGI, AND DETERMINING THEIR ECOLOGICAL ROLE WITHIN THE BIOLOGICAL SOIL CRUST CONSORTIUM

Erin C. Carr

University of Nebraska, 2022

Advisors: Wayne R. Riekhof & Steven D. Harris

The ecological niche of polyextremotolerant fungi within oligotrophic ecosystems such as biological soil crusts has not yet been determined. These fungi persist in locations where nutrients are depleted while simultaneously surrounded by autotrophic microbes such as algae and cyanobacteria. Yet it has not been shown that they are engaging in any exchange of nutrients the way lichens do. However, there is seemingly no other way for these fungi to obtain vital nutrients, such as carbon or nitrogen, other than from these microbes. Here we have isolated polyextremotolerant fungi from cold desert biological soil crusts which are a microbial biofilm that form on the surfaces of non-vegetative soils and contain an abundance of autotrophic microbes. The presence of free-living fungi in these biofilms has recently been verified, but only a few fungi have been cultured directly from them, therefore the ecological role of fungi in the biological soil crust remains unknown. With work presented here, we have shown that polyextremotolerant fungi are present within the biological soil crust. Additionally, we have provided potential leads to the ecological niches of these organisms within the biological soil crust. *Exophiala viscosium* and *Exophiala limosus,* tentatively named, are two novel species described here, which have been observed to secrete excess amounts of melanin into their media.

Since melanin is a carbon-expensive product to make, we believe they are secreting it to protect the biological soil crust from UV and desiccation. Additionally, we have identified what we believe to be a polyextremotolerant fungus with endosymbiotic bacteria, Crusty and its *Methylobacterium* symbionts Light Pinky and Dark Pinky. While we have not directly confirmed the basis of their endosymbiosis, we believe it is to allow the bacteria to optimally perform aerobic anoxygenic photosynthesis and auxin production, due to the genetic confirmation of the mechanisms required for these processes within the genomes of these bacteria, and the significant increase in active metabolism of Crusty-Pinky when grown in the presence of light. Detailed descriptions of the methods of experiments performed and the results of this study will provide a basis for research in the future on polyextremotolerant fungi, and determine the microbial interactions that allow them to survive oligotrophic conditions.

ACKNOWLEDGEMENTS

First, I would like to thank my advisors, Steve Harris and Wayne Riekhof. Even though Dr. Harris "abandoned me" to go on to another institution, our weekly virtual meetings and his regular visits were comforting and made me feel guided through this process no matter what. I will be forever grateful to Dr. Harris for introducing me to the world of fungi and for supporting me through this creative research track. And I am thankful that Dr. Riekhof rescued me from a difficult position, allowing me to continue with my own research, and always providing me with useful ideas and insights. He has saved the mental wellbeing and careers of many grad students in his short time here, and for that I will always be grateful. They both provided me irreplaceable guidance, non-stop ideas bouncing, and patience with my sometimes-chaotic way of tackling science and life. I would like to thank my committee members, Dr. Kristi Montooth, Dr. Etsuko Moriyama, and Dr. Christian Elowsky. Kristi Montooth and Colin Meiklejohn were there for me from the beginning, providing me with a job that gave me essential experience learning how to be a part of a scientific community, ever-essential lab upkeep skills, and continuous guidance throughout my PhD. Christian Elowsky for being himself, always looking out for me, reeling me in when I was over-doing things, and always willing to tell me the hard truths. Etsuko Moriyama for providing me with kind and useful feedback, and always being flexible to whatever the circumstances may be.

This research would not have been possible without the help of my many undergraduate students, who not only assisted in research but provided me with essential experience in mentorship: Cecile Renfro, Javier Omar, Mitchell Sullivan, Alex Corrifan, Sarah Grambo, Jeremy Vinton, Stephen Allen, Mia Kennedy, Elizabeth Shouseck,

Armando Flores, and Quin Barton. I must thank my labmates past and present, which have provided me so much support and feedback throughout the years, sometimes unwarranted, but always useful. So, thank you, Dr. Jyothi Kumar, Lakshmi Yerra, Dr. Jithesh Vijayan, Caleb Wheling, Morgan Siemek, and Amanda Maliva. Particular thanks to the best lab mate I could have ever asked for, Dr. Samantha Reese, whom grad school would have been much more boring without. Additional thanks to Eddie Hillman, who during his brief time in my presence was able to concentrate a lifetime of friendship, though I wish it could have continued onto our grumpy old professorial days, like we always talked about eventually happening.

I would not be here today without the constant love and support from my family. Thank you to my parents, Joan and Jon Creasey, and my Nana and Papa, Barbara and Joe Sabia, for instilling in me a love of science, and for always supporting me in my endeavors. Thank you to my in-laws, who have always been loving and supportive of me and Sean, Judy and John Carr, and my sister Mandi Carr. Thank you to my Lincoln family aka the D&D crew, who have always been there for me, helping me get through the rollercoaster that is grad school, and for a constant stream of entertainment: Amy Ort, Adelle Burk, Julien Gradnigo, Sam McCarthy, Justin Buchanan, and Mandy Kottas. Finally, I would like to thank my wonderful husband Sean Carr, without him I would not be here getting a PhD and finding my passion. You are my rock, and my honey bun, thank you for countless hours of ideas-bouncing, helping me whenever I needed, sparing practice, and support. I can’t wait to see what we do next.

“Polish comes from the cities; wisdom from the desert”- Frank Herbert, Dune

GRANT INFORMATION

This research was supported by grants awarded to Dr. Steven Harris including NASA grant 80NSSC17K0737.

TABLE OF CONTENTS

LIST OF MULTI-MEDIA OBJECTS

INTRODUCTION

Biological soil crusts, also known as cryptogamic soils and biocrusts (Johansen, 1993), are microbial biofilms that form on the surface of any mineral soils (Colesie et al., 2014; Lange et al., 1997) but are most known for their stabilization of xeric desert soils (Belnap et al., 2001; Pointing & Belnap, 2012). Complete taxa-specificity within biological soil crusts is not yet established. However, ecological factors surrounding biological soil crusts are thought to select for multi-stress tolerating microbes (Bates et al., 2010; Bowker et al., 2010; Colesie et al., 2014; Couradeau et al., 2019; Lan et al., 2012; Maier et al., 2016). Microbial members of the biological soil crust consortium include: cyanobacteria, lichens, mosses, fungi, bacteria, algae, and archaea (Bates et al., 2010; Belnap et al., 2001; Bowker et al., 2010; Csotonyi et al., 2010; Li et al., 2012; Maier et al., 2016; Steven et al., 2013).

One essential taxa that has so far been found in all biological soil crusts is cyanobacteria, particularly *Microcoleus vaginatus* and other species (Couradeau et al., 2019). *Microcoleus* is usually the seed microbe, which begins the formation of new biological soil crusts (Garcia-Pichel et al., 2001; Rajeev et al., 2013), much like cyanobacteria's role in altering the Earth's atmosphere (Berman-Frank et al., 2003). Features that make *Microcoleus* essential to the biological soil crust community are its ability to fix nitrogen, fix carbon, and interestingly its excessive secretion of extracellular polysaccharide matrix (Couradeau et al., 2019; Garcia-Pichel & Wojciechowski, 2009). This trifecta of features makes *Microcoleus*, and cyanobacteria with similar features, essential for the formation of biological soil crusts and ultimately the colonization of land in the Late Precambrian era (Golubic & Campbell, 1979; Horodyski & Knauth, 1994;

Labandeira, 2005; Prave, 2002). It is believed that the modern biological soil crust community reflects early terrestrial ecosystems, before plants were able to colonize land (Kenrick et al., 2012; Mitchell et al., 2021). As such, it is thought that microbial symbioses, such as lichens, may have evolved from ancient versions of biological soil crusts (Mitchell et al., 2016; Mitchell et al., 2021).

Some abiotic stresses of early Earth still remain in the desert soils that modern biological soil crusts inhabit, maintaining these environmental stresses that select for symbioses. Multiple abiotic factors influence the ecology of biological soil crusts, such as temperature fluctuations and UV exposure (Belnap & Lange, 2001; Belnap et al., 2007; Kuske et al., 2012). However, the main abiotic factors that allow for active metabolism in the microbes are nutrient and water availability (Belnap & Lange, 2001; Belnap et al., 2004; Couradeau et al., 2019). Beyond the physical perimeters of the biological soil crust, nutrients are practically nonexistent (Couradeau et al., 2019). However, within the confines of the biological soil crust, the autotrophic members of the community are able to produce organic nitrogen and carbon compounds, creating a nutrient-rich pocket that the heterotrophic microbes use as their sole source of nutrients (Belnap, 2002; Couradeau et al., 2019; Li et al., 2012). As such, biological soil crusts play a critical role in servicing entire desert and soil ecosystems by limiting soil erosion, reducing desertification of non-desert ecosystems, and performing bioremediation both in the desert and in anthropogenically contaminated soils (Belnap, 2002; Belnap & Büdel, 2016; Gretarsdottir et al., 2004; Kuske et al., 2012; Nevins et al., 2021; Wu et al., 2013; Yan et al., 2021).

Lichens seem well-adapted to ecosystems of biological soil crusts. This is owing to their well-established symbiosis between a photoautotrophic partner (cyanobacteria or algae) providing carbon and sometimes nitrogen, and the fungal partner forming structures and recruiting bacteria (Ahmadjian & Jacobs, 1981; Honegger, 1991; Spribille, 2018). This symbiosis prevails without the biological soil crust community with many rocks, trees, and some human-built surfaces providing substrates for lichens to grow. Lichens are so successful, that they have been estimated to cover almost 7% of Earth's surface (Nelsen et al., 2020). Although, much like the biological soil crust community, lichens are being shown to include more than just a fungus and an algae or cyanobacteria (Bates et al., 2011; Cardinale et al., 2006; Cardinale et al., 2008). Metabolic functions within these larger consortia are not yet fully understood, but it is very likely that lichens without cyanobacterial partners rely on diazotrophic bacteria for nitrogen sources as it is thought to occur in biological soil crusts (Cardinale et al., 2008).

Although each member of a biological soil crust is thought to possess a specific ecological function, not every niche in these communities has been scientifically determined. In this study we wish to establish a greater understanding of the roles of non-lichenized fungi within biological soil crusts, by isolating, identifying, and extrapolating as much information as possible from genomics, genetics, metabolite manipulation, and microbial interaction experimentations. Specifically, we focused our efforts on obtaining information about the polyextremotolerant fungi that are found within biological soil crusts.

Polyextremotolerant fungi, also known as black yeasts or meristematic fungi, are a paraphyletic group of fungi that are characterized by their melanized cell wall (Quan et

al., 2020; Sterflinger, 2006; Teixeira et al., 2017). Melanin imbues these fungi with a vast range of abiotic resistances and is likely the main cause of their polyextremotolerance. With their melanin coating, these fungi have been able to occupy spaces where they otherwise might not have such as rock surfaces, marble, brick walls, dishwashers, and biological soil crusts (Bates et al., 2006; Gorbushina, 2007; Gostincar et al., 2010; Sterflinger, 2000; Zalar et al., 2011). Locations where these fungi are found have little external organic carbon or nitrogen sources, and these fungi are not known chemolithotrophs (rock degrading). Therefore, as many have noted, their sources of nutrients seem to be limited to their autotrophic microbial neighbors in these same ecosystems (Gorbushina et al., 2005; Gostinčar et al., 2012; Grube et al., 2013; Muggia et al., 2013). Yet there has been little direct evidence of these fungi's capability to engage in symbiosis with autotrophic microbes.

Polyextremotolerant fungi of the order Chaetothyriales are a part of Eurotiomycetes, which is the most lifestyle-diverse class of fungi, with taxa representing all known fungal lifestyles, including lichenization (Geiser et al., 2006; Naranjo-Ortiz & Gabaldón, 2019; Schoch et al., 2009). Fungi of Chaetothyriales occupy many of these fungal lifestyles, which has been attributed to their polyextremotolerant capabilities (Badali et al., 2008; Gostinčar et al., 2012; Gostinčar et al., 2018; Grube et al., 2013; Réblová et al., 2016; Sterflinger, 2006). Chaetothyriales and Verrucariales, a primarily lichen-forming clade, share a most recent common ancestor that was likely a rock-dwelling melanized polyextremotolerant fungus (Gueidan et al., 2008). Indicating that these fungi's polyextremotolerant nature is likely the ancestral link to the eventual evolution of lichen-association, such as that which occurred in Verrucariales However,

there is a lack of understanding in the mechanisms of the evolutionary leap from polyextremotolerant fungi to lichenized fungi when it comes to their microbial interactions, which are essential to the lichen symbiosis.

We believe that polyextremotolerant fungi of Chaetothyriales found on surfaces where there are no external nutrient sources, are capable of transient interactions with the autotrophic microbes in their environment. This hypothesis can then be extended to polyextremotolerant fungi found within biological soil crusts. We hypothesize the non-lichenized microbes of the biological soil crust are engaged in transient interactions. These interactions are parallel to those of the lichen symbiosis, such as exchange of nutrients (carbohydrates and ammonia) and abiotic resistance factors (melanin, carotenoids, extracellular polymeric substances, and phytohormones). However, without the evolutionary strain causing species-specificity and propagule necessities found in lichenization, these organisms never evolved to form highly-specific lichens, instead these interactions can be considered “lichen-like”. To test this hypothesis and further tease apart ideas within the lichen symbiosis to correlate them to non-lichen fungi, I have: detailed the similarities between lichens and fungal biofilms, described the unique melanization properties of two novel *Exophiala* species isolated from a biological soil crust, and I have identified a novel polyextremotolerant fungi with *Methylobacterium* symbionts whose metabolic capabilities make them uniquely fit for optimal survival within a melanized fungus in a biological soil crust consortium.

Chapter one is a review article which describes the similarities between lichens and biofilms. With that chapter I have teased apart three vital developmental strategies that lichens and fungal biofilms share: their growth stages, extracellular matrix

production, and abiotic resistance. These three features are key to both lifestyles which links two seemingly different entities. This shows that lichens and biofilms are actually extremely similar, and that lichens themselves probably started as biofilms before evolving into lichens.

Chapter two describes two novel *Exophiala* species, and how the regulation of their melanin production, and secretion/excretion of such melanin, is likely useful in protecting the greater biological soil crust community from abiotic factors. Use of secreted melanin into the biological soil crust's extracellular matrix would increase the survival of the autotrophic members of the community, therefore ensuring continual production of essential carbon and nitrogen sources for these fungi.

Chapter three focuses on a novel polyextremotolerant fungi currently named "Crusty", and its Methylobacterium symbionts called "Pinky". This symbiosis is thought to be an endosymbiosis but is not yet confirmed. However, the basis for this symbiosis is believed to rely on the *Methylobacterium*'s ability to perform phytohormone production to increase algal, cyanobacterial, and fungal growth, and perform aerobic anoxygenic photosynthesis. Aerobic anoxygenic photosynthesis uses a bacteriochlorophyll that is excited in the ~800 nm light range, beyond the range melanin is capable of blocking. Instead, melanin is blocking the UV range of light, which would normally degrade bacteriochlorophyll. This optimal cross-over of light absorption properties allows the *Methylobacterium* to perform aerobic anoxygenic photosynthesis within the cell wall of the melanized fungi, and produce phytohormones to increase the growth capabilities of the fungi. Then when the bacteria is outside of the fungal cell it can provide those same phytohormones for the rest of the biological soil crust community, optimizing the growth

rate of autotrophs during the short window of optimal growing conditions for biological soil crusts.

Unique features of the *Exophiala* species' melanin secretion and the Crusty-Pinky symbiosis, are novel in understanding the role of non-lichenized fungi's role within the biological soil crust and in other ecological locations where polyextremotolerant fungi are found. Previous literature showed that these fungi are capable of growth in seemingly uninhabitable places but does not further explore what these fungi's ecological roles are within these habitats. This research aimed to decipher the roles of polyextremotolerant fungi within the biological soil crust consortium, to determine if they are indeed interacting in a lichen-like manner.

References

Ahmadjian, V., & Jacobs, J. B. (1981). Relationship between fungus and alga in the lichen Cladonia cristatella Tuck. *Nature*, *289*(5794), 169-172.

Badali, H., Gueidan, C., Najafzadeh, M. J., Bonifaz, A., van den Ende, A. H., & de Hoog, G. S. (2008). Biodiversity of the genus Cladophialophora. *Stud Mycol*, *61*, 175-191. https://doi.org/10.3114/sim.2008.61.18

Bates, S. T., Cropsey, G. W., Caporaso, J. G., Knight, R., & Fierer, N. (2011). Bacterial communities associated with the lichen symbiosis. *Applied and environmental microbiology*, *77*(4), 1309-1314.

Bates, S. T., Garcia-Pichel, F., & Nash III, T. (2010). Fungal components of biological soil crusts: insights from culture-dependent and culture-independent studies. *Bibliotheca Lichenologica*, *105*, 197-210.

Bates, S. T., Reddy, G. S., & Garcia-Pichel, F. (2006). Exophiala crusticola anam. nov.(affinity Herpotrichiellaceae), a novel black yeast from biological soil crusts in the Western United States. *International journal of systematic and evolutionary microbiology*, *56*(11), 2697-2702.

Belnap, J. (2002). Nitrogen fixation in biological soil crusts from southeast Utah, USA. *Biology and fertility of soils*, *35*(2), 128-135.

Belnap, J., & Büdel, B. (2016). Biological soil crusts as soil stabilizers. In *Biological soil crusts: an organizing principle in drylands* (pp. 305-320). Springer.

Belnap, J., Büdel, B., & Lange, O. L. (2001). Biological soil crusts: characteristics and distribution. In *Biological soil crusts: structure, function, and management* (pp. 3-30). Springer.

Belnap, J., & Lange, O. L. (2001). *Biological soil crusts: structure, function, and management* (Vol. 150). Springer.

Belnap, J., Phillips, S. L., & Miller, M. E. (2004). Response of desert biological soil crusts to alterations in precipitation frequency. *Oecologia*, *141*(2), 306-316. https://doi.org/10.1007/s00442-003-1438-6

Belnap, J., Phillips, S. L., & Smith, S. D. (2007). Dynamics of cover, UV-protective pigments, and quantum yield in biological soil crust communities of an undisturbed Mojave Desert shrubland. *Flora-Morphology, Distribution, Functional Ecology of Plants*, *202*(8), 674-686.

Berman-Frank, I., Lundgren, P., & Falkowski, P. (2003). Nitrogen fixation and photosynthetic oxygen evolution in cyanobacteria. *Res Microbiol*, *154*(3), 157-164. https://doi.org/10.1016/S0923-2508(03)00029-9

Bowker, M. A., Soliveres, S., & Maestre, F. T. (2010). Competition increases with abiotic stress and regulates the diversity of biological soil crusts. *Journal of Ecology*, *98*(3), 551-560.

Cardinale, M., Puglia, A. M., & Grube, M. (2006). Molecular analysis of lichen-associated bacterial communities. *FEMS Microbiol Ecol*, *57*(3), 484-495. https://doi.org/10.1111/j.1574-6941.2006.00133.x

Cardinale, M., Vieira de Castro, J., Müller, H., Berg, G., & Grube, M. (2008). In situ analysis of the bacterial community associated with the reindeer lichen Cladonia arbuscula reveals predominance of Alphaproteobacteria. *FEMS Microbiol Ecol*, *66*(1), 63-71. https://doi.org/10.1111/j.1574-6941.2008.00546.x

Colesie, C., Allan Green, T. G., Haferkamp, I., & Büdel, B. (2014). Habitat stress initiates changes in composition, CO2 gas exchange and C-allocation as life traits in biological soil crusts. *The ISME Journal*, *8*(10), 2104-2115. https://doi.org/10.1038/ismej.2014.47

Couradeau, E., Giraldo-Silva, A., De Martini, F., & Garcia-Pichel, F. (2019). Spatial segregation of the biological soil crust microbiome around its foundational cyanobacterium, Microcoleus vaginatus, and the formation of a nitrogen-fixing cyanosphere. *Microbiome*, *7*(1). https://doi.org/10.1186/s40168-019-0661-2

Csotonyi, J. T., Swiderski, J., Stackebrandt, E., & Yurkov, V. (2010). A new environment for aerobic anoxygenic phototrophic bacteria: biological soil crusts. *Environmental Microbiology Reports*, *2*(5), 651-656.

Garcia-Pichel, F., López-Cortés, A., & Nübel, U. (2001). Phylogenetic and morphological diversity of cyanobacteria in soil desert crusts from the Colorado plateau. *Appl Environ Microbiol*, *67*(4), 1902-1910. https://doi.org/10.1128/AEM.67.4.1902-1910.2001

Garcia-Pichel, F., & Wojciechowski, M. F. (2009). The Evolution of a Capacity to Build Supra-Cellular Ropes Enabled Filamentous Cyanobacteria to Colonize Highly Erodible Substrates. *PLoS ONE*, *4*(11), e7801. https://doi.org/10.1371/journal.pone.0007801

Geiser, D. M., Gueidan, C., Miadlikowska, J., Lutzoni, F., Kauff, F., Hofstetter, V., . . . Aptroot, A. (2006). Eurotiomycetes: Eurotiomycetidae and Chaetothyriomycetidae. *Mycologia*, *98*(6), 1053-1064. https://doi.org/10.3852/mycologia.98.6.1053

Golubic, S., & Campbell, S. E. (1979). Analogous microbial forms in recent subaerial habitats and in Precambrian cherts: Gloethece coerulea Geitler and Eosynechococcus moorei Hofmann. *Precambrian Research*, *8*(3-4), 201-217. https://doi.org/https://doi.org/10.1016/0301-9268(79)90029-9

Gorbushina, A. A. (2007). Life on the rocks. *Environmental microbiology*, *9*(7), 1613-1631.

Gorbushina, A. A., Andreas, B., & Schulte, A. (2005). Microcolonial rock inhabiting fungi and lichen photobionts: evidence for mutualistic interactions. *Mycological Research*, *109*(11), 1288-1296.

Gostincar, C., Grube, M., de Hoog, S., Zalar, P., & Gunde-Cimerman, N. (2010). Extremotolerance in fungi: evolution on the edge. *FEMS Microbiol Ecol*, *71*(1), 2-11. https://doi.org/10.1111/j.1574-6941.2009.00794.x

Gostinčar, C., Muggia, L., & Grube, M. (2012). Polyextremotolerant black fungi: oligotrophism, adaptive potential, and a link to lichen symbioses. *Frontiers in Microbiology*, *3*, 390.

Gostinčar, C., Zajc, J., Lenassi, M., Plemenitaš, A., De Hoog, S., Al-Hatmi, A. M. S., & Gunde-Cimerman, N. (2018). Fungi between extremotolerance and opportunistic pathogenicity on humans. *Fungal Diversity*, *93*(1), 195-213. https://doi.org/10.1007/s13225-018-0414-8

Gretarsdottir, J., Aradottir, A. L., Vandvik, V., Heegaard, E., & Birks, H. (2004). Long-term effects of reclamation treatments on plant succession in Iceland. *Restoration Ecology*, *12*(2), 268-278.

Grube, M., Muggia, L., & Gostinčar, C. (2013). Niches and adaptations of polyextremotolerant black fungi. In *Polyextremophiles* (pp. 551-566). Springer.

Gueidan, C., Villaseñor, C. R., De Hoog, G. S., Gorbushina, A. A., Untereiner, W. A., & Lutzoni, F. (2008). A rock-inhabiting ancestor for mutualistic and pathogen-rich fungal lineages. *Studies in Mycology*, *61*, 111-119. https://doi.org/10.3114/sim.2008.61.11

Honegger, R. (1991). Functional aspects of the lichen symbiosis. *Annual review of plant biology*, *42*(1), 553-578.

Horodyski, R. J., & Knauth, L. P. (1994). Life on land in the precambrian. *Science*, *263*(5146), 494-498. https://doi.org/10.1126/science.263.5146.494

Johansen, J. R. (1993). Cryptogamic crusts of semiarid and arid lands of North America. *Journal of phycology*, *29*(2), 140-147.

Kenrick, P., Wellman, C. H., Schneider, H., & Edgecombe, G. D. (2012). A timeline for terrestrialization: consequences for the carbon cycle in the Palaeozoic. *Philosophical Transactions of the Royal Society B: Biological Sciences*, *367*(1588), 519-536.

Kuske, C. R., Yeager, C. M., Johnson, S., Ticknor, L. O., & Belnap, J. (2012). Response and resilience of soil biocrust bacterial communities to chronic physical disturbance in arid shrublands. *The ISME Journal*, *6*(4), 886-897. https://doi.org/10.1038/ismej.2011.153

Labandeira, C. C. (2005). Invasion of the continents: cyanobacterial crusts to tree-inhabiting arthropods. *Trends Ecol Evol*, *20*(5), 253-262. https://doi.org/10.1016/j.tree.2005.03.002

Lan, S., Wu, L., Zhang, D., & Hu, C. (2012). Successional stages of biological soil crusts and their microstructure variability in Shapotou region (China). *Environmental Earth Sciences*, *65*(1), 77-88.

Lange, O. L., Belnap, J., Reichenberger, H., & Meyer, A. (1997). Photosynthesis of green algal soil crust lichens from arid lands in southern Utah, USA: role of water content on light and temperature responses of CO2 exchange. *Flora*, *192*(1), 1-15. https://doi.org/10.1016/s0367-2530(17)30749-1

Li, X., Zhang, P., Su, Y., & Jia, R. (2012). Carbon fixation by biological soil crusts following revegetation of sand dunes in arid desert regions of China: a four-year field study. *Catena*, *97*, 119-126.

Maier, S., Muggia, L., Kuske, C. R., & Grube, M. (2016). Bacteria and non-lichenized fungi within biological soil crusts. In *Biological Soil Crusts: An Organizing Principle in Drylands* (pp. 81-100). Springer.

Mitchell, R. L., Cuadros, J., Duckett, J. G., Pressel, S., Mavris, C., Sykes, D., . . . Kenrick, P. (2016). Mineral weathering and soil development in the earliest land plant ecosystems. *Geology*, *44*(12), 1007-1010.

Mitchell, R. L., Strullu-Derrien, C., Sykes, D., Pressel, S., Duckett, J. G., & Kenrick, P. (2021). Cryptogamic ground covers as analogues for early terrestrial biospheres: Initiation and evolution of biologically mediated proto-soils. *Geobiology*, *19*(3), 292-306. https://doi.org/10.1111/gbi.12431

Muggia, L., Gueidan, C., Knudsen, K., Perlmutter, G., & Grube, M. (2013). The Lichen Connections of Black Fungi. *Mycopathologia*, *175*(5-6), 523-535. https://doi.org/10.1007/s11046-012-9598-8

Naranjo-Ortiz, M. A., & Gabaldón, T. (2019). Fungal evolution: diversity, taxonomy and phylogeny of the Fungi. *Biological Reviews*, *94*(6), 2101-2137. https://doi.org/10.1111/brv.12550

Nelsen, M. P., Lücking, R., Boyce, C. K., Lumbsch, H. T., & Ree, R. H. (2020). No support for the emergence of lichens prior to the evolution of vascular plants. *Geobiology*, *18*(1), 3-13. https://doi.org/10.1111/gbi.12369

Nevins, C. J., Inglett, P. W., & Strauss, S. L. (2021). Biological soil crusts structure the subsurface microbiome in a sandy agroecosystem. *Plant and Soil*, *462*(1-2), 311-329. https://doi.org/10.1007/s11104-021-04868-2

Pointing, S. B., & Belnap, J. (2012). Microbial colonization and controls in dryland systems. *Nature Reviews Microbiology*, *10*(8), 551-562. https://doi.org/10.1038/nrmicro2831

Prave, A. R. (2002). Life on land in the Proterozoic: Evidence from the Torridonian rocks of northwest Scotland. *Geology*, *30*(9), 811-814. https://doi.org/10.1130/0091-7613(2002)030<0811:lolitp>2.0.co;2

Quan, Y., Muggia, L., Moreno, L. F., Wang, M., Al-Hatmi, A. M. S., Da Silva Menezes, N., . . . De Hoog, S. (2020). A re-evaluation of the Chaetothyriales using criteria of comparative biology. *Fungal Diversity*, *103*(1), 47-85. https://doi.org/10.1007/s13225-020-00452-8

Rajeev, L., Da Rocha, U. N., Klitgord, N., Luning, E. G., Fortney, J., Axen, S. D., . . . Mukhopadhyay, A. (2013). Dynamic cyanobacterial response to hydration and dehydration in a desert biological soil crust. *The ISME Journal*, *7*(11), 2178-2191. https://doi.org/10.1038/ismej.2013.83

Réblová, M., Hubka, V., Thureborn, O., Lundberg, J., Sallstedt, T., Wedin, M., & Ivarsson, M. (2016). From the Tunnels into the Treetops: New Lineages of Black Yeasts from Biofilm in the Stockholm Metro System and Their Relatives among Ant-Associated Fungi in the Chaetothyriales. *PLoS One*, *11*(10), e0163396. https://doi.org/10.1371/journal.pone.0163396

Schoch, C. L., Wang, Z., Townsend, J. P., & Spatafora, J. W. (2009). <I>Geoglossomycetes</I> cl. nov., <I>Geoglossales</I> ord. nov. and taxa above class rank in the <I>Ascomycota</I> Tree of Life. *Persoonia - Molecular Phylogeny and Evolution of Fungi*, *22*(1), 129-138. https://doi.org/10.3767/003158509x461486

Spribille, T. (2018). Relative symbiont input and the lichen symbiotic outcome. *Curr Opin Plant Biol*, *44*, 57-63. https://doi.org/10.1016/j.pbi.2018.02.007

Sterflinger, K. (2000). Fungi as Geologic Agents. *Geomicrobiology Journal*, *17*(2), 97-124. https://doi.org/10.1080/01490450050023791

Sterflinger, K. (2006). Black yeasts and meristematic fungi: ecology, diversity and identification. In *Biodiversity and ecophysiology of yeasts* (pp. 501-514). Springer.

Steven, B., Gallegos-Graves, L. V., Belnap, J., & Kuske, C. R. (2013). Dryland soil microbial communities display spatial biogeographic patterns associated with soil depth and soil parent material. *FEMS microbiology ecology*, *86*(1), 101-113.

Teixeira, M. M., Moreno, L. F., Stielow, B. J., Muszewska, A., Hainaut, M., Gonzaga, L., . . . de Hoog, G. S. (2017). Exploring the genomic diversity of black yeasts and

relatives (Chaetothyriales, Ascomycota). *Studies in mycology*, *86*, 1-28. https://doi.org/https://doi.org/10.1016/j.simyco.2017.01.001

Wu, Y., Rao, B., Wu, P., Liu, Y., Li, G., & Li, D. (2013). Development of artificially induced biological soil crusts in fields and their effects on top soil. *Plant and soil*, *370*(1), 115-124.

Yan, S., Yang, J., Zhou, S., Yan, Y., Tang, X., Ma, Y., . . . Ye, W. (2021). Biological soil crusts alleviate the stress of arsenic on rice germination and the underlying immobilization mechanisms. *Ecotoxicology and Environmental Safety*, *227*, 112839.

Zalar, P., Novak, M., de Hoog, G. S., & Gunde-Cimerman, N. (2011). Dishwashers – A man-made ecological niche accommodating human opportunistic fungal pathogens. *Fungal Biology*, *115*(10), 997-1007. https://doi.org/https://doi.org/10.1016/j.funbio.2011.04.007

Chapter 1

Lichens and Biofilms: Common Collective Growth Imparts Similar Developmental Strategies

This chapter represents the contents of: Erin C. Carr, Steven D. Harris, Joshua R. Herr, Wayne R. Riekhof; Lichens and biofilms: Common collective growth imparts similar developmental strategies. Algal Research, 54, 102217.
https://doi.org/10.1016/j.algal.2021.102217

Abstract

Lichens are traditionally defined as a symbiotic relationship between fungi and algae and/or cyanobacteria. This union forms a unique structure called the thallus, which attaches to surfaces such as rocks and tree bark. Recent reports challenge the view that lichens are comprised of one fungus and one photobiont, and instead suggest that they are a consortium of microbes. Much of lichen biology remains unknown as most of our knowledge of lichens is limited to morphological characteristics with little to no functional analysis of lichen genes. However, lichens and biofilms share many similar physiological traits which when compared may assist in our understanding of lichens. Similarities between the two are rooted in their lifestyle, where these microbes and their extracellular products attach themselves to a surface and grow in a community structure. Biofilms and lichens alike have distinct features that allow for their lifestyle and identification, such as specific developmental patterns, formation of an extracellular matrix, and their ability to resist abiotic stressors. We argue here that one can gain insight

into the cellular processes and evolutionary origins of lichens, which are currently undetermined, by applying knowledge gleaned from studies on microbial biofilms, with a particular focus on fungal biofilms.

Introduction to Lichens and Biofilms

The lichen lifestyle represents over half of all Ascomycetes with theoretically five evolutionary origins of the lifestyle amongst fungi, which makes this fungal form a highly successful yet still confounding entity (Gargas et al., 1995; Lutzoni & Miadlikowska, 2009) (**Figure 1**). Lichens have been observed by scientists and used for medicinal purposes and dyes since ancient times - they were even studied by Aristotle (Plitt, 1919) (**Figure 2**). Since their initial discovery our understanding of lichens has drastically altered and is still changing today. Lichens were originally described and recognized as plants. However, in 1867, Herman Schwendener proposed that lichens were instead a conglomerate of fungi (the mycobiont), and algae or cyanobacteria (the photobiont/phycobiont and cyanobiont respectively) (Honegger, 2000). Until recently this was the reigning paradigm of lichen symbiosis, but with the advent of modern sequencing technologies we have amended our understanding of what constitutes a lichen.

Researchers are now beginning to understand that lichens do not contain just two organisms or “partners”, but rather an entire consortium of microbes, which can even include bacteria and archaea (Cardinale et al., 2008; Goodenough & Roth, 2020b; Grube & Berg, 2009; Grube et al., 2015; Hodkinson & Lutzoni, 2009). As these developments have only been made in the past 10 years, many scientists are still under the assumption that lichens contain only the mycobiont and the photobiont. A shift in the accepted

definition of a lichen to encompass a wider array of organismal participants is slowly gaining acceptance, but more research is needed to characterize the involvement of bacteria and other microbes in the lichen symbiosis before a consensus is reached. Presently, no published research characterizes the roles of the other microbes found in lichens, therefore we still know very little about how these organisms are involved in the lichen symbiosis and interact to form a uniquely complex 3-D structure.

Lichens are extremely difficult to grow, maintain, and study in a laboratory setting, growing extremely slowly compared to other microbes, with some slow growing lichens growing only 0.01 – 0.33 mm in a year (Armstrong & Bradwell, 2011; Hale, 1959). Whereas faster lichens can cover up to 64 mm a year, most lichens fall between those growth extremes (Armstrong & Bradwell, 2011; Webster & Brown, 1997). Reasons for their slow growth remain enigmatic, but many researchers have attempted to understand this phenomenon. Past and current hypotheses have relied on modeling to determine growth rate factors, with multiple factors having been tested (Armstrong & Bradwell, 2011; Seminara et al., 2018). It is currently thought that growth rate is limited by the ability for lichens to both shuttle around nutrients, such as carbohydrates, and the rate at which carbon dioxide is taken up for photosynthesis to occur (Lange & Tenhunen, 1981; Seminara et al., 2018). These, and possibly other factors that contribute to the slow growth of lichens, remain issues that confront those who study these unique symbioses.

Additionally, the diverse polyphyletic evolutionary origins of lichens coupled with the availability of multiple prospective partners within a given “species”, contributes to their enigmatic nature (Gargas et al., 1995; Honegger, 1991). Lichens are classified based on several features, but typically the photobiont taxon and structural morphology

of the thallus provides the basis for classification of a lichen type, such as *Xanthoria parietina,* which is a Trebouxiod foliose type lichen. While the taxon name given to the lichen is also given to the mycobiont (or vice versa), for example: *Endocarpon pusillum* the lichen with the mycobiont species *Endocarpon pusillum* and photobiont species *Diplosphaera chodatii*. Phenotypic plasticity can then lead to unnecessary taxonomic separation and confusion in understanding lichen biology and diversity. Lichens that contain multiple photobionts (or mycobionts), and promiscuous lichens that can choose between multiple partners further increases confusion in nomenclature. Examples of phenotypic specificities leading to nomenclature issues include: recent indications that some lichens contain multiple fungal partners (ascomycete and basidiomycete) that are required for lichen speciation (Spribille et al., 2016; Tuovinen et al., 2019), mycobionts that are capable of associating with a variety of photobiont partners (Blaha et al., 2006; Piercey-Normore, 2006; Piercey-Normore & DePriest, 2001), and lichens that can contain more than one photobiont simultaneously (Galun & Bubrick, 1984; Henskens et al., 2012). For the sake of simplicity, lichen features and descriptions referred to here will be broad and not specific to any particular lichen morphotype and may not represent all lichen taxa. This diversity of life history strategies has also caused the understanding of lichens to lag behind those of other organisms, but more recent nucleotide sequencing technologies have helped further our knowledge of these communities. In order to understand the life history of lichens it is appropriate to make sense of their biology by focusing on the fact that they exist in a similar fashion to microbial biofilms.

Biofilms are defined as an aggregation of microbes and their extracellular products attached to a surface (visual examples in **Figure 2**) (Donlan, 2002). This simple,

overarching definition is widely accepted by microbiologists, which deconvolutes the study of this microbial form. In a laboratory setting, such as in a petri dish or shaking flask, microbes are typically grown in monoculture under conditions that are not conducive to biofilm formation, although many argue that a simple colony could be a biofilm (Branda et al., 2005; Friedman & Kolter, 2004; Kowalski et al., 2019). While some microbes may still form biofilms at the air-liquid interface of shaking flasks, they are more notable in stable ecosystems where biofilms attach to surfaces such as rocks, fermentation tanks, PVC pipes, soil, plant roots, teeth, etc. (Davey & O'Toole, 2000). Growth on surfaces is only capable due to formation of a biofilm, and therefore it is assumed that all microbes form biofilms in their natural habitats at some point (Davey & O'Toole, 2000; Watnick & Kolter, 2000). Much research on biofilms has been invested into those that cause diseases or possess the ability to disrupt and destroy man-made structures (walls, plumbing, statues, etc.), with little work devoted to non-destructive biofilms. Because of their broad impacts on human welfare, there has been a lot of research on the genetics and molecular basis of biofilm formation, which stands as a stark contrast to our relatively poor understanding of thallus development in lichens. To date, a small number of lichen mycobiont genomes have been sequenced and only a few have been transcriptionally analyzed (Junttila & Rudd, 2012; Kono et al., 2020; Kuske et al., 2015; Wang et al., 2014). Due to this lack of knowledge, our understanding of exactly how lichens form is unknown. However, a comparison of the similarities between lichens and biofilms may facilitate the generation of hypotheses for the establishment and function of the multi-species lichen consortium.

Following the definition of a biofilm, lichens represent one of the most successful surface-attached microbial symbiotic architectures covering 8% of total land surface on Earth (Lutzoni & Miadlikowska, 2009). One could even posit that lichens began as biofilms, and through millions of years of co-evolution with symbiotic partners (Lutzoni et al., 2018), developed into the highly coordinated and more permanent lichen thallus. However, our understandings of the lichen symbiosis and biofilms as a microbial phenomenon have been historically realized via different fields of study and, as a result, available information regarding these two biological entities differs despite the many connections that can be made. In this review, we will reflect on similarities and differences between biofilms and lichens by focusing on perhaps the three most important aspects of a biofilm and lichens: (1) the development and microbial interactions of microbial communities; (2) the extracellular matrix (ECM) structure and function; and (3) the role of community growth in resistance to abiotic factors (summarized in **Table 1**). We will also discuss how lichens may be analogous to biofilms due to potential evolutionary origins and identify gaps of knowledge in both phenomena that will help link our understandings of these ecologically and economically important microbial communities.

Microbial Development and Interactions in Biofilms

Stages of Development

Stages of biofilm development have been extensively described in many microorganisms, meaning we now have mostly complete models of the genetic cascade involved in forming microbial biofilms (Finkel & Mitchell, 2011; López et al., 2010;

Vlamakis et al., 2008). The same cannot be said for lichens. Our knowledge of lichen thallus development relies heavily on re-synthesis experiments- observations of the separation and re-constitution of the mycobiont and photobiont. These experiments have mostly employed scanning electron microscopy (SEM) and transmission electron microscopy (TEM) to characterize the changing morphology of the two partners and their interactions in forming the lichen thallus (Ahmadjian & Jacobs, 1981; Honegger, 1982, 1991, 1992, 1993; Honegger, 2000, 2009; Honegger & Haisch, 2001; Jacobs & Ahmadjian, 1969). In 1993, a model for lichen formation was proposed by Honegger using morphological data, which has been widely adopted. But we can build upon this work by delving into the literature of the cellular processes involved in biofilm formation, particularly in the fungi *Candida albicans* and *Aspergillus fumigatus*. We can then hypothesize and more readily focus lichen research on biofilm-specific genes for example, that likely have led to the same biological phenomena in lichen thallus formation.

Biofilm development follows four main stages: 1) adherence, 2) initiation, 3) maturation, and 4) dispersal (Finkel & Mitchell, 2011; Watnick & Kolter, 2000). Each stage has specific microbial requirements and genetic switches, which change between stages of formation (Vlamakis et al., 2008). These stages resemble those of lichen thallus development as described in the literature on morphological succession of lichenization. According to Honegger (1993), the stages of lichenization are: 1) non-specific contact and recognition, 2) pre-thallus formation, 3) thallus stratification, and 4) mature thallus reproduction and dispersal (**Figure 3**). Although the terminology may differ between the developmental stages of biofilms and lichens, the biologically significant processes are

aligned across the four stages. The first stage includes adherence to the surface, or to the partner in the lichen literature, and identifying neighboring organisms. The second stage involves a switch in the type of cell growth. The third stage is the differentiation of cell morphotypes and matrix formation. The final stage is dispersal of cells via spores or vegetative propagules. Notably, the time it takes the cells to go through each stage varies significantly between these communities. Lichens take years to grow, whereas some biofilms take only hours. Regardless of the timescale, these two communities share great biological similarities in each stage of their development (**Figure 3**).

Adherence/Non-specific Contact Stage

Biofilm formation begins with the adherence stage. For both bacteria and fungi, this stage consists of "pioneer cells" that adhere to a surface and seed biofilm formation. Surface types that many biofilms adhere to are typically hydrophobic and non-polar, such as silicone (Andes et al., 2004; Donlan, 2002). This is mostly due to the nature of structures that aid in adhesion to surfaces, which are typically hydrophobic in nature (Blankenship & Mitchell, 2006; Davey & O'Toole, 2000; Krasowska & Sigler, 2014). In bacteria this phenomenon is typically initiated by type IV pili, flagella, fimbriae, hydrophobins, and adhesin proteins (Davey & O'Toole, 2000). Most fungal species that form biofilms do not contain flagellar-like structures, and instead rely on adhesins, hydrophobins, agglutinin-like sequence proteins, and other proteins for their adherence step (Finkel & Mitchell, 2011; Lipke, 2018).

Akin to monotypic fungal biofilms, lichens also readily attach to hydrophobic surfaces such as rock surfaces, tree bark, and leaves, all of which can present a

hydrophobic point of attachment for a lichen spore or propagule, however their mechanism of adherence is poorly understood. One confounding issue with lichen adherence and their non-specific contact stage is the variety of ways that lichen taxa disperse their cells. While many lichens disperse via vegetative means with both mycobiont and photobiont traveling together (for example, soredia and isidia), there are a number of well-known spore-forming lichens which disperse the mycobiont spores alone (Sanders & Lücking, 2002). This variety in dispersal methods likely results in diverse attachment modes based on the "preferred" method of dispersal and attachment surface for given lichen taxa. Since vegetative propagule dispersal contains a pre-established symbiosis composed of mycobiont and photobiont cells, it is likely that these structures rely on fungal proteins for adhesion that might be similar to those that underlie adhesion of biofilm constituents.

One prevailing feature of most Ascomycete spores and particularly those of biofilm-forming *Aspergillus spp*. is their hydrophobic outer layer. This layer contains hydrophobins that together form a rodlet layer surrounding the spores' matrix (Dynesen & Nielsen, 2003; Girardin et al., 1999; Priegnitz et al., 2012; Wösten, 2001). This rodlet layer allows for the spores to attach to hydrophobic surfaces to begin forming colonies then, biofilms. Similarly, *Magnaporthe spp*. also use hydrophobins on their spore surface to attach to hydrophobic plant cuticles (Inoue et al., 2016; Talbot et al., 1996). Without their hydrophobic surface outside of the matrix layer, it has been shown many times that both *Aspergillus spp*. and *Magnaporthe spp*. are severely reduced in adhesion to their substrates (Inoue et al., 2016; Priegnitz et al., 2012; Talbot et al., 1996).

Lichens are reported to use similar types of hydrophobic proteins, particularly the class I hydrophobins XEH1 and XPH1, for interactions between the mycobiont and their photosynthetic partners, and theoretically also surfaces (Scherrer et al., 2000; Wessels, 2000). Hydrophobins surround the outside of the extracellular matrix that encompasses the mycobiont and photobiont, as seen by the distinct rodlet layer produced by the hydrophobin proteins, which can only be observed through freeze-etch electron microscopy (Honegger, 1982; Honegger, 1984). No cytological studies, particularly no electron microscopy studies, have been performed on the spores of lichens, therefore we cannot be sure if their spores also contain the distinctive hydrophobin rodlet layer of other Ascomycete spores. However, since the alternative method of lichen reproduction is via vegetative structures directly derived from lichen thalli, it seems reasonable to speculate that the hydrophobic layer surrounding the ECM plays a role in surface adhesion similar to that of fungal biofilms and fungal spores (Scherrer et al., 2000; Wösten et al., 1994). Once fungal biofilm cells have bound to their substrate it has been observed that the hydrophobicity of the cells decreases and they instead become hydrophilic (Dague et al., 2008). This observation is linked to multiple instances of germinating sporelings of both lichens and biofilm-forming fungi creating or possibly exposing their hydrophilic polysaccharide ECM (Clayden, 1998; Dague et al., 2008; González-Ramírez et al., 2016; Meeßen & Ott, 2013; Ott, 1987). This shift in hydrophobicity allows for the success of the next step in biofilm and lichen formation, which is characterized by binding to other cells.

Initiation/Pre-thallus Stage

The second stage of biofilm formation is the initiation stage, which includes cell differentiation, cell-cell adhesion, and filamentation in fungal biofilms specifically (Finkel & Mitchell, 2011). During this stage, the ability to adhere is vital to forming a cohesive biofilm of cells adhering to other cells. Therefore, many times there is less of a distinct separation of the adherence stage from the initiation stage, which is indicated by similarly important genes being expressed and the continuing functional role of adhesion proteins (Finkel & Mitchell, 2011). For lichens this cell-cell adhesion step is required for mycobiont-photobiont interactions. This step is called the pre-thallus stage in lichen formation and is critical for the ability of mycobionts to engage with prospective photobionts. However, if the lichen reproduces via vegetative propagules then the photobiont and mycobiont travel as a unit and therefore do not require partner recruitment, which presumably leads to quicker lichen development that "skips" the pre-thallus stage (Honegger, 1993).

Complete coherence between the mycobiont and photobiont is a result of the surface layer hydrophobins of the fungal extracellular matrix encompassing cells of both the photobiont and mycobiont (Honegger, 1991). Two Class I hydrophobin proteins of fungal origin are involved in adherence between mycobiont and photobiont cells in the lichens *Xanthoria parietina* and *X. ectaneoides*; the proteins are XPH1 and XEH1 respectively (Scherrer et al., 2000). These proteins make up the distinctive rodlet layer that surrounds these lichens' ECM within certain structures, similar to other fungal rodlet layers (Scherrer et al., 2000). Timing of photobiont-mycobiont adherence is not entirely understood but is observed to occur very early in the pre-thallus stage, or the late non-specific contact stage (Clayden, 1998). Cell-cell adherence in fungal biofilms has not

been fully characterized either, but this is the result of the complicated nature of binding through a variety of mechanisms. Fungal cell-cell adherence has been said to be mediated by GPI-linked adhesin proteins (Li et al., 2007; Nobile et al., 2006; Nobile et al., 2008), hydrophobins (Dynesen & Nielsen, 2003), and polysaccharides of the ECM (Beauvais et al., 2007; Gravelat et al., 2013), with hydrophobins possibly not playing a role in certain species.

In *C. albicans* biofilm formation, cell-cell adherence is triggered by a switch from yeast growth to hyphal growth, and involves key genes, such as *epa1*, *hwp1,* and *als1/3*. These genes encode GPI-anchored adhesin proteins, which aid in cell-cell adherence and cell-surface adherence in *C. albicans* (Finkel & Mitchell, 2011; Li et al., 2007; Nobile et al., 2006; Nobile et al., 2008). The filamentous fungus *Aspergillus fumigatus* has also recently been identified as a biofilm forming fungus. *Aspergillus fumigatus* biofilms were initially thought to use hydrophobins like RodB for cell-cell adherence (Beauvais et al., 2007). However, after a full deletion screen of hydrophobin-coding genes, it was determined that hydrophobins are not used for cell-cell adherence in *A. fumigatu*s (Valsecchi et al., 2018). On the other hand, deletion of *rodA* in *Aspergillus nidulans* revealed a decrease in cell-cell adherence, likely due to nucleation effects and species-specific processes (Dynesen & Nielsen, 2003). In lichens, it has been observed that both spore-initiated and vegetative starting structures contain ECM and secrete more once attached to their substrate (Clayden, 1998). Beyond this observation not much is known about mycobiont-mycobiont cell adherence. Nevertheless, the ability of biofilm-forming fungi to utilize adhesin proteins for cell-cell adherence suggests that mycobionts do as well. Additionally, mycobionts are known to use a combination of class I hydrophobins

and ECM for mycobiont-photobiont and also potentially mycobiont-bacterial cell adherence (Goodenough & Roth, 2020b; Honegger & Haisch, 2001).

The initiation stage is also the point at which cell differentiation occurs and microcolonies form (Finkel & Mitchell, 2011; Vlamakis et al., 2008; Watnick & Kolter, 2000). This stage is particularly important for multi-species biofilms since it is the first step towards niche determination within the cells. The differentiation and arrangement of niches allows for optimal usage of "microniches" that form within the biofilm, such as anaerobic zones. When a microbe fills a specific niche, it increases overall biofilm fitness (Van Gestel et al., 2015; Watnick & Kolter, 2000). How these microcolonies form and how cell differentiation occurs has been the topic of recent research, and although this is still poorly understood, the current consensus is that numerous factors trigger cell differentiation (Van Gestel et al., 2015). Various conditions that contribute to the formation of cell differentiation and microniches include abiotic factors, the organisms involved in the biofilm, and specific gene switches. For example, Vlamakis et al. (2008) investigated the spatiotemporal shift of three types of differentiated cells in *Bacillus subtilis* biofilms, where they observed a shift in cell types. Observed cell types varied in abundance over time, with motile cells being the first type of cells (which formed the initial biofilm), then matrix cells becoming the majority of the second stage, and finally sporulating cells to allow for dispersal of the microbes. All three types of cells were observed at each time point but in different locations within the biofilm and in varying abundance. This evidence suggests that even within a mono-cultured biofilm, diversification of cell type is both present and essential to the overall fitness of the biofilm.

Quorum sensing molecules (QSM) or cell-signaling chemicals have also been linked to cell differentiation in both fungal and bacterial biofilms (Davey & O'Toole, 2000). When the gene *lasI*, which encodes for the formation of acyl-homoserine lactones (acyl-HSLs), was deleted from *Pseudomonas aeruginosa*, it formed flat-nondifferentiated biofilms that were easily disrupted by a detergent such as SDS, but recovered after addition of external acyl-HSL (Davies et al., 1998). QSMs are not specific to bacteria, as farnesol has been identified as a quorum sensing molecule produced by the fungal pathogen *Candida albicans* in its planktonic state (Hornby et al., 2001). However, exposure of *C. albicans* or its close relative *C. dubliniensis,* to 10x the normal amount of farnesol disrupts biofilm formation (Jabra-Rizk et al., 2006; Ramage et al., 2002). *Candida albicans* is unable to form biofilms in the presence of farnesol because it blocks the switch to hyphal growth (Hornby et al., 2001; Jabra-Rizk et al., 2006; Ramage et al., 2002), and the switch from white to opaque cells, which are both vital to the formation of biofilms during the initiation step (Baillie & Douglas, 1999). Since increased farnesol inhibits the progression into the filamentous form, it in turn inhibits biofilm formation (Jabra-Rizk et al., 2006; Ramage et al., 2002). In most Ascomycete biofilm-forming fungi, hyphal growth is necessary for biofilm production, (Blankenship & Mitchell, 2006; Fanning & Mitchell, 2012; Finkel & Mitchell, 2011). This phenomenon is found mainly in Pezizomycotina, the fungal subdivision where the majority of lichen-forming fungi are phylogenetically derived (Gargas et al., 1995; Mitchell et al., 2016).

Lichen cell differentiation is very understudied, and there is little to no understanding of pre-thallus cell differentiation. Most studies in this area have focused more on the later aspects of cell differentiation. However, cell differentiation is vital to

the initial formation of the lichen thallus (i.e., body), which is composed of 4 (or more) distinct zones: the upper cortex, the algal layer, the medullary thalline layer, and the lower cortex (Honegger, 1992). Separation into these layers and cell types allows for the algae to be exposed to light, for gas and water to exchange between layers, and reduced desiccation (Honegger, 1992; Honegger & Haisch, 2001). This degree of cell differentiation is believed to form after much of the initial growth, and therefore this stratification occurs during the aptly named stratified thallus/stratification stage (Honegger, 1991; Stocker-Wörgötter & Türk, 1991). A recent publication by Roth et al. (2020) have indicated that lichen cell differentiation occurs in a stem cell-like fashion, in which the outer cortical fungal cells differentiate by emerging from internal medullary hyphae "stem cells". Unlike *C. albicans,* mycobionts have been known to maintain their hyphal state even outside of the lichen symbiosis and only one mycobiont (*Umbilicaria muhlenbergii*) recently has been identified to have a yeast state outside of the symbiosis (Wang et al., 2020). Notably, hyphal branching is more vital in lichen formation and biofilm-forming filamentous fungi (Harris, 2008; Roth et al., 2020), while hyphal branching is not commonly observed in *C. albicans* biofilms (Barelle et al., 2006). Lichen cell differentiation is vital for structural differences, which are not obvious until later stages, understanding the factors that drive thallus stratification and cell differentiation in the mycobiont cells will greatly contribute to our knowledge of lichen development. As *C. albicans* uses QSM to block biofilm formation, one would hypothesize that a quorum sensing molecule in lichens- whether sourced from fungal, algal, or both partners- may also play a role in lichen cell differentiation.

Maturation/Stratification Stage

The third stage of biofilm formation is the maturation stage. This stage is characterized by more pronounced cell differentiation or stratification, the formation of ECM, and the development of stress resistance mechanisms. At this stage only physical removal can disrupt biofilm organization (Donlan & Costerton, 2002). The combination of matrix formation, cell differentiation, and the subsequent development of specific structures provides biofilms with increased resilience relative to their planktonic form. In lichens, this stage is called the stratified thallus stage, where individual structural layers form to provide different functions, and subsequently this is the stage the lichen will remain in for many years (Honegger, 1993; Stocker-Wörgötter & Türk, 1991). ECM formation is one of the main features of the maturation stage of biofilms (Davey & O'Toole, 2000; Finkel & Mitchell, 2011; López et al., 2010). Similarly, the stratification of lichen thalli is also marked by the formation of "conglutinate zones", or the formation of the lichen matrix, by fungal (and likely photobiont) secretion of the mucilaginous matrix (Honegger, 1993). This matrix layer that forms around biofilms, and easily recognized in the lichen thallus, is important to the survival of both communities.

For biofilms and lichens alike, this stage is most important to the structural architecture that allows for optimal microbial interactions and survivability of all cells in the community. The initial parts of this stage are key to the shifting of cell types, which precedes structure formation. Although pili and flagella are integral to this shifting stage of many bacterial biofilms there are no known lichen-forming fungi capable of such coordinated movement in this way (Davey & O'Toole, 2000; Donlan, 2002). Like other filamentous fungi, lichen mycobionts employ polar growth and hyphal branching to

interact with partner algae and to develop the thallus (Armaleo, 1991; Harris, 2008; Joneson et al., 2011; Joneson & Lutzoni, 2009; Roth et al., 2020). Fungal biofilms formed by *C. albicans* have similar structural changes since, they also rely on polar growth of their hyphae to create a biofilm (Finkel & Mitchell, 2011).

Re-positioning of cells during this stage of lichen or biofilm development allows for tunnels to form, which are key to gas and liquid exchange. In biofilms, these structures are termed interstitial voids and are typically located at the base of the biofilm (Donlan, 2002). In lichens these structures are traditionally called pseudoparenchyma and are on the surface of the lichen (Ahmadjian, 1962). Recent research suggests that they may be a result of hydrophobic layers formed between clumps of mycobiont and photobiont cells (Goodenough et al., 2021; Honegger & Haisch, 2001). Nonetheless, both biofilms and lichens require mechanisms for gas and water exchange throughout the entire structure, to ensure availability of nutrients for all cells.

The formation of upper and lower conglutinate cortices of lichens seemingly permits no way for air or water exchange to occur within the thallus. However, the matrix that coats the cells of the lichen contains an outer hydrophobic layer surrounding the matrix, allowing for gas exchange within an optimally wetted thallus (Goodenough & Roth, 2020a, 2020b; Goodenough et al., 2021; Honegger, 2012; Honegger & Haisch, 2001) (**Figure 5**). When air moisture levels are low, the hydrophilic matrix shrinks like a dried dish sponge, allowing desiccation to occur. Desiccation shuts down cellular processes, which increases resistance to many stressors but also poses an issue by halting photosynthesis at peak UV exposure (Honegger, 1997; Lange & Tenhunen, 1981; Nybakken et al., 2004). When air moisture is high, the hydrophobic layer surrounding the

matrix subsequently reduces over wetting of the thallus and increases the timespan for photosynthesis, by allowing gas exchange to still occur as the hydrophilic matrix expands like a wetted dish sponge (Honegger & Haisch, 2001). This process of passive water regulation is called poikilohydry, as it uses no active cellular processes to regulate water retention (Honegger, 1997; Lange & Tenhunen, 1981; Nybakken et al., 2004). Although, at full hydration photobionts are still unable to perform photosynthesis (Lange & Tenhunen, 1981). The process is not a perfect solution, but without this hydrophobic layer the timespan for photosynthesis to occur would be much shorter (**Figure 5**).

Mycobiont cell polarization facilitates arrangement of photobiont cells for optimal light exposure – arguably the most important trait to the success of the lichen symbiosis. Mycobiont hyphae will grow in such a way to shift the photobiont to the upper medullary thalline layer (surface layer) and position the photobiont cells so they will be exposed to sunlight (Armaleo, 1991; Goodenough et al., 2021). Fungal positioning of the photobiont cells removes the responsibility of optimizing light exposure from the photobiont, and instead placing all the work on the fungal partner. Other fungal-photosynthetic organism interactions, such as mycorrhizal fungal symbioses, rely on the photosynthetic partner as the organism responsible for orienting towards the light. This is one argument that has been made for the symbiosis of lichens to be mutualistic instead of parasitic, because the mycobiont is providing a vital resource in the form of cell movement to the non-motile photobiont (Honegger, 1991; Lawrey, 2009). Without the proper structural organization to allow for gas and water exchange, and the correct positioning of the photobiont cells photosynthesis would not occur, compromising the lichen symbiosis.

A similar phenomenon can be accounted for in all microbial biofilms as their specific structural organization – the formation of interstitial voids – is optimized for the air and water exchange required by each organism in the biofilm (Donlan, 2002; López et al., 2010). In some multi-species biofilms, anaerobic zones within the biofilm allow specific syntrophys to form between anaerobic organisms, such as anaerobic archaea and aerophilic bacteria (Davey & O'Toole, 2000). Microniches that form within microbial biofilms via cell differentiation and community diversity accommodate specific interactions that may not have formed outside of the biofilm. The effect is an increase of the overall fitness of the microbial collective, which is hypothesized as one initiating factor driving these interactions toward mutualism (Yamamura, 1993). This may be how lichen interactions originally formed, via aggregation within a biofilm, then co-evolving over millions of years to form the more permanently structured lichen thallus.

Reproduction and Dispersal Stage

The last stage in biofilm formation is the dispersal stage, which allows the biofilm to spread to new locations, and is characterized by sporulation, shedding of vegetative cells, or cellular detachment (Donlan, 2002; Finkel & Mitchell, 2011). This stage resembles the end-stage growth of most microbes, but for some biofilm-forming microbes the ability to sporulate or disassociate requires they be in a biofilm. In both lichens and biofilms, dispersal may be non-sexual (vegetative spreading) or an asexual/sexual sporulation event. Vegetative spreading of biofilms may result from loss of a vital nutrient source, shearing caused by fluid movement, or by an autoinducer chemical signal (Hall-Stoodley et al., 2004; Hunt et al., 2004; Kaplan, 2010). Biofilm

dispersal promotes survival, allowing the biofilm to persist elsewhere. Although this process occurs throughout biofilm-forming organisms, the environmental and chemical triggers can vary across species and conditions.

Compared to biofilms, lichens' propensity for and mechanism of dispersal is comparatively much less understood. It has been noted that lichens are sometimes incapable of dispersing very far (Dettki et al., 2000); however, the production of various sporulating and vegetative structures is very well characterized in lichens, suggesting dispersal is vital in their development (Clayden, 1998; Honegger, 1993; Honegger, 2012; Sanders & Lücking, 2002). Spore-formation varies widely between lichen taxa, but one common theme is that no lichen separation experiments have observed sporulation events of the mycobiont when it is grown axenically and sporulation has been observed to be restored by re-synthesis (Ahmadjian, 1966; Cubero et al., 1999; del Carmen Molina & Crespo, 2000; Mcdonald et al., 2013; Molina et al., 1997). Overall, mating in fungal organisms is very complex and well-studied in only a few model organisms, particularly yeasts such as *Saccharomyces cerevisae*. For example, in *C. albicans* the genes required for biofilm formation (ex: the switch from white to opaque cells, and adhesin proteins: Eap1, Pga10, Hwp1, Hwp2, & Rbt1) are also important for mating (Ene & Bennett, 2009; Finkel & Mitchell, 2011). The link between mating and biofilm-formation in *C. albicans* is novel to fungal mating and it will be important to elucidate mating across other biofilm forming fungi and lichens. Notably, the presence of canonical mating components in sequenced lichen genomes suggest similar mechanisms of *C. albicans* mating and those employed through the lichen symbiosis (Armaleo et al., 2019).

Interactions

In multi-species biofilms, interactions between microbes tend to be symbiotic or syntrophic in nature, such that one microbe produces a product that another uses as a substrate (Davey & O'Toole, 2000). Biofilms promote persistent interactions between microorganisms and, in an economic sense, allow for nutrient niche economy such that the organisms always are within "flagella's reach" of what they collectively need. This phenomenon can be observed in anaerobic digestion vessels during wastewater treatment, which contain fermentative bacteria, acetogenic bacteria, and methanogens. Fermentative bacteria produce alcohols, which are used by acetogenic bacteria as a carbon source, who then produce acetate as a byproduct that is used by the anaerobic Methanogens as a carbon source - the final step in the carbon cycle (Schink, 1997). This exemplifies the typical biotic interactions that occur and are vital to a well-developed biofilm (Burmølle et al., 2014; Davey & O'Toole, 2000; Watnick & Kolter, 2000).

Lichens are a prime example of microbial syntrophy, where the mycobiont creates the "home" for the photobiont protecting it from the external stressors and orienting the photobiont for optimal UV exposure, while the photobiont in turn produces carbohydrates and occasionally reduced nitrogen (from cyanobacteria) (Honegger, 1993). Bacterial involvement in lichens is still poorly understood but likely is involved with nitrogen production in non-cyanolichens by utilizing other nitrogen-fixing bacteria from the order Rhizobiales to obtain reduced nitrogen, since they are the most abundant order found on lichens thus far (Grube et al., 2009; Hodkinson & Lutzoni, 2009). Microbial syntrophy allows biofilms and lichens to rely less on external abiotic acquisition of nutrients, in favor of becoming self-sustainable and more persistent. Lichens have co-opted this

strategy to their evolutionary advantage. By leveraging the combination of photosynthetic partners and flexible carbohydrate consumers in fungi, lichens have practically everything they need from biotic origins.

Recognition between the surrounding microbial species is also crucial to both biofilm and lichen formation. Quorum sensing molecules such as acyl-HSLs are one mechanism that microbial biofilms use to determine the identity of neighboring species and facilitate formation of multispecies biofilms (Keller & Surette, 2006). These compounds are species- and even strain-specific, which allows organisms to identify self, "friend", and "foe"- allowing for precise interactions between organisms within the biofilm (Davey & O'Toole, 2000). These QSM are utilized in almost every stage of biofilm formation but are especially important in the development of interactions between microbes in the biofilm. One prime example of interactions between biofilm-forming microbes and their QSM is the interactions of *C. albicans* with *P. aeruginosa* and *Streptococcus gordonii* (Hogan et al., 2004; Silverman et al., 2010). *Candida albicans* is known for producing the QSM farnesol, which has been studied for its multiple roles in the *C. albicans* lifestyle (Hornby et al., 2001). For instance, when *C. albicans* and *P. aeruginosa* are near one another, their respective QSM inhibit each other's growth. Farnesol will prevent *P. aeruginosa* from producing the toxic phenazine pyocyanin, which in turn reduces its virulence (Cugini et al., 2007). Simultaneously, *P. aeruginosa* produces its QSM called 3-oxo-C12-homoserine lactone, which represses filamentous growth in *C. albicans* reducing its biofilm forming abilities (Hogan et al., 2004). Alternatively, *S. gordonii* promotes the production of *C. albicans* hyphae and therefore biofilm development in the oral cavity (Bamford et al., 2009). This

phenomenon is believed to be regulated via secretion of Autoinducer 2 by *S. gordonii* indicating a different microbial interaction caused by similar chemical interactions (Bamford et al., 2009).

No QSM or other known interactive secondary metabolites have been identified in lichens so far, but it is likely that they utilize chemical signaling due to their well noted abundance of secondary metabolites. Even amongst eukaryotes QSMs are poorly understood. However, recent studies show that the alga *Chlorella sorokiniana* produces the auxin family of phytohormones (Khasin et al., 2018). Because this alga belongs to the same class as most lichen photobionts (Trebouxiophyaceae), this observation suggests a role for phytohormones in mediating mycobiont-photobiont interactions. Additionally, multiple studies implicate lichen-made secondary metabolites (e.g., usnic acid and evernic acid) in the prevention of unwanted bacterial growth in *Streptococcus spp.* and *P. aeruginosa* biofilms respectively (Gökalsın & Sesal, 2016; Nithyanand et al., 2015). These biofilm-reducing secondary metabolites resemble the role of farnesol in their capacity to disrupt bacterial biofilms. Since farnesol is a QSM capable of reducing biofilm formation in *P. aeruginosa* and other bacteria, it is not surprising that usnic acid and evernic acid are also capable of dispersing biofilms, and as such they may be later termed lichen QSM or, at the very least, communication molecules (Gökalsın & Sesal, 2016; Nithyanand et al., 2015).

During lichen partner recognition, lectin-mediated interactions between mycobionts and photobionts trigger either a compatibility or incompatibility reaction by the photobiont (Singh & Walia, 2014). Lectins, which are carbohydrate-binding proteins, are used frequently by pathogenic fungi, bacteria, and viruses to identify their hosts

(Rutishauser & Sachs, 1975). Certain lichens will only form between specific species of a mycobiont and a photobiont, while other partner interactions are much less specific, as some mycobionts can utilize more than one type of photobiont (Piercey-Normore & DePriest, 2001; Yahr et al., 2004). However, lectin recognition only occurs after the mycobiont has made physical contact with the potential photobiont. Other studies have shown that there may be some form of unknown chemical signaling occurring between the symbionts before physical contact is made (Meeßen & Ott, 2013). These chemical signals are photobiont-specific, in that when multiple photobiont supernatants were exposed to a single mycobiont each of the supernatants caused different growth forms of the mycobiont. Exposure to the correct photobiont's supernatant resulted in increased ECM production, increased hyphal growth, and increased hyphal branching, all important aspects of initial thallus development (Meeßen & Ott, 2013). Although this is only one example of pre-contact interactions between lichen symbionts, it is still strong evidence for the importance of chemical interactions in lichen development, which are analogous in biofilm development.

Insight into that unknown mechanism can be gained from interactions between plants and mycorrhizal fungi. Though mycorrhizal fungi-plant interactions are not generally thought of as biofilms, the manner in which ectomycorrhizal (or "sheathing") fungi attach and surround the roots of plants by use of an extracellular matrix strongly resembles biofilm formation (Fox, 1987; Harding et al., 2009). For mycorrhizal fungi to identify their plant host, the plant and mycorrhizal fungi secrete specific phytohormones, similar to that of QSM in fungal and bacterial biofilms (Felten et al., 2009). Plant phytohormones secreted by mycorrhizal fungi are typically auxins, and plants in turn

secrete strigolactones that the fungus may identify. After their chemical signals are exchanged, both organisms exhibit lateral growth towards the source of the chemical signal to locate their symbiont (Akiyama et al., 2005; Felten et al., 2009; Hanlon & Coenen, 2011; Sirrenberg et al., 2007).

Microbial interactions within biofilms and lichens are very complex in nature and inherently difficult to study. We still are lacking most information regarding how microbes interact within consortia. These few specific interactions represent only a fraction of what actually facilitates or regulates biofilms and lichens in their natural environments. Even amongst lichenologists, the nature of the lichen relationship is contested; it may be true symbiosis, or controlled parasitism (Ahmadjian & Jacobs, 1981; Richardson, 1999). To elucidate the complex relationships between microorganisms, researchers are moving towards systems-biology approaches to simultaneously probe the multi-species transcriptome (Kuske et al., 2015) and characterize their phylogenetic diversity in microbial communities (Herr et al., 2015; Hibbett et al., 2016). Subsequently, biologically important mechanisms can be deduced from those vast libraries of knowledge and utilized to perform specific experiments based on the information from the systems-level approaches. In order for microbial ecology and interactions to be resolved we must expand the use of these and other approaches.

Extracellular Matrix

Matrix Details from Biofilms and Lichens

One of the most important features of a biofilm is their extracellular polymeric substance or the extracellular matrix (Branda et al., 2005; Mitchell et al., 2016). In

biofilms, this matrix contains polysaccharides, proteins, nucleic acids, lipids, and secondary metabolites – all of which vary in composition due to the overall species diversity, abundance, and specific chemical interactions (Flemming & Wingender, 2010). The ECM is seen in the initial formation of the biofilm but is not fully formed until the biofilm reaches maturity. Not only is the ECM essential for maintenance of structural integrity, but it also plays a key role in resistance to abiotic stresses such as desiccation, as well as external stress caused by antimicrobial drugs or the human immune system (Flemming & Wingender, 2010). Although it has been established that inner layers of the ECM contain mostly hydrophilic polysaccharides that mediate desiccation resistance (Flemming & Wingender, 2010), they also possess outer hydrophobic layers to allow for hydrophobic substrate binding and prevent water loss from the hydrated inner structures of the ECM (Arnaouteli et al., 2016; Beauvais et al., 2007; Dague et al., 2008; Wösten, 2001). Additionally, the hydrophobicity of the substance the biofilm is attached to has been shown to alter the hydrophobicity of the outer matrix layer (Bruinsma et al., 2001). This allows biofilms to adapt to surfaces as they attach, allowing for both hydrophobic and hydrophilic attachments.

Our understanding of the ECM in lichens is largely confined to that which surrounds the cells. Additionally, the variable nomenclature for the lichen ECM, which ranges from regular “extracellular polymeric substance”, to the aptly named “gelatinous matrix”, and the structural term “conglutinate” (Ahmadjian & Jacobs, 1981; Honegger, 1993; Honegger & Haisch, 2001) has likely hindered attempts to understand its properties. However, with the help of two recent publications (Goodenough & Roth, 2020a, 2020b; Goodenough et al., 2021; Roth et al., 2020; Spribille et al., 2020) and

information on the lichen ECM scattered throughout the literature, we can construct a loose understanding of the structural composition and biological role of the ECM, that bears similarity to biofilm matrices. We know for certain that the lichen matrix contains a variety of polysaccharides (Spribille et al., 2020), crystalline secondary metabolites such as usnic acid, and proteins; and that parts of the lichen thallus' ECM are surrounded in a hydrophobic outer layer (Goodenough & Roth, 2020a; Honegger, 1982; Honegger & Haisch, 2001; Scherrer et al., 2000). This composition is therefore extremely similar to the extracellular matrix of biofilms (Harding et al., 2009; Mitchell et al., 2016).

Another feature of the biofilm matrix is the presence of external DNA, which promotes horizontal gene transfer between the biofilm members (Antonova & Hammer, 2011; Flemming & Wingender, 2010; Lebeaux et al., 2014; Roberts et al., 1999). Although the presence of external DNA in the lichen ECM remains untested, multiple horizontal gene transfer events have been observed within various lichens (Armaleo et al., 2019; Beck et al., 2015; Carniel et al., 2016; McDonald et al., 2012). In particular, the lichen *Xanthoria parietina*'s genome harbors three genes that were likely transferred from the mycobiont to the photobiont several millions of years ago (Beck et al., 2015). Phylogenetic analysis suggests that this transfer preceded the origins of the lichen symbiosis, which implies that fungi and algae have a long history of intimate interactions (Beck et al., 2015; Lutzoni et al., 2018). Accordingly, it is tempting to speculate that such "proto-lichens" might have existed within a protective biofilm-like matrix that facilitated interactions and enabled gene transfer.

Currently, the matrix-containing components of lichens have been isolated to the upper and lower cortices which are called "conglutinate zones" (Honegger, 1992). The

lower cortex allows for attachment to the substrate, and the upper cortex controls the transfer of liquids and gases and provides environmental protection. The isolation of the lichen matrix to these two zones is not confirmed, and it is likely that a variety of matrix layers coat all of the lichen cells based on the images captured by Honegger & Haisch (2001) and Roth et al. (2020). Biofilms are completely coated by their ECM, which implies that lichens would presumably also have a complete coating of matrix material, instead of ECM isolated to specific layers. The similarities between lichen and biofilm matrices detailed above suggest lichens do indeed have an extracellular matrix analogous to biofilms, which is vital to the persistence of these communities within the extreme environments they typically inhabit. The successful lifestyles of lichens and biofilms are undoubtedly dependent upon the ability of the matrix to contain water, mediate environmental resistance, and promote cell-cell adhesion.

Closer Look at the Matrices of the Filamentous Fungus Aspergillus fumigatus and the Lichen Cetraria islandica

Studies have focused on the filamentous fungus *Aspergillus fumigatus*, a human pathogen, regarding its biofilm-forming capabilities (Beauvais et al., 2007; Mowat et al., 2009). These studies have concluded that *A. fumigatus* is indeed capable of forming an extracellular matrix and therefore is also capable of forming a biofilm. The matrix of *A. fumigatus* contains polysaccharides (particularly galactomannan and α-1,3-glucans), monosaccharides and polyols, secondary metabolites (like melanin), as well as proteins (Beauvais et al., 2007). One of the most intriguing findings from Beauvis et al. (2007) was the location of α-1,3-glucans within the extracellular matrix. Via immunogold

labeling, they identified α-1,3-glucans in the matrix and right on the outer edge of the cell wall, but not within the cell wall.

Similarly, Honegger and Haisch (2001) observed the β-1,3-glucan lichenin in the lichen *Cetraria islandica* in the same locations as *A. fumigatus*. In both studies, polysaccharides were only located in the extracellular matrix and not in the cell wall, where fungal glucans are also known to be located. In addition, both authors commented on the location of hydrophobic versus hydrophilic substances and proteins in relation to the cell wall and matrix. In *A. fumigatus*, hydrophobin proteins were said to be located within the matrix but with no further details on localization mentioned. Whereas, in *C. islandica* it was noted that the matrix itself was hydrophilic with a thin hydrophobic proteinaceous outer layer (Beauvais et al., 2007; Honegger & Haisch, 2001) (**Figure 4**). The thin hydrophobic layer is thought to allow photosynthesis to continue when the lichen is wetted and the extracellular matrix is expanded (Honegger & Haisch, 2001). Without the hydrophobic layer the photobiont would be incapable of gas exchange, and therefore photosynthesis (**Figure 5**). If there are indeed differences between the matrices, they are likely influenced by the differences in life-history of these two different entities. Lichens exist in xeric conditions with quickly fluctuating periods of wetting and drying, whereas *A. fumigatus* is found in the misty environment of the lungs. In both cases, the presence of the glucans in their extracellular matrix is likely to facilitate the agglutination of the fungal cells to form a lichen thallus or a biofilm.

Resistances to Environmental Stressors

Environmental Stress Resistance of Biofilms and Lichens

An evolutionarily selected for trait of the biofilm lifestyle is an increase in resistance to a variety of stressors (Stewart & Costerton, 2001). This key feature is frequently used to test whether an organism is biofilm-forming, and whether knocking-out a key gene affects biofilm formation in certain species (Lewis, 2001; Mah & O'Toole, 2001). All biofilms that have been studied so far are noted to have multiple environmental resistances that include antimicrobial drug resistance, ultraviolet (UV) radiation, metal toxicity, osmotic shock resistance, desiccation resistance, and pH shift resistance (Davey & O'Toole, 2000; Flemming, 1993). Lichens share this multi-resistance phenotype with biofilms, and numerous studies have been performed to understand lichen resistances to various abiotic stresses. Most notably, lichens are known to be resistant to UV radiation, metal ion toxicity, desiccation, and extreme temperatures simultaneously (Meeßen et al., 2013). As an example of this extreme multi-resistance, the survivability of the lichen *Xanthoria elegans* was tested in the exposed vacuum of space for 1.5 years (Onofri et al., 2012; Sancho et al., 2007). These experiments revealed that *X. elegans* survives the vacuum of space by exploiting its poikilohydric lifestyle to shut down metabolism while in extreme xeric conditions and restarting metabolism when humidity levels were optimal upon their return. Although a complete understanding of the variety of resistance factors is far from being understood, it is clear that one of the main contributors to abiotic resistance is their ECM coating (Baillie & Douglas, 2000; Gilbert et al., 1997). How important the matrix is, and other factors that may be involved in resistance mechanisms varies between environmental stressors, so taking a closer look at each external factor, the cause of resistances, and the shared themes between lichens and biofilms will be explored here.

Metal Toxicity Resistance

Lichens have long been recognized as biomonitors for their ability to absorb multiple types of pollutants such as heavy metals and atmospheric pollutants like sulfuric and nitrous oxides (SOX and NOX) (Sarret et al., 1998; Skye, 1979; Szczepaniak & Biziuk, 2003). Consequently, lichens have been used to identify common air pollutants in some cities as lichen distribution patterns and extracted compounds may serve as an indicator of air quality (Skye, 1979). Unlike metal resistance mechanisms of some bacteria, the ability of lichens to resist metals is not a result of changing the chemical state of the metal. Instead, lichens typically sequester the metal ions into their cellular structures (Ekmekyapar et al., 2006; Gadd, 2010; Honegger, 2009). Metal ions are known to adhere to the chitinous cell wall of most fungi, but especially lichen forming fungi. Lichens are even recognized for the coloration that results from the sequestering of metals onto their thallus (Honegger, 2009). This makes lichens and other fungi prime candidates for bioremediation since they absorb metal ions from their surroundings instead of merely changing the state of the metal ions. Alternative forms of metal resistance in lichens include binding of metal to intracellular spaces of hyphal filaments (likely the matrix), binding of metals to metallothioneins (small cysteine proteins), and complexing of metal ions to organic acids produced by lichens such as oxalate and evernic acid (Sarret et al., 1998). Each of these methods allow lichens to be hyper-resistant to harmful metals.

Biofilms are also recognized for the ability to sequester metal ions (Huang et al., 2000; Teitzel & Parsek, 2003). Metal ions typically adhere to the ECM of biofilms,

instead of the cells themselves, which protects the microbes from metal toxicity (Kazy et al., 2002). Additional methods of metal resistance in biofilms include: siderophore production, persister cells, metal metabolic processes (found in specific bacteria), and overall reduced metabolic processing (Harrison et al., 2007). Multi-metal resistance capabilities of biofilms have also led researchers to investigate their bioremediation capabilities, even utilizing biofilms in water purification techniques (Uluozlu et al., 2008). The capacity for both lichens and biofilms to resist metal toxicity shows their capability to survive in more hash environments than most planktonic microbes. Through their microbial community they are more resistant together than they are as individual cells.

UV & Desiccation Resistance

Resistance to UV radiation and desiccation are crucial for sun-exposed microbes. For example, living on a rock or tree leads to intense UV along with dramatic daily and seasonal shifts in water activity. The properties of biofilms and lichens suggest that they might play a key role in mitigating the impacts of these stresses. Ultraviolet light radiation is recognized for its ability to cause DNA damage (Matsumura & Ananthaswamy, 2004) such as misincorporation of nucleotides during transcription and translation, direct oxidative damage, or nucleotide modification such as thymine-thymine dimers (Rastogi et al., 2010). While low levels of UV radiation are easily repaired by normal DNA repair mechanisms, surface dwelling microorganisms are subjected to higher levels of UV (Rastogi et al., 2010). Alternative mechanisms of UV radiation resistance rely on the initial blocking of UV exposure, typically via secondary

metabolites such as carotenoids, melanin, and other UV-absorbing compounds (Matsumura & Ananthaswamy, 2004).

Lichens are well-known for their UV resistance capabilities. They are some of the only organisms that can grow in extreme UV conditions such as the arctic poles, on mountains, and desert conditions (Solhaug et al., 2003). Furthermore, when lichens are exposed to peak UV radiation at midday, they are also typically in a desiccated state which halts all cellular processes to prevent death by desiccation, a process attributed to their poikilohydric lifestyle (Nybakken et al., 2004). This means lichens are incapable of performing DNA-repair while desiccated and exposed to high amounts of UV radiation, therefore, they have evolved alternative UV resistance measures. Lichens utilize their capability to produce extensive amounts and types of secondary metabolites as their main source of defense against UV radiation. Numerous compounds produced by lichens that are resistant to UV radiation include melanin, carotenoids, usnic acid, parietin, polyketides, and other secondary metabolites which are all mycobiont-sourced, whereas mycosporin is one of the only UV resistant compounds that is only produced by cyanobacteria in cyanolichens (Nguyen et al., 2013). These compounds are typically bound to the fungal cell walls of the mycobiont, particularly in the upper cortex and medullary layers, where exposure to UV radiation is the highest (Mcevoy et al., 2006). Whether the mycobiont partner can create an array of UV protectant compounds when grown in isolation has not yet been studied. However, it seems likely that the UV protective nature of secondary compounds produced by the mycobiont would have been selective for the photobiont to form a lichen symbiosis.

Biofilm resistance to UV radiation is mainly dependent on the capability of the extracellular matrix to block UV from penetrating far through the biofilm. Researchers previously determined that *P. aeruginosa* extracellular matrices have a very strong capacity to block UV exposure, only allowing 13% UV-C, 31% UV-B, and 33% of UV-A to penetrate the matrix, with UV-C being the most harmful (Elasri & Miller, 1999). Most microbial biofilms surveyed to date rely primarily on DNA repair mechanisms in addition to their matrix to resist UV-induced damage (Fernández Zenoff et al., 2006). To date, the mechanism underlying UV absorptive properties of the ECM remain unknown, but the presence of copious polysaccharides is thought to play a role (Elasri & Miller, 1999). In addition, it would not be surprising to find secondary metabolites within the biofilm matrix that contribute to UV resistance like that in lichens. Additionally, one of the most successful ways for a microbial biofilm to resist UV damage is to incorporate already extremely UV resistant microbes, into their matrix, as observed in biofilms that formed on the Chernobyl nuclear reactor cooling towers (Ragon et al., 2011). These biofilms contain melanized fungi, as well as bacterial and fungal species that are known to be radiation resistant, and even non-UV resistant microbes such as *S. cerevisiae* (Ragon et al., 2011). This observation suggests that microbes that possess only "standard" UV resistance mechanisms can survive high levels of UV radiation by co-inhabiting in biofilms with UV resistant organisms.

Desiccation resistance in biofilms and lichens largely stem from their ECM. In both communities the ability to resist desiccation is attributed to their thick extracellular matrix, which can hold water within their excess of hygroscopic polysaccharides (Kranner et al., 2008; Ophir & Gutnick, 1994). In biofilms formed by *P. aeruginosa* and

other Pseudomonads, it has been determined that the polysaccharide alginate located in the extracellular matrix is the main contributor of desiccation resistance (Chang et al., 2007). Within lichens, many polysaccharides have been identified all of which are noted to have hygroscopic tendencies that aid in desiccation resistance (Honegger & Haisch, 2001; Spribille et al., 2020). However, additional desiccation resistance in lichens can be attributed to the outer layer of hydrophobic proteins on the outside of the extracellular matrix, possibly acting like the cuticle of plant leaves (Honegger & Haisch, 2001; Scherrer et al., 2000). This allows the water to be maintained within the matrix reducing evaporation through the matrix. This additional layer contributes a higher degree of desiccation resistance in lichens which is vital to the specific niche they hold amongst the surface-attached microbes.

Concluding Remarks

An abundance of similarities between lichens and microbial biofilms allow us to make many connections between the two consortia. The stages of their development both follow a regimented progression with surface adherence as the first stage, cell morphological transition in the second stage, stratification of cell types in the third stage, and dispersal of cells as the final stage. Both position their cells in ways that allow for proper gas and water exchange, either through interstitial voids or the medullary thalline layer. Similar protein types are used for cell-surface adherence and cell-cell adherence. Quorum sensing molecules and lectins provide biofilms and lichen-related organisms the ability to identify the microbes around them, allowing for specific positive and negative interactions such as syntrophy and competition. Additionally, they both contain an

extracellular matrix which is essential to their cohesion and stress resistance to various environmental factors. Understanding of these attributes has been arguably more researched in biofilm literature. Thus, providing lichenologists a potential starting point when identifying cellular processes for these features.

With this starting point, further identification of specialized properties of lichens can be elucidated. Are quorum sensing molecules important in mycobiont-photobiont interactions? What triggers mycobiont cells undergo cell differentiation to begin stratification of the thallus? How extensive is the extracellular matrix in lichens, and what does it specifically contain? Finally, one of the most sought-after questions of lichenologists, how did lichens come to exist and evolve? Similarities between lichens and biofilms listed here in our review point to the concept that lichens likely started out as a biofilm, then over millions of years of co-evolution between the partners they formed the unique structure that we know of as the lichen. These questions and many others can be extrapolated from focusing on the cellular processes within biofilms and determining how they may overlap with lichens.

Acknowledgements

Funding for this work was provided by NASA (grant number 80NSSC17K0737). We would like to thank Ursula Goodenough and Toby Spribille for helpful communications, edits early on, and for providing unpublished manuscripts related to this work, and Kristi Montooth and Etsuko Moriyama for their useful insight into early versions of this manuscript. Additional thanks to Sean Carr for idea-bouncing as well as intellectual and emotional support.

References

Ahmadjian, V. (1962). Investigations on lichen synthesis. *American Journal of Botany*, *49*(3), 277-283.

Ahmadjian, V. (1966). Artificial Reestablishment of the Lichen Cladonia cristatella. *Science*, *151*(3707), 199-201. https://doi.org/10.1126/science.151.3707.199

Ahmadjian, V., & Jacobs, J. B. (1981). Relationship between fungus and alga in the lichen Cladonia cristatella Tuck. *Nature*, *289*(5794), 169-172. https://doi.org/10.1038/289169a0

Akiyama, K., Matsuzaki, K., & Hayashi, H. (2005). Plant sesquiterpenes induce hyphal branching in arbuscular mycorrhizal fungi. *Nature*, *435*(7043), 824-827. https://doi.org/10.1038/nature03608

Andes, D., Nett, J., Oschel, P., Albrecht, R., Marchillo, K., & Pitula, A. (2004). Development and characterization of an in vivo central venous catheter Candida albicans biofilm model. *Infect Immun*, *72*(10), 6023-6031. https://doi.org/10.1128/IAI.72.10.6023-6031.2004

Antonova, E. S., & Hammer, B. K. (2011). Quorum-sensing autoinducer molecules produced by members of a multispecies biofilm promote horizontal gene transfer to Vibrio cholerae. *FEMS Microbiol Lett*, *322*(1), 68-76. https://doi.org/10.1111/j.1574-6968.2011.02328.x

Armaleo, D. (1991). Experimental microbiology of lichens: mycelia fragmentation, a novel growth chamber, and the origins of thallus differentiation. *Symbiosis*.

Armaleo, D., Müller, O., Lutzoni, F., Andrésson, Ó. S., Blanc, G., Bode, H. B., . . . Xavier, B. B. (2019). The lichen symbiosis re-viewed through the genomes of

Cladonia grayi and its algal partner Asterochloris glomerata. *BMC Genomics*, *20*(1), 605. https://doi.org/10.1186/s12864-019-5629-x

Armstrong, R. A., & Bradwell, T. (2011). Growth of foliose lichens: A review. *Symbiosis*, *53*(1), 1-16. https://doi.org/10.1007/s13199-011-0108-4

Arnaouteli, S., MacPhee, C. E., & Stanley-Wall, N. R. (2016). Just in case it rains: building a hydrophobic biofilm the Bacillus subtilis way. *Curr Opin Microbiol*, *34*, 7-12. https://doi.org/10.1016/j.mib.2016.07.012

Baillie, G. S., & Douglas, J. L. (1999). Role of dimorphism in the development of Candida albicans biofilms. *Journal of Medical Microbiology*, *48*(7), 671-679. https://doi.org/10.1099/00222615-48-7-671

Baillie, G. S., & Douglas, L. J. (2000). Matrix polymers of Candida biofilms and their possible role in biofilm resistance to antifungal agents. *J Antimicrob Chemother*, *46*(3), 397-403. https://doi.org/10.1093/jac/46.3.397

Bamford, C. V., d'Mello, A., Nobbs, A. H., Dutton, L. C., Vickerman, M. M., & Jenkinson, H. F. (2009). Streptococcus gordonii modulates Candida albicans biofilm formation through intergeneric communication. *Infect Immun*, *77*(9), 3696-3704. https://doi.org/10.1128/IAI.00438-09

Barelle, C. J., Richard, M. L., Gaillardin, C., Gow, N. A., & Brown, A. J. (2006). Candida albicans VAC8 is required for vacuolar inheritance and normal hyphal branching. *Eukaryot Cell*, *5*(2), 359-367. https://doi.org/10.1128/EC.5.2.359-367.2006

Beauvais, A., Schmidt, C., Guadagnini, S., Roux, P., Perret, E., Henry, C., . . . Latgé, J. P. (2007). An extracellular matrix glues together the aerial-grown hyphae of

Aspergillus fumigatus. *Cellular Microbiology*, *9*(6), 1588-1600. https://doi.org/10.1111/j.1462-5822.2007.00895.x

Beck, A., Divakar, P. K., Zhang, N., Molina, M. C., & Struwe, L. (2015). Evidence of ancient horizontal gene transfer between fungi and the terrestrial alga Trebouxia. *Organisms Diversity & Evolution*, *15*(2), 235-248. https://doi.org/10.1007/s13127-014-0199-x

Blaha, J., Baloch, E., & Grube, M. (2006). High photobiont diversity associated with the euryoecious lichen-forming ascomycete Lecanora rupicola (Lecanoraceae, Ascomycota). *Biological Journal of the Linnean Society*, *88*(2), 283-293. https://doi.org/10.1111/j.1095-8312.2006.00640.x

Blankenship, J. R., & Mitchell, A. P. (2006). How to build a biofilm: a fungal perspective. *Current Opinion in Microbiology*, *9*(6), 588-594. https://doi.org/10.1016/j.mib.2006.10.003

Branda, S. S., Vik, Å., Friedman, L., & Kolter, R. (2005). Biofilms: The matrix revisited. *Trends in Microbiology*, *13*(1), 20-26. https://doi.org/10.1016/j.tim.2004.11.006

Bruinsma, G. M., van der Mei, H. C., & Busscher, H. J. (2001). Bacterial adhesion to surface hydrophilic and hydrophobic contact lenses. *Biomaterials*, *22*(24), 3217-3224. https://doi.org/10.1016/s0142-9612(01)00159-4

Burmølle, M., Ren, D., Bjarnsholt, T., & Sørensen, S. J. (2014). Interactions in multispecies biofilms: do they actually matter? *Trends Microbiol*, *22*(2), 84-91. https://doi.org/10.1016/j.tim.2013.12.004

Cardinale, M., Vieira De Castro Jr, J., Müller, H., Berg, G., & Grube, M. (2008). In situ analysis of the bacterial community associated with the reindeer lichen Cladonia

arbuscula reveals predominance of Alphaproteobacteria. *FEMS Microbiology Ecology*, *66*(1), 63-71. https://doi.org/10.1111/j.1574-6941.2008.00546.x

Carniel, F. C., Gerdol, M., Montagner, A., Banchi, E., De Moro, G., Manfrin, C., . . . Tretiach, M. (2016). New features of desiccation tolerance in the lichen photobiont Trebouxia gelatinosa are revealed by a transcriptomic approach. *Plant Mol Biol*, *91*(3), 319-339. https://doi.org/10.1007/s11103-016-0468-5

Chang, W. S., van de Mortel, M., Nielsen, L., Nino de Guzman, G., Li, X., & Halverson, L. J. (2007). Alginate production by Pseudomonas putida creates a hydrated microenvironment and contributes to biofilm architecture and stress tolerance under water-limiting conditions. *J Bacteriol*, *189*(22), 8290-8299. https://doi.org/10.1128/JB.00727-07

Clayden, S. R. (1998). Thallus initiation and development in the lichen Rhizocarpon lecanorinum. *New Phytologist*, *139*(4), 685-695. https://doi.org/10.1046/j.1469-8137.1998.00243.x

Cubero, O. F., Crespo, A., Fatehi, J., & Bridge, P. D. (1999). DNA extraction and PCR amplification method suitable for fresh, herbarium-stored, lichenized, and other fungi. *Plant Systematics and Evolution*, *216*(3), 243-249.

Cugini, C., Calfee, M. W., Farrow, J. M., Morales, D. K., Pesci, E. C., & Hogan, D. A. (2007). Farnesol, a common sesquiterpene, inhibits PQS production in Pseudomonas aeruginosa. *Mol Microbiol*, *65*(4), 896-906. https://doi.org/10.1111/j.1365-2958.2007.05840.x

Dague, E., Alsteens, D., Latgé, J. P., & Dufrêne, Y. F. (2008). High-resolution cell surface dynamics of germinating Aspergillus fumigatus conidia. *Biophysical Journal*, *94*(2), 656-660. https://doi.org/10.1529/biophysj.107.116491

Davey, M. E., & O'Toole, G. A. (2000). Microbial biofilms: From ecology to molecular genetics. *Microbiology and Molecular Biology Reviews*, *64*(4), 847-867. https://doi.org/10.1128/MMBR.64.4.847-867.2000

Davies, D. G., Parsek, M. R., Pearson, J. P., Iglewski, B. H., Costerton, J. W., & Greenberg, E. P. (1998). The involvement of cell-to-cell signals in the development of a bacterial biofilm. *Science*, *280*(5361), 295-298. https://doi.org/10.1126/science.280.5361.295

del Carmen Molina, M., & Crespo, A. (2000). Comparison of development of axenic cultures of five species of lichen-forming fungi. *Mycological Research*, *104*(5), 595-602.

Dettki, H., Klintberg, P., & Esseen, P.-A. (2000). Are epiphytic lichens in young forests limited by local dispersal? *Ecoscience*, *7*(3), 317-325.

Donlan, R. M. (2002). Biofilms: Microbial life on surfaces. *Emerging Infectious Diseases*, *8*(9), 881-890. https://doi.org/10.3201/eid0809.020063

Donlan, R. M., & Costerton, J. W. (2002). Biofilms: survival mechanisms of clinically relevant microorganisms. *Clinical microbiology reviews*, *15*(2), 167-193.

Dynesen, J., & Nielsen, J. (2003). Surface hydrophobicity of Aspergillus nidulans conidiospores and its role in pellet formation. *Biotechnology Progress*, *19*(3), 1049-1052. https://doi.org/10.1021/bp0340032

Ekmekyapar, F., Aslan, A., Bayhan, Y. K., & Cakici, A. (2006). Biosorption of copper(II) by nonliving lichen biomass of Cladonia rangiformis hoffm. *J Hazard Mater*, *137*(1), 293-298. https://doi.org/10.1016/j.jhazmat.2006.02.003

Elasri, M. O., & Miller, R. V. (1999). Study of the response of a biofilm bacterial community to UV radiation. *Appl Environ Microbiol*, *65*(5), 2025-2031. https://doi.org/10.1128/AEM.65.5.2025-2031.1999

Ene, I. V., & Bennett, R. J. (2009). Hwp1 and related adhesins contribute to both mating and biofilm formation in Candida albicans. *Eukaryot Cell*, *8*(12), 1909-1913. https://doi.org/10.1128/EC.00245-09

Fanning, S., & Mitchell, A. P. (2012). Fungal biofilms. *PLoS pathogens*, *8*(4). https://doi.org/10.1371/journal.ppat.1002585

Felten, J., Kohler, A., Morin, E., Bhalerao, R. P., Palme, K., Martin, F., . . . Legué, V. (2009). The ectomycorrhizal fungus Laccaria bicolor stimulates lateral root formation in poplar and Arabidopsis through auxin transport and signaling. *Plant Physiol*, *151*(4), 1991-2005. https://doi.org/10.1104/pp.109.147231

Fernández Zenoff, V., Siñeriz, F., & Farías, M. E. (2006). Diverse responses to UV-B radiation and repair mechanisms of bacteria isolated from high-altitude aquatic environments. *Appl Environ Microbiol*, *72*(12), 7857-7863. https://doi.org/10.1128/AEM.01333-06

Finkel, J. S., & Mitchell, A. P. (2011). Genetic control of Candida albicans biofilm development. *Nature Reviews Microbiology*, *9*(2), 109-118. https://doi.org/10.1038/nrmicro2475

Flemming, H.-C. (1993). Biofilms and environmental protection. *Water Science and Technology*, *27*(7-8), 1-10.

Flemming, H.-C., & Wingender, J. (2010). The biofilm matrix. *Nature reviews microbiology*, *8*(9), 623-633.

Fox, F. M. (1987). Ultrastructure of mycelial strands of Leccinum scabrum, ectomycorrhizal on birch (Betula spp.). *Transactions of the British Mycological Society*, *89*(4), 551-560.

Friedman, L., & Kolter, R. (2004). Genes involved in matrix formation in Pseudomonas aeruginosa PA14 biofilms. *Molecular Microbiology*, *51*(3), 675-690. https://doi.org/10.1046/j.1365-2958.2003.03877.x

Gadd, G. M. (2010). Metals, minerals and microbes: geomicrobiology and bioremediation. *Microbiology (Reading)*, *156*(Pt 3), 609-643. https://doi.org/10.1099/mic.0.037143-0

Galun, M., & Bubrick, P. (1984). Physiological Interactions Between the Partners of the Lichen Symbiosis. *In Cellular interactions (Pp. 362–401)*.

Gargas, A., DePriest, P. T., Grube, M., & Tehler, A. (1995). Multiple origins of lichen symbioses in fungi suggested by SSU rDNA phylogeny. *Science*, *268*(5216), 1492-1495. https://doi.org/10.1126/science.7770775

Gilbert, P., Das, J., & Foley, I. (1997). Biofilm susceptibility to antimicrobials. *Adv Dent Res*, *11*(1), 160-167. https://doi.org/10.1177/08959374970110010701

Girardin, H., Paris, S., Rault, J., Bellon-Fontaine, M. N., & Latgé, J. P. (1999). The role of the rodlet structure on the physicochemical properties of Aspergillus conidia.

Letters in Applied Microbiology, *29*(6), 364-369. https://doi.org/10.1046/j.1472-765X.1999.00643.x

González-Ramírez, A. I., Ramírez-Granillo, A., Medina-Canales, M. G., Rodríguez-Tovar, A. V., & Martínez-Rivera, M. A. (2016). Analysis and description of the stages of Aspergillus fumigatus biofilm formation using scanning electron microscopy. *BMC Microbiology*, *16*(1), Article 243. https://doi.org/10.1186/s12866-016-0859-4

Goodenough, U., & Roth, R. (2020a). Lichen 2: constituents. *Algal Res.*

Goodenough, U., & Roth, R. (2020b). Lichen 5: medullary and bacterial biofilms. *Algal Res.*

Goodenough, U., Wagner, R., & Roth, R. (2021). Lichen 4. The Algal Layer. *Algal Research*, *58*, 102355.

Gravelat, F. N., Beauvais, A., Liu, H., Lee, M. J., Snarr, B. D., Chen, D., . . . Sheppard, D. C. (2013). Aspergillus Galactosaminogalactan Mediates Adherence to Host Constituents and Conceals Hyphal β-Glucan from the Immune System. *PLoS Pathogens*, *9*(8), Article e1003575. https://doi.org/10.1371/journal.ppat.1003575

Grube, M., & Berg, G. (2009). Microbial consortia of bacteria and fungi with focus on the lichen symbiosis. *Fungal Biology Reviews*, *23*(3), 72-85. https://doi.org/10.1016/j.fbr.2009.10.001

Grube, M., Cardinale, M., de Castro, J. V., Müller, H., & Berg, G. (2009). Species-specific structural and functional diversity of bacterial communities in lichen symbioses. *ISME J*, *3*(9), 1105-1115. https://doi.org/10.1038/ismej.2009.63

Grube, M., Cernava, T., Soh, J., Fuchs, S., Aschenbrenner, I., Lassek, C., . . . Berg, G. (2015). Exploring functional contexts of symbiotic sustain within lichen-associated bacteria by comparative omics. *ISME Journal*, *9*(2), 412-424. https://doi.org/10.1038/ismej.2014.138

Gökalsın, B., & Sesal, N. C. (2016). Lichen secondary metabolite evernic acid as potential quorum sensing inhibitor against Pseudomonas aeruginosa. *World J Microbiol Biotechnol*, *32*(9), 150. https://doi.org/10.1007/s11274-016-2105-5

Hale, M. E. (1959). Studies on lichen growth rate and succession. *Bulletin of the Torrey Botanical Club*, *86*(2), 126-129.

Hall-Stoodley, L., Costerton, J. W., & Stoodley, P. (2004). Bacterial biofilms: from the Natural environment to infectious diseases. *Nature Reviews Microbiology*, *2*(2), 95-108. https://doi.org/10.1038/nrmicro821

Hanlon, M. T., & Coenen, C. (2011). Genetic evidence for auxin involvement in arbuscular mycorrhiza initiation. *New Phytol*, *189*(3), 701-709. https://doi.org/10.1111/j.1469-8137.2010.03567.x

Harding, M. W., Marques, L. L., Howard, R. J., & Olson, M. E. (2009). Can filamentous fungi form biofilms? *Trends Microbiol*, *17*(11), 475-480. https://doi.org/10.1016/j.tim.2009.08.007

Harris, S. D. (2008). Branching of fungal hyphae: regulation, mechanisms and comparison with other branching systems. *Mycologia*, *100*(6), 823-832. https://doi.org/10.3852/08-177

Harrison, J. J., Ceri, H., & Turner, R. J. (2007). Multimetal resistance and tolerance in microbial biofilms. *Nat Rev Microbiol*, *5*(12), 928-938. https://doi.org/10.1038/nrmicro1774

Henskens, F. L., Green, T. G., & Wilkins, A. (2012). Cyanolichens can have both cyanobacteria and green algae in a common layer as major contributors to photosynthesis. *Annals of botany*, *110*(3), 555-563. https://doi.org/10.1093/aob/mcs108

Herr, J. R., Opik, M., & Hibbett, D. S. (2015). Towards the unification of sequence-based classification and sequence-based identification of host-associated microorganisms. *New Phytol*, *205*(1), 27-31. https://doi.org/10.1111/nph.13180

Hibbett, D., Abarenkov, K., Kõljalg, U., Öpik, M., Chai, B., Cole, J., . . . Geiser, D. M. (2016). Sequence-based classification and identification of Fungi. *Mycologia*, *108*(6), 1049-1068. https://doi.org/10.3852/16-130

Hodkinson, B. P., & Lutzoni, F. (2009). A microbiotic survey of lichen-associated bacteria reveals a new lineage from the Rhizobiales. *Symbiosis*, *49*(3), 163-180. https://doi.org/10.1007/s13199-009-0049-3

Hogan, D. A., Vik, A., & Kolter, R. (2004). A Pseudomonas aeruginosa quorum-sensing molecule influences Candida albicans morphology. *Mol Microbiol*, *54*(5), 1212-1223. https://doi.org/10.1111/j.1365-2958.2004.04349.x

Honegger, R. (1982). Cytological aspects of the triple symbiosis in Peltigera aphthosa. *J. Hattori Bot. Lab.*, *52*, 379-391.

Honegger, R. (1984). Cytological Aspects of the Mycobiont-Phycobiont Relationship in Lichens. *The Lichenologist*, *16*(2), 111-127. https://doi.org/10.1017/S0024282984000293

Honegger, R. (1991). Functional aspects of the lichen symbiosis. *Annual review of plant biology*, *42*(1), 553-578.

Honegger, R. (1992). Lichens: Mycobiont-photobiont relationships. *Algae and Symbioses*, 255-275.

Honegger, R. (1993). Developmental biology of lichens. *New Phytologist*, *125*(4), 659-677. https://doi.org/10.1111/j.1469-8137.1993.tb03916.x

Honegger, R. (1997). Metabolic interactions at the mycobiont-photobiont interface in lichens. In *Plant relationships* (pp. 209-221). Springer.

Honegger, R. (2000). Simon Schwendener (1829-1919) and the dual hypothesis of lichens. *Bryologist*, *103*(2), 307-313. https://doi.org/10.1639/0007-2745(2000)103[0307:SSATDH]2.0.CO;2

Honegger, R. (2009). Lichen-forming fungi and their photobionts. *Plant Relationships*, 307-333.

Honegger, R. (2012). 15 The Symbiotic Phenotype of Lichen-Forming Ascomycetes and Their Endo-and Epibionts. In *Fungal associations* (pp. 287-339). Springer.

Honegger, R., & Haisch, A. (2001). Immunocytochemical location of the (1→ 3)(1→ 4)-β-glucan lichenin in the lichen-forming ascomycete Cetraria islandica (Icelandic moss). *New phytologist*, *150*(3), 739-746.

Hornby, J. M., Jensen, E. C., Lisec, A. D., Tasto, J. J., Jahnke, B., Shoemaker, R., . . . Nickerson, K. W. (2001). Quorum Sensing in the Dimorphic Fungus Candida

albicans Is Mediated by Farnesol. *Applied and Environmental Microbiology*, *67*(7), 2982-2992. https://doi.org/10.1128/AEM.67.7.2982-2992.2001

Huang, Y. B., Wang, W. H., & Peng, A. (2000). Accumulation of Cu (II) and Pb (II) by biofilms grown on particulate in aquatic systems. *Journal of Environmental Science & Health Part A*, *35*(4), 575-592.

Hunt, S. M., Werner, E. M., Huang, B., Hamilton, M. A., & Stewart, P. S. (2004). Hypothesis for the Role of Nutrient Starvation in Biofilm Detachment. *Applied and Environmental Microbiology*, *70*(12), 7418-7425. https://doi.org/10.1128/aem.70.12.7418-7425.2004

Inoue, K., Kitaoka, H., Park, P., & Ikeda, K. (2016). Novel aspects of hydrophobins in wheat isolate of Magnaporthe oryzae: Mpg1, but not Mhp1, is essential for adhesion and pathogenicity. *Journal of General Plant Pathology*, *82*(1), 18-28. https://doi.org/10.1007/s10327-015-0632-9

Jabra-Rizk, M. A., Shirtliff, M., James, C., & Meiller, T. (2006). Effect of farnesol on Candida dubliniensis biofilm formation and fluconazole resistance. *FEMS Yeast Research*, *6*(7), 1063-1073. https://doi.org/10.1111/j.1567-1364.2006.00121.x

Jacobs, J. B., & Ahmadjian, V. (1969). THE ULTRASTRUCTURE OF LICHENS. I. A GENERAL SURVEY. *Journal of Phycology*, *5*(3), 227-240. https://doi.org/10.1111/j.1529-8817.1969.tb02608.x

Joneson, S., Armaleo, D., & Lutzoni, F. (2011). Fungal and algal gene expression in early developmental stages of lichen-symbiosis. *Mycologia*, *103*(2), 291-306. https://doi.org/10.3852/10-064

Joneson, S., & Lutzoni, F. (2009). Compatibility and thigmotropism in the lichen symbiosis: A reappraisal. *Symbiosis*, *47*(2), 109-115. https://doi.org/10.1007/bf03182294

Junttila, S., & Rudd, S. (2012). Characterization of a transcriptome from a non-model organism, Cladonia rangiferina, the grey reindeer lichen, using high-throughput next generation sequencing and EST sequence data. *BMC Genomics*, *13*(1), Article 575. https://doi.org/10.1186/1471-2164-13-575

Kaplan, J. B. (2010). Biofilm dispersal: mechanisms, clinical implications, and potential therapeutic uses. *J Dent Res*, *89*(3), 205-218. https://doi.org/10.1177/0022034509359403

Kazy, S. K., Sar, P., Singh, S. P., Sen, A. K., & D'Souza, S. F. (2002). *World Journal of Microbiology and Biotechnology*, *18*(6), 583-588. https://doi.org/10.1023/a:1016354713289

Keller, L., & Surette, M. G. (2006). Communication in bacteria: an ecological and evolutionary perspective. *Nat Rev Microbiol*, *4*(4), 249-258. https://doi.org/10.1038/nrmicro1383

Khasin, M., Cahoon, R. R., Nickerson, K. W., & Riekhof, W. R. (2018). Molecular machinery of auxin synthesis, secretion, and perception in the unicellular chlorophyte alga Chlorella sorokiniana UTEX 1230. *PloS one*, *13*(12), e0205227.

Kono, M., Kon, Y., Ohmura, Y., Satta, Y., & Terai, Y. (2020). In vitro resynthesis of lichenization reveals the genetic background of symbiosis-specific fungal-algal interaction in Usnea hakonensis. *BMC Genomics*, *21*(1), Article 671. https://doi.org/10.1186/s12864-020-07086-9

Kowalski, C. H., Kerkaert, J. D., Liu, K. W., Bond, M. C., Hartmann, R., Nadell, C. D., . . . Cramer, R. A. (2019). Fungal biofilm morphology impacts hypoxia fitness and disease progression. *Nature Microbiology*, *4*(12), 2430-2441. https://doi.org/10.1038/s41564-019-0558-7

Kranner, I., Beckett, R., Hochman, A., & Nash III, T. H. (2008). Desiccation-tolerance in lichens: a review. *The Bryologist*, *111*(4), 576-593.

Krasowska, A., & Sigler, K. (2014). How microorganisms use hydrophobicity and what does this mean for human needs? *Frontiers in Cellular and Infection Microbiology*, *4*(AUG), Article Article 112. https://doi.org/10.3389/fcimb.2014.00112

Kuske, C. R., Hesse, C. N., Challacombe, J. F., Cullen, D., Herr, J. R., Mueller, R. C., . . . Vilgalys, R. (2015). Prospects and challenges for fungal metatranscriptomics of complex communities. *Fungal Ecology*, *14*, 133-137. https://doi.org/10.1016/j.funeco.2014.12.005

Lange, O. L., & Tenhunen, J. D. (1981). Moisture content and CO2 exchange of lichens. II. Depression of net photosynthesis in Ramalina maciformis at high water content is caused by increased thallus carbon dioxide diffusion resistance. *Oecologia*, *51*(3), 426-429. https://doi.org/10.1007/BF00540917

Lawrey, J. D. (2009). Chemical defense in lichen symbioses. *Defensive Mutualism in Microbial Symbiosis*, 167-176.

Lebeaux, D., Ghigo, J. M., & Beloin, C. (2014). Biofilm-related infections: bridging the gap between clinical management and fundamental aspects of recalcitrance

toward antibiotics. *Microbiol Mol Biol Rev*, *78*(3), 510-543. https://doi.org/10.1128/MMBR.00013-14

Lewis, K. (2001). Riddle of biofilm resistance. *Antimicrob Agents Chemother*, *45*(4), 999-1007. https://doi.org/10.1128/AAC.45.4.999-1007.2001

Li, F., Svarovsky, M. J., Karlsson, A. J., Wagner, J. P., Marchillo, K., Oshel, P., . . . Palecek, S. P. (2007). Eap1p, an adhesin that mediates Candida albicans biofilm formation in vitro and in vivo. *Eukaryotic Cell*, *6*(6), 931-939. https://doi.org/10.1128/EC.00049-07

Lipke, P. N. (2018). What we do not know about fungal cell adhesion molecules. *Journal of Fungi*, *4*(2), Article 59. https://doi.org/10.3390/jof4020059

Lutzoni, F., & Miadlikowska, J. (2009). Lichens. *Current Biology*, *19*(13), R502-R503. https://doi.org/10.1016/j.cub.2009.04.034

Lutzoni, F., Nowak, M. D., Alfaro, M. E., Reeb, V., Miadlikowska, J., Krug, M., . . . Magallón, S. (2018). Contemporaneous radiations of fungi and plants linked to symbiosis. *Nature Communications*, *9*(1), Article 5451. https://doi.org/10.1038/s41467-018-07849-9

López, D., Vlamakis, H., & Kolter, R. (2010). Biofilms. *Cold Spring Harbor perspectives in biology*, *2*(7). https://doi.org/10.1101/cshperspect.a000398

Mah, T. F., & O'Toole, G. A. (2001). Mechanisms of biofilm resistance to antimicrobial agents. *Trends Microbiol*, *9*(1), 34-39. https://doi.org/10.1016/s0966-842x(00)01913-2

Matsumura, Y., & Ananthaswamy, H. N. (2004). Toxic effects of ultraviolet radiation on the skin. *Toxicol Appl Pharmacol*, *195*(3), 298-308. https://doi.org/10.1016/j.taap.2003.08.019

McDonald, T. R., Dietrich, F. S., & Lutzoni, F. (2012). Multiple horizontal gene transfers of ammonium transporters/ammonia permeases from prokaryotes to eukaryotes: toward a new functional and evolutionary classification. *Mol Biol Evol*, *29*(1), 51-60. https://doi.org/10.1093/molbev/msr123

Mcdonald, T. R., Gaya, E., & Lutzoni, F. (2013). Twenty-five cultures of lichenizing fungi available for experimental studies on symbiotic systems. *Symbiosis*, *59*(3), 165-171. https://doi.org/10.1007/s13199-013-0228-0

Mcevoy, M., Nybakken, L., Solhaug, K. A., & Gauslaa, Y. (2006). UV triggers the synthesis of the widely distributed secondary lichen compound usnic acid. *Mycological Progress*, *5*(4), 221-229. https://doi.org/10.1007/s11557-006-0514-9

Meeßen, J., & Ott, S. (2013). Recognition mechanisms during the pre-contact state of lichens: I. Mycobiont-photobiont interactions of the mycobiont of Fulgensia bracteata. *Symbiosis*, *59*(3), 121-130. https://doi.org/10.1007/s13199-013-0232-4

Meeßen, J., Sánchez, F. J., Brandt, A., Balzer, E. M., de la Torre, R., Sancho, L. G., . . . Ott, S. (2013). Extremotolerance and resistance of lichens: comparative studies on five species used in astrobiological research I. Morphological and anatomical characteristics. *Orig Life Evol Biosph*, *43*(3), 283-303. https://doi.org/10.1007/s11084-013-9337-2

Mitchell, K. F., Zarnowski, R., & Andes, D. R. (2016). Fungal Super Glue: The Biofilm Matrix and Its Composition, Assembly, and Functions. *PLoS Pathogens*, *12*(9), Article e1005828. https://doi.org/10.1371/journal.ppat.1005828

Molina, M., Stocker-Wörgötter, E., Türk, R., & Vicente, C. (1997). Axenic culture of the mycobiont of Xanthoria parietina in different nutritive media effect of carbon source in spore germination. *Endocytobiosis and Cell Research*, *12*, 103-110.

Mowat, E., Williams, C., Jones, B., McChlery, S., & Ramage, G. (2009). The characteristics of Aspergillus fumigatus mycetoma development: is this a biofilm? *Med Mycol*, *47 Suppl 1*, S120-126. https://doi.org/10.1080/13693780802238834

Nguyen, K. H., Chollet-Krugler, M., Gouault, N., & Tomasi, S. (2013). UV-protectant metabolites from lichens and their symbiotic partners. *Nat Prod Rep*, *30*(12), 1490-1508. https://doi.org/10.1039/c3np70064j

Nithyanand, P., Beema Shafreen, R. M., Muthamil, S., & Karutha Pandian, S. (2015). Usnic acid, a lichen secondary metabolite inhibits Group A Streptococcus biofilms. *Antonie Van Leeuwenhoek*, *107*(1), 263-272. https://doi.org/10.1007/s10482-014-0324-z

Nobile, C. J., Nett, J. E., Andes, D. R., & Mitchell, A. P. (2006). Function of Candida albicans adhesin hwp1 in biofilm formation. *Eukaryotic Cell*, *5*(10), 1604-1610. https://doi.org/10.1128/EC.00194-06

Nobile, C. J., Schneider, H. A., Nett, J. E., Sheppard, D. C., Filler, S. G., Andes, D. R., & Mitchell, A. P. (2008). Complementary Adhesin Function in C. albicans Biofilm Formation. *Current Biology*, *18*(14), 1017-1024. https://doi.org/10.1016/j.cub.2008.06.034

Nybakken, L., Solhaug, K. A., Bilger, W., & Gauslaa, Y. (2004). The lichens Xanthoria elegans and Cetraria islandica maintain a high protection against UV-B radiation in Arctic habitats. *Oecologia*, *140*(2), 211-216.

Onofri, S., de la Torre, R., de Vera, J. P., Ott, S., Zucconi, L., Selbmann, L., . . . Horneck, G. (2012). Survival of rock-colonizing organisms after 1.5 years in outer space. *Astrobiology*, *12*(5), 508-516. https://doi.org/10.1089/ast.2011.0736

Ophir, T., & Gutnick, D. L. (1994). A role for exopolysaccharides in the protection of microorganisms from desiccation. *Appl Environ Microbiol*, *60*(2), 740-745. https://doi.org/10.1128/aem.60.2.740-745.1994

Ott, S. (1987). Sexual reproduction and developmental adaptations in Xanthoria parietina. *Nordic Journal of Botany*, *7*(2), 219-228. https://doi.org/10.1111/j.1756-1051.1987.tb00933.x

Piercey-Normore, M. D. (2006). The lichen-forming ascomycete Evernia mesomorpha associates with multiple genotypes of Trebouxia jamesii. *New Phytologist*, *169*(2), 331-344. https://doi.org/10.1111/j.1469-8137.2005.01576.x

Piercey-Normore, M. D., & DePriest, P. T. (2001). Algal switching among lichen symbioses. *American Journal of Botany*, *88*(8), 1490-1498.

Plitt, C. C. (1919). A short history of lichenology. *Bryologist*, *22*(6), 77-85.

Priegnitz, B. E., Wargenau, A., Brandt, U., Rohde, M., Dietrich, S., Kwade, A., . . . Fleißner, A. (2012). The role of initial spore adhesion in pellet and biofilm formation in Aspergillus niger. *Fungal Genetics and Biology*, *49*(1), 30-38. https://doi.org/10.1016/j.fgb.2011.12.002

Ragon, M., Restoux, G., Moreira, D., Møller, A. P., & López-García, P. (2011). Sunlight-exposed biofilm microbial communities are naturally resistant to chernobyl ionizing-radiation levels. *PLoS One*, *6*(7), e21764. https://doi.org/10.1371/journal.pone.0021764

Ramage, G., Saville, S. P., Wickes, B. L., & López-Ribot, J. L. (2002). Inhibition of Candida albicans biofilm formation by farnesol, a quorum-sensing molecule. *Applied and Environmental Microbiology*, *68*(11), 5459-5463. https://doi.org/10.1128/AEM.68.11.5459-5463.2002

Rastogi, R. P., Kumar, A., Tyagi, M. B., & Sinha, R. P. (2010). Molecular mechanisms of ultraviolet radiation-induced DNA damage and repair. *Journal of nucleic acids*, *2010*.

Richardson, D. H. (1999). War in the world of lichens: parasitism and symbiosis as exemplified by lichens and lichenicolous fungi. *Mycological Research*, *103*(6), 641-650.

Roberts, A. P., Pratten, J., Wilson, M., & Mullany, P. (1999). Transfer of a conjugative transposon, Tn5397 in a model oral biofilm. *FEMS Microbiol Lett*, *177*(1), 63-66. https://doi.org/10.1111/j.1574-6968.1999.tb13714.x

Roth, R., Wagner, R., & Goodenough, U. (2020). Lichen 3: outer layers. *Algal Res.*

Rutishauser, U., & Sachs, L. (1975). Cell-to-cell binding induced by different lectins. *J Cell Biol*, *65*(2), 247-257. https://doi.org/10.1083/jcb.65.2.247

Sancho, L. G., de la Torre, R., Horneck, G., Ascaso, C., de Los Rios, A., Pintado, A., . . . Schuster, M. (2007). Lichens survive in space: results from the 2005 LICHENS experiment. *Astrobiology*, *7*(3), 443-454. https://doi.org/10.1089/ast.2006.0046

Sanders, W. B., & Lücking, R. (2002). Reproductive strategies, relichenization and thallus development observed in situ in leaf-dwelling lichen communities. *New Phytologist*, *155*(3), 425-435. https://doi.org/10.1046/j.1469-8137.2002.00472.x

Sarret, G., Manceau, A., Cuny, D., Van Haluwyn, C., Déruelle, S., Hazemann, J.-L., . . . Menthonnex, J.-J. (1998). Mechanisms of lichen resistance to metallic pollution. *Environmental Science & Technology*, *32*(21), 3325-3330.

Scherrer, S., De Vries, O. M. H., Dudler, R., Wessels, J. G. H., & Honegger, R. (2000). Interfacial self-assembly of fungal hydrophobins of the lichen-forming ascomycetes Xanthoria parietina and X. ectaneoides. *Fungal Genetics and Biology*, *30*(1), 81-93. https://doi.org/10.1006/fgbi.2000.1205

Schink, B. (1997). Energetics of syntrophic cooperation in methanogenic degradation. *Microbiol Mol Biol Rev*, *61*(2), 262-280. https://doi.org/10.1128/mmbr.61.2.262-280.1997

Seminara, A., Fritz, J., Brenner, M. P., & Pringle, A. (2018). A universal growth limit for circular lichens. *Journal of the Royal Society Interface*, *15*(143), Article 20180063. https://doi.org/10.1098/rsif.2018.0063

Silverman, R. J., Nobbs, A. H., Vickerman, M. M., Barbour, M. E., & Jenkinson, H. F. (2010). Interaction of Candida albicans cell wall Als3 protein with Streptococcus gordonii SspB adhesin promotes development of mixed-species communities. *Infect Immun*, *78*(11), 4644-4652. https://doi.org/10.1128/IAI.00685-10

Singh, R. S., & Walia, A. K. (2014). Characteristics of lichen lectins and their role in symbiosis. *Symbiosis*, *62*(3), 123-134. https://doi.org/10.1007/s13199-014-0278-y

Sirrenberg, A., Göbel, C., Grond, S., Czempinski, N., Ratzinger, A., Karlovsky, P., . . . Pawlowski, K. (2007). Piriformospora indica affects plant growth by auxin production. *Physiol Plant*, *131*(4), 581-589. https://doi.org/10.1111/j.1399-3054.2007.00983.x

Skye, E. (1979). Lichens as biological indicators of air pollution. *Annual Review of Phytopathology*, *17*(1), 325-341.

Solhaug, K. A., Gauslaa, Y., Nybakken, L., & Bilger, W. (2003). UV-induction of sun-screening pigments in lichens. *New Phytologist*, *158*(1), 91-100. https://doi.org/10.1046/j.1469-8137.2003.00708.x

Spribille, T., Tagirdzhanova, G., Goyette, S., Tuovinen, V., Case, R., & Zandberg, W. F. (2020). 3D biofilms: in search of the polysaccharides holding together lichen symbioses. *FEMS Microbiol Lett*, *367*(5). https://doi.org/10.1093/femsle/fnaa023

Spribille, T., Tuovinen, V., Resl, P., Vanderpool, D., Wolinski, H., Aime, M. C., . . . McCutcheon, J. P. (2016). Basidiomycete yeasts in the cortex of ascomycete macrolichens. *Science*, *353*(6298), 488-492. https://doi.org/10.1126/science.aaf8287

Stewart, P. S., & Costerton, J. W. (2001). Antibiotic resistance of bacteria in biofilms. *Lancet*, *358*(9276), 135-138. https://doi.org/10.1016/s0140-6736(01)05321-1

Stocker-Wörgötter, E., & Türk, R. (1991). Artificial resynthesis of thalli of the cyanobacterial lichen peltigera praetextata under laboratory conditions. *The Lichenologist*, *23*(2), 127-138. https://doi.org/10.1017/S0024282991000294

Szczepaniak, K., & Biziuk, M. (2003). Aspects of the biomonitoring studies using mosses and lichens as indicators of metal pollution. *Environ Res*, *93*(3), 221-230. https://doi.org/10.1016/s0013-9351(03)00141-5

Talbot, N. J., Kershaw, M. J., Wakley, G. E., De Vries, O. M. H., Wessels, J. G. H., & Hamer, J. E. (1996). MPG1 encodes a fungal hydrophobin involved in surface interactions during infection-related development of Magnaporthe grisea. *Plant Cell*, *8*(6), 985-999. https://doi.org/10.1105/tpc.8.6.985

Teitzel, G. M., & Parsek, M. R. (2003). Heavy metal resistance of biofilm and planktonic Pseudomonas aeruginosa. *Appl Environ Microbiol*, *69*(4), 2313-2320. https://doi.org/10.1128/AEM.69.4.2313-2320.2003

Tuovinen, V., Ekman, S., Thor, G., Vanderpool, D., Spribille, T., & Johannesson, H. (2019). Two Basidiomycete Fungi in the Cortex of Wolf Lichens. *Current Biology*, *29*(3), 476-483.e475. https://doi.org/10.1016/j.cub.2018.12.022

Uluozlu, O. D., Sari, A., Tuzen, M., & Soylak, M. (2008). Biosorption of Pb(II) and Cr(III) from aqueous solution by lichen (Parmelina tiliaceae) biomass. *Bioresour Technol*, *99*(8), 2972-2980. https://doi.org/10.1016/j.biortech.2007.06.052

Valsecchi, I., Dupres, V., Stephen-Victor, E., Guijarro, J. I., Gibbons, J., Beau, R., . . . Beauvais, A. (2018). Role of hydrophobins in aspergillus fumigatus. *Journal of Fungi*, *4*(1), Article 2. https://doi.org/10.3390/jof4010002

Van Gestel, J., Vlamakis, H., & Kolter, R. (2015). Division of labor in biofilms: The ecology of cell differentiation. *Microbiology Spectrum*, *3*(2), Article Mb-0002-2014. https://doi.org/10.1128/microbiolspec.MB-0002-2014

Vlamakis, H., Aguilar, C., Losick, R., & Kolter, R. (2008). Control of cell fate by the formation of an architecturally complex bacterial community. *Genes and Development*, *22*(7), 945-953. https://doi.org/10.1101/gad.1645008

Wang, Y., Wei, X., Bian, Z., Wei, J., & Xu, J. R. (2020). Coregulation of dimorphism and symbiosis by cyclic AMP signaling in the lichenized fungus. *Proc Natl Acad Sci U S A*, *117*(38), 23847-23858. https://doi.org/10.1073/pnas.2005109117

Wang, Y. Y., Liu, B., Zhang, X. Y., Zhou, Q. M., Zhang, T., Li, H., . . . Wei, J. C. (2014). Genome characteristics reveal the impact of lichenization on lichen-forming fungus Endocarpon pusillum Hedwig (Verrucariales, Ascomycota). *BMC Genomics*, *15*(1), Article 34. https://doi.org/10.1186/1471-2164-15-34

Watnick, P., & Kolter, R. (2000). Biofilm, city of microbes. *Journal of Bacteriology*, *182*(10), 2675-2679. https://doi.org/10.1128/JB.182.10.2675-2679.2000

Webster, M., & Brown, D. H. (1997). Preliminary observations on the growth of transplanted Peltigera cainina under semi-natural conditions. *Lichenologist*, *29*(1), 91-96. https://doi.org/10.1006/lich.1996.0063

Wessels, J. G. H. (2000). Hydrophobins, unique fungal proteins. *Mycologist*, *14*(4), 153-159. https://doi.org/10.1016/S0269-915X(00)80030-0

Wösten, H. A. B. (2001). Hydrophobins: Multipurpose proteins. In *Annual Review of Microbiology* (Vol. 55, pp. 625-646).

Wösten, H. A. B., Schuren, F. H. J., & Wessels, J. G. H. (1994). Interfacial self-assembly of a hydrophobin into an amphipathic protein membrane mediates fungal attachment to hydrophobic surfaces. *EMBO Journal*, *13*(24), 5848-5854. https://doi.org/10.1002/j.1460-2075.1994.tb06929.x

Yahr, R., Vilgalys, R., & Depriest, P. T. (2004). Strong fungal specificity and selectivity for algal symbionts in Florida scrub Cladonia lichens. *Mol Ecol*, *13*(11), 3367-3378. https://doi.org/10.1111/j.1365-294X.2004.02350.x

Yamamura, N. (1993). Vertical transmission and evolution of mutualism from parasitism. *Theoretical Population Biology*, *44*(1), 95-109.

Table 1: Similar features between biofilms and lichens.

Feature	Fungal Biofilm	Lichen
Surfaces adhered to	Hydrophobic; nonpolar; rough	Hydrophobic; rough
Stages of Development	Adherence to surface, cell communication and differentiation, matrix and microniche formation, dispersal	Adherence to surface, cell communication and differentiation, matrix formation and tissue development, dispersal
Cell Differentiation	Microniches; Interstitial voids; sporulating	Layered tissue differences: upper and lower conglutinate cortexes, medullary thalline layer, algal layer, sporulation structures and vegetative propagules
Cell Interactions	Synergies between metabolically linked organisms; antagonism between non-matching QSM	Syntrophy between mycobiont and photobiont
Extracellular Matrix	Generally Hydrophilic with hydrophobic coating; Known to contain: Hygroscopic Polysaccharides, eDNA, lipids, and proteins	Hydrophilic with hydrophobic coating; Known to contain: Hygroscopic Polysaccharides, and proteins; potentially eDNA
Stress Resistances	Antimicrobials, UV, desiccation, metal toxicity	UV, desiccation, metal toxicity, extreme temperatures

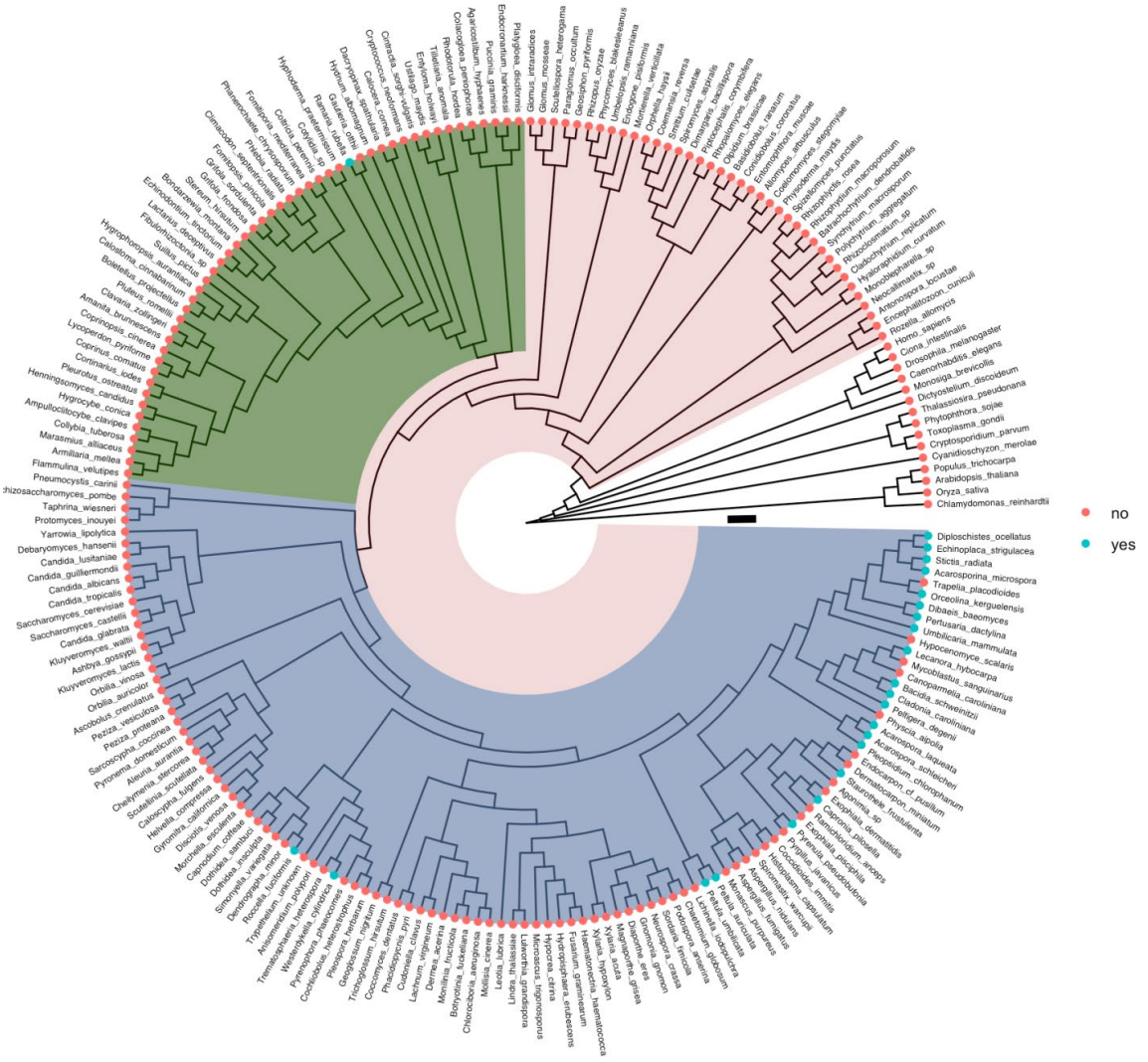

Figure 1: Phylogenetic tree of the fungal lineages that have developed the lichen form. Tree was constructed with data derived from Hibbett et al. (2016) of 23 single copy genes derived from whole genome sequences. The morphology of lichen habit was mapped across the fungal phylogeny. The complete Fungal lineage is represented in the pink portion of the tree, with the green wedge representing the Basidiomycete lineage, and the blue portions representing Ascomycete fungi.

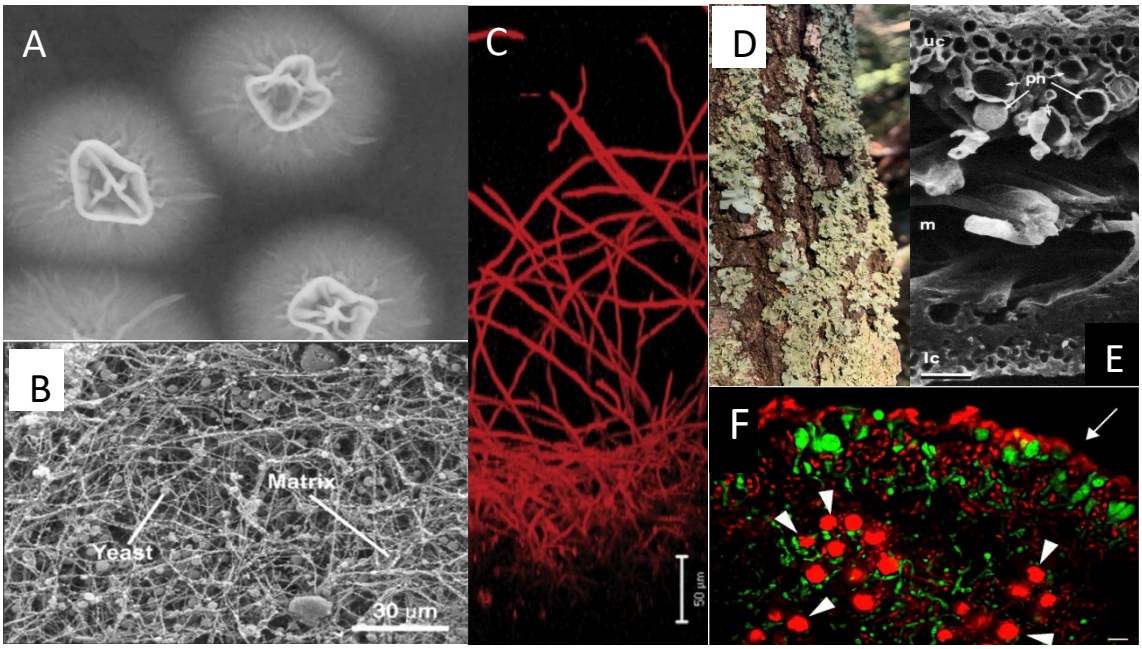

Figure 2: Photographic and microcopy images of different details of biofilms and lichens. (A-C) Biofilm images of the fungus *Candida albicans*. A) Photo of a C. albicans colony/biofilms with inner hyphal layer and outer yeast layer (credit: Surabhi Naik). B) SEM photo of *C. albicans* biofilm, showing hyphal cells, yeast cells, and matrix that forms around the entire biofilm (Andes et al., 2004). C) Fluorescent image of the cross section of a *C. albicans* biofilm (Nobile et al., 2008). A dense layer of hyphae and yeast is seen on the bottom, and a looser layer of hyphae protrude out the top. (D-F) Images of various lichens. D) A photograph of the lichen *Parmotrema* sp. on a Live Oak tree in central Florida (credit: Erin Carr) E) SEM of a cross section of the lichen *Xanthoria parietina* (Honegger, 1993). uc= upper cortex; ph= photobiont; m= medullary thalline layer; lc= lower cortex. F) Fluorescent cross section of lichen thallus of *Letharia vulpina* (Tuovinen et al., 2019). Arrow is pointing to autofluorescence and the arrow heads are pointing to the algal photobionts below the upper cortex.

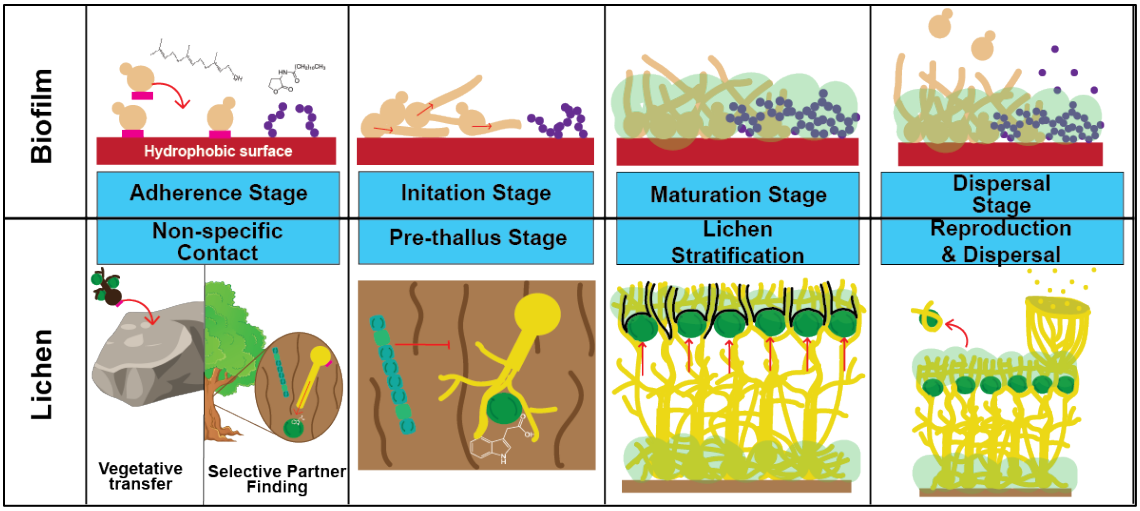

Figure 3: Summary of the stages of development of biofilms, represented by *Candida albicans* (tan) and *Streptococcus gordonii* (purple), and lichens with the mycobiont *Xanthoria paretina* in yellow and the photobionts in green (algae and cyanobacteria). Adherence and Non-specific contact stage are the first stages of biofilm and lichen development respectively. Both are known for the binding of cells to a hydrophobic surface (rock, bark, or catheter tube) via various hydrophobic proteins represented with a pink rectangle. Initiation and Pre-thallus stages are the second stages of development. This stage is linked to cell differentiation, where *C. albicans* initiates the switch into hyphal growth, and mycobionts initiate hyphal branching. The third stages are the maturation stage and the lichen stratification stage. In these stages both biofilms and lichens create differential zones of cells and form their extracellular matrix. Biofilms form microniches which lead to microcolonies, and interstitial voids which allow for some gas exchange. Lichens separate into 3 main sections the upper cortex where the majority of ECM is contained and the photobiont cells are positioned right below, the medullary thalline layer that is thought to be made up of mostly air or unknown substances (Honegger, 2001; Goodenough & Roth, 2020), and the lower cortex layer which is considered to also have ECM and is responsible for lichen-surface attachment. The final stage is the dispersal stage, or reproduction and dispersal in lichens. This stage can be caused by reproduction or vegetative release of cells by external disturbance or intent by the community.

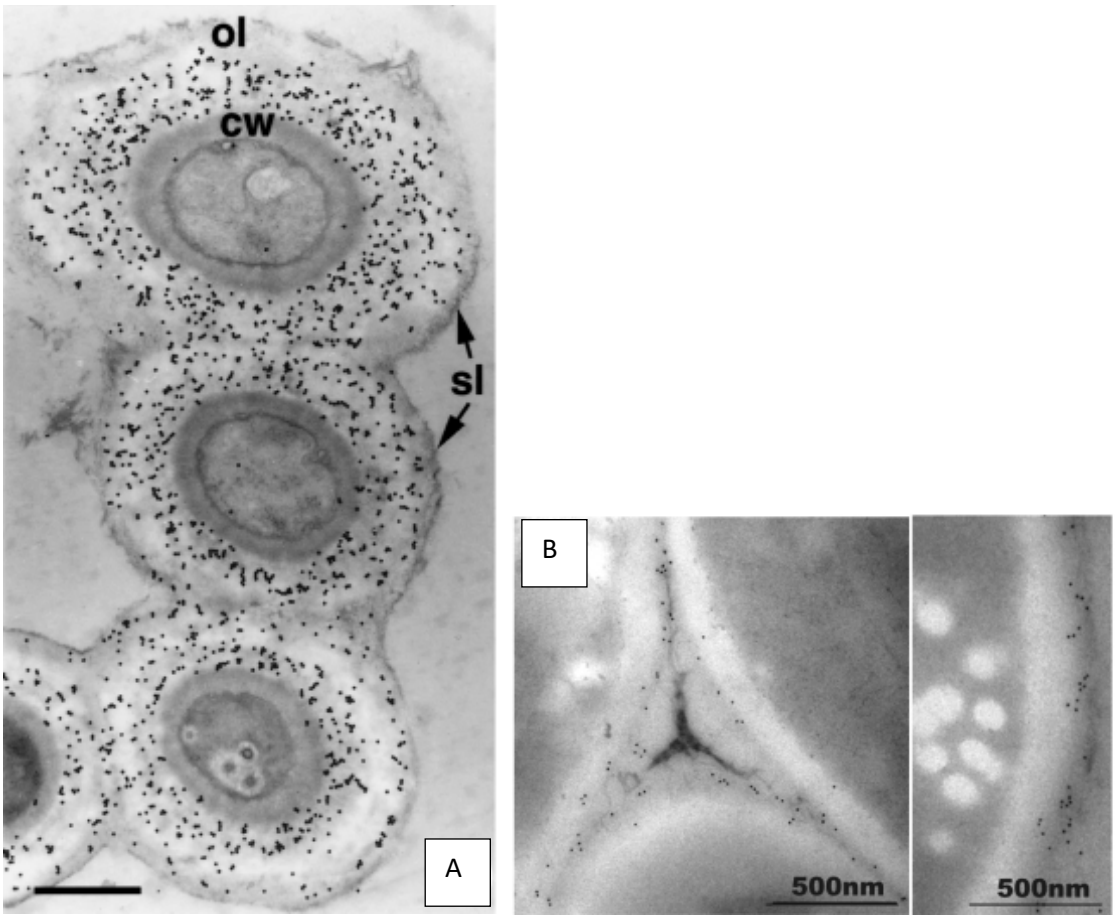

Figure 4: Transmission Electron Microscopy images of immunogold labeling experiments locating 1,3-Glucans in the lichen *C. islandica* (A) and *A. fumigatus* (B). (A): Immunogold labeling of β-1,3-Glucans in the lichen *C. islandica* (Honegger & Haisch, 2001). Lichenin is presumed to be the glucan that is labeled, which is shown to be mainly accumulated in the outer layer (ol), which is indicated to be the extracellular matrix of the lichen; bar=1μm; cw= mycobiont Cell wall; sl= surface layer. (B): Immunogold labeling of α-1,3-Glucans in the fungus *A. fumigatus* (Beauvis et al., 2007). The α-1,3-Glucans are also observed to be accumulated in the extracellular matrix of *A. fumigatus* biofilms as well. Indicating that both lichens and fungal biofilms create extracellular matrixes that contain extracellular polysaccharides.

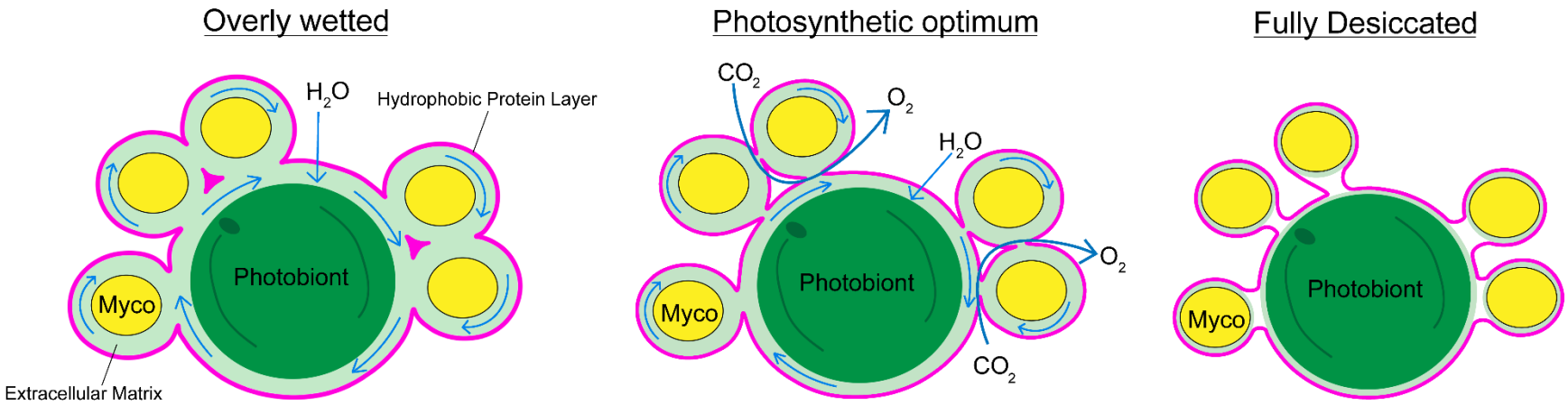

Figure 5: Illustration of the lichen extracellular matrix in relation to the mycobiont and photobiont cell walls, and its effect on lichens' poikilohydric lifestyle. The matrix is located beyond the mycobiont's cell wall, it is hydrophilic due to its excess in hygroscopic glucans allowing for water accumulation and exchange. Additionally, there is a thin hydrophobic proteinaceous coat that surrounds the extracellular matrix and photobiont cells, indicated here with a thick pink line. This is presumed to prevent over wetting of the lichen thallus, to allow for important gas exchange to occur that is vital to photosynthesis, and also to aid in the water retention of the matrix acting like a plant's cuticle.

Chapter 2

Deciphering the potential niche of two novel black yeast fungi, *Exophiala viscosium* and *Exophiala limosus*, from a biological soil crust using their genomes, phenotypes, and melanin regulation

This chapter represents the contents of: Carr, E.C., Barton, Q., Grambo, S., Sullivan, M., Renfro, C.M., Kuo, A., Pangilinan, J., Lipzen, A., Keymanesh, K., Savage, E., Barry, K., Grigoriev, I.V., Riekhof, W.R., Harris, S.D., 2021. Deciphering the potential niche of novel black yeast fungal isolates in a biological soil crust based on genomes, phenotyping, and melanin regulation. BioRxiv, March 2nd, 2022 doi:10.1101/2021.12.03.471027.

Abstract

Black yeasts are polyextremotolerant fungi that contain high amounts of melanin in their cell wall and maintain a primarily yeast form. These fungi grow in xeric, nutrient deplete environments which implies that they require highly flexible metabolisms and the ability to form lichen-like mutualisms with nearby algae and bacteria. However, the exact ecological niche and interactions between these fungi and their surrounding community is not well understood. We have isolated two novel black yeast fungi of the genus *Exophiala*: *E. viscosium* and *E. limosus*, which are from dryland biological soil crusts. A combination of whole genome sequencing and various phenotyping experiments have been performed on these isolates to determine their fundamental niches within the biological soil crust consortium. Our results reveal that these *Exophiala* spp. are capable of utilizing a wide

variety of carbon and nitrogen sources potentially from symbiotic microbes, they can withstand many abiotic stresses, and can potentially provide UV resistance to the crust community in the form of secreted melanin. Besides the identification of two novel species within the genus *Exophiala*, our study also provides new insight into the regulation of melanin production in extremotolerant fungi.

Introduction

Polyextremotolerant fungi are a polyphyletic group that can be divided morphologically into black yeast and microcolonial/meristematic fungi types (Gostinčar et al., 2012). These two sub-types are distinct in their morphology; black yeast fungi are usually only yeasts but can be dimorphic, whereas microcolonial fungi are typically filamentous, pseudohyphal, or possess other unique morphologies such as spherical cells (Ametrano et al., 2017; De Hoog et al., 2003; Gostinčar et al., 2011). However, all polyextremotolerant fungi share the capacity to produce melanin, which presumably accounts for much of their polyextremotolerance. Most polyextremotolerant fungi are in the subdivision Pezizomycotina, residing mainly within Eurotiomycetes and Dothidiomycetes, but one could argue that any fully melanized fungus could be a polyextremotolerant fungi (Gostinčar et al., 2009).

Melanin is arguably a defining feature of polyextremotolerant fungi given that they form unmistakably black colonies. Because of its structure and association with the cell wall, melanin imbues polyextremotolerant fungi with resistance to multiple forms of stress. Most commonly known is ultraviolet (UV) light resistance, as melanin absorbs light in the UV part of the spectrum (Kobayashi et al., 1993). However, melanin is also

capable of absorbing reactive oxygen species (ROS), reactive nitrogen species (RNS), providing tolerance to toxic metals, reducing desiccation, and potentially using ionizing radiation as an energy source (Cordero & Casadevall, 2017; Dadachova et al., 2007; Gessler et al., 2014; Płonka & Grabacka, 2006; Zanne et al., 2020). Collectively, these functions of melanin are thought to enhance the ability of polyextremotolerant fungi to colonize habitats that are otherwise inhospitable to most forms of life.

The production of melanin is a key functional trait observed in fungi spanning the fungal kingdom (Bell & Wheeler, 1986; Zanne et al., 2020). The diverse protective functions of melanin (e.g., metal resistance, ROS and RNS tolerance, UV resistance) underscores its broad utility in mitigating the impacts of stress despite the potential cost of its synthesis (Schroeder et al., 2020). Fungi are capable of producing three different types of melanin: pheomelanin, allomelanin, and pyomelanin, all of which have their own independent biosynthetic pathways (Pal et al., 2014; Perez-Cuesta et al., 2020). Allomelanin, is formed from the polymerization of 1,8-DHN, which requires the use of polyketide synthase for initial steps in production (Perez-Cuesta et al., 2020; Płonka & Grabacka, 2006) (**Figure 1**). Pyomelanin and pheomelanin share an initial substrate of Tyrosine, but pheomelanin derives from L-DOPA, whereas pyomelanin is created via tyrosine degradation (Perez-Cuesta et al., 2020; Płonka & Grabacka, 2006) (**Figure 1**). Allomelanin and pheomelanin are often referred to as DHN melanin and DOPA melanin respectively, given their chemical precursors. Unfortunately, due to the unique characteristics of melanins and their association with larger biomolecules, we do not know the complete structure of any type of melanin (Cao et al., 2021). However, given that we do know their chemical constituents, it is possible to draw some inferences about

the relationship between structure and function of a particular type of melanin. For instance, out of the three types of melanin fungi can produce, only pheomelanin has a chemical precursor, 5-CysDOPA, with both Nitrogen and Sulfur in its structure (Płonka & Grabacka, 2006). Notably, all three fungal melanins are synthesized via independent pathways, which enables the targeted use of chemical inhibitors to block one pathway without interfering with the others. For example, previous studies have extensively used the chemical melanin blockers kojic acid and phthalide to block pheomelanin and allomelanin respectively (Pal et al., 2014) (**Figure 1**). Use of these chemical blockers allowed previous studies to identify the primary melanin biosynthetic pathway employed by individual fungal species (Pal et al., 2014).

Polyextremotolerant fungi tend to occupy extreme niches such as rock surfaces, external brick and marble walls, soil surfaces, and even the inside of dishwashers (Gostinčar et al., 2009; Zupančič et al., 2016). Characteristic features of these environments includes the relative paucity of nutrients and the frequent presence of a community biofilm consisting of photosynthetic organisms and/or bacteria (Gostinčar et al., 2012). Strikingly, these species are rarely found alone in their habitats, which suggests that multi-species interactions between fungi, bacteria, and photosynthetic organisms underlie the formation and function of these communities. That is, the ability of polyextremotolerant fungi to successfully adapt to their niche must depend on complex yet poorly understood interactions with other microbes.

We have isolated two polyextremotolerant fungi from a biological soil crust (BSC) in B.C., Canada. These novel fungi are of the genus *Exophiala*, which has previously been found in BSCs (Bates et al., 2006). Biological soil crusts are unique

dryland biofilms that form on the surface of xeric desert soils where little to no plants are able to grow (Belnap, 2003; Belnap et al., 2001). They are notable for their extensive cyanobacteria population, which seeds the initial formation of all biological soil crusts and creates the main source of nitrogen for the rest of the community (Belnap, 2002). Once the initial crust is established, it is then inundated with a consortium of bacteria, fungi, algae, archaea, lichens, and mosses (Bates et al., 2010; Lan et al., 2012; Maier et al., 2016). This community is a permanent fixture on the land they occupy unless physically disturbed, much like other biofilms (Belnap & Eldridge, 2001; Donlan & Costerton, 2002). As a result of the desert conditions BSCs reside in, the microbes found there are constantly exposed to extreme abiotic factors which they must tolerate simultaneously (Bowker et al., 2010). Some of these abiotic extremes are: UV radiation (especially at higher altitudes and closer to the poles) (Bowker et al., 2002), desiccation and osmotic pressures (Rajeev et al., 2013), and temperature fluctuations both daily and annually (Belnap et al., 2001; Bowker et al., 2002; Pócs, 2009). Microbes that reside in these biological soil crusts have therefore adapted mechanisms to withstand these abiotic extremes.

An extensive amount of research has been dedicated to certain members of the biological soil crust community, but one such less studied microbe has been the “free-living” fungal taxa. These fungi are non-lichenized (Teixeira et al., 2017) yet are still thriving in an environment where there are no plants to infect or decompose (Belnap & Lange, 2003), and no obvious source of nutrients besides contributions from the other members of the biological soil crust community (Belnap & Lange, 2003). This would imply that even though these fungi are not lichenized per say, they would have to be

engaging in lichen-like interactions with the biological soil crust community to obtain vital nutrients for proliferation. While the idea of transient interactions between non-lichenized fungi and other microbes has been floated by previous researchers in other systems (Gostinčar et al., 2012; Grube et al., 2015; Hom & Murray, 2014), it will be a difficult task to strongly confirm in biological soil crusts given their taxonomic complexity.

Despite the importance of microbial interactions in enabling the successful formation of BSCs in a niche characterized by poor nutrient and water availability, the fungal components of BSCs and their relative functions within the interaction network remain poorly understood. Here, we combine genome sequencing with computational tools and culture-based phenotyping to describe two new species of black yeast fungi associated with BSCs. We report on their carbon and nitrogen utilization profiles, stress responses, and lipid accumulation patterns. In addition, we characterize their capacity for melanin production and generate valuable insight into mechanisms that might be involved in regulating the synthesis of these compounds and how their melanin production contributes to the BSC community.

Methods

General Methods

Fungal Strains and Media

Two novel species of fungi are described here: *Exophiala viscosium* JF 03-3F Goopy CBS 148801 and *Exophiala limosus* JF 03-4F Slimy CBS 148802. Their genomes and transcriptomes are deposited at the Department of Energy's (DOE) Joint Genome

Institute (JGI) on their Mycocosm website under their genus species names, and the National Center for Biotechnological Information (NCBI) under accession numbers JALDXI000000000 for *E. viscosium* and JALDXH000000000 for *E. limosus.* Their type strains have been deposited to the Westerdijk institute for access to the scientific community. *E. viscosium* and *E. limosus* are typically grown in malt extract medium (MEA; see **Table 1** for media recipe) at room temperature in an Erlenmeyer flask at $1/10^{th}$ the volume of the flask, shaking at 200 rpm. Additional strains used in this study were *Saccharomyces cerevisiae* ML440 and BY4741, and *E. dermatitidis* wild type (WT) strain ATCC 34100. *S. cerevisiae* strains are grown in Yeast Peptone Dextrose medium (YPD; see **Table 1** for media recipe), and *E. dermatitidis* is grown in MEA.

Fungal isolation and identification methods

Fungi were isolated from a biological soil crust in B.C., Canada. Soil samples were taken from the top 2 cm of the biological soil crust. A 0.1 g portion of the crust was re-suspended in 1 mL of water, ground with a sterile micropestle, and diluted with a dilution factor (DF) of 10 till they reached 10,000x dilution. Each dilution was then spread out onto two different MEA petri plate containing either no antibiotics or containing: Ampicillin (100 mg/L), Chloramphenicol (50 mg/L), Gentamycin (10 mg/L), and Cycloheximide (100 mg/L). The plates were then incubated in a Percival light incubator at 23 °C with a 12 hr light/dark cycle and examined daily using a dissection microscope to check for small black colonies. Once a potential black colony was seen, half of it was removed and transferred to a new MEA (no antibiotics) petri plate. It was vital to examine the plates daily, because even in the presence of antibiotics many unwanted fast-growing microbes would grow on the plates and cover up the slower

growing polyextremotolerant fungal colonies. Once a pure culture of each isolate was grown up (approximately 2 weeks), they were preserved in 30% Glycerol and stored in the -80 °C freezer. DNA sequencing of amplified internal transcribed spacer (ITS) sequences was used to identify the isolates. DNA was extracted using the Qiagen DNeasy Powersoil DNA extraction kit. Primers used to isolate the ITS region were: ITS1- (5'-TCC GTA GGT GAA CCT GCG G-3') and ITS4- (5'-TCC TCC GCT TAT TGA TAT GC-3') (White et al., 1990). A BioRad MJ Mini Personal Thermal Cycler was used, with the program set as: 1) 95 °C for 5:00 (5 minutes), 2) 94 °C for 0:30 (30 seconds), 3) 55 °C for 0:30, 4) 72 °C for 1:30, 5) Return to 2 35 times, 6) 72 °C for 5:00. Resulting PCRs were then checked via gel electrophoresis in 1% agar run at 80 V for 1 hr. Isolated ITS regions were sequenced using the Eurofins sequencing facility, and the sequences were subsequently identified using the basic locally aligned search tool (BLAST) of the National Center for Biotechnological Information (NCBI) database to look for potential taxa matches.

DNA extraction and RNA extraction for whole genome sequencing

A Cetyltrimethylammonium bromide (CTAB) based DNA extraction method was performed to obtain high molecular weight DNA for whole genome sequencing. The DNA extraction method used was derived from (Cubero et al., 1999). Changes to the original protocol include switching PVPP for the same concentration of PVP, use of bead beating tubes with liquid nitrogen-frozen cells and the extraction buffer instead of a mortar and pestle for breaking open the cells, and heating up the elution buffer to 65 °C before eluting the final DNA. These changes were made to optimize the protocol for liquid-grown yeast cells instead of lichen material. Cells for the DNA extraction were

grown up in 25 mL of liquid MEA in 250 mL Erlenmeyer flasks for 5 days, 1 mL of those grown cells was used for the DNA extraction after washing with water twice. RNA was obtained using the Qiagen RNeasy mini kit (Cat. No. 74104). Cells were grown in 25 mL of three different liquid media types (MEA, YPD, and MNV; see **Table 1**) in 250 mL Erlenmeyer flasks at room temperature for 5 days, and 1-2 mL of cells were used for the RNA extraction. Cells were washed with DEPC-treated water and flash frozen in liquid nitrogen in 1.5 mL microcentrifuge tubes. RNA extraction was then performed according to the methods by the RNeasy kit.

Genome assembly and annotation

Both genomes and transcriptomes were sequenced using Illumina technology. For transcriptomes, a plate-based RNA sample prep was performed on the PerkinElmer Sciclone next generation sequencing (NGS) robotic liquid handling system using Illuminas TruSeq Stranded mRNA high throughput (HT) sample prep kit utilizing poly-A selection of mRNA following the protocol outlined by Illumina in their user guide: https://support.illumina.com/sequencing/sequencing_kits/truseq-stranded-mrna.html, and with the following conditions: total RNA starting material was 1 μg per sample and 8 cycles of PCR was used for library amplification. The prepared libraries were quantified using KAPA Biosystems' next-generation sequencing library qPCR kit and run on a Roche LightCycler 480 real-time PCR instrument. The libraries were then multiplexed and prepared for sequencing on the Illumina NovaSeq sequencer using NovaSeq XP v1 reagent kits, S4 flow cell, following a 2x150 indexed run recipe.

Using BBDuk (https://sourceforge.net/projects/bbmap/), raw reads were evaluated for artifact sequence by kmer matching (kmer=25), allowing 1 mismatch and detected

artifact was trimmed from the 3' end of the reads. RNA spike-in reads, PhiX reads and reads containing any Ns were removed. Quality trimming was performed using the phred trimming method set at Q6. Finally, following trimming, reads under the length threshold were removed (minimum length 25 bases or 1/3 of the original read length - whichever is longer). Filtered reads were assembled into consensus sequences using Trinity ver. 2.3.2 (Grabherr et al., 2011).

For genomes, DNA library preparation for Illumina sequencing was performed on the PerkinElmer Sciclone NGS robotic liquid handling system using Kapa Biosystems library preparation kit. 200 ng of sample DNA was sheared to 300 bp using a Covaris LE220 focused-ultrasonicator. The sheared DNA fragments were size selected by double-SPRI and then the selected fragments were end-repaired, A-tailed, and ligated with Illumina compatible sequencing adaptors from IDT containing a unique molecular index barcode for each sample library. The prepared libraries were quantified using KAPA Biosystems' next-generation sequencing library qPCR kit and run on a Roche LightCycler 480 real-time PCR instrument. The quantified libraries were then multiplexed with other libraries, and the pool of libraries was then prepared for sequencing on the Illumina HiSeq sequencing platform utilizing a TruSeq paired-end cluster kit, v4, and Illumina's cBot instrument to generate a clustered flow cell for sequencing. Sequencing of the flow cell was performed on the Illumina HiSeq2500 sequencer using HiSeq TruSeq SBS sequencing kits, v4, following a 2x150 indexed run recipe.

An initial assembly of the target genome was generated using VelvetOptimiser version 2.1.7 (3) with Velvet version 1.2.07 (Zerbino & Birney, 2008) using

the following parameters; "--s 61 --e 97 --i 4 --t 4, --o "-ins_length 250 -min_contig_lgth 500"". The resulting assembly was used to simulate 28X of a 2x100 bp 3000 +/- 300bp insert long mate-pair library with wgsim version 0.3.1-r13 (https://github.com/lh3/wgsim) using "-e 0 -1 100 -2 100 -r 0 -R 0 -X 0 -d 3000 -s 30". 25X of the simulated long mate-pair was then co-assembled together with 125X of the original Illumina filtered fastq with AllPathsLG release version R49403 (Gnerre et al., 2011) to produce the final nuclear assembly. The genome was annotated using JGI Annotation pipeline (Grigoriev et al., 2014). The assemblies and annotations of both genomes are available at the fungal genome portal MycoCosm ((Grigoriev et al., 2014); https://mycocosm.jgi.doe.gov) and in the DDBJ/EMBL/GenBank repository under accessions X and X.

Phylogenetic analysis

Our approximate maximum likelihood phylogenetic tree was constructed from the protein sequences of 24 taxa which represent a sampling of the family Herpotrichielleaceae in which *E. viscosium* and *E. limosus* reside. We created this tree using the pipeline described in Kuo et al. (Kuo et al., 2014). We wanted to obtain the largest set of data for phylogenetic analysis available by defining homologous proteins across all 24 genomes using Best Bidirectional Blast pairs via BlastP across all proteins of all the genomes from their FilteredModels or ExternalModels files available on Mycocsm. Resulting defined homologous proteins across all 24 genomes were then used as our sequences for the rest of the pipeline. These sequences were aligned with Mafft v7.123b with no alterations (Katoh et al., 2002). That alignment was then trimmed using Gblocks 0.91b with options -b4=5 -b5=h to have a minimum of 5 positions per block and

allowing up to half of those to be gaps (Castresana, 2000). The resulting trimmed alignment was then input into FastTree version 2.1.5 SSE3 with options -gamma -wag (Price et al., 2009). The tree file was then input into iTOL for visual optimization (Letunic & Bork, 2021).

Mating type locus identification

Mating loci for *E. viscosium* and *E. limosus* were determined using the methods described by (Teixeira et al., 2017). Genes known to flank the MAT loci of most Chaetothyriales species include: *APN2*, *SLA2*, *APC5*, and *COX13*. The protein sequences of these genes from *Aspergillus nidulans* were used to BLASTP against the genomes of the new fungi. These gene sequences were obtained from Aspergillus Genome Database and BLASTed using JGI's Mycocosm. Once those genes were found, analysis of upstream and downstream flanking genes was performed until the mating gene MAT1-1 was located. Genes close to MAT1-1 and within the span of genes listed above were considered part of the MAT locus.

Phenotyping experiments

Characterization of *E. viscosium* and *E. limosus* was performed to provide us with the knowledge of these new species' capabilities. Experiments performed were carbon utilization, nitrogen utilization, UV resistance, metal resistance, growth temperature range, budding patterns, lipid profiles, and growth capabilities on various fungal medias as described below.

Budding Pattern determination

Protocols for observing the budding patterns of these new species were derived from methods in (Mitchison-Field et al., 2019). A 1:1:1 ratio by weight of Vaseline, Parafin, and Lanolin (VALAP) was combined in a glass bottle and heated to 115 °C to melt completely and kept at room temperature for later use. Heated solid MEA was aliquoted into a 50mL tube for agar slab making. Isolates were grown in liquid MEA for 5 days prior to inoculation of slides. First, the VALAP was brought back up to 115 °C to melt completely for application. Then 5 µL of the 5-day old cells were diluted in 995 µL of liquid MEA. Agar slabs of MEA were made by microwaving the 50 mL tube of solid MEA until it melted, then pipetting 1 mL of the hot agar into a 1 cm x 2 cm mold formed out of cut strips of silicone and laid down in a sterile petri dish. This agar slab was allowed to solidify and was then cut in half to be 1 cm x 1 cm. Both the cover slip and the slide were wiped down with ethanol to ensure clean and sterile growth conditions for the cells. 8 µL of the diluted cells was pipetted onto the center of the sterile slide, then one square of the agar slab was carefully placed on top of the cells in media, 8 µL of MEA was pipetted onto the top of the agar slab, and the coverslip was placed over the agar slab. Using a small paintbrush, the melted VALAP was carefully painted onto the gap between the coverslip and the microscope slide to seal off the coverslip. Finally, a 23-gauge needle was used to poke holes in the solidified VALAP to allow for gas exchange. The slide was then placed with the slide facing down onto the inverted microscope EVOS fl. Once an adequate number of cells was observed in frame, the cells were allowed to settle for 2 hours before imaging began. Images were then automatically taken every 30 mins for 72 hours. Videos of the budding pattern were created using Adobe Premiere Pro.

Growth of E. viscosium and E. limosus on different medias

Eight different fungal media were used to observe the growth of these novel fungi. These media have been used for identification purposes and will be useful for future identification of these species from other locations. Media used in this experiment were: MAG, MEA, MN, MNV, MN+NAG, PDA, Spider, YPD, V8 (**Table 1**). Both isolates were first grown in 25 mL of liquid MEA at room temperature, shaking at 200 rpm for 5 days. Then 1 mL of each species was aliquoted and washed 3 times with water. Washed cells were then applied to the media in three ways: 5 µL spotting (pipetting 5 µL of cells onto the plate), toothpick poking (poking a sterile toothpick tip into the suspended cells and then onto a plate), and metal loop streaking (placing sterile metal loop into suspended cells, then spreading cells onto plate in a decreasing manner). This provided us with different plating techniques that could potentially yield different morphologies.

Carbon Utilization

Carbon utilization of each isolate was determined using a BioMerieux ID C32 carbon utilization strip (Cat. No. 32200-1004439110). These strips have 30 different carbon sources in individual wells, one well with no carbon source for a negative control, and one well with Ferric citrate. The inoculated strips were kept in a plastic box container with a lid and lined with moist paper towels to reduce drying. The initial inoculum of cells was prepared in 25 mL of MEA shaking at room temp for 5 days. Inoculation of the strips was done according to the instructions provided by the vendor, and each strain was inoculated in three separate strips for triplicate replication. Cells were diluted to the kit requirement of McFarland standard #3 (McFarland, 1907) before starting the inoculum. Growth in the ID strip lasted 10 days before evaluation. Growth in each well was

observed and evaluated by eye. Each well was compared to the negative control (no carbon) and the positive control (dextrose). Initial growth was evaluated on a: +, V, -, and - - scale. If a well had the same growth as the negative control it was given a "-", meaning no growth; if the well had less growth than the negative control it was given a "- -", meaning growth was inhibited by the carbon source; if a well had growth equal to or more than the dextrose well then it was given "+", meaning it was capable of growth on the carbon substrate; finally if the well was in between the negative control and positive control it was given a "V", for variable growth. Nuances of the fungal growth on individual carbon sources required a more gradual scale, and so scores were adjusted to form a range of 1-5 to allow for more accurate average calculation between the three replicates. For this scale: one was no growth or equal to the kits "-", five was the most growth and equivalent to the kit's "+"; numbers in between allowed us to average out the replicates to ensure we had a sliding scale of utilization rather than multiple variable "V" utilizations without a clear idea of how variable the utilization was.

Nitrogen utilization

Nitrogen utilization tests were performed using ten different nitrogen conditions. 100 mM was the concentration used for all compounds that contained one nitrogen atom per molecule: Proline, Ammonium tartrate dibasic, Serine, Sodium Nitrate, Glycine, Glutamate, and Aspartate; 50 mM was the concentration used for Urea because it has two atoms of nitrogen per molecule; 1% w/v of Peptone was used as a positive control; and no nitrogen was added as a condition for a negative control (**Table 2**). Liquid minimal media (MN) with MN salts (not 20x Nitrate salts) was used with the varying nitrogen sources to ensure that no alternative nitrogen source would be available to the fungi.

Fungi were first grown up in liquid MEA for 5 days at room temperature to reach maximum density. Then, 1 mL of cells was removed and washed three times with water. 99 µL of each nitrogen source-containing medium was added to six wells in a 96-well plate, for six replicates, and 1 µL of the washed cells was added to each well. 100 µL of each medium was also added to one well each without cells to blank each condition, because the different nitrogen sources created different colors of medium. Daily growth was measured from day 0 to day 7 at 420 nm, using the BioTek Synergy H1 hybrid spectrophotometer.

Optimal growth temperature and range of growth temperatures

To determine the temperature resistance range and optimal growth temperature for each isolate, we grew both fungi at 4 °C, 15 °C, 23 °C (i.e., ambient room temperature), 28 °C, 37 °C, and 42 °C. Isolates were first grown up in 25 mL of MEA for 5 days at room temperature to maximum density. Then 1 mL of cells was removed, and a 10x serial dilution was made from 0x to 100,000x, using pre-filled 1.5mL tubes with 900 µL of MEA and adding 100 µL of the previous tubes each time. Then 5 µL of each serial dilution was spotted onto a square MEA plate which allowed us to determine the carrying capacity of each isolate at the different temperatures. Plates were kept at their respective temperatures for 7 days before observations were made, however the 37 °C and 42 °C incubators required cups of water inside of them to prevent the plates from dehydrating. Plates grown in 42 °C and 37 °C were then allowed to grow at room temp for up to a week to determine if the isolates died at these temperatures or if their growth was just arrested.

UV resistance

Resistance to UV light was observed to determine if these black fungi, with highly melanized cell walls and constant exposure to sunlight in their natural habitat, were in fact UV resistant. To determine this, we used the UVP HL-2000 HybriLinker UV crosslinker as our source of UV light, which has a UV wavelength of 254 nm. Lower wavelengths (100-280 nm) are of the UV-C range, they are considered ionizing radiation and are the most detrimental to living organisms, but are completely blocked by the ozone layer (Molina & Molina, 1986; Schreier et al., 2015). Therefore, using this wavelength we are able to push our organisms beyond the UV limits found in their natural habitat and test extreme amounts of UV exposure. The fungi were inoculated in 25 mL of MEA in a 250 mL Erlenmeyer flask and let grow under shaking conditions at 200 rpm for 5 days at room temperature to reach maximum density. 100 µL of this culture was then spread out onto 6 MEA plates, using a glass spreader. Three plates were kept as the control growth, to compare to the three other plates which were exposed to the UV light. Experimental plates were placed inside of the crosslinker with their lids taken off. Then the plates were exposed to 120 seconds of UV light from a distance of 9.5 cm to the light source at 10,000 µJ/cm^2 (254 nm) (Frases et al., 2007). We then wrapped all plates in aluminum foil and placed them in the Percival light incubator set at 23 °C for 2 days. Placing UV-exposed cells in complete dark after exposure is essential for preventing native cell repair mechanisms to act upon any potential mutations, allowing for only those cells that are capable of withstanding the UV exposure without repair mechanisms to grow (Weber, 2005). After 2 days the plates were removed from the aluminum foil and left in the incubator for 5 more days before final observations. To

determine whether a particular isolate was resistant to UV exposure, the growth of the isolate exposed to UV was compared to the control growth.

Metal Resistance

Metal resistance is a relatively universal trait in many polyextremotolerant fungal species. Due to the under-studied nature of this particular characteristic in biological soil crusts and fungi, we decided to test if any of our isolates were resistant to any heavy metals which would indicate possible bioremediation capacity. In order to test metal resistance, we used the antibiotic disc method by aliquoting metal solutions onto paper discs and observing zones of clearance. Metals and concentrations used are listed in **Table 3.** For testing, 5 µL of each metal solution was aliquoted onto a dry autoclaved Wattman filter paper disc which was created using a standard hole puncher. These discs were then allowed to air dry and kept at 4 °C for up to a week. Initial growth of the fungal isolates was done in 25 mL of MEA, shaking at 200 rpm for 5 days at room temperature. We then spread 100 µL of each fungal isolate onto 100 mm sized MEA plates using a glass spreader to create a lawn. Using flame sterilized tongs our metal paper discs were placed onto the center of the petri dish on top of the fungal lawn and lightly pressed down to ensure the metal disc was touching the plate completely. These plates were then placed in the Percival light incubator at 23 °C with a 12 hr light/dark cycle for up to 2 weeks. Once a zone of clearing was clearly visible amongst the fungal growth (1-2 weeks), the zone of clearing was then measured in cm. Generally, large zones of clearing indicated sensitivity to the metal, whereas zones of reduced size were consisted with resistance to the metal.

Lipid profiles

Comparison of the lipid production of *S. cerevisiae*, *E. dermatitidis*, *E. viscosium*, and *E. limosus* was performed in the presence of fermentable vs. non-fermentable sugars in high and low nitrogen. To test these conditions we grew all four species in four different media types. 1) MEA; 2) MEA + 20 g/L of peptone instead of 2 g/L; 3) MEA with the dextrose replaced with the same weight amount of glycerol; 4) MEA with glycerol instead of dextrose and 20 g/L of peptone instead of 2 g/L. All four fungal species were first inoculated in 25 mL of liquid MEA in a 250 mL Erlenmeyer flask and shaken at 200 rpm for 5 days at room temperature to reach peak density. Then 100 µL was inoculated into 5 mL of each media in a size 25 mm tube, placed in a roller drum and allowed to grow at room temperature for 5 days.

To observe their lipid profile, we performed a standard Bligh Dyer lipid extraction (Bligh & Dyer, 1959). Equal wet weight of each organisms' cells was pelleted and re-suspended in 2 mL of methanol inside of 16 mm glass tubes. Tube openings were covered in Durafilm before applying the lid of the tube, then samples were boiled for 5 minutes and let cool for 10 minutes. Then 2 mL of chloroform and 1.6 mL of 0.9% NaCl were added, and the tubes were vortexed to fully mix. Tubes were then centrifuged at 5000 rpm for 5 minutes to separate the layers. The bottom lipid layer of the suspension was removed and placed in a new glass tube which was then dehydrated using nitrogen gas till the samples became fully dry. Dehydrated samples were then re-suspended with 100 µL of a 9:1 ratio of chloroform : methanol to run the thin layer chromatography (TLC) with. For all samples except the *S. cerevisiae*, 7 µL of the lipid suspension was used to dot the TLC. For *S. cerevisiae,* 10 µL of the lipid suspension was needed. The solvent systems used for TLC were Chloroform : methanol : glacial acetic acid: water

85:12.5:12.5:3 for the Polar lipid solvent system, and Petroleum ether : Diethyl ether : acetic acid 80:20:1 for the neutral lipid solvent system. The TLC plates were loaded with 7 or 10 µL of the re-suspended samples, and they were placed in the Polar solvent system for approximately 30 minutes (half-way up the plate) before transferring to the Neutral Lipid solvent system in a separate container till the solvent front reached just a few cm below the top of the plate. The plate was then removed and dried for 15 minutes, until the solution on the plate was no longer volatile, and the plate was placed in the presence of iodine (Sigma-Aldrich cat. No. 207772) in a glass chamber for 5 minutes until all the lipids were visible. The plates were then immediately placed in plastic covers and scanned and photographed for visualization and documentation.

Melanin experiments

Melanin biosynthesis gene annotation

Melanin biosynthesis in fungi occurs via three different pathways: the DHN pathway which creates allomelanin, the DOPA pathway which creates pheomelanin, and the tyrosine degradation pathway which creates pyomelanin (Cao et al., 2021; Gessler et al., 2014). Most fungal species only contain one melanin biosynthetic pathway, but there are many species in Pezizomycotina, particularly in the genera *Aspergillus* and *Exophiala*, which are capable of producing two or all three forms of melanin (Teixeira et al., 2017). For that reason, we decided to manually annotate the genes involved in all three melanin biosynthetic pathways in *E. viscosium* and *E. limosus* to determine if they too possessed all three melanin biosynthetic pathways. In all cases, the relevant *A. niger* genes were used as queries (Teixeira et al., 2017). Protein sequences for each gene were

found using the Aspergillus genome database (AspGD) and were tested using BLAST-P against the filtered model proteins database of *E. viscosium and E. limosus* on Mycocosm. Since *A. niger* contains paralogs for some melanin biosynthetic genes, all genes listed in (Teixeira et al., 2017) were used as queries for BLAST searches. Once the melanin biosynthetic genes in *E. viscosium* and *E. limosus* were identified, their highest matching protein sequences were then reverse BLASTed to the *A. niger* genome to determine the reciprocal best hit and ensure true homology.

Regulation of Melanin production using chemical blockers

Once it was established that both isolates contain the potential for production of all three fungal melanins, the effects of known chemical blockers of the DHN and DOPA melanin pathways was used to investigate melanin production. DHN melanin blocker Phthalide and the DOPA melanin blocker Kojic acid were both used in hopes of blocking melanin production in these isolates. Stock solutions were made according to (Pal et al., 2014): Phthalide was diluted in 70% ethanol, and Kojic acid in DMSO. Three separate experiments were performed using these melanin blockers, to determine which method would provide the most informative results.

The first was the disc diffusion method whereby Whatman filter paper discs were autoclaved and impregnated with 5 µL of either 10 mM of Phthalide or 10 mg/mL of Kojic acid. Impregnated filter paper discs were then placed on top of freshly spread lawns of either isolates on both MEA and YPD. Lawns were of 50:50 diluted 5-day old cells grown in MEA, and 100 µL of this dilution was spread onto the petri plates with a glass spreader. These plates were then grown at 23 °C with 12 hr light/dark cycles for 5 days. Additionally, both a Kojic acid disc and Phthalid discs were placed on fungal lawns ~4

cm apart simultaneously to observe their specific melanin-blocking capabilities on the same cells.

Next, we tried adding the melanin blockers directly to the medium as was done in (Pal et al., 2014). Since melanin is more universally distributed in *Exophiala* cells compared to *Aspergillus* cells, we decided to use the highest concentration of both Kojic acid and Phthalide that was used by (Pal et al., 2014), which was 100 mM of each compound. This concentration was added to both solid YPD and MEA after autoclaving, individually and combined. These plates were then used for two forms of growth experiments. Alternatively, we spread a lawn onto YPD and MEA with and without Kojic acid, Phthalide, and both compounds at 100 mM each. Finally, we performed a 10x serial dilution of both *E. viscosium* and *E. limosus* up to 10,000x diluted, and spotted 5 µL of each dilution onto MEA plates with and without Kojic acid, Phthalide, and both compounds. We let both growth experiments grow at 23 °C for 5 days with a 12 hr light/dark cycle.

Melanin Extraction and spectrophotometric measurements

Extraction of melanin from a variety of sources has been performed with two main categories of methods: chemical extraction and enzymatic extraction (Pralea et al., 2019). We were unsure which extraction method would be most applicable to these species, so both were performed. The enzymatic extraction method that was used came from (Rosas et al.) (2000). Alternatively, the chemical extraction method, which has been used more extensively in previous works, was derived from (Pal et al., 2014). Their method for extraction and purification of melanin from culture filtrate was adapted and used for all future secreted melanin extractions. Adjustments to the Pal et al. method

included: the 6M HCl precipitation took multiple days instead of overnight for melanin to precipitate, then stopping the protocol when 2M NaOH was added to the extracted melanin. We did not continue on to re-precipitation and drying of the melanin as this product did not reprecipitate in any solvents used.

Exact methods are as follows. 10 mL of culture was centrifuged at 3,000x g for 5 minutes, and the resulting supernatant was filter sterilized through a 2 μm filter to ensure all cells were removed. The filtered supernatant was then transferred into a 50 mL centrifuge tube, and 40 mL of 6M HCl was added to the tube. The filtrate was then allowed to precipitate out for up to two weeks. Precipitated solutions were then centrifuged at 4000 rpm for 3 minutes, and the resulting supernatant was discarded. The pellet was washed with 2 mL of dd H_2O, vortexed, centrifuged, and the supernatant discarded. Then 3 mL of 1:1:1 Chloroform : ethyl acetate : ethanol was added to the samples and vortexed vigorously to ensure as much re-distribution of the melanin was accomplished. The tubes were then centrifuged again, and any resulting clear layers (top and or bottom) were discarded, leaving behind the dark layer. 2 mL of water was added to the sample for washing, and the tubes were centrifuged again, and the entire supernatant was discarded. Finally, 1 mL of 2M NaOH was added to each sample to allow for a standard volume added even if the melanin amount and therefore the final volume varied.

Extracted melanin samples suspended in 1 mL of 2M NaOH were then diluted 5 μL into 195 μL of 2M NaOH into a 96-well plate, with a 200 μL 2M NaOH blank well. These diluted samples were then read using the BioTek Synergy H1 hybrid spectrophotometer. The settings were for a full spectrum read from 230 nm to 700 nm,

with 10 nm steps. However, the machine could not read ODs above 4.0, and therefore only data from 300 nm to 700 nm was used.

Melanin secretion and its concentration in the supernatant

To confirm that *E. viscosium* and *E. limosus* are actively secreting melanin, as opposed to dead cells lysing and releasing it, we grew up both species and took daily aliquots for melanin extraction. Additionally, we wanted to compare the melanin secretion capabilities of these species to *E. dermatitidis* for a baseline comparison. All three species were grown up in liquid MEA shaking at room temperature for 5 days. Then 2 mL of cells were washed with water three times. 500 μL of washed cells were then inoculated into 100 mL of MEA and YPD in 500 mL flasks. We let the cells grow at 23 °C shaking at 200 rpm for 7 days, removing 11 mL of cells and supernatant daily and pipetting them into 15 mL centrifuge tubes. The tubes of cells were then centrifuged at 3000 rpm for 5 minutes, the supernatant was removed, filter sterilized through a 2 μm filter, and placed into a new tube. We filter sterilized the supernatant to ensure that no cells remained in the supernatant, therefore all of the melanin extracted came only from secreted melanin. Melanin was then extracted using the chemical method explained above. Resulting pure melanin for all samples was read with the full spectrum as stated above, and both standard OD and log scale graph were created to confirm the presence of melanin with the proper R^2 value above 0.9 (Pralea et al., 2019).

Increasing amounts of peptone

To assess the role of nitrogen levels in melanin secretion, we initially switched the concentration of peptone added to YPD and MEA media; the new media would be: YPD + 0.2% peptone, and MEA + 2% peptone. We then took both *E. viscosium* and *E. limosus*

that was grown in liquid MEA for 5 days shaking at room temperature and plated out the species onto these new media using the same technique as described above for growth comparison on different media. To determine if a more gradual increase in peptone would correlate with a gradual secretion of melanin, we took the base media of MEA (solid) and changed the concentration of peptone to: 0.1%, 0.5%, 1%, 1.5%, 2%, 2.5%, 3%, 3.5%, 4%, and 5%. We then spotted 5 μL of both species onto the plates after performing a 10x serial dilution up to 10,000x dilution. The plates were grown at 23° for 10 days with a 12 hr light/dark cycle.

Albino mutant experiments

Creation of EMS mutants and annotation of their mutations

Genetic modification of these species has not been established yet. However, random mutagenesis via chemical mutagens was performed in the hopes of finding albino mutants, to provide greater insight into the regulation of melanin production. UV exposure which is used frequently as a mutagen for random mutagenesis was attempted, but never resulted in phenotypically distinct mutants or albino mutants. Instead, we used ethyl methyl sulfonate (EMS) to induce G:C to A:T mutations randomly within the genomes of our two species. This was performed using the method by Winston (Winston, 2008). Albino mutants and other interesting pigmentation or morphological mutants were isolated from the resulting mutagenesis, and their DNA was extracted using the same CTAB extraction manner stated above. Their DNA was then sent to the Microbial Genome Sequencing Center (MiGS) for genome re-sequencing and base-called against the wild-type DNA. Resulting mutations were then manually annotated using the JGI

Mycocosm genome "search" tool to determine if any genes were disrupted by the mutations to cause the phenotype observed.

Recovery of melanin production in albino mutants

Following recovery of our albino mutant, we attempted to restore melanin production via chemical induction of the other melanin biosynthetic pathways. We did this using hydroxyurea (HU), L-DOPA, and 1,8-DHN. Hydroxyurea has been shown to enhance melanin production in *E. dermatitidis*, and L-DOPA is needed for certain fungi to produce melanized structures, including the albino mutant form of *E. dermatitidis* WdPKS1 (Dadachova et al., 2007; Paolo et al., 2006; Schultzhaus et al., 2020). Both YPD and MEA medium was made up and 20 mM of HU, 1 mM of L-DOPA, or 1 mM of 1,8-DHN was added to the medium after autoclaving. Our albino mutant was then grown up in the same way as our wild type cells. 5 µL of grown cells were spotted onto these media with added compounds and they were grown for 10 days at 23 °C 12 hr light/dark cycle.

Data Availability

All data generated is available through the JGI Mycocosm website under *E. viscosium* and *E. limosus,* or at NCBI under accession numbers JALDXI000000000 for *E. viscosium* and JALDXH000000000 for *E. limosus.* Transcriptomes for these fungi can be found at NCBI using the SRA numbers: SRX5076261 for *E. viscosium,* and SRX5077344 for *E. limosus*. The type strains of *E. viscosium* CBS 148801 and *Exophiala limosus* CBS 148802 have also been deposited to the Westerdijk institute for access to the scientific community, but all strains used in this study can also be obtained from the corresponding author upon request. Finally, if any additional details or questions are

required for the replication of any experiments listed above, one may reach out to the corresponding author.

Results

Description of Exophiala viscosium and Exophiala limosus

Exophiala viscosium JF 03-3F Goopy CBS 148801 was isolated from Jackman Flats Provincial Park in British Columbia, Canada (52.931383 N, 119.372059 W). Initial ITS sequencing was performed to obtain potential taxonomic matches. BLAST results to its ITS sequence matched 97.57% to "*Exophiala nigra* strain CBS 535.95" accession number: MH862481.1. Whole genome sequencing and further phylogenetic analyses subsequently revealed that *E. viscosium* is a novel species closely related to *E. sideris* (**Figure 2**). Morphological characterization of *E. viscosium* demonstrated that compared to *E. dermatitidis*, *E. viscosium* has much darker pigmentation, and is also a more viscous cell culture. When scraping a colony off the plate it comes up like stretchy tar usually leaving a string of cells hanging off the sterile loop. *E. viscosium* does not disperse in water easily when re-suspending, but it does pellet easily at 10,000x g for 1 minute. When grown up on a MEA plate for a week or more, it will begin to form a rainbow sheen like an oil slick (**Figure 3A**). Hyphal growth will begin to form into the agar when the plate is left alone at room temperature for more than three weeks. Interestingly, secretion of melanin into the agar can be observed after two weeks on MEA and one week on YPD plates. In liquid culture, this occurs more quickly, with melanin observed in the supernatant starting at 5 days in MEA and 3 days in YPD. The cellular morphology of *E. viscosium* is that of a true yeast. It has large tear-drop shaped cells that usually bud

one at a time but can sometimes bud 2-3 times simultaneously (**Figure 3B**). Lipid bodies are frequently observed, as the large circles within cells (**Figure 3B**) and have been confirmed by Nile red staining (data not shown). This isolate grows to its maximum density in 7 days at 23 °C in 25 mL of MEA in a 250 mL Erlenmeyer flask shaken at 200 rpm. *Exophiala viscosium* was originally referred to as "Goopy" due to the nature of its morphology. Accordingly, we have formally named it *Exophiala viscosium* for the Latin term of viscous.

Exophiala limosus JF 03-4F Slimy CBS 148802 was isolated from a biological soil crust on public land in B.C. Canada. The ITS region of *E. limosus* most strongly matched "*Exophiala nigra* strain CBS 535.95" accession number: MH862481.1 with an identify of 97.67%. Although both *E. viscosium* and *E. limosus* have similar phylogenetic placement, their cellular morphology and budding patterns differ drastically (**Figures 3** & **5**). As seen in **Figure 3D**, the cellular morphology of *E. limosus'* resembles that of *Horatea werneckii* as observed by (Mitchison-Field et al., 2019). Cells are more elongated than *E. viscosium*, and when grown up to maximum density pipetting becomes difficult due to large clumps of cells formed by its more filamentous growth pattern. Both isolates have the consistency of sticky black tar, and an iridescent shine that forms after a week on an MEA plate. *Exophiala limosus* also fails to easily disperse when suspended in water but can be readily pelleted. These observations and the prominence of lipid bodies within the cells (**Figure 3D**) suggests that lipid-derived compounds could cause their sticky, water repelling, iridescent nature. This isolate grows to its maximum density in 7 days at 23 °C in 25 mL of MEA in a 250 mL Erlenmeyer flask shaken at 200 rpm. Originally, *E. limosus* was named "Slimy" to reflect its colony characteristics.

Accordingly, we have formally named it *Exophiala limosus* for the Latin term of muddy. Notably, *E. limosus* possesses a looser pellet and is less refractory to re-suspension than *E. viscosium*.

Genome description

The genome assembly sizes of these two novel *Exophiala* species are: 28.29 Mbp for *E. viscosium* and 28.23 Mbp for *E. limosus* (**Table 4**). These sizes are similar to other yeasts in the genus *Exophiala* and are only a bit smaller than their closest relative *E. sideris* (29.51 Mbp). Although their genomes are smaller than *E. sideris*, predicted gene content is relatively higher; 11344 for *E. viscosium* and 11358 for *E. limosus* as compared to 11120 for *E. sideris* (**Table 4**). However, *E. sideris* appears to possess longer genes, transcripts, exons, and introns compared to *E. limosus* and *E. viscosium,* which could also contribute to the gene number to genome size differences (**Table 4**). *E. viscosium* contains the highest GC% amongst the *Exophiala* species listed in **Table 4**. *E. viscosium*'s GC content is even higher than *E. limosus* by 2.65%, which given their genetic similarities is quite interesting.

Mating type

Exophiala species are one of the many fungal genera whose mating capabilities remain incompletely understood and vary across the genus (Teixeira et al., 2017). The closest species to *E. viscosium* and *E. limosus* is *E. sideris,* within which both mating types have been characterized as a single fused gene (Teixeira et al., 2017). Given the known order of genes in regions flanking the MAT locus in *Exophiala* species, we used comparative approaches to determine the mating identities of the sequenced *E. viscosium* and *E. limosus* isolates, and to look for possible evidence of homothallism that is also

presumed in *E. sideris*. Homologues of the genes *APN2*, *SLA2*, *APC5*, *COX13*, and *MAT1* (*MAT1-1/alpha*) in *E. viscosium* and *E. limosus* were identified via BLAST searches. We found that *APN2* and *SLA2* flank the *MAT* gene of both species, and they also contain the Herpotrichalleaceae-specific mating gene *MAT1-1-4* (**Figure 4**). These results are not surprising, in that this is the exact same order of these genes in *E. sideris*. Interestingly, as Teixeira et al. indicate, in *E. sideris* the *MAT* gene is a fused *MAT1-1/MAT1-2* gene with the HMG domain in the middle splitting the α-box in half (Teixeira et al., 2017). When the MAT gene protein sequences of *E. viscosium* and *E. limosus* are aligned with the *MAT* gene of *E. sideris*, we see very high homology indicating that these fungi also contain a fused *MAT* gene. This fused *MAT* gene is theorized to allow these species to be homothallic, although this has not been confirmed experimentally in any of these three species. Additionally, neither *E. viscosium* nor *E. limosus* contain an additional gene between *APN2* and the *MAT1-1-4* that is found in *E. sideris* (Teixeira et al., 2017). Furthermore, *COX13* and *APC5* are about 7,000 bp downstream of the MAT locus in both species, but *COX13* is on the opposite strand in *E. limosus* (**Figure 4**).

Phenotyping of *E. viscosium* and *E. limosus*

To further understand the morphology, growth capabilities, and stress responses of *E. viscosium* and *E. limosus*, we performed multiple phenotyping experiments. The intent of these experiments was to provide a broader perspective on the potential adaptations that would support the ability of these fungi to successfully colonize biological soil crusts and other extreme niches.

Budding patterns

Due to these species' similarities in colony morphology, observations of budding patterns in these new species became an essential task for differentiation. Microscopy was initially performed on cells grown from solid agar plates, which provided us with basic information that their cell morphology was different, with *E. viscosium* being very round and yeast-shaped and *E. limosus* having more elongated, connected cells. But details regarding their budding patterns and cell polarity we're also needed. Using adapted protocols from (Mitchison-Field et al., 2019) we were able to perform a long-term microscopy time-lapse of the budding patterns of these species using the VALAP (1:1:1 Vasoline: Lanolin: Parafin) method to seal the edges of a coverslip while allowing gas exchange for cells to actively grow (**Figure 6**).

From this we were able to observe dramatic differences in the budding types of *E. viscosium* and *E. limosus*. *E. viscosium* buds with round cells in initially a distal fashion where the new bud forms 180° from the mother cell origination site, but also forms new buds at a ~90° angle from where the mother bud was formed in a proximal manner (**Figure 5; Video 1**). *E. limosus* on the other hand forms elongated cells in a distal manner, forming longer chains of cells instead of clusters, with axial buds forming at later timepoints (**Figure 5; Video 2**). These morphological differences in budding patterns influences the way these two species grow in a shaking flask. For example, *E. limosus* forms more elongated cells and buds distally which while does not create true hyphae, still creates larger clumps of cells which are not easily pipetted. However, *E. viscosium* since it forms rounder cells and buds with both distal and proximal patterns, does not form extensive clumps in a shaking flask and is more easily pipetted. *E. limosus*

also forms more extensive biofilms at the liquid-air interface than *E. viscosium*, likely also due to the elongated cell morphology.

Growth of E. viscosium and E. limosus on 8 different medias

Growth of *E. viscosium* and *E. limosus* on a variety of different media was done to evaluate growth requirements and their impact on pigmentation (**Figure 6**). The media used are described in **Table 1**, and include MAG, MEA, MN+NAG, MNV, PDA, Spider, YPD, and V8. The addition of Vitamin mix (**Table 1**) to any medium, but specifically to MAG and MN, caused the growth of both isolates to become much shinier, blacker (vs. browner), and more yeast-like. Growth on MEA causes the formation of a rainbow sheen, which is not seen on any other medium. Spider medium and YPD caused the formation of a dark-colored halo around colonies of both species. However, the halo around colonies grown on YPD is much darker and extends further than on Spider medium, and *E. viscosium* showed a more extensive halo than *E. limosus*. The ability of both species to grow on V8 medium implies that they can use cellulosic material as a carbon source. Overall, colony growth and pigmentation were similar across of media types for both species (**Figure 6**).

Carbon and nitrogen utilization

Carbon source utilization was determined using Biomerieux C32 carbon strips, which are typically used for identification of human pathogens (Tragiannidis et al., 2012). Following the protocols provided by the vendor, we were able to show that *E. viscosium* and *E. limosus* can utilize a wide range of carbon sources. Triplicates were performed on these strips to ensure results were uniform and representative. Overall, a variety of carbon sources supported robust growth of both species (e.g., D-glucose, L-

sorbose, D-galactose, N-acetyl glucosamine, D-sorbitol, D-xylose, glycerol, L-rhamnose, L-arabinose, D-celliobiose, and maltose), and there are only a few quantitative differences in utilization patterns (**Figure 7; Tables 5 & 6**). Carbon sources that could not support growth include D-rafinose, D-melibiose, methyl-aD-glucopyranoside, and D-lactose. Both species were resistant to cycloheximide and were capable of producing a black color in the presence of esculin ferric citrate (**Figure 7**). Notably, for both *E. viscosium* and *E. limosus*, growth on some carbon sources, particularly sorbose, levulinic acid, and N-acetyglucosamine, lead to enhanced pigmentation (**Figure 7**).

We were particularly interested in patterns of nitrogen utilization for *E. viscosium* and *E. limosus* given their isolation from a nutrient deplete niche with extensive nitrogen-fixing bacterial populations. Nine different nitrogen sources were tested: five amino acids (aspartate, glutamate, glycine, proline, serine), ammonium tartrate, sodium nitrate, urea, peptone (mixed short chain amino acids) as a positive control, and no nitrogen as a negative control. Both species are incapable of utilizing Aspartate and Glutamate as nitrogen sources (**Figure 8**). Preferred nitrogen sources for both species include ammonia and proline. However, they differ in that *E. viscosium* also prefers urea while *E. limosus* also prefers serine (**Figure 8**). Otherwise, patterns of nitrogen utilization appear generally similar across both species.

Optimal Growth Temperature and Range of growth temperatures

E. viscosium and *E. limosus* were isolated from an environment that experiences wide seasonal and diurnal temperature changes. As such, we wanted to determine both the optimal growing temperature for these species, as well as the limits at which they are capable of survival. Both isolates were serial diluted and spotted onto MEA plates to

determine the carrying capacity at different temperatures. Both *E. viscosium and E. limosus* were capable of growth at 4 °C, 15 °C, 23 °C, and 27 °C, but could not grow at 37 °C and 42 °C (**Figure 9**). Optimal growth temperature of both *E. viscosium* and *E. limosus* was 23 °C (**Figure 9**). Growth at 4 °C was slow, but after a year the isolates both species formed extensive colonies and flooded the agar with melanin (**Figure 10**). Although neither species grew at 37 °C, they retained viability as they were able to resume growth following return to 23 °C after three days exposure to 37 °C (**Figure 10**). In contrast, a similar experiment showed that incubation at 42 °C is lethal.

UV and metal resistance

Melanized fungi are recognized for their resistance to UV light, and the possibility of using ionizing radiation as an energy source (Dadachova et al., 2007). To assess the response of *E. viscosium* and *E. limosus* to UV radiation, they were each exposed to a dose (120 seconds of 10,000 μJ/cm^2 at 254 nm) that was lethal to *S. cerevisiae* and *E. dermatitidis* (data not shown). The same level of exposure did not kill either *E. viscosium* or *E. limosus* (**Figure 11**) but did significantly reduce the number of viable colonies. Strikingly, surviving colonies showed no evidence of induced mutagenesis based on the absence of altered morphologies or pigmentation (**Figure 11**). Polyextremotolerant fungi have been previously noted as having increased metal resistances as a result of their melanized cell wall and other adaptations to harsh environments (Gadd & de Rome, 1988). To test if these two new *Exophiala* spp. possess increased metal resistances when compared to *E. dermatitidis* and *S. cerevisiae*, we impregnated Whatman filter discs with various metals of different concentrations. Diameters of zones of clearing revealed no evidence for enhanced metal resistance in *E.*

viscosium or *E. limosus* (**Table 6**). On the other hand, both species appear to be moderately more sensitive to $NiCl_2$ and $CdCl_2$ (**Table 6**).

Lipid Profiles

Both *E. viscosium* and *E. limosus* appear to possess abundant lipid bodies (**Figure 3**). This observation along with the unique sticky morphology of both species led us to the idea that they might contain unique or copious amounts of lipids. We performed a Bligh and Dyer lipid extraction followed by thin layer chromatography (TLC) to observe patterns of lipid accumulation in *E. viscosium* and *E. limosus* grown on media that contained fermentable or non-fermentable sugars, both with high nitrogen and low nitrogen. These iterations creating four unique medias would allow us to cover as much of a spread of lipid changes as possible. *S. cerevisiae* and *E. dermatitidis* were also similarly analyzed. Results from this lipid extraction showed that our two new species did not seem to produce any unique or novel amounts or types of lipids when compared to *S. cerevisiae* and *E. dermatitidis* (**Figure 12**).

Melanin production and regulation in E. viscosium and E. limosus

Melanin biosynthesis gene annotation

A defining feature of black yeasts such as *E. viscosium* and *E. limosus* is their pigmentation caused by the accumulation of melanin (Bell & Wheeler, 1986). Given the presumed importance of melanin to a polyextremotolerant lifestyle, we are interested in understanding how melanin production is regulated in response to environmental inputs. A first step in this process is to determine the types of melanin that *E. viscosium* and *E. limosus* are capable of producing. To accomplish this, the sequenced genomes of *E.*

viscosium and *E. limosus* were annotated using protein sequences for all three melanin biosynthetic pathways in *Aspergillus niger* (Teixeira et al., 2017). The list of *A. niger* genes and their homologs in both *E. viscosium* and *E. limosus* are summarized in **Table 7**. Manual annotation and reverse BLASTP of the melanin biosynthesis pathway genes showed that both *E. viscosium* and *E. limosus* have the genetic capability to produce all three forms of known fungal melanins: DOPA melanin (pheomelanin), DHN melanin (allomelanin), and L-tyrosine derived pyomelanin.

Regulation of Melanin production using chemical blockers

Because *E. viscosium* and *E. limosus* possess the capability to produce all three forms of fungal melanin, we asked whether they were all being produced simultaneously or if one was preferred for production versus secretion. We used chemical blockers for both DOPA melanin and DHN melanin to determine the predominant type of melanin produced on MEA and YPD. Kojic acid blocks the production of DOPA melanin, whereas Phthalide inhibits the synthesis of DHN melanin; both are effective at doses of 1, 10, and 100 μg/mL (Pal et al., 2014).

First, we used 100 mM of phthalide and 100 mg/mL of kojic acid in a filter disc assay. Placing drug-impregnated filter discs on freshly spread lawns of cells either individually or with both drugs combined did not block melanin production even though the concentrations of the drugs were higher than that of previous studies (**Figure 13**). Then using Pal et al.'s method of melanin blocking (Pal et al., 2014), we added the highest dosage (100 μg/mL) of Phthalide and Kojic acid individually and combined to agar-solidified MEA, and both spread a lawn of cells and spotted serially diluted cells onto the plates. Neither assay resulted in blockage of melanin production in *E. viscosium*

or *E. limosus* (**Figure 13**). However, addition of 100 µg/mL of Phthalide alone did result in their apparent secretion of a dark substance into MEA (**Figure 14**). Overall, chemical inhibition of DOPA melanin or DHN melanin production did not qualitatively reduce colony pigmentation, possibly suggesting that the tyrosine-derived pyomelanin is still being produced.

Melanin Secretion

The appearance of a dark pigment surrounding colonies of *E. viscosium* and *E. limosus* under specific conditions raised the idea that these yeasts are able to secrete melanin into their local environment. The presence of dark pigments in the supernatants of liquid cultures lent further support to this.

Initial studies were performed to determine which media triggered the release of melanin. Both *E. viscosium* and *E. limosus* were capable of releasing the most melanin and in the shortest growth time on YPD, with *E. viscosium* seemingly secreting more than *E. limosus* (**Figure 5**). Because YPD and MEA only differ in yeast vs. malt extract as well as the percentage of peptone (2% in YPD, 0.2% in MEA), we first determined if the peptone differences impacted melanin secretion. By switching the peptone amounts in YPD and MEA, we demonstrated that *E. viscosium* acquired the ability to secrete melanin on MEA if it was supplemented with 2% peptone. To extend this observation, we added progressively higher amounts of peptone to MEA media (i.e., 10 different concentrations of peptone ranging from 0.1% to 5%). We observed that *E. viscosium* starts secreting melanin on MEA at a peptone amount of 2%, and *E. limosus* starts secreting melanin at about 4% peptone (**Figure 16**).

Confirmation of active melanin secretion from living cells

To confirm that the dark pigment in culture supernatants is indeed melanin, we performed a melanin extraction using previously described methods (Pal et al., 2014; Pralea et al., 2019). Although both enzymatic and chemical extraction of melanin was attempted, the chemical extraction process proved to be more efficient at recovering secreted melanin (**Figure 17**). Therefore, all extractions going forward were performed using the chemical extraction method to ensure all melanin was precipitated out of the solution.

Growth of *E. viscosium, E. limosus,* and *E. dermatitidis* on YPD and MEA were observed daily for melanin secretion; 11 mL aliquots of their supernatant were removed daily, and the melanin was extracted from each sample. As the experiment progressed, it was obvious that *E. viscosium* and *E. limosus* began secreting melanin on day 3 and secreted more in YPD than in MEA (**Figure 18**). *E. dermatitidis* on the other hand seemed to have a slower build-up of melanin, and melanin wasn't truly obvious in the medium until day 6 in MEA though it can be seen in MEA day 3 in **Figure 18**. Analysis of the optical density (OD) of extracted melanin revealed that melanin amount increased over the course of the experiment, and that greater amounts of melanin are released in YPD for *E. viscosium* and *E. limosus* compared to MEA for *E. dermatitidis* (**Figure 17**). Interestingly, for both *E. viscosium* and *E. limosus*, their peak melanin secretion was on day 6 and not on day 7 (**Figure 19**). There was actually less melanin on day 7 for both species, indicating that the melanin after day 6 was either degrading, or was being taken back up by the cells. This was only obvious with reading the OD results of the extracted melanin, as the supernatants themselves day 5 and on were all strikingly dark and hard to differentiate visually (**Figure 18**). Extracted melanin from all *E. viscosium* and *E. limosus*

samples displayed the typical results from a full spectrum read on pure melanin, *E. dermatitidis* did not show typical melanin spectrum results until day 6 in YPD but were typical every day in MEA. When graphed with OD to Wavelength the sample should have an exponentially decreasing OD as wavelength increases, and when the OD is changed to a log scale, the full spectrum read should be a linear regression with an R^2 value of 0.97 or higher (Pralea et al., 2019). All *E. viscosium* and *E. limosus* samples displayed these features, and therefore we can confirm that the dark nature of their supernatants is caused by actively secreted melanin.

Genetic analysis of Melanin Production

Creation of an albino mutant

At this time, molecular tools for the manipulation of *E. viscosium* and *E. limosus* are not yet available. Therefore, we combined classical genetics with genome re-sequencing to initially investigate the regulation of melanin production. Following mutagenesis with the alkylating agent ethyl methyl sulfonate (EMS), mutants following into four distinct phenotypic classes were recovered: pink/albino, crusty, brown, and melanin over-secretion (Data not shown). The most intriguing of these phenotypes was the pink/albino phenotype found in a mutant of *E. limosus* we called EMS 2-11 (**Figure 20**). This mutant is considered albino but colored pink likely due to *Exophiala* spp. production of carotenoids. It has already been shown that blockage of melanin production in *E. dermatitidis* by mutations in *pks1* results in pink instead of white albino colonies because they also produce carotenoids and by-products such as flavolin that are normally masked by melanin (Geis & Szaniszlo, 1984; Geis et al., 1984).

Genome re-sequencing of high molecular weight DNA from mutant EMS 2-11 and comparison to the reference *E. limosus* genome revealed a deleterious SNP causing a nonsense mutation in *pks1*. This mutation was on position 2,346,590 in scaffold 3, located in the *pks1* gene, which caused an C -> T mutation on the first position of the codon such that it became a stop codon, Q814STOP. Interestingly, *pks1* only functions in one of the three melanin biosynthetic pathways found in *E. limosus*. Only two of the other random mutations found in EMS 2-11 were missense or nonsense mutations. One is a mutation in a transcriptional repressor EZH1, and another is in alcohol dehydrogenase GroES-like/Polyketide synthase enolreductase. Although either of these mutations could contribute to the pink phenotype, it is more likely that a nonsense mutation in *pks1* is solely responsible for the loss of melanin production despite the lack of mutations in the other melanin biosynthetic pathways.

Recovery of melanin production in albino mutant

Pks1 is a polyketide synthase that is essential for the first step in the DHN-melanin/Allomelanin production pathway. To test if "activation" of an alternative melanin production pathway could restore melanin production to the EMS 2-11 mutant, we substituted 1 mM of L-DOPA into the medium. As L-DOPA was shown to recover melanization in a *pks1* deletion mutant of *E. dermatitidis*, thus presumed that it would be taken up by our EMS 2-11 mutant and activate the DOPA melanin/pheomelanin biosynthesis pathway (Dadachova et al., 2007; Paolo et al., 2006). However, substitution of 1 mM L-DOPA into either MEA or YPD did not induce melanin production in the EMS 2-11 *pks1* mutant (**Figure 20**). These plates were grown in the dark for 10 days, as L-DOPA will auto polymerize into a melanin precursor in the presence of light, and still

no melanin production was observed. Hydroxyurea is another compound that in other *Exophiala* species induces melanin production, however addition of 20 mM of Hydroxyurea also did not activate melanin production in our EMS 2-11 albino mutant (**Figure 20**) (Schultzhaus et al., 2020). Finally, we substituted in 1 mM of 1,8-DHN into their media which is the immediate precursor to DHN melanin, in hopes of recovering the expected melanin biosynthetic process with a *pks1* mutant. This did result in recovery of melanized colonies, while on MEA they do not form extensive growth, their cells are still dark, and on YPD active dark colony growth is observed (**Figure 20**).

Discussion

A major limitation to our understanding of the roles played by BSCs in semi-arid ecosystems is our lack of insight into the microbial components of these biofilms and the nature of their functional interactions (Carr et al., 2021). As photoautotrophs, the roles of cyanobacteria and algae in BSCs are clear (Belnap, 2002), but the importance of other residents such as fungi and bacteria is less so. Here, we identify two novel species of black yeasts from BSCs; *E. viscosium* and *E. limosus*. In addition to presenting the complete annotated genome sequence for each species, we also provide a relatively detailed profile of their ability to utilize diverse carbon and nitrogen sources, as well as their response to different forms of stress. Most importantly, we demonstrate that *E. viscosium* and *E. limosus* are capable of producing excessive amounts of melanin, including melanin that is secreted at high levels. Our results suggest that by making melanin available as a public good, black yeasts provide a critical service to the broader BSC community.

Description and genome features of E. viscosium and E. limosus

E. viscosium and *E. limosus* are two novel fungi from the family Herpotrichielleaceae that we isolated from a lichen-dominated BSC. Distinguishing features of these isolates includes their yeast morphology, pronounced melanization, and production of extracellular material that leads to the formation of "goopy" or "slimy" colonies. Notably, numerous other melanized fungi with filamentous or polymorphic characteristics were isolated from the same BSC communities. These fungi, which will be described in detail elsewhere, grow much more slowly than *E. viscosium* or *E. limosus* and also release much less melanin.

Phylogenetic comparisons suggest that the closest relative of *E. viscosium* and *E. limosus* is *E. sideris*. Comparison of their respective annotated genome sequences revealed that overall gene content and characteristics are similar across all three species. *E. sideris* belongs to the *jeanselmei*-clade of *Exophiala* species; it is typically recovered from highly polluted environments and is not known to be pathogenic (Seyedmousavi et al., 2011). The failure of *E. viscosium* and *E. limosus* to grow at 37 ºC reinforces the point that species within this clade are less likely to possess the capacity of causing disease in mammals. One interesting feature that the genome comparisons of *E. sideris* to *E. viscosium* and *E. limosus* revealed was that *E. sideris* contains a lower predicted gene content than the other two isolates. This could be a factor of their differences in their ecology and lifestyles. *E. sideris* was isolated from a highly toxic environment containing arsenate, hydrocarbons, and other toxins meaning this species had to specialize in withstanding these toxins rather than generalizing its survival genetic toolbox (Seyedmousavi et al., 2011). MAT organization of the MAT locus between these

homothallic species is very similar, all containing a fused *MAT* gene, with the exception of different transcript directionality for the flanking *cox13* and *apc5* genes. Many *Exophiala* species are indicated to be heterothallic, even closely related species to *E. sideris* such as *E. oligosperma* and *E. spinifera* are heterothallic (Teixeira et al., 2017; Untereiner & Naveau, 1999). Whereas *E. sideris* itself and now *E. viscosium* and *E. limosus* all contain a fused or cryptic MAT gene which has been hypothesized to cause homothallism as a result of a parasexual cycle that occurred (Teixeira et al., 2017). Further investigation of these ideas will require demonstration that these *Exophiala* species undergo sexual development.

Phenotypic characterization of E. viscosium and E. limosus

Our results show that *E. viscosium* and *E. limosus* are capable of using a diverse array of carbon sources. These include mannitol, ribitol, and glucose, which are considered the main carbon sources exchanged between photobionts and their mycobiont partners in lichens (Richardson et al., 1967; Yoshino et al., 2020). Although, *E. viscosium* and *E. limosus* are able to use most nitrogen sources provided, glutamate and aspartate are clearly not being taken up or used, unlike in yeasts such as *S. cerevisiae* where glutamate is a more favorable nitrogen source used for multiple core metabolism and amino acid production processes (Ljungdahl & Daignan-Fornier, 2012). Because peptone is a favorable nitrogen source for *E. viscosium* and *E. limosus*, it is likely that these species can import peptides and degrade them as sources of ammonia. Their preferred nitrogen source is ammonium/ammonia though, which in their ecological environment would likely be produced by cyanobacteria and other nitrogen-fixing bacteria (Belnap,

2002). However, they can also use nitrate and urea as nitrogen sources, again pointing to their metabolic flexibility in their nutrient deplete ecosystem.

A characteristic feature of BSCs is the inherently stressful nature of these ecosystems. Of note, *E. viscosium* and *E. limosus* were isolated from a site that can experience extremes in temperature, UV exposure, and soil wetness/osmotic pressure. Although the optimal growth range for these species is from 15 °C to 27 °C, they are capable of slow growth at 4 °C and while they do not grow at 37 °C, they do remain viable after 72 consecutive hours of exposure to this temperature. The ability to grow at 4ºC, albeit slowly, presumably contributes to the success of fungi such *E. viscosium* and *E. limosus* in adapting to BSCs in colder drylands. A broader comparison of microbiomes and associated functional traits between cold-adapted BSCs and those found in hot deserts would be an informative approach to identifying microbial species and/or physiological factors that underlie temperature adaptation.

As for resistance to UV radiation, *E. viscosium* and *E. limosus* were both able to survive the high exposure of UV-C that was used and were uniquely resistant to standard UV mutagenesis conditions. Potential mechanisms that might contribute to UV resistance include the presence of melanin or other defensive compounds, some of which could be public goods provided by other constituents of the BSC community, or an enhanced capacity to repair damaged DNA. This will ultimately be an interesting topic to investigate in the future.

One feature we expected to find in *E. viscosium* and *E. limosus* but we did not necessarily observe was higher metal resistance. Melanin is known to enhance resistances to metals (Bell & Wheeler, 1986; Gadd, 1994; Gorbushina, 2007; Purvis et al., 2004), and

so we predicted that these species would have increased metal tolerance when compared to non-melanized fungi. However, of the metals tested, only $AgNO_3$ and $CuCl_2$ showed a decreased zone of clearing in *E. viscosium* and *E. limosus*, compared to *S. cerevisiae* and *E. dermatitidis*. A potential explanation for the latter observation is that melanin has a higher affinity for copper due to the phenolic compounds within the polymer (Gadd & de Rome, 1988).

Secretion of melanin by E. viscosium and E. limosus

Melanin is considered an expensive secondary metabolite to produce because it is made up of conglomerates of polyphenols and as such contains many carbons (Schroeder et al., 2020). Therefore, it would be assumed that an organism would not want to create melanin just to export it out of the cell unless there was a beneficial reason behind it. Additionally, there are not many fungi known to secrete melanin and few in the genus *Exophiala*, so the possibility of novel species that secrete melanin into their surroundings was intriguing. Both novel fungi have the genetic makeup to produce all three types of fungal melanin: allomelanin (DHN derived), pyomelanin (L-tyrosine derived), and pheomelanin (L-DOPA derived); but it is still unknown how these melanin biosynthetic pathways are regulated, and which are being actively produced.

In our attempts to understand the regulation of melanin production by *E. viscosium* and *E. limosus* we tried blocking individual pathways using known chemical blockers of DHN and DOPA melanin, phthalide and kojic acid respectively. Neither blocker, nor their combination at the highest amounts used were able to block the production of melanin in either species. If these species have the capability to produce all three melanins, then it is possible that they are producing more than one at the same time.

This could be the case here, since the combination of both kojic acid and phthalide still resulted in melanized cells which would indicate that tyrosine-derived pyomelanin was the cause of melanization.

Linked regulation of potentially multiple forms of melanin was observed with our EMS-induced mutant in which the *pks1* gene contained a nonsense mutation. Although *pks1* is the first enzyme involved in only the production of DHN-derived allomelanin, the cells that resulted from this mutation were albino. Theoretically, these cells should have still been capable of producing the two other melanins as their pathways were seemingly not disrupted by any mutations, but this was not the case. Addition of L-DOPA has been shown to induce melanization in a *pks1* deletion mutant of *E. dermatitidis* (Paolo et al., 2006), which would indicate that it is capable of producing both pheomelanin and allomelanin. However, the same experiment performed on *E. limosus*' *pks1* nonsense mutant did not recover melanization. Therefore, it is possible that; (i) *E. viscosium* and *E. limosus* only produce DHN-derived allomelanin and disruption of *pks1* causes all melanin production to shut down, (ii) *pks1* (or downstream creation of allomelanin) is essential for the regulation of other melanin productions, or (iii) pheomelanin and pyomelanin are only produced under specific conditions that were not used during analysis of the mutants.

Our experiments also showed that *E. viscosium* and *E. limosus* actively secrete melanin when they are viable and growing. We observed that melanin began to accumulate starting as early as day 2, therefore suggesting live cells are secreting melanin and not leaked from dead lysed cells. We also observed a decrease in melanin

concentrations after day 6 in both YPD and MEA, which raises the intriguing potential for melanin uptake or degradation by *E. viscosium* and *E. limosus*.

The medium that stimulated the most melanin secretion is YPD which has 10x more nitrogen (2% vs. 0.2%) than the alternative medium we use, MEA, which neither fungus secrete melanin into when plated on solid media. This led us to believe that nitrogen amount could potentially have an effect on the production of secreted melanin, which we did observe as we increased peptone amounts in the medium. Interestingly, the only fungal melanin that has nitrogen in its precursor structure is the DOPA derived pheomelanin. This was one of two melanins that could be produced in the presence of phthalide, which we observed also induced the secretion of melanin in these fungi. This provides support that the secreted melanin is either pheomelanin, as it requires more nitrogen in order to be produced, or that the production of pheomelanin (DOPA) and the water soluble pyomelanin (Turick et al., 2010) are linked.

Insights into the niche of polyextremotolerant fungi within the biological soil crust consortium

Fungal residents of BSC communities include lichenized mycobionts, lichenicolous fungi, endolichenic fungi, and free-living fungi. Although the latter are likely not directly associated with lichens themselves, they are surrounded by algae, cyanobacteria, and other bacteria in the same way that lichen-associated fungi are surrounded by a similar community of microbes. This raises the intriguing possibility that fungi such as *E. viscosium* and *E. limosus* might transiently associated with phototrophs in response to specific environmental conditions. Members of the genus *Exophiala* (Class Eurotiomycetes) are phylogenetically related to the lichen-forming Verrucariales,

and reside between Lecanoromycetes and Lichinomycetes (James et al., 2006). Additionally, lifestyle changes within Eurotiomycetes contributed to the polyphyletic nature of lichenization within the Ascomycetes, but since surrounding taxa are lichenized it is more likely that these species lost lichenization than three distinct lichenization events occurring within closely related species (Lutzoni et al., 2001). Because *E. viscosium* and *E. limosus* have lichenized ancestors, they could conceivably have lost their "true lichenization" capabilities, but maintained the genetic tools to interact with algae, cyanobacteria, and other bacteria to form lichen-like symbioses. As these are two newly identified species, more extensive ecological and molecular investigation is needed to determine the extent to which these taxa are found in BSCs and to elucidate their species interaction networks.

Correlation between environmental nitrogen availability and secreted melanin amounts could have strong implications for interactions between these fungi found in BSCs and their nitrogen-fixing community partners. The presumed source of nitrogen used to enhance the secretion of melanin would be from nitrogen-fixing prokaryotes such as cyanobacteria, other bacteria, and archaea in the community. Our results suggest that the availability of these nitrogen-fixers to provide fungal cells with ammonia could subsequently induce the secretion of melanin that then provides protective services to the broader BSC community. Secreted melanin could function at the community-level to maintain respiration and growth under varying temperature conditions while also mitigating the effects of desiccation and exposure to UV, extending the window of time allotted for optimal photosynthetic capabilities (Carr et al., 2021; Honegger, 1997; Honegger & Haisch, 2001; Lange & Tenhunen, 1981; Nybakken et al., 2004). Moreover,

the secreted melanin could simultaneously serve as an external source of carbon used by the fungi and possibly others when the environment does not allow for photosynthesis. In either scenario, the seemingly wasteful secretion of melanin by *E. viscosium* and *E. limosus* instead represents the optimal sharing of an expensive public good for the overall betterment of the BSC community in which they reside.

The availability of complete, annotated genome sequences for *E. viscosium* and *E. limosus* will enable more detailed investigations of the mechanisms that support the adaptation of these fungi to extreme environments. This in turn should provide greater insight into the roles that these fungi play in the BSC community. Of particular interest will be the regulatory mechanisms that coordinate the production of different types of melanin in response to environmental and chemical inputs. Moreover, the broad applicability of melanin as a bioproduct has triggered growing interest in microorganisms that secrete this polymer. In this context, *E. viscosium* and *E. limosus* could potentially serve as excellent platforms for additional engineering focused on optimizing or tailoring the type of melanin produced in responses to specific applications.

Acknowledgements

The authors would like to acknowledge Dr. Rajib Saha for providing a pre-print review of this work, with his guidance we were able to make this manuscript as clear and concise as possible, Dr. Christian Elowsky for acquiring beautiful microscopic and plate photos of these new species, and Darwyn S. Coxson for assistance in obtaining soil samples for isolation of these fungi. The work (proposal: 10.46936/10.25585/60001081) conducted by the U.S. Department of Energy Joint Genome Institute, a DOE Office of

Science User Facility, is supported by the Office of Science of the U.S. Department of Energy under Contract No. DE-AC02-05CH11231. Funding for this work was provided by NASA grant number 80NSSC17K0737.

References

Ametrano, C. G., Selbmann, L., & Muggia, L. (2017). A standardized approach for co-culturing Dothidealean rock-inhabiting fungi and lichen photobionts in vitro. *Symbiosis*, *73*(1), 35-44.

Bates, S. T., Garcia-Pichel, F., & Nash III, T. (2010). Fungal components of biological soil crusts: insights from culture-dependent and culture-independent studies. *Bibliotheca Lichenologica*, *105*, 197-210.

Bates, S. T., Reddy, G. S., & Garcia-Pichel, F. (2006). Exophiala crusticola anam. nov.(affinity Herpotrichiellaceae), a novel black yeast from biological soil crusts in the Western United States. *International journal of systematic and evolutionary microbiology*, *56*(11), 2697-2702.

Bell, A. A., & Wheeler, M. H. (1986). Biosynthesis and functions of fungal melanins. *Annual review of phytopathology*, *24*(1), 411-451.

Belnap, J. (2002). Nitrogen fixation in biological soil crusts from southeast Utah, USA. *Biology and fertility of soils*, *35*(2), 128-135.

Belnap, J. (2003). The world at your feet: desert biological soil crusts. *Frontiers in Ecology and the Environment*, *1*(4), 181-189.

Belnap, J., Büdel, B., & Lange, O. L. (2001). Biological soil crusts: characteristics and distribution. In *Biological soil crusts: structure, function, and management* (pp. 3-30). Springer.

Belnap, J., & Eldridge, D. (2001). Disturbance and recovery of biological soil crusts. In *Biological soil crusts: structure, function, and management* (pp. 363-383). Springer.

Belnap, J., & Lange, O. L. (2003). *Biological soil crusts: structure, function, and management* (Vol. 150). Springer.

Bligh, E. G., & Dyer, W. J. (1959). A rapid method of total lipid extraction and purification. *Canadian journal of biochemistry and physiology*, *37*(8), 911-917.

Bowker, M. A., Reed, S., Belnap, J., & Phillips, S. (2002). Temporal variation in community composition, pigmentation, and Fv/Fm of desert cyanobacterial soil crusts. *Microbial Ecology*, 13-25.

Bowker, M. A., Soliveres, S., & Maestre, F. T. (2010). Competition increases with abiotic stress and regulates the diversity of biological soil crusts. *Journal of Ecology*, *98*(3), 551-560.

Cao, W., Zhou, X., McCallum, N. C., Hu, Z., Ni, Q. Z., Kapoor, U., . . . Mantanona, A. J. (2021). Unraveling the structure and function of melanin through synthesis. *Journal of the American Chemical Society*, *143*(7), 2622-2637.

Carr, E. C., Harris, S. D., Herr, J. R., & Riekhof, W. R. (2021). Lichens and biofilms: Common collective growth imparts similar developmental strategies. *Algal Research*, *54*, 102217.

Castresana, J. (2000). Selection of conserved blocks from multiple alignments for their use in phylogenetic analysis. *Molecular biology and evolution*, *17*(4), 540-552.

Cordero, R. J., & Casadevall, A. (2017). Functions of fungal melanin beyond virulence. *Fungal Biology Reviews*, *31*(2), 99-112.

Cubero, O. F., Crespo, A., Fatehi, J., & Bridge, P. D. (1999). DNA extraction and PCR amplification method suitable for fresh, herbarium-stored, lichenized, and other fungi. *Plant Systematics and Evolution*, *216*(3), 243-249.

Dadachova, E., Bryan, R. A., Huang, X., Moadel, T., Schweitzer, A. D., Aisen, P., . . . Casadevall, A. (2007). Ionizing radiation changes the electronic properties of melanin and enhances the growth of melanized fungi. *PloS one*, *2*(5), e457.

De Hoog, G., Vicente, V., Caligiorne, R., Kantarcioglu, S., Tintelnot, K., Gerrits van den Ende, A., & Haase, G. (2003). Species diversity and polymorphism in the Exophiala spinifera clade containing opportunistic black yeast-like fungi. *Journal of Clinical Microbiology*, *41*(10), 4767-4778.

Donlan, R. M., & Costerton, J. W. (2002). Biofilms: survival mechanisms of clinically relevant microorganisms. *Clinical microbiology reviews*, *15*(2), 167-193.

Frases, S., Salazar, A., Dadachova, E., & Casadevall, A. (2007). Cryptococcus neoformans can utilize the bacterial melanin precursor homogentisic acid for fungal melanogenesis. *Applied and environmental microbiology*, *73*(2), 615-621.

Gadd, G. M. (1994). Interactions of fungi with toxic metals. *The Genus Aspergillus*, 361-374.

Gadd, G. M., & de Rome, L. (1988). Biosorption of copper by fungal melanin. *Applied microbiology and biotechnology*, *29*(6), 610-617.

Geis, P. A., & Szaniszlo, P. J. (1984). Carotenoid pigments of the dematiaceous fungus Wangiella dermatitidis. *Mycologia*, *76*(2), 268-273.

Geis, P. A., Wheeler, M. H., & Szaniszlo, P. J. (1984). Pentaketide metabolites of melanin synthesis in the dematiaceous fungus Wangiella dermatitidis. *Archives of microbiology*, *137*(4), 324-328.

Gessler, N., Egorova, A., & Belozerskaya, T. (2014). Melanin pigments of fungi under extreme environmental conditions. *Applied Biochemistry and Microbiology*, *50*(2), 105-113.

Gnerre, S., MacCallum, I., Przybylski, D., Ribeiro, F. J., Burton, J. N., Walker, B. J., . . . Jaffe, D. B. (2011). High-quality draft assemblies of mammalian genomes from massively parallel sequence data. *Proceedings of the National Academy of Sciences*, *108*(4), 1513-1518. https://doi.org/10.1073/pnas.1017351108

Gorbushina, A. A. (2007). Life on the rocks. *Environmental microbiology*, *9*(7), 1613-1631.

Gostinčar, C., Grube, M., De Hoog, S., Zalar, P., & Gunde-Cimerman, N. (2009). Extremotolerance in fungi: evolution on the edge. *FEMS microbiology ecology*, *71*(1), 2-11.

Gostinčar, C., Grube, M., & Gunde-Cimerman, N. (2011). Evolution of fungal pathogens in domestic environments? *Fungal biology*, *115*(10), 1008-1018.

Gostinčar, C., Muggia, L., & Grube, M. (2012). Polyextremotolerant black fungi: oligotrophism, adaptive potential, and a link to lichen symbioses. *Frontiers in Microbiology*, *3*, 390.

Grabherr, M. G., Haas, B. J., Yassour, M., Levin, J. Z., Thompson, D. A., Amit, I., . . . Zeng, Q. (2011). Full-length transcriptome assembly from RNA-Seq data without a reference genome. *Nature biotechnology*, *29*(7), 644-652.

Grigoriev, I. V., Nikitin, R., Haridas, S., Kuo, A., Ohm, R., Otillar, R., . . . Shabalov, I. (2014). MycoCosm portal: gearing up for 1000 fungal genomes. *Nucleic Acids Research*, *42*(D1), D699-D704. https://doi.org/10.1093/nar/gkt1183

Grube, M., Cernava, T., Soh, J., Fuchs, S., Aschenbrenner, I., Lassek, C., . . . Sensen, C. W. (2015). Exploring functional contexts of symbiotic sustain within lichen-associated bacteria by comparative omics. *The ISME journal*, *9*(2), 412-424.

Hom, E. F., & Murray, A. W. (2014). Niche engineering demonstrates a latent capacity for fungal-algal mutualism. *Science*, *345*(6192), 94-98.

Honegger, R. (1997). Metabolic interactions at the mycobiont-photobiont interface in lichens. In *Plant relationships* (pp. 209-221). Springer.

Honegger, R., & Haisch, A. (2001). Immunocytochemical location of the (1→ 3)(1→ 4)-β-glucan lichenin in the lichen-forming ascomycete Cetraria islandica (Icelandic moss). *New phytologist*, *150*(3), 739-746.

James, T. Y., Kauff, F., Schoch, C. L., Matheny, P. B., Hofstetter, V., Cox, C. J., . . . Miadlikowska, J. (2006). Reconstructing the early evolution of Fungi using a six-gene phylogeny. *Nature*, *443*(7113), 818-822.

Katoh, K., Misawa, K., Kuma, K. i., & Miyata, T. (2002). MAFFT: a novel method for rapid multiple sequence alignment based on fast Fourier transform. *Nucleic acids research*, *30*(14), 3059-3066.

Kobayashi, N., Muramatsu, T., Yamashina, Y., Shirai, T., Ohnishi, T., & Mori, T. (1993). Melanin reduces ultraviolet-induced DNA damage formation and killing rate in cultured human melanoma cells. *Journal of investigative dermatology*, *101*(5), 685-689.

Kuo, A., Bushnell, B., & Grigoriev, I. V. (2014). Fungal genomics: sequencing and annotation. *Advances in Botanical Research*, *70*, 1-52.

Lan, S., Wu, L., Zhang, D., & Hu, C. (2012). Successional stages of biological soil crusts and their microstructure variability in Shapotou region (China). *Environmental Earth Sciences*, *65*(1), 77-88.

Lange, O., & Tenhunen, J. (1981). Moisture content and CO2 exchange of lichens. II. Depression of net photosynthesis in Ramalina maciformis at high water content is caused by increased thallus carbon dioxide diffusion resistance. *Oecologia*, *51*(3), 426-429.

Letunic, I., & Bork, P. (2021). Interactive Tree Of Life (iTOL) v5: an online tool for phylogenetic tree display and annotation. *Nucleic acids research*, *49*(W1), W293-W296.

Ljungdahl, P. O., & Daignan-Fornier, B. (2012). Regulation of amino acid, nucleotide, and phosphate metabolism in Saccharomyces cerevisiae. *Genetics*, *190*(3), 885-929.

Lutzoni, F., Pagel, M., & Reeb, V. (2001). Major fungal lineages are derived from lichen symbiotic ancestors. *Nature*, *411*(6840), 937-940.

Maier, S., Muggia, L., Kuske, C. R., & Grube, M. (2016). Bacteria and non-lichenized fungi within biological soil crusts. In *Biological Soil Crusts: An Organizing Principle in Drylands* (pp. 81-100). Springer.

McFarland, J. (1907). The nephelometer: an instrument for estimating the number of bacteria in suspensions used for calculating the opsonic index and for vaccines. *Journal of the American Medical Association*, *49*(14), 1176-1178.

Mitchison-Field, L. M. Y., Vargas-Muñiz, J. M., Stormo, B. M., Vogt, E. J. D., Van Dierdonck, S., Pelletier, J. F., . . . Gladfelter, A. S. (2019). Unconventional Cell Division Cycles from Marine-Derived Yeasts. *Current Biology*, *29*(20), 3439-3456.e3435. https://doi.org/10.1016/j.cub.2019.08.050

Molina, L., & Molina, M. (1986). Absolute absorption cross sections of ozone in the 185- to 350-nm wavelength range. *Journal of Geophysical Research: Atmospheres*, *91*(D13), 14501-14508.

Nybakken, L., Solhaug, K. A., Bilger, W., & Gauslaa, Y. (2004). The lichens Xanthoria elegans and Cetraria islandica maintain a high protection against UV-B radiation in Arctic habitats. *Oecologia*, *140*(2), 211-216.

Pal, A. K., Gajjar, D. U., & Vasavada, A. R. (2014). DOPA and DHN pathway orchestrate melanin synthesis in Aspergillus species. *Medical mycology*, *52*(1), 10-18.

Paolo, W. F., Dadachova, E., Mandal, P., Casadevall, A., Szaniszlo, P. J., & Nosanchuk, J. D. (2006). Effects of disrupting the polyketide synthase gene WdPKS1 in Wangiella [Exophiala] dermatitidis on melanin production and resistance to killing by antifungal compounds, enzymatic degradation, and extremes in

temperature. *BMC microbiology*, *6*(1), 1-16. https://doi.org/https://doi.org/10.1186/1471-2180-6-55

Perez-Cuesta, U., Aparicio-Fernandez, L., Guruceaga, X., Martin-Souto, L., Abad-Diaz-de-Cerio, A., Antoran, A., . . . Rementeria, A. (2020). Melanin and pyomelanin in Aspergillus fumigatus: from its genetics to host interaction. *International Microbiology*, *23*(1), 55-63.

Pralea, I.-E., Moldovan, R.-C., Petrache, A.-M., Ilieș, M., Hegheș, S.-C., Ielciu, I., . . . Radu, M. (2019). From extraction to advanced analytical methods: The challenges of melanin analysis. *International journal of molecular sciences*, *20*(16), 3943.

Price, M. N., Dehal, P. S., & Arkin, A. P. (2009). FastTree: computing large minimum evolution trees with profiles instead of a distance matrix. *Molecular biology and evolution*, *26*(7), 1641-1650.

Purvis, O. W., Bailey, E. H., McLean, J., Kasama, T., & Williamson, B. J. (2004). Uranium biosorption by the lichen Trapelia involuta at a uranium mine. *Geomicrobiology Journal*, *21*(3), 159-167.

Pócs, T. (2009). Cyanobacterial crust types, as strategies for survival in extreme habitats. *Acta Botanica Hungarica*, *51*(1-2), 147-178.

Płonka, P., & Grabacka, M. (2006). Melanin synthesis in microorganisms: biotechnological and medical aspects. *Acta Biochimica Polonica*, *53*(3).

Rajeev, L., Da Rocha, U. N., Klitgord, N., Luning, E. G., Fortney, J., Axen, S. D., . . . Kerfeld, C. A. (2013). Dynamic cyanobacterial response to hydration and dehydration in a desert biological soil crust. *The ISME journal*, *7*(11), 2178-2191.

Richardson, D., Smith, D., & Lewis, D. (1967). Carbohydrate movement between the symbionts of lichens. *Nature*, *214*(5091), 879-882.

Rosas, Á. L., Nosanchuk, J. D., Gómez, B. L., Edens, W. A., Henson, J. M., & Casadevall, A. (2000). Isolation and serological analyses of fungal melanins. *Journal of immunological methods*, *244*(1-2), 69-80.

Schreier, W. J., Gilch, P., & Zinth, W. (2015). Early events of DNA photodamage. *Annual review of physical chemistry*, *66*, 497-519.

Schroeder, W. L., Harris, S. D., & Saha, R. (2020). Computation-driven analysis of model polyextremo-tolerant fungus exophiala dermatitidis: defensive pigment metabolic costs and human applications. *IScience*, *23*(4), 100980.

Schultzhaus, Z., Romsdahl, J., Chen, A., Tschirhart, T., Kim, S., Leary, D., & Wang, Z. (2020). The response of the melanized yeast Exophiala dermatitidis to gamma radiation exposure. *Environmental microbiology*, *22*(4), 1310-1326.

Seyedmousavi, S., Badali, H., Chlebicki, A., Zhao, J., Prenafeta-Boldu, F. X., & De Hoog, G. S. (2011). Exophiala sideris, a novel black yeast isolated from environments polluted with toxic alkyl benzenes and arsenic. *Fungal biology*, *115*(10), 1030-1037.

Teixeira, M. M., Moreno, L. F., Stielow, B. J., Muszewska, A., Hainaut, M., Gonzaga, L., . . . de Hoog, G. S. (2017). Exploring the genomic diversity of black yeasts and relatives (Chaetothyriales, Ascomycota). *Studies in mycology*, *86*, 1-28. https://doi.org/https://doi.org/10.1016/j.simyco.2017.01.001

Tragiannidis, A., Fegeler, W., Rellensmann, G., Debus, V., Müller, V., Hoernig-Franz, I., . . . Groll, A. (2012). Candidaemia in a European Paediatric University Hospital: a

10-year observational study. *Clinical Microbiology and Infection*, *18*(2), E27-E30.

Turick, C. E., Knox, A. S., Becnel, J. M., Ekechukwu, A. A., & Milliken, C. E. (2010). Properties and function of pyomelanin. *Biopolymers*, *449*, 72.

Untereiner, W. A., & Naveau, F. A. (1999). Molecular systematics of the Herpotrichiellaceae with an assessment of the phylogenetic positions of Exophiala dermatitidis and Phialophora americana. *Mycologia*, *91*(1), 67-83.

Weber, S. (2005). Light-driven enzymatic catalysis of DNA repair: a review of recent biophysical studies on photolyase. *Biochimica et Biophysica Acta (BBA)-Bioenergetics*, *1707*(1), 1-23.

White, T. J., Bruns, T., Lee, S., & Taylor, J. (1990). 38 - AMPLIFICATION AND DIRECT SEQUENCING OF FUNGAL RIBOSOMAL RNA GENES FOR PHYLOGENETICS. In M. A. Innis, D. H. Gelfand, J. J. Sninsky, & T. J. White (Eds.), *PCR Protocols* (pp. 315-322). Academic Press. https://doi.org/https://doi.org/10.1016/B978-0-12-372180-8.50042-1

Winston, F. (2008). EMS and UV mutagenesis in yeast. *Current protocols in molecular biology*, *82*(1), 13.13 B. 11-13.13 B. 15. https://doi.org/https://doi.org/10.1002/0471142727.mb1303bs82

Yoshino, K., Yamamoto, K., Masumoto, H., Degawa, Y., Yoshikawa, H., Harada, H., & Sakamoto, K. (2020). Polyol-assimilation capacities of lichen-inhabiting fungi. *The Lichenologist*, *52*(1), 49-59.

Zanne, A. E., Abarenkov, K., Afkhami, M. E., Aguilar-Trigueros, C. A., Bates, S., Bhatnagar, J. M., . . . Crowther, T. W. (2020). Fungal functional ecology:

bringing a trait-based approach to plant-associated fungi. *Biological Reviews*, *95*(2), 409-433.

Zerbino, D. R., & Birney, E. (2008). Velvet: algorithms for de novo short read assembly using de Bruijn graphs. *Genome research*, *18*(5), 821-829.

Zupančič, J., Novak Babič, M., Zalar, P., & Gunde-Cimerman, N. (2016). The black yeast Exophiala dermatitidis and other selected opportunistic human fungal pathogens spread from dishwashers to kitchens. *PLoS One*, *11*(2), e0148166.

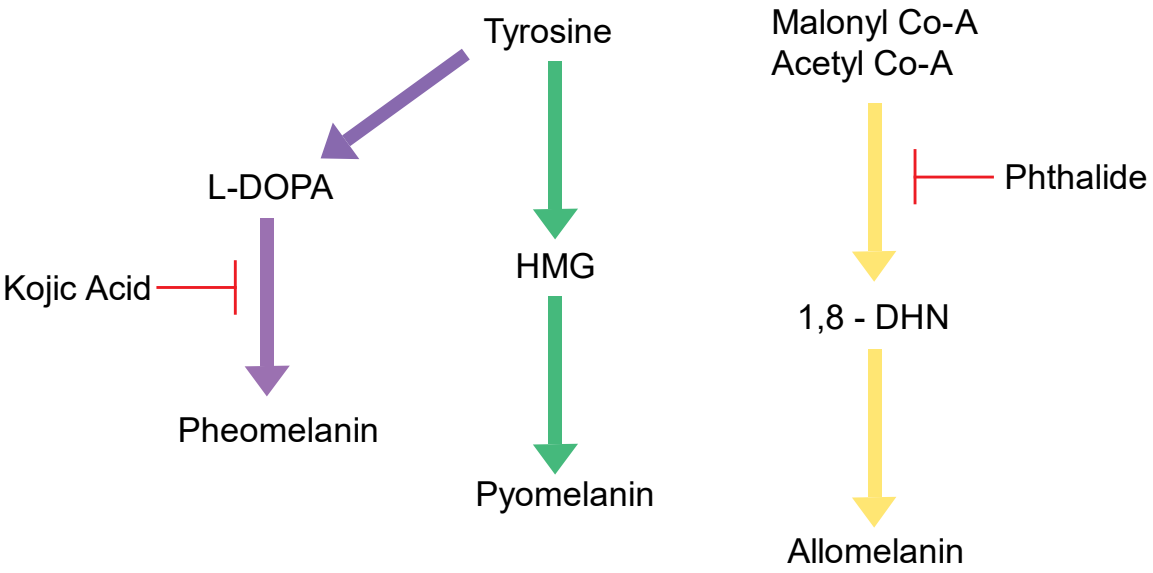

Figure 1: Visual summary of generalized fungal melanin production and the chemicals that block each pathway. Pheomelanin and Pyomelanin both use tyrosine as their starting reagent but have different biosynthesis pathways. However, pheomelanin uses L-DOPA as a precursor to the final product and pyomelanin uses HMG as a precursor. Allomelanin's starting components are malonyl co-A and acetyl co-A, and its immediate precursor is 1,8-DHN. Kojic acid is a chemical blocker that blocks production of pheomelanin, and phthalide blocks production of allomelanin.

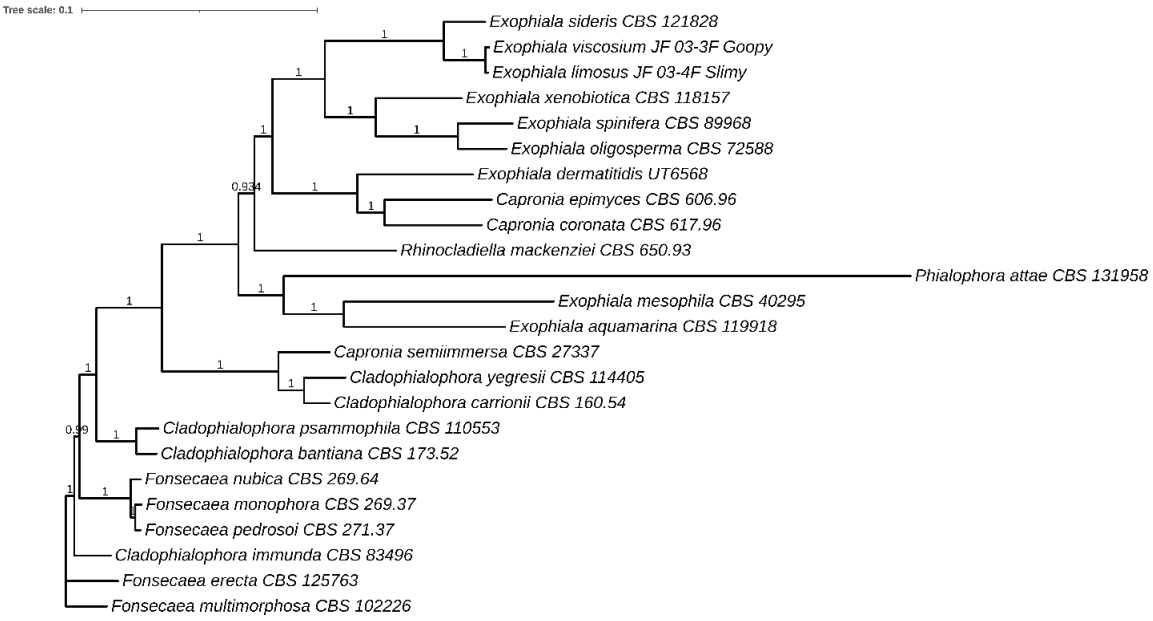

Figure 2: Homologous protein sequence approximate maximum likelihood phylogenetic tree of taxa of the family Herpotrichielleaceae all of which have been whole genome sequenced and annotated. *E. viscosium* and *E. limosus* are shown to be most closely related to *E. sideris*.

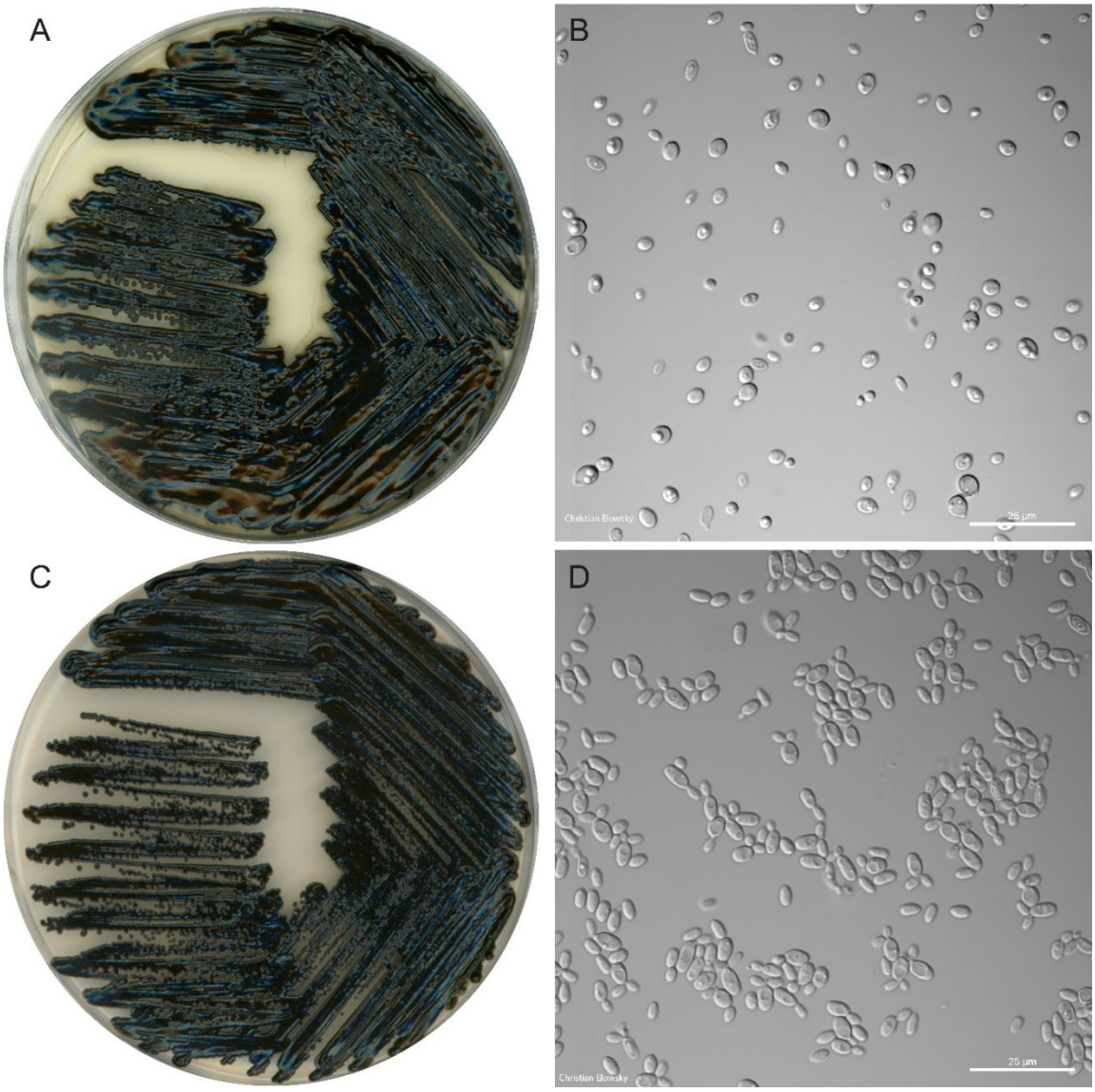

Figure 3: A) *E. viscosium* plate morphology; grown on an MEA plate for 10 days. *B) E. viscosium* cell morphology; grown in liquid MEA for 5 days; 60x objective lens. C) *E. limosus* plate morphology; grown on a MEA plate for 10 days. D) *E. limosus* cell morphology; grown in liquid MEA for 5 days; 60x objective lens. (Both plate photos and microscopy photos were taken by Christian Elowsky)

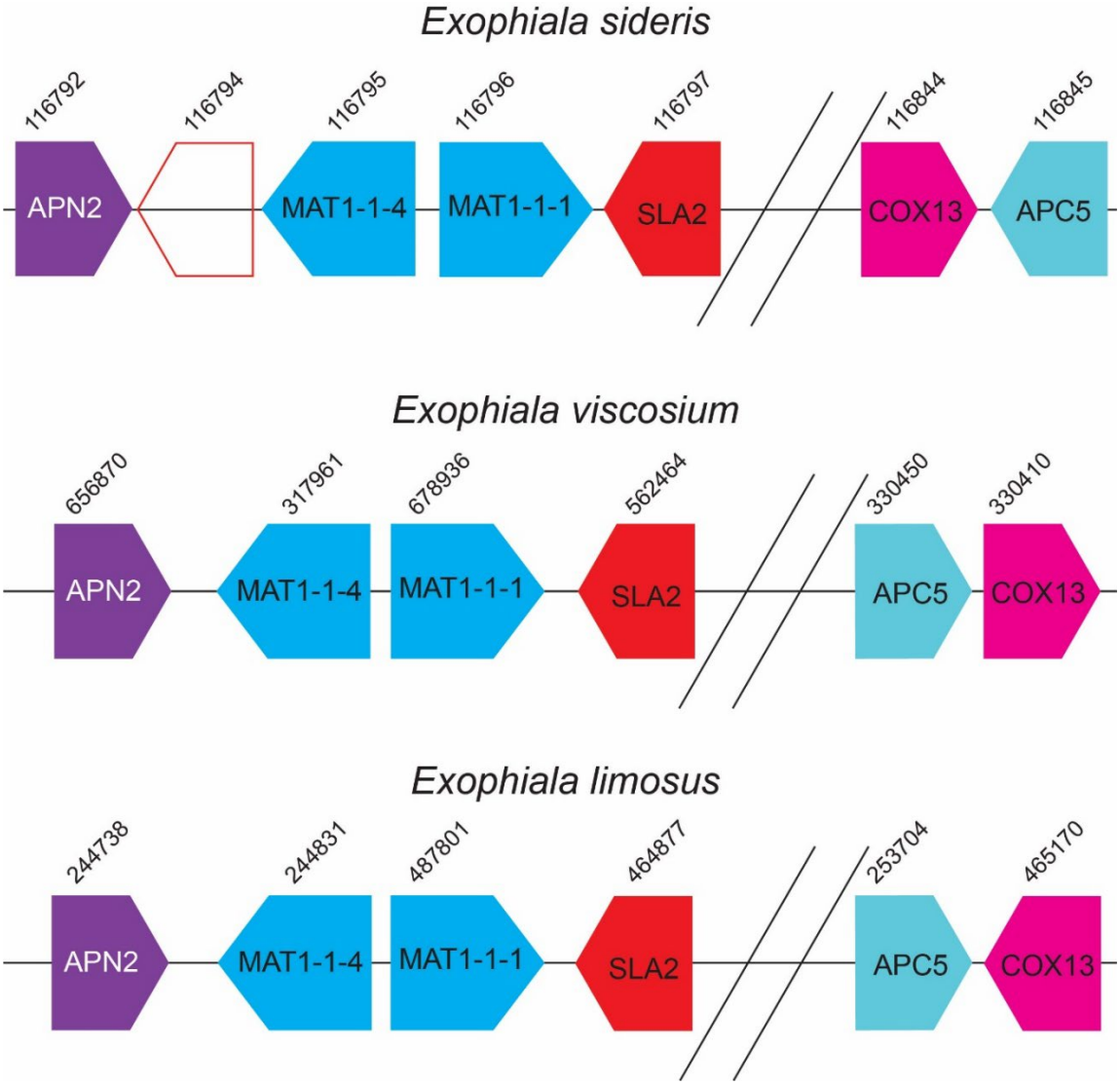

Figure 4: MAT loci gene order for *E. viscosium*, *E. limosus*, and *E. sideris*. In all three species the same genes are present within the MAT locus. *E. sideris* is indicated to have a hypothetical protein between APN2 and MAT1-1-4, whereas *E. viscosium and E. limosus* were not predicted to have that gene. Additionally, all three species have COX 13 and APC5 downstream of their mat loci, but the gene order or orientation is different amongst the three species.

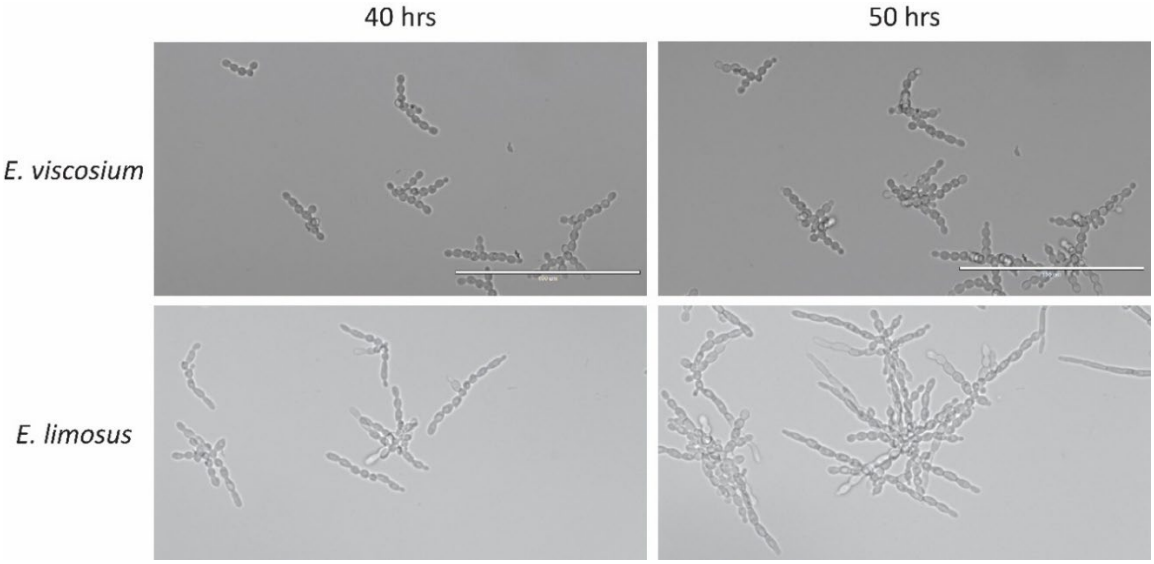

Figure 5: Budding styles of *E. viscosium* and *E. limosus*. Rate of budding is higher in *E. limosus* than in *E. viscosium*, as seen at the 50 hr mark. Budding style is also different between the species, *E. viscosium* buds both distal polarly and proximal at close to a 90° angle, whereas *E. limosus* buds almost exclusively as a distal polar. *E. limosus*'s cells also elongate with every bud, forming almost hyphal-like structures at the 50 hr timepoint (scale bars apply to all images).

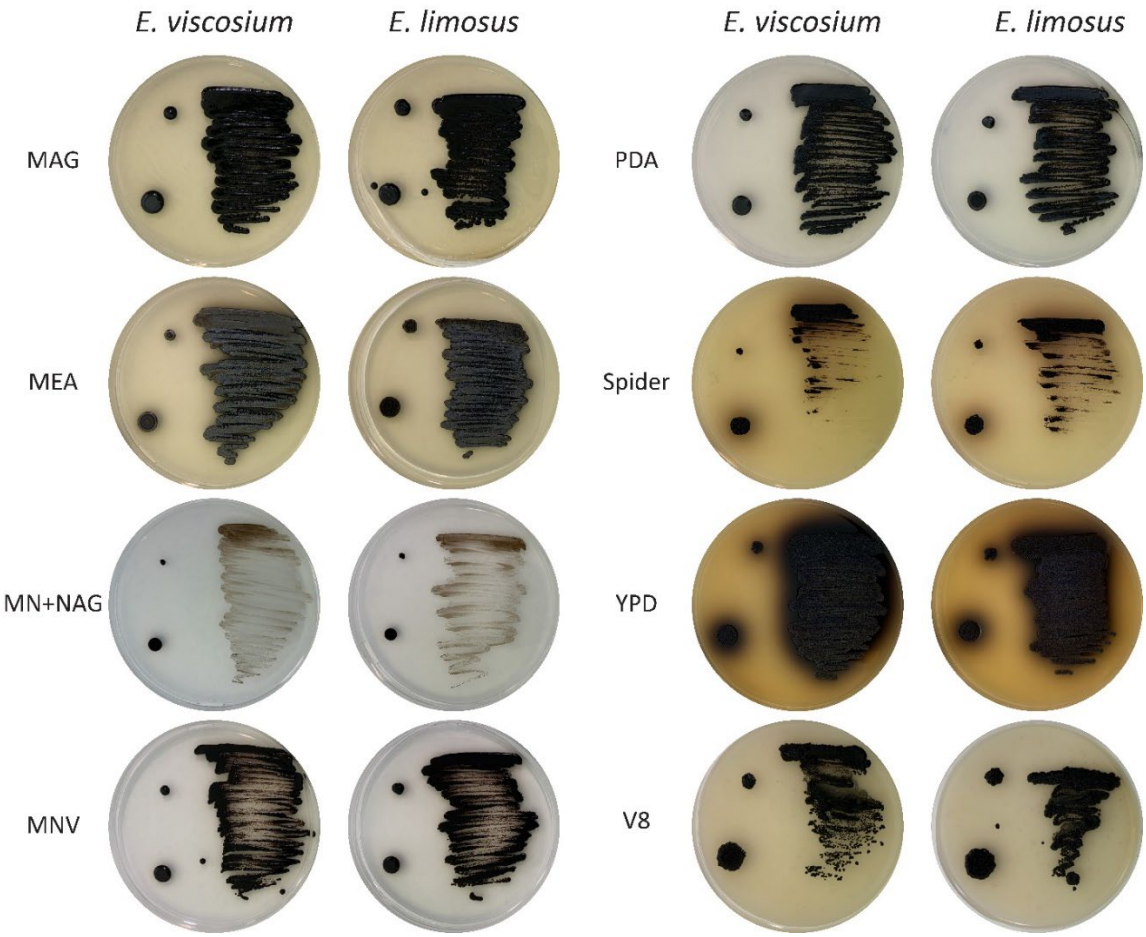

Figure 6: Growth of *E. viscosium* and *E. limosus* on eight different media types. Both species were capable of growth on all medias tested, but growth on MN+NAG showed the least amount of growth. PDA, MAG, and MNV allowed for very shiny and dark colonies to form in both species. Growth on V8 medium confirms potential for saprotrophic growth. Colorful secretions were observed on both Spider media and YPD for both species, though *E. viscosium* has more secretion into YPD than *E. limosus*.

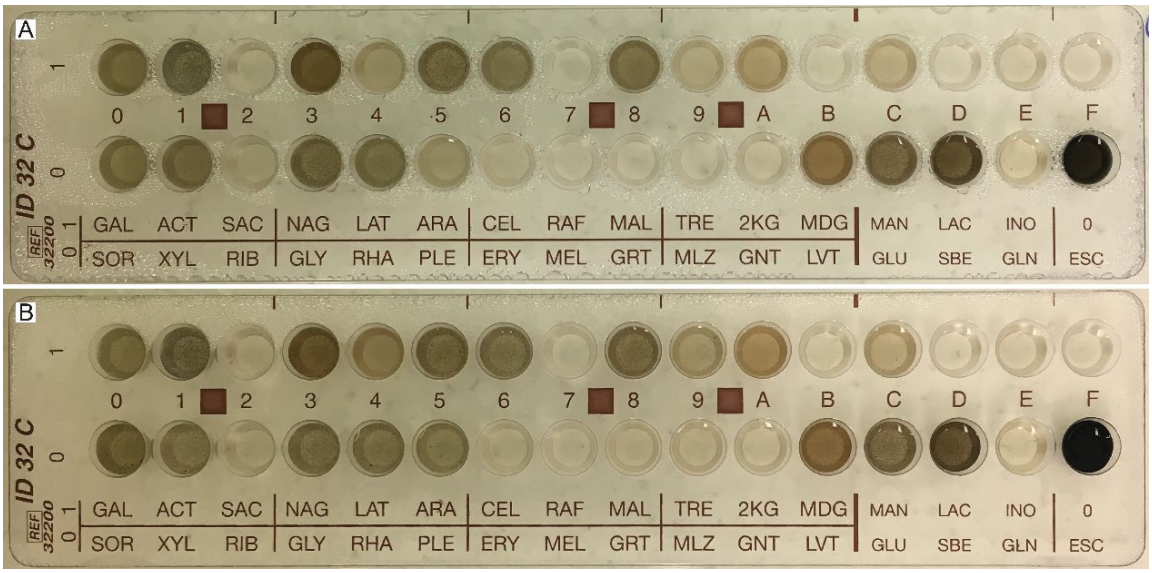

Figure 7: Growth of (A) *E. viscosium* and (B) *E. limosus* on C32 strips for determining carbon utilization. Both species were capable of using the same carbon sources, though some variations are seen. *E. limosus* was better at growing on palatinose, trehalose, potassium 2-ketogluconate, and mannitol than *E. viscosium*. *E. viscosium* was not better at growing on any carbon sources than *E. limosus*.

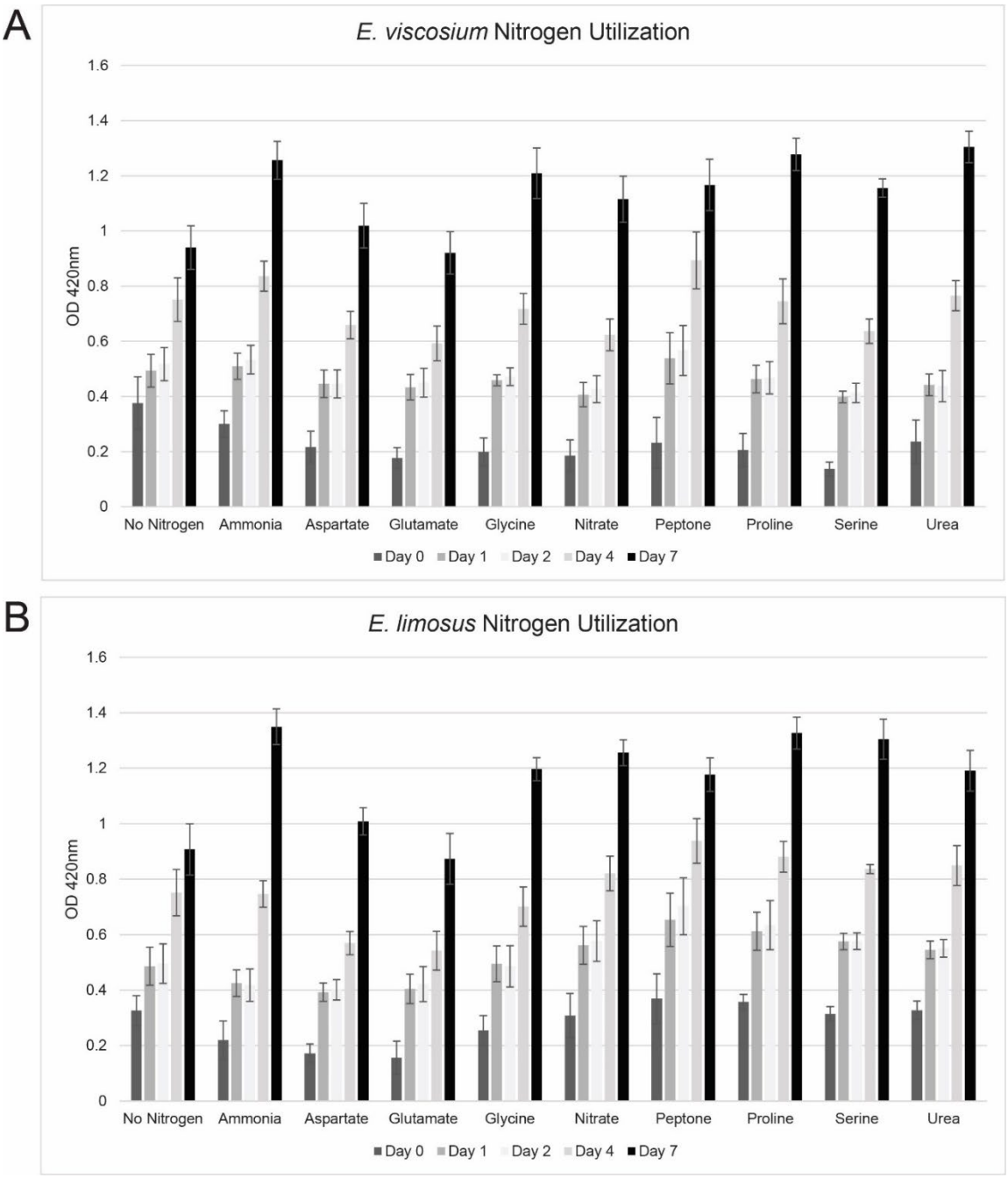

Figure 8: Nitrogen source utilization of (A) *E. viscosium* and (B) *E. limosus* in liquid culture. Neither species was capable of using aspartate or glutamate as a nitrogen source, as their growth amount were equivalent to no nitrogen. All other nitrogen sources tested were used by both species with varying preference. Ammonium was the preferred nitrogen source for *E. limosus*, and *E. viscosium* preferred urea and proline for nitrogen sources.

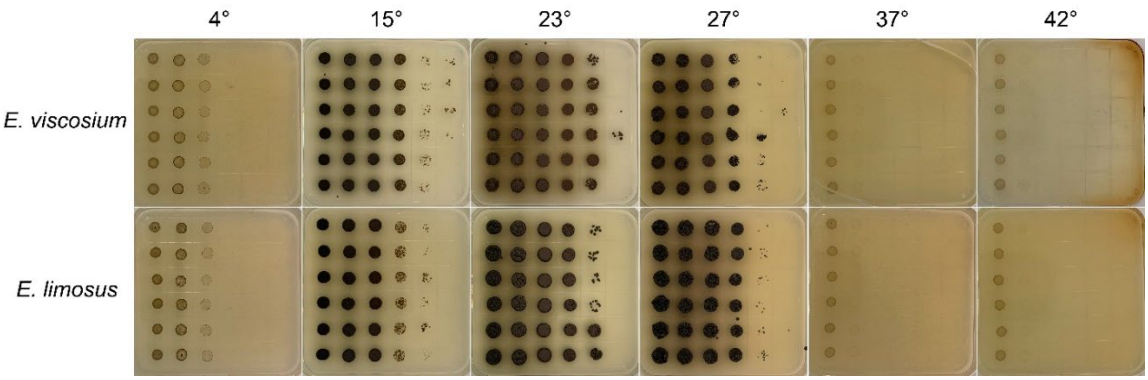

Figure 9: Growth of *E. viscosium* and *E. limosus* at varying temperatures. Neither species was capable of growth at or above 37 °C, implying they are not human pathogens. Both species optimally grew at 23 °C, but were capable of growth down to 4 °C.

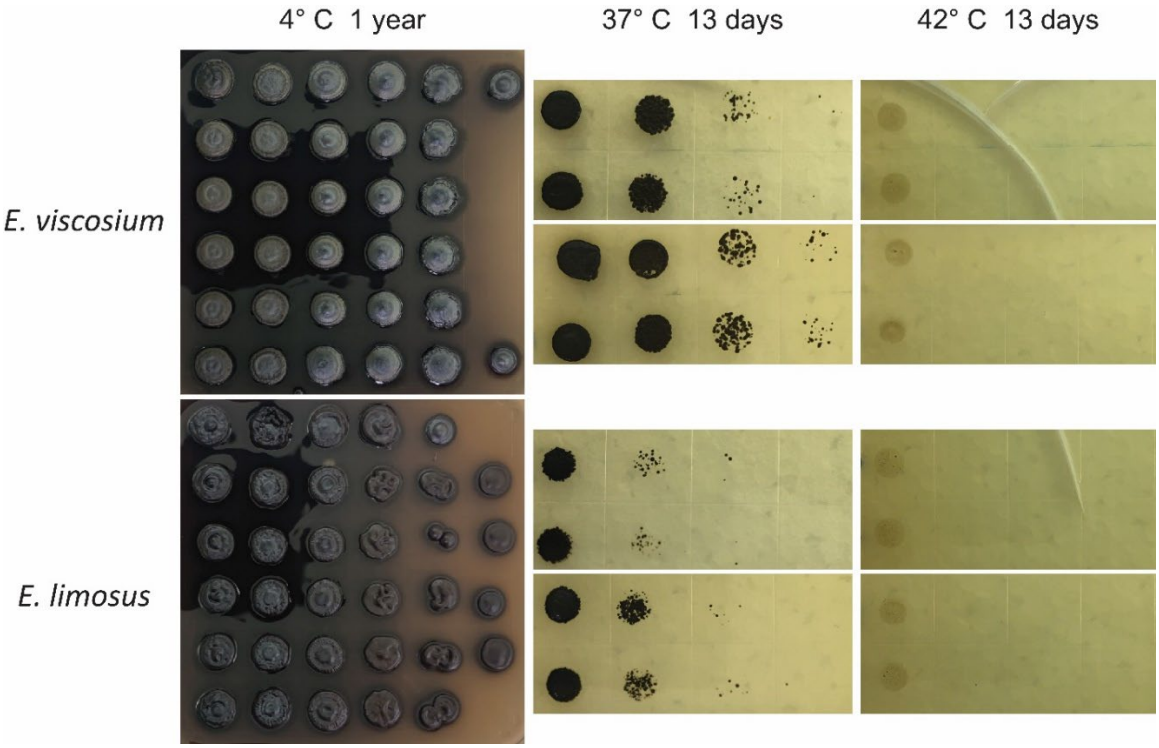

Figure 10: Growth of *E. viscosium* and *E. limosus* at the lowest and highest temperatures tested, after prolonged periods of time. Growth at 4 °C continued for a year in both species, indicating that they can grow at these lower temperatures for extended periods of time. Additionally, we observed that while neither species was capable of active growth at 37 °C, 48 hours was not too long of an exposure time to kill these cells. Whereas at 42 °C neither species was capable of growth, and both were killed after 48 hours of exposure.

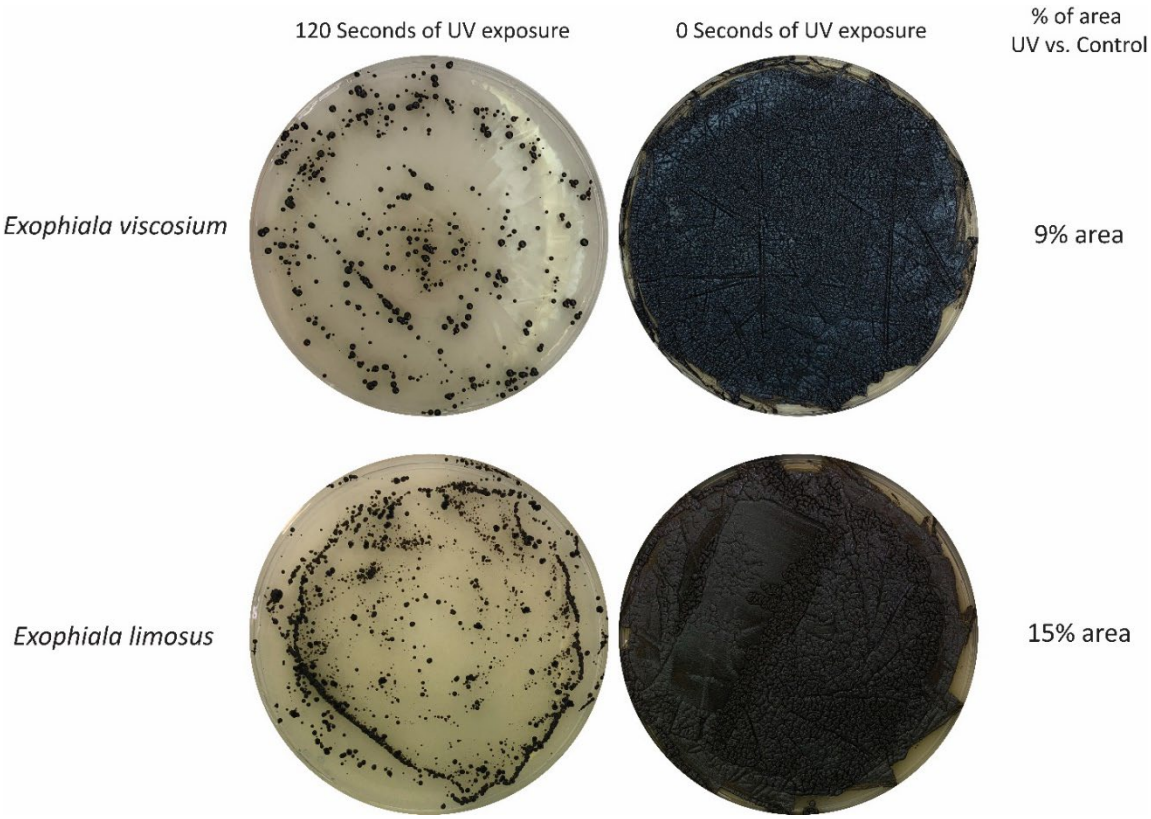

Figure 11: Difference in growth of *E. viscosium* and *E. limosus* with and without exposure to UV light. *E. viscosium* showed slightly less resistance to the UV exposure than *E. limosus*. Neither species was mutated from 120 seconds of UV exposure, normally *S. cerevisiae* and *E. dermatitidis* are incapable of growth after the same amount of UV exposure (data not shown).

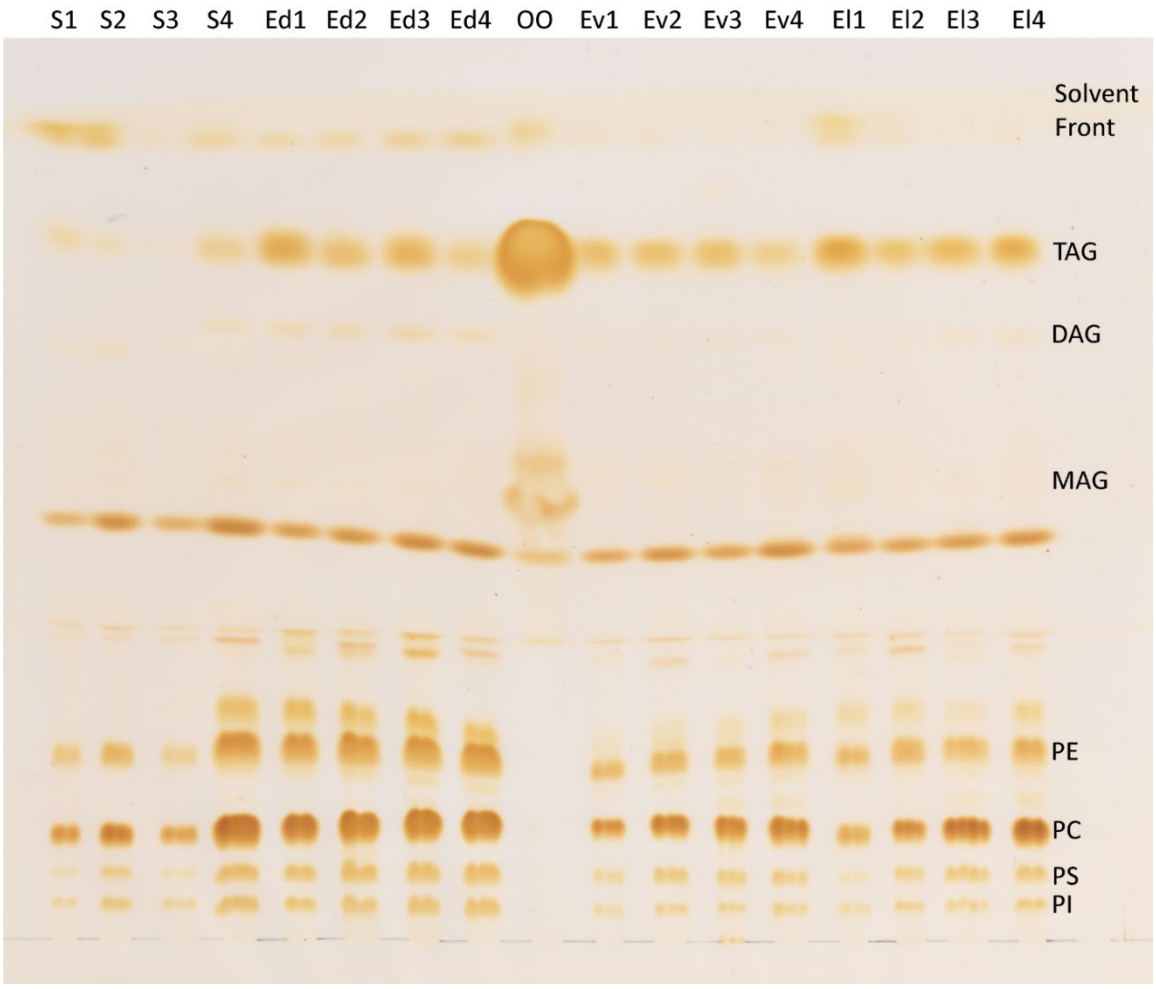

Figure 12: Lipid profile of *S. cerevisiae* (Sc), *E. dermatitidis* (Ed), *E. viscosium* (Ev), and *E. limosus* (El) using four different medias (1: MEA, 2: MEA + % peptone, 3: MEA + glycerol, 4: MEA + glycerol + % peptone). Differences in fermentable vs. non-fermentable carbon sources and amount of nitrogen source did not alter the amount or types of lipids produced by either *E. viscosium or E. limosus*. These fungi also showed no unique lipid production or any extreme accumulations of any lipids when compared to other fungi.

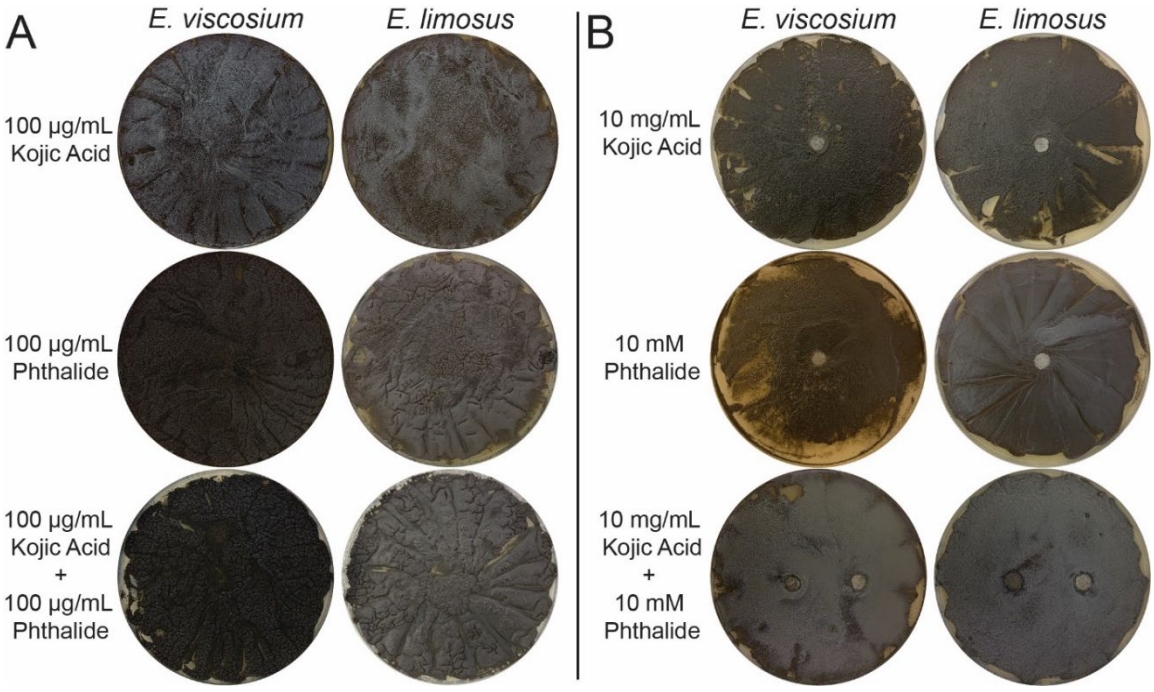

Figure 13: (A) *E. viscosium* and *E. limosus* lawns grown on MEA media contain either 100 µg/mL of kojic acid, 100 µg/mL of phthalide, or both in hopes of blocking melanin production through chemical means. Neither the individual melanin blockers nor their combined efforts were able to block melanin production in either fungus. (B) The same chemicals were used to attempt a different method of melanin blocking but at different concentrations, 10 mg/mL for kojic acid and 10 mM for phthalide. These compounds were added to filter discs and placed on lawns of *E. viscosium* and *E. limosus*. Neither the individual compounds nor the combined compounds blocked melanin production.

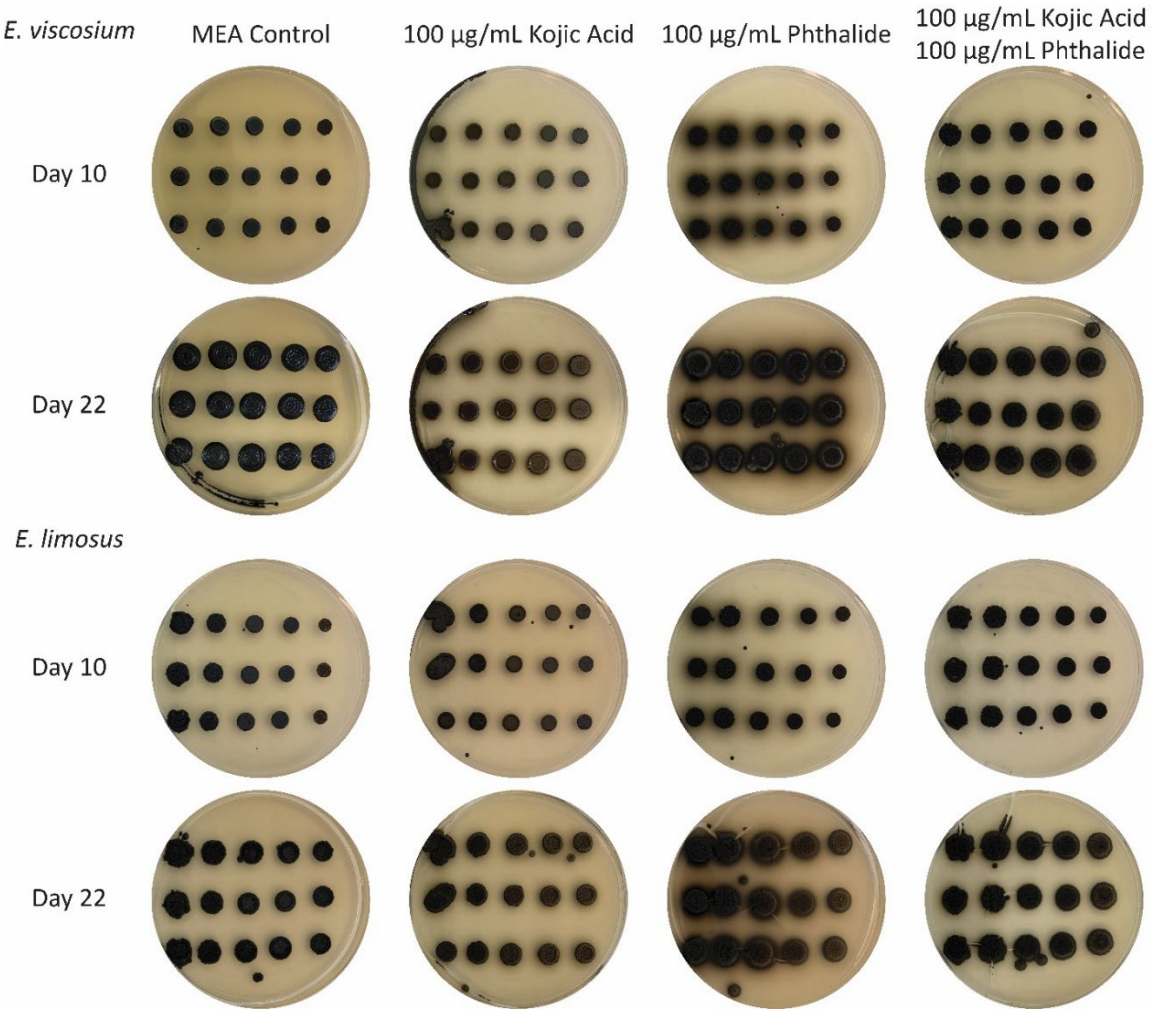

Figure 14: Growth of *E. viscosium* and *E. limosus* in the presence of melanin blockers kojic acid and phthalide. Neither chemcial melanin blocker was capable of blocking melanin production in either fungi even when both chemical blockers were used simultaneously. Additionally, use of phthalide on *E. viscosium* induced melanin secretion on a medium where this does not usually occur. The melanin halo around *E. viscosium*'s colonies on medium containing phthalide was replaced with hyphal growth after 22 days.

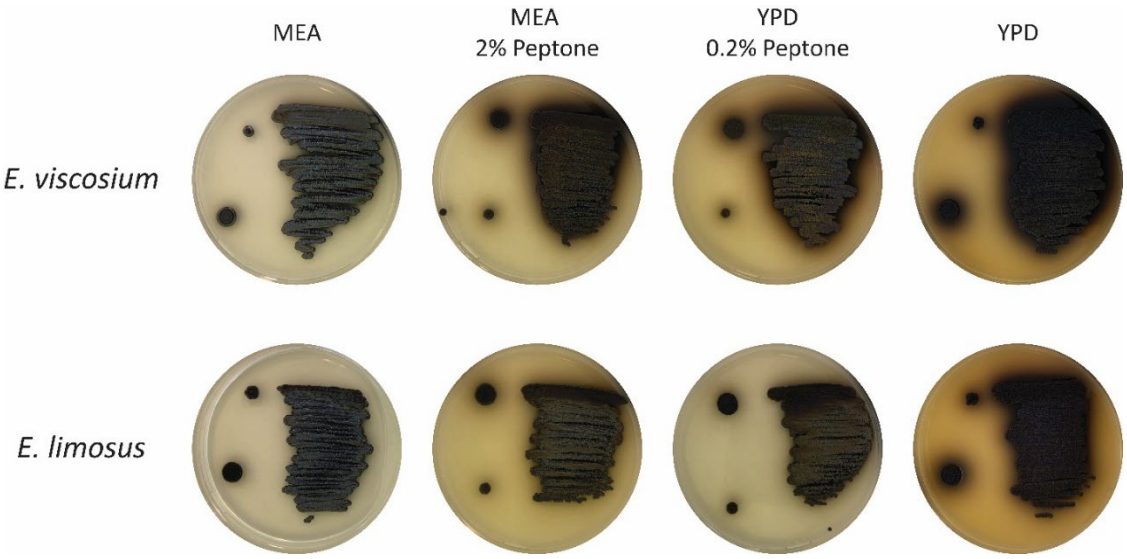

Figure 15: E. viscosium and *E. limosus* grown on MEA and YPD with different concentrations of peptone. *E. viscosium* is capable of melanin secretion on MEA with 2% peptone, which is the same amount of peptone in regular YPD. *E. limosus* was not as capable of secreting melanin in the MEA + 2% peptone, but there is a slight amount of secreted melanin. *E. viscosium* was also capable of secreting melanin on YPD with 0.2% peptone, indicating that yeast extract might have more available nitrogen than malt extract.

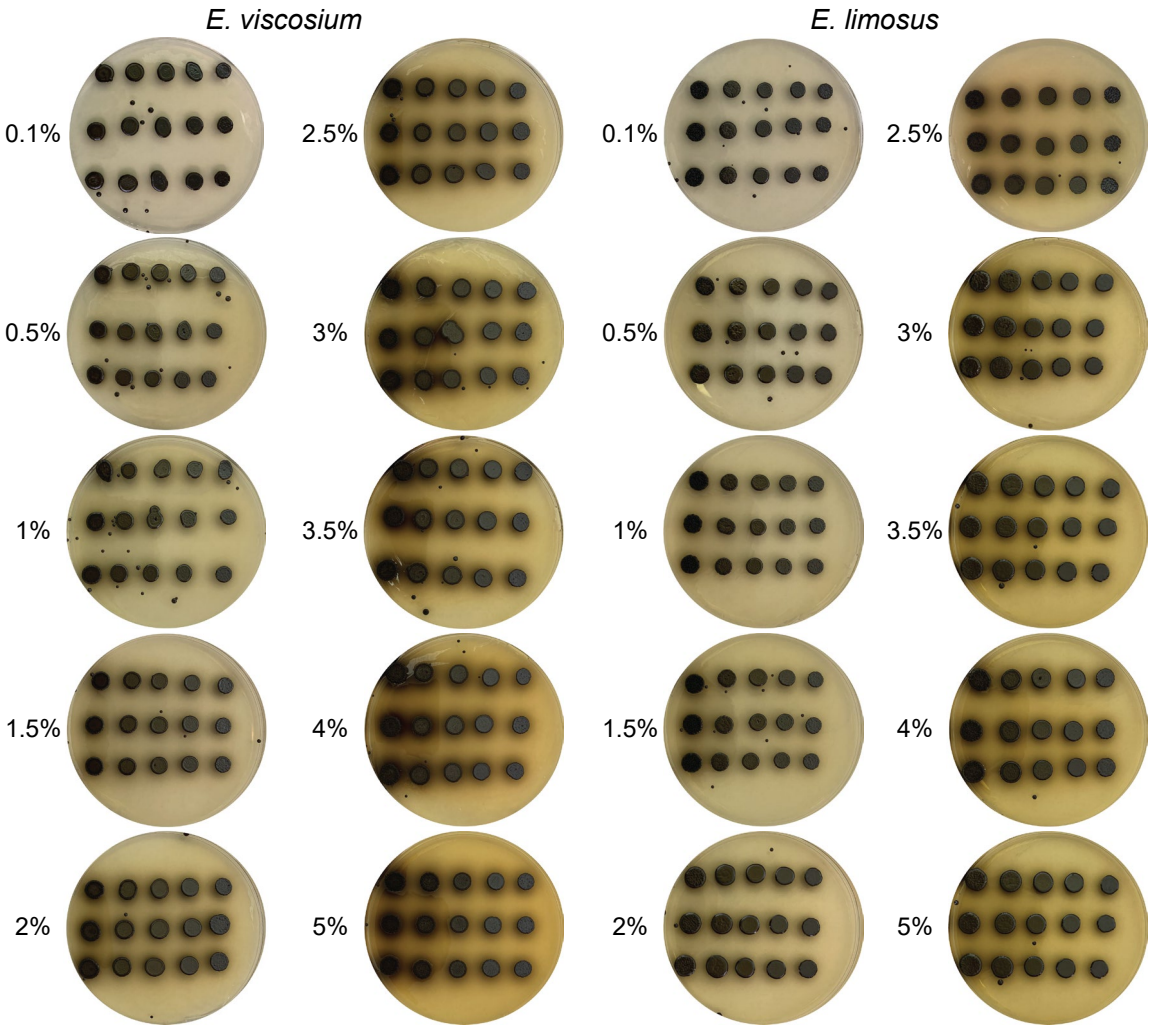

Figure 16: *E. viscosium* and *E. limosus* grown on MEA with increasing amounts of peptone. The higher the amount of peptone in the medium, the more melanin was secreted. *E. viscosium* started secreting melanin at 2%, and *E. limosus* at 4%.

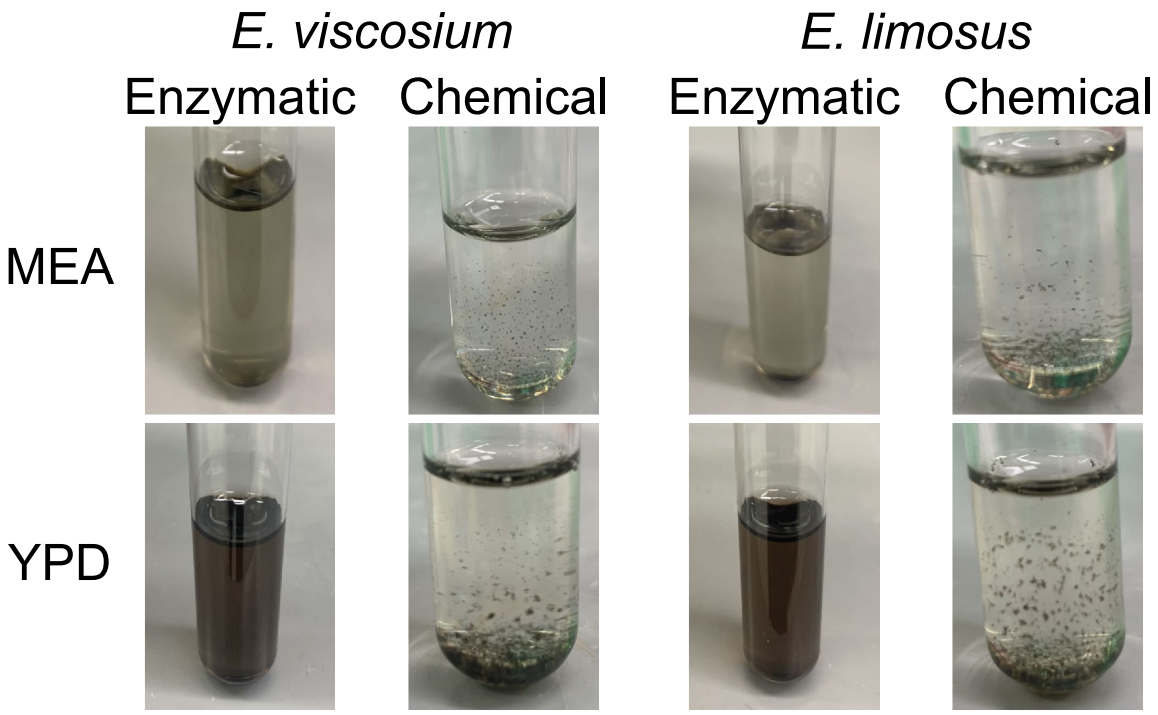

Figure 17: Extraction of melanin from supernatants of *E. viscosium* and *E. limosus* using both enzymatic and chemical methods described in (Pralea et al., 2019). Enzymatic extraction methods were incapable of extracting all the melanin, leaving behind a dark supernatant in the last step. However, melanin extracted by chemical extraction methods had complete extraction of the secreted melanin.

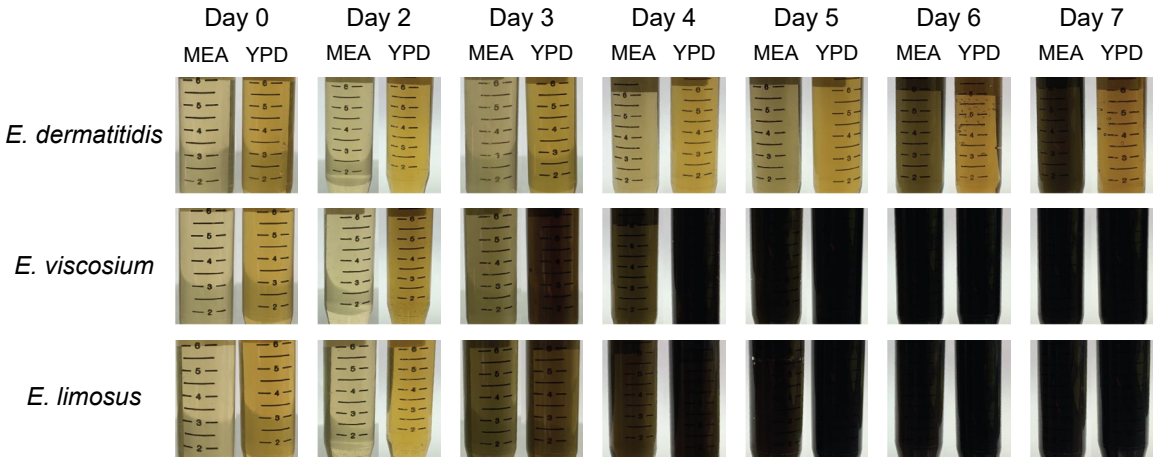

Figure 18: Daily melanin extraction from the supernatant of *E. dermatitidis*, *E. viscosium*, and *E. limosus*. Melanin began to accumulate in the supernatant of *E. viscosium* and *E. limosus* on day 3, with a steep increase in melanin in YPD. *E. dermatitidis* began melanin secretion at day 6, and only in MEA.

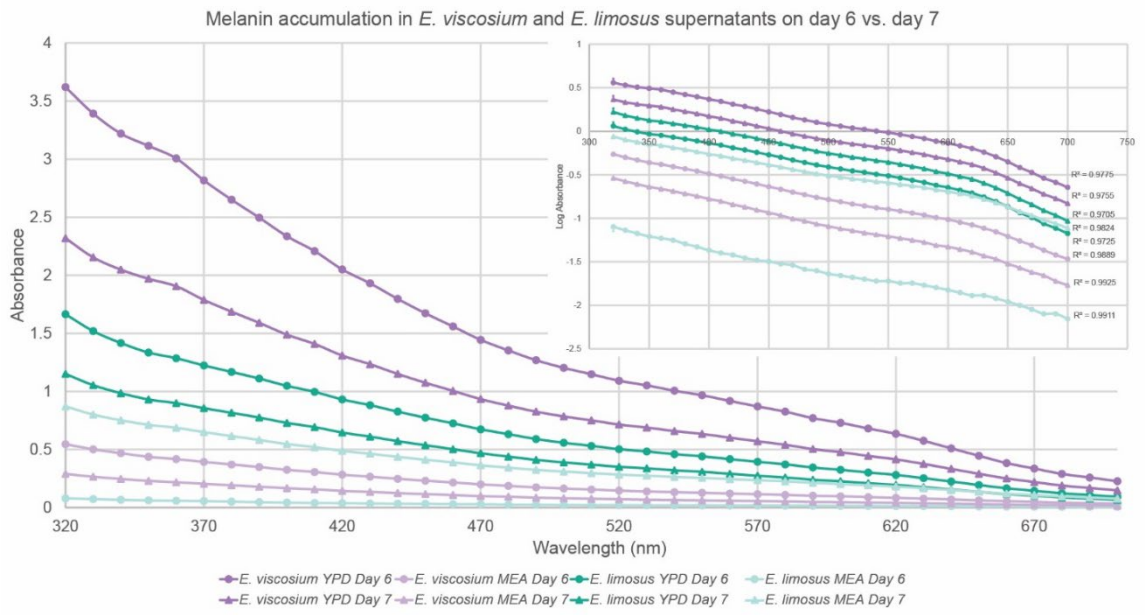

Figure 19: Day 6 and 7 results of daily melanin extraction from *E. viscosium* and *E. limosus*. Both samples display typical melanin properties with full spectrum light, in that all samples have a linear regression when their Log Absorbance is plotted against wavelength, with an R^2 value of 0.97 or higher (Pralea et al., 2019). The sample with the highest amount of secreted melanin was *E. viscosium* in YPD on day 6. Both *E. viscosium* and *E. limosus* had more secreted melanin when grown on YPD as opposed to MEA which showed lower melanin secretion for both species. Interestingly, both species had a decrease in melanin on day 7 when grown on YPD.

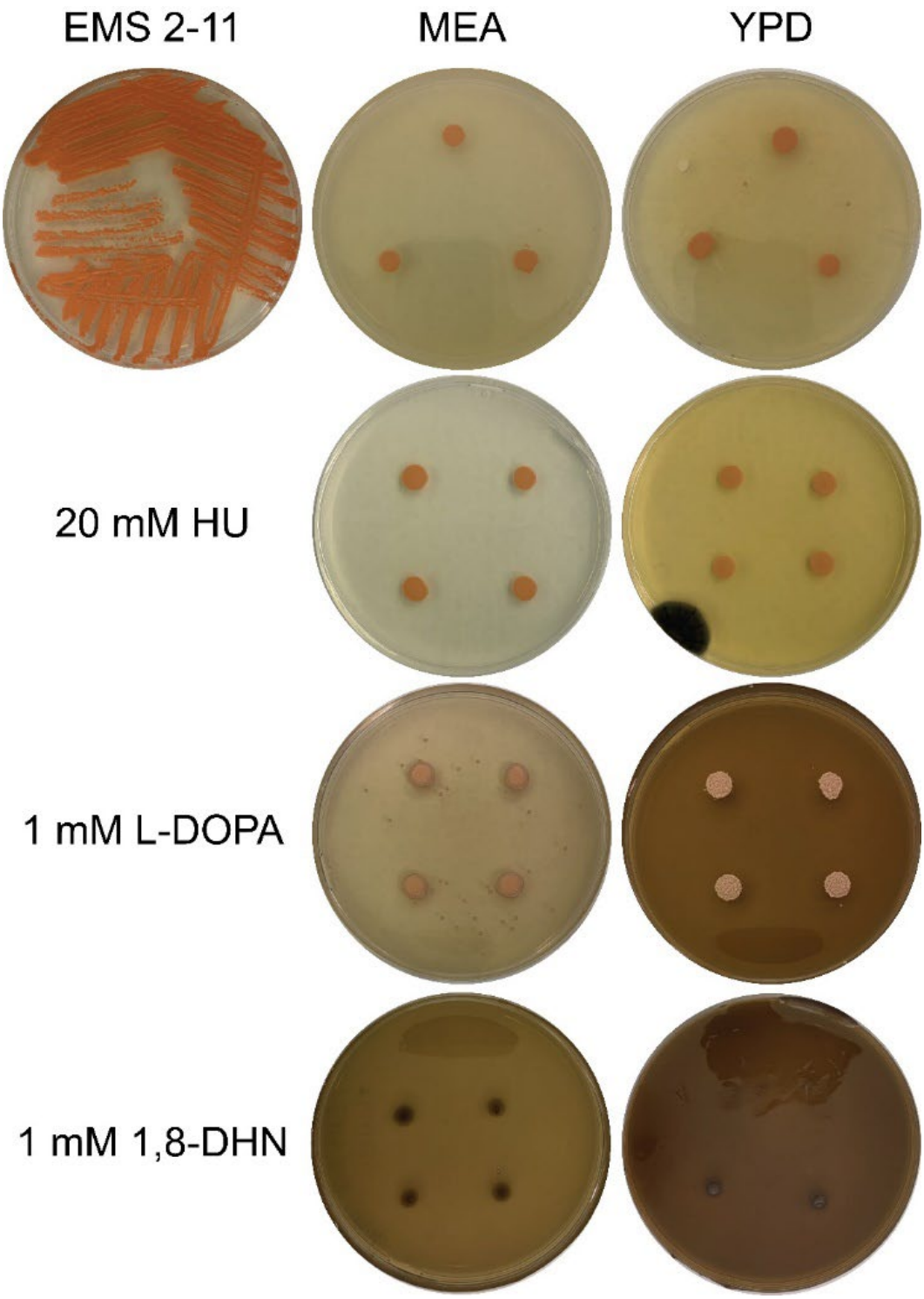

Figure 20: Phenotype of the EMS 2-11 mutant of *E. limosus* with *pks1* nonsense mutation Q814STOP, causing melanin production to be stopped hence the pink coloration. Attempts to recover melanin production were done with Hydroxyurea (HU), L-DOPA, and 1,8-DHN. Neither HU or L-DOPA were able to recover the melanin in the mutant, however 1,8-DHN was able to recover melanin production in this mutant.

Table 1: Medias used and their compositions

Media Name	**Acronym**	**Composition (L^{-1})**
Malt Extract Agar Glucose	MAG	20 g Dextrose 20 g Malt Extract 2 g Peptone 1 mL Hutner's Trace Elements 1 mL Vitamin Mix 15 g Agar
Malt Extract Agar	MEA	20 g Dextrose 20 g Malt Extract 2 g Peptone 15 g Agar
Minimal	MN	10 g Dextrose 50 mL 20x Nitrate salts 1 mL Hutner's Trace Elements
Minimal + Vitamins	MNV	10 g Dextrose 50 mL 20x Nitrate salts 1 mL Hutner's Trace Elements 1 mL Vitamin Mix
Minimal + N-acetyl Glucosamine	MN+NAG	10 g Dextrose 50 mL 20x Nitrate salts 1 mL Hutner's Trace Elements 4.74 g N-Acetyl Glucosamine (21.43 mM)
Potato Dextrose Agar	PDA	24 g Potato dextrose powder 15 g agar (if not in potato powder)
Spider	Spider	20 g Nutrient Broth 20 g Mannitol 4 g K_2HPO_4 27 g Agar pH adjusted to 7.2 with NaOH
Yeast Extract Peptone Dextrose	YPD	20 g Dextrose 20 g Peptone 10 g Yeast Extract 20 g Agar
V8	V8	200 mL V8 Juice 2 g $CaCO_3$ 15 g Agar
Additives	**Volume**	**Composition**
20X Nitrate Salts/MN salts	1 L	120 g $NaNO_3$ (remove for "MN salts") 10.4 g KCl 10.4 g $MgSO_4$-$7H_2O$ 30.4 g KH_2PO_4
Hutner's Trace Elements	100 mL	2.2 g $ZnSO_4$-$7H_2O$ 1.1 g H_3BO_3

		0.5 g $MnCl_2$-$4H_2O$ 0.5 g $FeSO_4$-$7H_2O$ 0.17 g $CoCL_2$-$6H_2O$ 0.16 g $CuSO_4$-$5H_2O$ 0.15 g Na_2MoO_4-$2H_2O$ 5 g EDTA (Disodium)
Vitamin Mix	100 mL	10 mg biotin 10 mg pyridoxin 10 mg thiamine 10 mg riboflavin 10 mg p-aminobenzoic acid (PABA) 10 mg nicotinic acid

Table 2: Nitrogen Sources, Concentrations, and Providers

Nitrogen Source	**Concentration**	**Catalog number**
No Nitrogen	N/A	N/A
Peptone	1% w/v	Fisher Brand: BP1420
L-Proline	100 mM	Sigma: P-0380
Ammonium tartrate	100 mM	Sigma: A2956
L-Serine	100 mM	Sigma: S4500
Sodium Nitrate	100 mM	Fisher Brand: S343
Glycine	100 mM	Fisher BioReagents: BP381
L-Glutamic acid	100 mM	Sigma: G1251
L-Aspartic acid	100 mM	Sigma: A9256
Urea	50 mM	Alfa Aesar: A12360

Table 3: Metals used and their concentration

Metal	**Concentration**	**Catalog Number**
$FeSO_4$	1 M	Fisher: I146
$CoCl_2$	0.5 M	Sigma: C-2644
$NiCl_2$	1.5 M	Sigma-aldrich: 223387
$CuCl_2$	1.5 M	Sigma: 203149
$CdCl_2$	10 mM	Fisher: 7790-84-3
$AgNO_3$	0.47 M	Alfa Aesar: 7761-88-8

Table 4: Genome descriptions of the novel *Exophiala* species and close relatives

Genome Assembly statistics	*E. viscosium*	*E. limosus*	*E. sideris*	*E. spinifera*	*E. xenobiotica*	*E. oligosperma*	*E. dermatitidis*
Accession #s	PRJNA501636	PRJNA501637	PRJNA325799	PRJNA325800	PRJNA325801	PRJNA325798	PRJNA225511
Genome Assembly size (Mbp)	28.29	28.23	29.51	32.91	31.41	38.22	26.35
Sequencing read coverage depth	147.3x	147.8x	NA	NA	NA	NA	NA
Number of contigs	35	27	69	143	64	287	10
Number of scaffolds	30	17	5	28	15	143	10
Number of scaffolds ≥ 2Kbp	25	17	5	20	11	129	10
Scaffold N50	4	5	2	4	3	5	4
Scaffold L50 (Mbp)	2.24	2.89	7.9	3.79	5.04	3.39	3.62
Number of gaps	5	10	64	115	49	144	0
% of scaffold length in gaps	0.00%	0.00%	0.10%	0.10%	0.10%	0.80%	0.00%
Three largest Scaffolds (Mbp)	5.39, 4.56, 2.49	4.57, 3.58, 2.93	9.94, 7.90, 7.15	6.18, 3.93, 3.92	5.55, 5.20, 5.04	4.47, 4.29, 4.12	4.25, 4.22, 3.71
GC content (%)	51.91	49.26	49.73	49.42	51.89	50.99	51.74
Gene statistics							
Number of genes	11344	11358	11120	12049	13187	13234	9562
Gene length (bp, Average)	1840	1844	2044	1593	2072	2090	2237
Gene length (bp, Median)	1666	1671	1823	1415	1845	1879	1923
Transcript length (bp, Average)	1740	1746	1933	1483	1941	1949	2122
Transcript length (bp, Median)	1564	1574	1710	1311	1710	1735	1794
Exon length (bp, Average)	705	707	776	621	738	743	896
Exon length (bp, Median)	410	414	452	339	430	426	513
Intron length (bp, Average)	70	69	74	81	80	85	85
Intron length (bp, Median)	56	56	56	61	57	61	62
Protein length (aa, Average)	488	489	500	494	492	488	501
Protein length (aa, Median)	428	430	434	437	431	429	429
Exons per gene (Average)	2.47	2.47	2.49	2.39	2.63	2.62	2.37
Exons per gene (Median)	2	2	2	2	2	2	2

Table 5: Carbon source utilization scores of *E. viscosium*

E. viscosium		***# 1***	***# 2***	***# 3***	***Average***	***Score***
D-galactose	GAL	4	5	4	4.3	+
D-sorbitol	SOR	4	4	4	4.0	+
Actidione (cycloheximide)	ACT	5	4	4	4.3	+
D-xylose	XYL	4	4	4	4.0	+
D-saccharose (sucrose)	SAC	1	1	1	1.0	-
D-ribose	RIB	2	2	2	2.0	V
N-acetyl-glucosamine	NAG	4	5	4	4.3	+
Glycerol	GLY	4	4	4	4.0	+
Lactic acid	LAT	3	3	3	3.0	V
L-rhamnose	RHA	4	4	4	4.0	+
L-arabinose	ARA	4	4	4	4.0	+
palatinose	PLE	3	3	3	3.0	V
D-cellobiose	CEL	4	4	4	4.0	+
Erythritol	ERY	2	2	2	2.0	V
D-raffinose	RAF	1	1	1	1.0	-
D-melibiose	MEL	1	1	1	1.0	-
D-maltose	MAL	4	4	4	4.0	+
sodium glucuronate	GRT	2	2	2	2.0	V
D-trehalose	TRE	3	3	3	3.0	V
D-melezitose	MLZ	2	2	2	2.0	V
potassium 2-ketogluconate	2KG	4	3	4	3.7	+
potassium gluconate	GNT	2	2	2	2.0	V
methyl-aD-glucopyranoside	MDG	1	1	1	1.0	-
levulinic acid (leuvulinate)	LVT	4	3	4	3.7	+
D-mannitol	MAN	3	3	3	3.0	V
D-glucose	GLU	5	5	5	5.0	+
D-lactose	LAC	1	1	1	1.0	-
L-sorbose	SBE	5	5	5	5.0	+
Inositol	INO	2	2	2	2.0	V
glucosamine	GLN	1	1	1	1.0	-
no substrate	No	1	1	1	1.0	-
Esculin ferric citrate	ESC	+	+	+	+	Black +

Table 6: Carbon source utilization of *E. limosus*

E. limosus		***# 1***	***# 2***	***# 3***	***Average***	***Score***
D-galactose	GAL	4	4	4	4.0	+
D-sorbitol	SOR	5	5	5	5.0	+
Actidione (cycloheximide)	ACT	4	4	4	4.0	+
D-xylose	XYL	4	4	4	4.0	+
D-saccharose (sucrose)	SAC	2	2	2	2.0	V
D-ribose	RIB	2	2	3	2.3	V
N-acetyl-glucosamine	NAG	4	4	4	4.0	+
Glycerol	GLY	4	4	4	4.0	+
Lactic acid	LAT	3	3	3	3.0	V
L-rhamnose	RHA	4	4	4	4.0	+
L-arabinose	ARA	4	4	4	4.0	+
palatinose	PLE	4	4	4	4.0	+
D-cellobiose	CEL	4	4	4	4.0	+
Erythritol	ERY	1	2	2	1.7	V
D-raffinose	RAF	1	1	1	1.0	-
D-melibiose	MEL	1	1	1	1.0	-
D-maltose	MAL	4	4	4	4.0	+
sodium glucuronate	GRT	2	2	2	2.0	V
D-trehalose	TRE	4	3	4	3.7	+
D-melezitose	MLZ	2	2	2	2.0	V
potassium 2-ketogluconate	2KG	3	3	4	3.3	V
potassium gluconate	GNT	2	2	2	2.0	V
methyl-aD-glucopyranoside	MDG	1	1	1	1.0	-
levulinic acid (leuvulinate)	LVT	3	4	3	3.3	V
D-mannitol	MAN	3	3	4	3.3	V
D-glucose	GLU	5	5	5	5.0	+
D-lactose	LAC	1	1	1	1.0	-
L-sorbose	SBE	5	5	5	5.0	+
Inositol	INO	2	2	2	2.0	V
glucosamine	GLN	2	2	1	1.7	V
no substrate	0	1	1	1	1.0	-
Esculin ferric citrate	ESC	+	+	+	+	Black +

Table 7: Diameter of the zone of clearing of *E. viscosium*, *E. limosus*, *E. dermatitidis*, and *S. cerevisiae* with various metals

Species	**$FeSO_4$ 1 M**	**$CoCl_2$ 0.5 M**	**$AgNO_3$ 0.47 M**	**$NiCl_2$ 1.5 M**	**$CuCl_2$ 1.5 M**	**$CdCl_2$ 10 mM**
E. viscosium	1.6 cm	1.5 cm	1.4 cm	3.9 cm	1.3 cm	4.5 cm
E. limosus	1.8 cm	1.8 cm	1.4 cm	4 cm	1.5 cm	3.9 cm
E. dermatitidis	1.3 cm	1 cm	1.5 cm	2 cm	2.5 cm	1.2 cm
S. cerevisiae	1 cm	1.9 cm	2 cm	2.1 cm	2 cm	2.5 cm

Table 8: Annotation of melanin biosynthetic genes for *E. viscosium* and *E. limosus*.

DHN/Allomelanin pathway		
Gene in *A. niger*	***E. viscosium* Homolog protein ID #**	***E. limosus* Homolog protein ID #**
Pks1	580617	463165
Ayg1	511449	494160
Arp2	676985	479993, 453709
Arp1	477931	210894
Abr2	603697, 153763	326274, 72468
Abr1	648725, 437535	258543, 441397
	387337, 648725	92776, 258543
	648725, 653857	258543, 102128
L-DOPA/Pheomelanin pathway		
Gene in *A. niger*	***E. viscosium* Homolog protein ID #**	***E. limosus* Homolog protein ID #**
MelC2	140179, 643161	84855
	140179	84855
MelO	-	-
McoJ	571417	465594
McoM	571417	465594
McoD	437535	441397
McoG	437535	441397
McoF	437535	441397
McoN	653857, 649741	102128, 454148
McoI	653857, 649741	102128, 454148
L-Tyrosine degradation/Pyomelanin pathway		
Gene in *A. niger*	***E. viscosium* Homolog protein ID #**	***E. limosus* Homolog protein ID #**
Tat	606461	34310
hppD	623446	39306
hmgA	617354, 102643, 403121	430149, 483886, 431641
fahA	617341	148504
maiA	213100	198633

Chapter 3

Crusty-Pinky: A Novel Polyextremotolerant Fungus and its *Methylobacterium* Symbionts Could be an Essential Symbiosis for the Biological Soil Crust Consortium

Abstract

JF2 08-2F Crusty is a novel melanized polyextremotolerant fungus isolated from a biological soil crust, which we believe harbors *Methylobacterium* spp. endosymbionts, called Pinky. Crusty is capable of utilizing many sources of carbon and nitrogen and is resistant to multiple metals and UV-C due to its melanized cell wall. We were unable to recover a Pinky-free culture of Crusty via usage of antibiotics. However, when exposed to antibiotics that kill or stop the growth of the Pinky, growth of Crusty is significantly stunted, implying that actively growing Pinky symbionts are needed for Crusty's optimal growth. The Crusty-Pinky symbiosis also seems to be able to perform active metabolism in carbonless and nitrogenless medium, which we believe is due to Pinky's ability to perform aerobic anoxygenic photosynthesis. Finally, Pinky was identified as being capable of growth stimulation of the algae *Chlorella sorokiniana*, indicating that Pinky likely produces cytokinins or auxins which *Methylobacterium* are known for. Features of this symbiosis provide us insight into the ecological roles of these microbes within the biological soil crust.

Introduction

Non-lichenized Fungi within Biological Soil Crusts

Biological soil crusts are dryland biofilms that form on the surface of non-vegetative mineral soils, primarily deserts, which rely on microbial interactions to survive the oligotrophic extremes of desert climates (Belnap et al., 2001; Belnap & Lange, 2003; Evans & Johansen, 1999). While the autotrophic members of the biological soil crust community (cyanobacteria, lichens, mosses, and algae) have relatively well established ecological niches, the niches of non-lichenized fungi and non-cyanobacteria bacteria are still yet to be discerned (Bates et al., 2006; Belnap, 2002; Belnap et al., 2001; Belnap & Lange, 2001; Csotonyi et al., 2010; Evans & Johansen, 1999; Harper & Marble, 1988; Johansen, 1993; Li et al., 2012; Maier et al., 2016; Steven et al., 2013). This is mostly due to the lack of research on these organisms within this ecosystem.

Deserts are notoriously harsh environments with extreme abiotic conditions such as intense UV exposure, diurnal temperature fluctuations, and osmotic pressures. Cold deserts often contain additional stressors such as light/dark annual extremes near the poles, drastic annual temperature changes, and excessive snow pack (Birkeland et al., 2020; Boulc'h et al., 2020). These extreme conditions create a difficult environment for active metabolism of the biological soil crust consortium, allowing for only short windows of opportunity with the optimal water availability and temperature conditions for active growth of the biological soil crust. Beyond that window, the community is in quiescence, and not actively respiring (Belnap, 2002; Belnap et al., 2004; Lange et al., 1997). Biological soil crust communities must cope with abiotic stressors simultaneously while relying on the autotrophic organisms to provide nutrients for the community during

this short growth time period (Belnap & Büdel, 2016; Li et al., 2012). Given the abundance of such abiotic extremes, the biological soil crust needs to harbor multiple highly tolerant microbes to combat all causes of stress. This is because mechanisms underlying a given stress response are to some extent unique to that form of stress (ie: UV exposure vs. water retention) (Bowker et al., 2002). Additionally, the sources of abiotic stress resistances are not well understood, partly because the microbes present within the biological soil crust are not very well characterized. One source of abiotic resistance that multiple microbes in the biological soil crust are known to possess is sunscreen-like compounds and other UV-resistant mechanisms such as carotenoids or melanin (Bowker et al., 2002; Gao & Garcia-Pichel, 2011).

Polyextremotolerant fungi are a paraphyletic group of fungi characterized by their melanized cell wall which has imbued them with high abiotic tolerance (Gostinčar et al., 2009; Gostinčar et al., 2012). These fungi have previously been isolated from biological soil crusts (Bates et al., 2006), but their ecological role within the crust is still unknown. Other ecosystems where these fungi are found also have no external carbon or nitrogen sources, and these fungi are not known chemolithotrophs (rock degrading) (Gorbushina, 2007; Teixeira et al., 2017). Therefore, their sources of nutrients seem to be limited to their autotrophic microbial neighbors in these same ecosystems, which many have observed but never experimentally shown (Gorbushina et al., 2005; Gostinčar et al., 2012; Grube et al., 2013; Muggia et al., 2013). Due to what we know about the metabolic capabilities of these fungi, where we find them, and their evolutionary relatives the lichen-forming Verrucariales, they are more than likely using carbon and nitrogen fixers in their environment for nutrition acquisition.

Endosymbiotic Bacteria of Fungi

While the concept of endosymbiosis has been around for many years, evidence of fungi containing endosymbiotic bacteria has been a relatively recent discovery (Bonfante, 2003; Kobayashi & Crouch, 2009). Most focus of bacterial-fungal endosymbiosis has been on the mycorrhizal fungi which associate with the roots of plants (Bianciotto et al., 2000; Lumini et al., 2007; Mondo et al., 2012). Even with more time and improved techniques, the diversity of fungi containing endosymbiotic bacteria has largely focused on plant-associated fungi (Bastías et al., 2020; Hoffman et al., 2013; Izumi et al., 2006; Pakvaz & Soltani, 2016; Ruiz-Herrera et al., 2015; Shaffer et al., 2017). Only very recently has a non-plant associated saprotrophic fungi, *Mortierella* spp., been identified to contain an endosymbiont (Büttner et al., 2021). Overall, the main role of bacteria in these symbioses has been in the direct production, or inducing the production, of a chemical to enhance survival of the fungus, with the implication that the bacteria is creating something for the benefit of the fungus and not necessarily benefiting the bacteria.

The scientific community's attention on obtaining axenic cultures for fungal type strain deposition has probably reduced the number of identified endosymbiotic bacterial-fungal symbioses. Additionally, overuse of antibiotics to ensure clean cultures for genome sequencing likely also contributes to this issue. Many microbes are considered unculturable, but it remains possible that these microbes require the presence of their microbial neighbors for survival. The more we dedicate our time and resources to culturing non-laboratory or "unculturable" fungi, the more likely we will find fungi with uncurable endosymbionts.

Methylobacterium's metabolic capabilities and their roles in symbioses

Methylobacterium is a Gram negative alphaproteobacterial genus of the order Rhizobiales, now called Hyphomicrobiales. Also known as pink facultative methylotrophs (PPFMs), they are characterized by their ability to utilize one-carbon molecules such as methanol as a carbon source (Chistoserdova et al., 2003). They are prominent members of the plant phyllosphere (Kutschera, 2007), with certain taxa capable of root nodulation (Jourand et al., 2004; Sy et al., 2001); however, they are ubiquitously found in all ecosystems (Hiraishi et al., 1995). Metabolically, members of this genus have been known to perform nitrogen fixation (Jourand et al., 2004; Madhaiyan et al., 2015; Raja et al., 2006), aerobic anoxygenic photosynthesis (Atamna-Ismaeel et al., 2012; Csotonyi et al., 2010; Tang et al., 2018), and phytohormone production (Ivanova et al., 2001; Ivanova et al., 2000; Koenig et al., 2002). These metabolic capabilities make them ideal partners for broader interactions within a microbial community, as they have the capability to produce a nitrogen source, growth stimulating compounds, and perform the first step of photosynthesis creating ATP for themselves.

As their ubiquitous nature would imply, many *Methylobacterium* spp. have been identified across multi-species symbioses. Importantly, *Methylobacterium* have been identified as a part of newly recognized lichen holobionts (Cardinale et al., 2006; Cardinale et al., 2008; Erlacher et al., 2015; Hodkinson & Lutzoni, 2009; Jiang et al., 2020). Their role in the lichen symbiosis is currently unknown, but many still hypothesize that the unique metabolic capacity of *Methylobacterium* spp.' allow them to engage in nitrogen fixation, some role possibly associated with their nodulation

capabilities, and phytohormone production for growth-promoting capabilities (Erlacher et al., 2015; Grube et al., 2009; Hodkinson & Lutzoni, 2009). Of particular interest to this study, *Methylobacterium* spp. have also been found within the biological soil crust consortium (Csotonyi et al., 2010; Tang et al., 2018). The ecological importance of *Methylobacterium* spp. within the biological soil crust seems to be significant, as enriching for *Methylobacterium* spp. via activation of aerobic anoxygenic photosynthesis increases the growth of the biological soil crust (Tang et al., 2018). It is likely that *Methylobacterium* spp. could play a pivotal role in the biological soil crust consortium, with their wide assortment of metabolic capabilities at the ready for microbial interaction optimization.

We describe here a novel polyextremotolerant fungal species and its presumptive *Methylobacterium* spp. endosymbionts. Full characterization of the fungus has been performed in lieu of its genome, which is still being sequenced and analyzed. Additional experiments have been performed to understand the basis for this fungal-bacterial symbiosis, to determine if it is a true endosymbiotic interaction, and the ecological niche this fungal-bacterial symbiosis might occupy within the biological soil crust consortium.

Methods

General methods

Microbial strains and growth conditions

This chapter describes one novel fungal species and its two *Methylobacterium spp*. symbionts. The novel species of fungi described here is currently named JF2 08-2F Crusty and will from here on be referred to as Crusty. The closest alignment to this

isolate's (ITS) fingerprint region is *Neophaeococcomyces* sp. Currently, it does not have a designated species name, as its genome sequencing and annotation is still being processed at the Joint Genome Institute (JGI). Once its genome and transcriptome are fully sequenced, they will be deposited at the Department of Energy (DOE) JGI's Mycocosm website under the designated species name, and at the National Center for Biotechnological Information (NCBI). The type strain will also be deposited to the Westerdijk institute for access to the greater scientific community.

Crusty is grown in malt extract medium (MEA; composition in **Table 1**) at room temperature in an Erlenmeyer flask at $1/10^{th}$ the volume of the flask, shaking at 200 rpm. *Methylobacterium* spp. symbionts of Crusty are called JF2 08-2LP Light Pinky and JF2 08-2DP Dark Pinky, and the combination of these two in culture is called JF2 08-2P Pinky (from here on called Light Pinky, Dark Pinky, and Pinky respectively). According to the results of nucleotide similarity search using the Basic Local Alignment Search Tool (BLASTn) against the 16S ribosomal RNA (rRNA) sequence database at NCBI, both Light Pinky and Dark Pinky were 100% identical with an E-value of 0.0 to multiple *Methylobacterium* species including: *Methylobacterium oryzae* strain 94-A4, *Methylobacterium phyllosphaerae* strain CBMB27, and *Methylobacterium radiotolerans* strain PPFM28. *Methylobacterium* spp. are maintained in MEA as well with the same conditions stated above.

Additional organisms used in this study were *Saccharomyces cerevisiae* strain BY4741, algae *Chlorella sorokiniana* strain UTEX 1230, and an additional *Methylobacterium* sp. wild isolate named P3 that was isolated from the North Antelope Valley Parkway canal in Lincon, NE. *S. cerevisiae* is grown in Yeast Peptone Dextrose

medium (YPD; composition in **Table 1**) with the same flask and shaking conditions as described above. *C. sorokiniana* is either grown up in a carbonless medium called Bold's basal Medium (BBM), or TAP which contains carbon, and is grown under 12 hr light/dark cycles with shaking at 200 rpm.

Fungal isolation and identification methods

Fungi were isolated from a biological soil crust located in Jackman Flats British Columbia, Canada (52.931383 N, 119.372059 W). Soil samples were taken from the top 2 cm of the biological soil crust. A 0.1 g portion of the crust was re-suspended in 1 mL of water, ground with a sterile micropestle, and diluted with a dilution factor (DF) of 10 until they reached 10,000x dilution. Each dilution was then spread out onto two different MEA petri plates containing either no antibiotics or containing: Ampicillin (100 mg/L), Chloramphenicol (50 mg/L), Gentamycin (10 mg/L), and Cycloheximide (100 mg/L). The plates were then incubated in a Percival light incubator at 23 °C with a 12 hr light/dark cycle and examined daily using a dissection microscope to check for small black colonies. Once a potential black colony was seen, half of it was removed and transferred to a new MEA (no antibiotics) petri plate. Plates were examined daily, because even in the presence of antibiotics many unwanted fast-growing microbes would grow on the plates and cover up the slower growing polyextremotolerant fungal colonies. Once a pure culture of each isolate was grown up (approximately 2 weeks), they were preserved in 30% Glycerol and stored at -80 °C.

DNA sequencing of amplified internal transcribed spacer (ITS) sequences was used to identify the isolates. DNA was extracted using the Qiagen DNeasy Powersoil DNA extraction kit. Primers used to isolate the ITS region were: ITS1- (5'-TCC GTA

GGT GAA CCT GCG G-3') and ITS4- (5'-TCC TCC GCT TAT TGA TAT GC-3') (White et al., 1990). A BioRad MJ Mini Personal Thermal Cycler was used, with the program set as: 1) 95 °C for 5 minutes; 2) 94 °C for 30 seconds; 3) 55 °C for 30 seconds; 4) 72 °C for 1 minute and 30 seconds; 5) Return to step 2, repeat 35 times; 6) 72 °C for 5 minutes; 7) END. Amplified products were then checked via gel electrophoresis in 1% agar run at 80 V for 1 hr. Isolated ITS regions were sequenced using the Eurofins sequencing facility. Subsequently, a nucleotide similarity search using BLASTn was performed against the NCBI database to identify their potential taxanomical matches.

Phylogenetic Analysis of Crusty's ITS Sequence

To further refine the identity of newly isolated strains, we generated a multi-loci gene tree using ribosomal ITS1, ITS2, LSU, SSU and 5.8S genetic markers. Because these markers are commonly sequenced through amplicon or Sanger sequencing, there is a higher availability of closely related species with representative markers than closely related species with whole genome sequences available for comparison. Fifty-seven sequences of strains from the NCBI and UNITE databases were collected based on the BLAST results of Crusty (Abarenkov et al., 2010). The program ITSx *v.1.1b* (Bengtsson-Palme et al., 2013) was used with the save_all tag to pull out the ITS1, ITS2, LSU, SSU and 5.8S regions from each read. As the data on NCBI were all collected using a variety of different primer and PCR set-ups, this program allows us to capture as much of the ribosomal regions as possible. The program MUSCLE *v.5.1* (Edgar, 2004) was used to align each fasta file containing ribosomal gene region. Clipkit *v.1.3.0* (Steenwyk et al., 2020), another program to help with overall alignment and trimming strategy, was used to retain parsimony informative sites that are known to be more phylogenetically

informative. A python script (combine_multiseq_aln.py found in PHYling_united utilities folder https://github.com/stajichlab/PHYling_unified) was used to combine all aligned sequences into a fasta sequence. This python script also takes the length of each region into consideration as it builds the larger fasta file from a separate text file. The fasta files aligned and trimmed by MUSCLE and clipkit were each used and run with the nucleotide tag. Phylogenetic analysis was performed using IQ-Tree *v.2.2.0* (Minh et al., 2020), which was used in two main ways. Initially 1000 bootstrap Ultrafast (-b 1000) was used while also calling IQ-Tree automatic selection of substitution models for each ITS and rDNA region, specified as a partition. Standard evolutionary rates for branch lengths were used for each partition. The details along with the length of each region is added into a partitioning NEXUS file for multi-gene alignments and used to run IQ-Tree a second time and generate a composite ML phylogenetic tree. To reduce the computational burden that occurs with including a large number of organism ribosomal sequences, we used the relaxed hierarchical clustering algorithm, automatic model selection and best-fit partitioning scheme (Lanfear et al., 2014) were performed using the option "-m MF+MERGE".

Bacterial isolation and identification methods

Bacterial isolates were obtained after streaking out Crusty from frozen stocks. If antibiotics are not present in the media used to streak out a frozen stock of Crusty, then pink bacterial colonies always form. The difference in colony color allowed the isolation of the two bacteria. Identification of these bacteria was done by extracting DNA as explained above, and then using PCR to amplify their 16S ribosomal DNA (rDNA) region using the primers: 8F (5'-AGA GTT TGA TCC TGG CTC AG-3'), and 1492R

(5'- GGT TAC CTT GTT ACG ACT T-3') (Turner et al., 1999). A BioRad MJ Mini Personal Thermal Cycler was used for performing the PCR, with the program set to 1) 95 °C for 5 mins; 2) 95 °C for 1 min; 3) 51 °C for 1 min; 4) 72 °C for 2 mins; Go to step 2, repeat 30 times; 5) 72 °C for 10 mins; 6) END. PCR products were run on a 1x TAE 1% agarose gel electrophoresis at 80V for one hour for verification. Sequencing of the PCR products was performed by MWG Eurofins using the 8F primer. The obtained sequences were analyzed using BLASTn nucleotide similarity search against the NCBI nr/nt database, and the closest matching bacterial species were determined.

Phylogenetic Analysis of Methylobacterium spp. using 16S rDNA Sequences

Phylogenetic analysis of Light Pinky and Dark Pinky was performed using their 16S rDNA marker region. We downloaded all 16S rDNA sequences from the NCBI database using the *Methylobacterium* 16S rDNA Gene search. We also downloaded a selection of 16S rDNA sequences from *Microvirga* to use as an outgroup for the tree. Alignment of the 16S rDNA sequences was done in MEGAX using Muscle alignment's standard parameters. After alignment, the ends of the 16S rDNA sequences were trimmed due to size differences across the various sequences. No trimming was performed within the sequences beyond the end regions. On the very rare occasion that there was a strain with an insert, these regions were kept because it would be important for the further analysis to differentiate the closely related strains. A maximum likelihood tree was reconstructed in MEGAX using the GTR+G+I model with 1000 bootstrap values.

Methylobacterium spp. Genome Assembly and Annotation

Since the clarity of bacterial identification using the 16S rDNA sequence was not enough to obtain exact species identification, we performed sequencing of the whole

genome of the two *Methylobacterium* spp. we isolated from Crusty's culture: Light Pinky and Dark Pinky. DNA extraction of the isolates was done in the same way as described above for Crusty. The resulting genomes were sequenced using the Microbial Genome Sequencing Center (https://www.migscenter.com) using their 300 Mbs sequencing service. Resulting sequences were uploaded to the Galaxy web platform for computational analyses (Afgan et al., 2018). Bacterial genomes were aligned on Galaxy using the standard functions of Unicycler (Wick et al., 2017). Then, automatic annotation was performed on Galaxy using Prokka (Seemann, 2014). BLAST databases for Light Pinky and Dark Pinky's genomes were also created on Galaxy using blastdbn (Camacho et al., 2009; Cock et al., 2015). Individual proteins were identified on the Dark Pinky genome using BLASTp which was ran on Galaxy (Camacho et al., 2009).

Initial Microscopy and Plate Imaging

Initial microscopic images were taken using an Olympus BX51 on the 40x objective lens, with an iPhone 6s against the ocular lens. Cells of JF2 08-2F Crusty were grown up as described above for 10 days. Then 8 µL of the grown cells was aliquoted onto a microscope slide with a 1.5 mm coverslip overtop. Plate imaging of Crusty, Light Pinky, and Dark Pinky was done using the iPhone 6s. Additional microscopy was done using the EVOS-fl at 4x-40x magnification.

Analysis of Budding Patterns

The protocol for observing the budding patterns of JF2 08-2F Crusty was derived from methods in (Mitchison-Field et al., 2019). A 1:1:1 ratio by weight of Vaseline, Paraffin, and Lanolin (VALAP) was combined in a glass bottle and heated to 115 °C to melt completely and kept at room temperature for later use. Heated solid MEA was

aliquoted into a 50mL tube for agar slab making. Isolates were grown in liquid MEA for 10 days prior to inoculation of slides. First, the VALAP was brought back up to 115 °C to melt completely for application. Then 5 µL of the 10-day old cells were diluted in 95 µL of liquid MEA. Agar slabs of MEA were made by microwaving the 50 mL tube of solid MEA until it melted, then pipetting 1 mL of the hot agar into a 1 cm x 2 cm mold formed out of cut strips of silicone and laid down in a sterile petri dish. This agar slab was allowed to solidify and was then cut in half to be 1 cm x 1 cm. Both the cover slip and the slide were wiped down with ethanol to ensure clean and sterile growth conditions for the cells. 8 µL of the diluted cells was pipetted onto the center of the sterile slide, then one square of the agar slab was carefully placed on top of the cells in media, 8 µL of MEA was pipetted onto the top of the agar slab, and the coverslip was placed over the agar slab. Using a small paintbrush, the melted VALAP was carefully painted onto the gap between the coverslip and the microscope slide to seal off the coverslip. Finally, a 23-gauge needle was used to poke holes in the solidified VALAP to allow for gas exchange. The slide was then placed face down onto the inverted microscope EVOS fl. Once an adequate number of cells was observed in frame, the cells were allowed to settle for 2 hours before imaging began. Images were then automatically taken every 30 mins for 96 hours. Videos of the budding pattern were created using Adobe Premiere Pro.

XTT Assay Optimization of XTT:Menadione for Live Cell Growth

Planktonically grown microbial organisms can be measured using optical density (OD) for their cell growth cell growth. However, for organisms such as *Candida albicans* and Crusty who grow almost exclusively in biofilms, this form of measurement is highly inaccurate and, as such, much past work has been done to develop an indirect

measurement of live cell growth. One such assay involves the use of sodium 3,3'-[l[(phenylamino)carbonyl]-3,4-tetrazolium]-bis(4-methoxy-6-nitro) benzene sulfonic acid hydrate (XTT) and Menadione for indirect measurement of live cells performing the TCA cycle via the production of red colored formazans (Berridge et al., 2005). This assay works by measuring trans-plasma membrane electron transport via reduction of menadione by XTT (Berridge et al., 2005). Although it is an indirect measurement, it is meant to be used as a comparison of the same organisms in different conditions allowing for an accurate comparison when no other means are viable.

Concentrations of XTT and menadione were optimized to measure live growth of JF2 08-2F Crusty (Antachopoulos et al., 2006). XTT is suspended in 1x PBS and menadione is suspended in acetone. A stock solution of XTT was made to the concentration of 0.5 mg/mL. Solutions of menadione were made up to the concentrations of 300 mM, 200 mM, and 50 mM. These solutions were then combined in a 20:5 XTT:menadione ratio and tested against a serial dilution of Crusty which was serial diluted with a dilution factor of 1.2 to allow for a gradual gradient of nine dilutions from 0-4.3x diluted. These dilutions were made by starting with 600 µL of cells in the 0x tube, and 100 µL of media in each dilution 1.5 mL tube. Then 500 µL of the previous dilution was added to the next dilution, mixed, and continued to the next dilution. Finally, 400 µL of fresh media was added back to the tubes to allow for a final volume of 500 µL for a proper volume to XTT:menadione mixture ratio of 500:25 (Moss et al., 2008). After the addition of the XTT:menadione, the cells were allowed to incubate at room temperature for 18 hours. The tubes were then centrifuged at 10,000 g, and 100 µL of the supernatant was aliquoted into a 96-well plate and measured at 460nm.

Comparison of the results of the individual XTT:menadione ratios to the serial dilution was performed. Linear regression analysis was performed on these values, and the optimal combination has the highest R^2 value.

Phenotypic Characterization of the Fungus Crusty

Carbon Source Utilization of Crusty

Carbon utilization of each isolate was determined using a BioMerieux ID C32 carbon utilization strip (Cat. No. 32200-1004439110). These strips have 30 different carbon sources in individual wells, one well with no carbon source for a negative control, and one well with esculin ferric citrate (**Table 2**). The esculin (β-glucose-6,7-dihydroxycoumarin) ferric citrate assay was originally used to identify Enterobacteria (Edberg et al., 1977), but was co-opted to identify *Cryptococcus neoformans* via melanin production and esculin degredation (Edberg et al., 1980).

The inoculated strips were kept in a plastic box container with a lid and lined with moist paper towels to reduce drying. The initial inoculum of cells was prepared in 25 mL of MEA shaking at room temp for 5 days. Inoculation of the strips was done according to the instructions provided by the vendor, and each strain was inoculated in three separate strips for triplicate replication. Cells were diluted to the kit requirement of McFarland standard #3 (McFarland, 1907) before starting the inoculum. Growth in the ID strip lasted 10 days before evaluation. Growth in each well was observed and evaluated by eye.

Each well was compared to the negative control (no carbon) and the positive control (dextrose/glucose). Growth was evaluated on a scale of 1-5: 1 being no growth or resembling the growth of the No carbon negative control, and 5 being the highest growth

resembling the growth on glucose. Three replicates were performed, and their averages were taken to determine the kit's final scale of: +, V, and -. For this scale: 1-1.9 was "-", 2.0-3.6 was "V", and 3.7-5.0 was "+".

Nitrogen Source Utilization of Crusty

Nitrogen utilization tests were performed using ten different nitrogen conditions. 100 mM was the concentration used for all compounds that contained one nitrogen atom per molecule: Proline, Ammonium tartrate dibasic, Serine, Sodium Nitrate, Glycine, Glutamate, and Aspartate; 50 mM was the concentration used for Urea because it has two atoms of nitrogen per molecule; 1% w/v of Peptone was used as a positive control; and no nitrogen was added as a negative control. This concentration of nitrogen sources was used because Crusty is typically grown on MEA or YPD which contain 0.2% and 2% peptone respectively. Total nitrogen content of Peptone is around ~15%, with our standard YPD media using 2% peptone that equates to 0.3% total nitrogen in the media which is 150-200 mM of nitrogen source (peptone's nitrogen content varies by batch). We decreased that molarity to 100 mM for ease of solution making but is meant to represent the amount of nitrogen source between MEA and YPD which is their standard growth media. Liquid minimal media (MN) with MN salts (not 20x Nitrate salts) (**Table 1**) was used with the varying nitrogen sources to ensure that no alternative nitrogen source would be available to the fungi. Fungi were first grown up in liquid MEA for 5 days at room temperature to reach maximum density. One mL of cells was removed and washed three times with water. 195 µL of each nitrogen source-containing medium was added to six wells in a 96-well plate, for six replicates, and 5 µL of the washed cells was added to each well. 200 µL of each medium was also added to one well each without

cells to blank each condition, because the different nitrogen sources created different colors of medium. After 7 days of incubation, growth of Crusty on each nitrogen source was measured via the XTT assay because extensive biofilms form on the bottom of the wells which are difficult to disrupt physically. Specifically, it was assumed that there was 200 µL total volume in each well and the XTT assay was scaled to that volume, where 10 µL of the XTT:Menadione was added to each well and the assay was carried out as described above.

UV-resistance of Crusty

To assess UV resistance, we used the UVP HL-2000 HybriLinker UV crosslinker as our source of UV light, which has a UV wavelength of 254 nm. Lower wavelengths (100-280 nm) are of the UV-C range, are considered ionizing radiation and are the most detrimental to living organisms, but are completely blocked by the ozone layer (Molina & Molina, 1986; Schreier et al., 2015). Therefore, using this wavelength we are able to push our organisms beyond the UV limits found in their natural habitat and test extreme amounts of UV exposure.

The fungi were inoculated in 25 mL of MEA in a 250 mL Erlenmeyer flask and let grow under shaking conditions at 200 rpm for 10 days at room temperature to reach maximum density. This culture was then washed, and serial diluted to 0x, 10x, and 100x dilution in water to ensure that as many individual cells were being exposed to the UV light as possible. 100 µL of each dilution was then spread out onto 6 MEA plates, using a glass spreader. Three plates were kept as the control growth, to compare to the three other plates which were exposed to the UV light. Experimental plates were placed inside of the crosslinker with their lids taken off. Then the plates were exposed to 120 seconds of UV

light from a distance of 9.5 cm to the light source at 10,000 μJ/cm^2 (254 nm) (Frases et al., 2007). We then wrapped all plates in aluminum foil and placed them in the Percival light incubator set at 23 °C for 2 days. Placing UV-exposed cells in complete dark after exposure is essential for preventing light-dependent photoreactivation of induced lesions (Weber, 2005). After 2 days the plates were removed from the aluminum foil and left in the incubator for 5 more days before final observations. To determine whether a particular isolate was resistant to UV exposure, the growth of the isolate exposed to UV was compared to the control growth.

Metal-Tolerance of Crusty

Metal resistance is a relatively universal trait in many polyextremotolerant fungal species. Due to the under-studied nature of this particular characteristic in fungi from biological soil crusts, we decided to test if any of our isolates were resistant to any heavy metals which would indicate possible bioremediation capacity. In order to test metal resistance, we used the antibiotic disc method by aliquoting metal solutions onto paper discs and observing zones of clearance. Metals and concentrations used are listed in **Table 3.** For testing, 5 μL of each metal solution was aliquoted onto a dry autoclaved Whatman filter paper disc which was created using a standard hole puncher. These discs were allowed to air dry and kept at 4 °C for up to a week. Initial growth of the fungal isolates was done in 25 mL of MEA, shaking at 200 rpm for 5 days at room temperature. We spread 100 μL of each fungal isolate onto 100 mm sized MEA plates using a glass spreader to create a lawn. Using flame sterilized forceps, our metal paper discs were placed onto the center of the petri dish on top of the fungal lawn and lightly pressed down to ensure the metal disc was touching the plate completely. These plates were placed in

the Percival light incubator at 23 °C with a 12 hr light/dark cycle for up to 2 weeks. Once a zone of clearing was clearly visible amongst the fungal growth (1-2 weeks), the zone of clearing was measured in cm. Generally, large zones of clearing indicated sensitivity to the metal, whereas zones of reduced size were consistent with resistance to the metal.

Temperature Growth Range of Crusty

To determine the temperature resistance range and optimal growth temperature for JF2 08-2F Crusty, we grew the fungus at 4 °C, 15 °C, 23 °C (i.e., ambient room temperature), 28 °C, 37 °C, and 42 °C. JF2 08-2F Crusty was first grown up in 25 mL of MEA for 10 days at room temperature to maximum density. One mL of cells was removed, and a 10x serial dilution was made from 0x to 100,000x, using pre-filled 1.5mL tubes with 900 µL of MEA and adding 100 µL of the previous tubes each time. Five µL of each serial dilution was spotted onto a square MEA plate which allowed us to determine the carrying capacity of each isolate at the different temperatures. Plates were kept at their respective temperatures for 7 days before observations were made, however the 37 °C and 42 °C incubators required cups of water inside of them to prevent the plates from dehydrating. Plates grown in 42 °C and 37 °C were allowed to grow at room temp for up to a week to determine if the isolates died at these temperatures or if their growth was just arrested.

Experiments to decipher the relationship between Crusty and its Methylobacterium spp. symbionts

Determination of Endosymbiosis via 16S rDNA Amplification Post-Chloramine-T Treatment

Multiple methods obtained from various other fungal-bacterial endosymbiont manuscripts were tested on Crusty and its *Methylobacterium* spp. co-occurring bacteria. One such experiment was to surface-sterilize the fungal cells using a combination of Tween-20, hydrogen peroxide, and Chloramine-T as described by (Mondo et al., 2012). Exact methods from Mondo et al. were followed; however, to make up for the clumped nature of Crusty, manual disruption of the clumps was done using a micropestle against 800 µL of Crusty that was grown up as previously stated above. This would ensure that as many cell surfaces were exposed as possible, to reduce the likelihood of bacterial cells being trapped between cell clumps. The treatment was then used on the "post-pestled" cells, and 16S PCR amplification as stated above was performed on pre- and post-Chloramine-T treated cells to determine if surface sterilization removed all signs of bacterial presence indicating non-endosymbiosis, or if a 16S signature remained, most likely indicating endosymbiosis.

Confocal Microscopy to Observe Bacterial Presence Inside Fungal Cells

To observe the presence of the bacterial symbionts inside of Crusty, we used a combination of Propidium Iodide (PI), SYTO9, and Calcofluor staining. PI and SYTO9 are considered a live/dead stain for bacteria where SYTO9 stains live cells in green (480nm/500nm) and PI stains dead cells in red (610nm). The protocol used for this method was done as follows, modified from (Partida-Martinez & Hertweck, 2005). Both PI and SYTO9 solutions were made up to 1.67 mM in DMSO, equal parts of each were added to a light-blocking 1.5 mL tube. 3 µL of that PI+SYTO9 mixture was added to 1 mL of washed (with water three times) Crusty cells that had grown up as described above

but only for 6 days. The stains stayed in the tube of cells for 15 minutes before 2 µL of 1 mg/mL calcofluor was added to the cells right before visualization.

Antibiotics to Treat Crusty of its Methylobacterium Co-occurring Bacteria

In hopes of creating a clean strain of Crusty which did not contain any *Methylobacterium* spp. in its culture as a control, we attempted to use multiple antibiotics to remove the bacteria without killing the fungus. Antibiotics used were the β-lactam Ampicillin 100 mg/mL stock, peptidyl transferase Chloramphenicol 30 mg/mL stock, aminoglycoside Gentamycin 10 mg/mL stock, aminoglycoside Kanamycin 50 mg/mL stock, rRNA binding Tetracycline 100 mg/mL stock, and the fungicide Cycloheximide 100 mg/mL stock. To determine which antibiotic would be most effective against the *Methylobacterium* spp., we used the antibiotic disc method on the mixed culture of Pinky. Pinky was grown in MEA liquid for 5 days at room temperature, then 100 µL of the culture was spread out onto 18 MEA plates. Then filter paper discs were impregnated with 5 µL of one of the above listed antibiotics and were placed in the middle of the Pinky lawns. The plates were allowed to grow up for 8 days at 23 °C, then the zone of clearing caused by the antibiotic discs was observed. Once the antibiotic with the most defined zone of clearing was identified, we went on to use it on Crusty to try to clear out the *Methylobacterium* spp. from Crusty.

Gentamycin Treatment of Crusty, Pinky, and S. cerevisiae

Gentamycin ended up being the second most effective antibiotic treatment against the Pinky in our antibiotic disc trials. We decided to use Gentamycin as our first antibiotic to attempt to remove the *Methylobacterium* spp. from Crusty because it is bactericidal. Crusty, Pinky, and *S. cerevisiae* were grown up as described above, then 100

µL of the fungal cultures or 10 µL of the bacterial culture were added to 1.9 mL of MEA in a 24-well plate. In triplicate, each organism either had 20 µL of 0.3 mg/mL Gentamycin added, or nothing for a control. Then the cultures were allowed to grow at 23 °C for 7 days, after which the XTT assay as described above was used to determine the viability of cells after treatment.

Testing Fungal and Bacterial Ability to Grow in the Presence of Tetracycline

To attempt to obtain a Pinky-free Crusty and determine a dosage effect of the antibiotic Tetracycline on Crusty's ability to grow, we exposed the fungus to increasing amounts of Tetracycline in liquid culture and then spread out the resulting growth on to plates with and without Tetracycline added. Crusty was grown up as described above, then 50 µL of cells were inoculated into size 25 tubes containing 5 mL of MEA. Each tube then received either 1 µL/mL, 2 µL/mL, 3 µL/mL, or 4 µL/mL of 100 mg/mL Tetracycline, 4 µL/mL of 100% Ethanol as a carrier control, or nothing as a standard control. This was done in triplicate tubes, and then they were put into a roller drum for 7 days. After 14 days of growth, 100 µL of each tube was spread out onto either a MEA plate with 1 µL/mL of Tetracycline added or no Tetracycline added. These plates were then allowed to grow up for 14 days, and then they were observed and imaged. To determine the effect of the Tetracycline treatment on Crusty, we then used ImageJ to calculate the pixel area of Crusty on each plate.

This same protocol was repeated using *S. cerevisiae* BY4741 and Light Pinky alone and in co-culture. This experiment allowed us to determine whether Tetracycline was affecting not only the bacteria, but also the fungus. We only used the highest

concentration of Tetracycline, 4 μL/mL, for optimum effect and compared it to the Ethanol carrier control.

Microbial Interaction Experiments

Tri-culture Experiments in Carbonless BBM

In lichens, the essential nutrient exchange process that is known is carried out by the photosynthetic partner providing a source of carbon to the fungal partner. We wanted to see if we could mimic this symbiotic phenomenon using Crusty, the algae *C. sorokiniana* UTEX 1230, and the addition of external Pinky. *C. sorokiniana* was chosen as the algal portion of this experiment because it is in the same class Tebouxiophyaceae as lichen forming algae of the genus *Trebouxia*. It was also chosen because of availability, it was the only algal culture in our collection at the time, and since it was related to *Trebouxioid* algae we believed it would be a comparable substitute for a *Trebouxia* spp.

This experiment was performed using the carbonless media Bold's basal medium (BBM) (Connon, 2007) with and without its nitrogen source, which is sodium nitrate. All three organisms were grown up in their standard manner as described above, the cells were washed with BBM-nitrate three times, then 100 μL of each organism was inoculated into non-tissue culture treated tissue culture flasks either in monoculture, co-culture, or tri-culture. We used non-tissue culture treated tissue culture flasks because they have not been treated with vacuum-gas plasm, keeping their surface hydrophobic, which is optimal for fungal biofilm formation (Silva-Dias et al., 2015). The cells were then grown at 23 °C in a 12 hr light/dark cycle for 30 days. After 30 days, pictures of the entire flasks were

taken and the XTT assay as described above was performed to determine the amount of active metabolism of Crusty in the various conditions. The XTT assay was not effective at determining the active metabolism of *C. sorokiniana*, but the images of flasks show where growth was capable or not capable.

Crusty-Pinky +/- Carbon, Nitrogen, Light

After performing the Tri-culture experiments there was uncertainty about how Crusty was capable of active metabolism when exposed to 30 days without a carbon source in the conditions that did not contain *C. sorokiniana*. Therefore, we decided to grow Crusty-Pinky (which is emphasized here as Crusty-Pinky due to Pinky's importance) in BBM with and without 27.4 mM of mannitol, with and without sodium nitrate, and with and without the addition of 12 hours of light per day. This experiment was done to determine if light was affecting Crusty-Pinky's ability to perform active metabolism in carbonless, nitrogenless medium. It was initially done to determine if the *Methylobacterium* spp. co-occurring with Crusty were capable of nitrogen or carbon fixation and therefore providing nutrients to Crusty allowing for active metabolism. However, this experiment was performed before we received the whole genomes of Light Pinky and Dark Pinky, where we discovered that Dark Pinky was capable of making bacteriochlorophyll and therefore capable of performing aerobic anoxygenic photosynthesis.

Crusty was grown up as described above, then an aliquot of cells was washed three times with water and let to sit in water for three hours. Then 20 mL of BBM either with or without 27.4 mM of mannitol and/or sodium nitrate was added to non-tissue culture treated flasks (25 cm^2, 70 mL volume Falcon brand), where 100 µL of the washed

cells were then added (n=3, 3 biological replicates for each condition). Flasks were placed inside of a Percival Scientific light incubator Model no.: CU-36L4, set to 23 °C with a 12-hour light/dark cycle. Flasks that were kept in the dark were kept in the same incubator but were wrapped entirely in aluminum foil to block all light. Cells were allowed to grow in these conditions for 14 days, and afterwards the XTT assay as described above was performed to determine active metabolism of Crusty-Pinky. Additionally, 100 μL of the culture was removed at day 7 and 14 to spread out onto MEA plates to determine if Pinky was growing or "escaping" Crusty, and if Crusty and/or Pinky was growing under each condition. Images of the bottom of the flasks were also taken at days 7 and 14 using an EVOS-fl, which has an inverted objective allowing us to not disturb the flasks for imaging.

Overlaying Algae over Methylobacterium spp. Spots

Methylobacterium spp. are known to enhance the growth of plants via the production of phytohormones (Ivanova et al., 2001). As such, we decided to determine if Light Pinky, Dark Pinky, their combination Pinky, and the North Antelope valley Parkway canal isolate P3, were capable of stimulating the growth of microscopic plants, aka algae. *Chlorella sorokiniana* has previously been identified as both responding to and producing its own auxins, which is why this strain was used in this experiment (Khasin et al., 2018). We tested this by spotting the bacteria onto MEA plates, then creating a semi-solid BBM overlay containing varying concentrations of *C. sorokiniana*.

The four bacterial cultures were first grown up as described above, then washed in fresh MEA three times. 5 μL of this culture was then spotted onto MEA plates nine times and repeated in triplicate plates for all three cultures with the intention to add algal

overlays of five concentrations for each bacterial strain (45 plates total). The MEA plates with spotted bacteria were allowed to grow at room temperature for three days before the algal overlays were added. For the overlays, *C. sorokiniana* UTEX 1230 was grown up as described above, then washed three times with fresh BBM. This culture was then diluted with a 10x dilution from 0x-10,000x dilution in 10 mL aliquots. A semi-solid BBM mixture was made with 0.5% agar, and 9 mL of that mixture was added to 15 mL falcon tubes. 1 mL of the individual *C. sorokiniana* serial dilutions was added to the 9 mL of 0.5% agar BBM when the agar was approximately 40 °C. The BBM and *C. sorokiniana* mixture was then carefully poured over the bacterial spotted plates, as to minimize disturbances to the bacterial colonies. These plates were then grown at 23 °C with a 12-hour light/dark cycle for five days, after which they were observed and photographed.

Results

Description of Crusty

JF2 08-2F Crusty was isolated from Jackman Flats Provincial Park in B.C. Canada. Initial ITS sequencing was performed to obtain potential taxonomic matches. The highest BLAST match was 92.91% identity against "*Exophiala placitae* strain CBS 121716" (MH863143.1). Whole genome sequencing is still being performed. However, phylogenetic analyses using ITS revealed that JF2 08-2F Crusty is a novel species closely related to the genera *Phaeococcomyces* and *Neophaeococcomyces* (**Figure 1**). Morphological characterization of Crusty demonstrated that it has a very sand-like colony texture, allowing for the colonies to easily fall off a sterile loop when transferring to a plate, hence the name Crusty (**Figure 2A**). The colonies are relatively tall in the z-axis

but hyphae do not tend to invade the agar itself. Crusty has a very dark black colony pigmentation, which is common to all polyextremotolerant fungi due to high melanin content in their cell walls (**Figure 2**). It also forms extensive biofilms on the air-liquid surface interface of flasks it's grown in (**Figure 2C**).

The Many Faces (Cell Morphologies) of Crusty

Cells of Crusty are a polymorphic in nature, ranging from perfect spheres (**Figure 2D**) typical of the microcolonial fungi group of polyextremotolerant fungi, all the way to the formation of yeast and pseudohyphal cells (**Figures 2F & 3**). Other times, very large spherical cells can be seen with no observable septa, which are possibly chlamydospores (**Figure 3;** black arrows), and additional curved cells are frequently observed (**Figure 3**; white arrows). Crusty's cell morphology also differs when grown in liquid medium versus growing on solid agar plates. In liquid it forms more pseudohyphae, and odd morphologies such as curved cells, meristematic cells, and large spherical cells are more commonly observed. Whereas, on solid media Crusty grows almost exclusively as perfect spherical cells in clumps and chains similar to *Knufia petricola*, and these cells are observed to release large amounts of lipid droplets from their surface (**Figures 2D & 2E**). Curved cells in fungi are usually a sign of chemotrophism attributed to the fungal cell's attraction to a chemical compound. At this time, it remains unclear whether Crusty exhibits true chemotrophism and the nature of any possible chemical attractant is unknown. Additionally, Crusty's cell division in liquid culture is similar to that of *Hortaea werneckii* and *Phaeotheca salicorniae*, in that it seems to both perform budding and binary fission in some aspects (**Figure 3B**), and also form meristematic cells and

hyphae in other parts of budding cells (Mitchison-Field et al., 2019; Sterflinger, 2006) (**Figures 2F & 3;** asterisks).

Discovery of Methylobacteria Associated with Crusty

Typically, when growing out Crusty, it is not obvious that there are bacteria present because no bacterial colonies form (**Figure 2A**). If the cell wall has been disrupted in some way (i.e., resurrection of frozen stocks, bead beating), then colonies of both Crusty and Pinky will form on the plate when plating out cells (**Figure 2B**). This is why it was not initially apparent that this fungus even had bacterial symbionts. There are other strains in our collection from the same location that are inundated with *Methylobacterium* colonies when they are plated out, to the point where it is almost impossible to keep the fungus alive without the use of antibiotics to kill off the bacteria. Further evidence for the presence of bacteria associated with Crusty arose from the analysis of genomic DNA prepared for sequencing by the Joint Genome Institute (JGI). The extracted DNA had seemingly come from a sample that was a pure culture by eye, but results from quality controls revealed that there were two *Methylobacterium* spp. contaminating our sample. After performing our own 16S rDNA PCR again on what presumably was a pure culture of Crusty, we were able to replicate these results implicating that Crusty had co-occurring bacterial members that were not obvious when streaked on a petri plate.

Spontaneous Albino (Pink) Mutant of Crusty

While Crusty was being domesticated in the lab, observations were made of pink colonies forming at random intervals that showed the same colony morphology and cell morphology as wild type Crusty (**Figure 4**). This is not a novel phenomenon for fungi of

the *Knufia*, *Phaeococcomyces*, and *Neophaeococcomyces* clade as it was first observed by Katja Sterflinger's group in *K. petricola,* with no follow-up however on the mechanism of its occurrence (Tesei et al., 2017).

Descriptions of Light Pinky and Dark Pinky, and Potential Metabolic Functions

Both of the bacteria found in association with Crusty are of the genus *Methylobacterium* according to their 16S rDNA and whole genome sequences. However, the species delineation between *Methylobacterium* spp. based solely on 16S rDNA is difficult to parse out (**Figure 5**). Therefore, assigning either JF2 08-2 LP Light Pinky or JF2 08-2 DP Dark Pinky to any known *Methylobacterium* spp. would require detailed genomic analyses. Nevertheless, we can still confirm that they are *Methylobacterium* spp., and with their genomes sequenced we will be able to understand what they are metabolically capable of as members of that genus. The relative abundance of these two bacterial strains within Crusty is unknown. It is even sometimes difficult to determine if they are both present simultaneously, if they are actually one strain, or if there is only one strain present using 16S rDNA PCR alone. Additionally, their genomes are highly similar, yet their morphologies remain distinctly different (**Figure 6**).

Both Light Pinky and Dark Pinky are single-celled rod-shaped bacteria. In MEA, they do not readily form any filamentation or clumpy forms, although filamentation has been observed when grown in BBM (Data not shown). They are both pink in color due to the production of carotenoids, but have a distinct difference in their pigmentation, hence their difference in names. Light Pinky is lighter in color than Dark Pinky, where it is most obvious when they are grown on Minimal (MN) media (**Figure 6A**).

Regarding their metabolic capacity, genomic annotation suggests that neither strain is capable of nitrogen fixation as observed in Rhizobiales, for which there are three separate genetic pathways. However, in annotating these genes, we confirmed that they do contain ancestrally related genes involved in light-independent (dark) protochlorophyllide reductase (DPOR) used for anoxygenic bacterial photosynthesis (Fujita & Bauer, 2000). We were able to identify homologs of every bacteriochlorophyll (*bch*) gene required for bacterial photosynthesis from the Dark Pinky annotation (**Table 4**). Other genes essential for oxygen sensing that are used for both nitrogen fixation and anaerobic anoxygenic bacterial photosynthesis, such as the *fix* genes and other nitrogen fixation (*nif*) genes besides Nitrogenase iron protein 1 (*nifH*), were also found in the genome. These genes could be used to assist the bacteria in sensing an oxygen-less environment, which is essential for anaerobic anoxygenic photosynthesis, but not aerobic anoxygenic photosynthesis (Madigan, 1995).

XTT Assay Optimization of XTT:Menadione for Live Cell Growth

Due to Crusty's clumpy morphology and biofilm formation, performing any experiments that require a plate reader (OD reads) is challenging. However, many studies of other biofilm-forming or clumping organisms have implemented an alternative colorimetric assay, which utilizes live cells' ability to transport electrons across their membrane during active metabolism as an alternative to direct OD reads (Berridge et al., 2005). Therefore, we decided to use this method to observe the growth patterns of Crusty in the variety of experiments we would impose upon it. This method needed to first be optimized for concentrations of the two substrates to Crusty before experiments could be performed.

Serial dilutions of Crusty were tested against the three different concentrations of XTT:Menadione of 0.5 mg/mL:50 µL, 0.5 mg/mL:100 µL, and 0.5 mg/mL:300 µL. Based on the resulting R^2 values, the optimal XTT:Menadione concentration that was tested was 0.5 mg/mL:50 µL, and therefore was used for future studies (**Figure 7**).

Phenotypic characterization of Crusty

Carbon Utilization of Crusty

Crusty was capable of utilizing 16 of the 30 carbon sources it was tested on in a positive manner, and 7 in a variable manner (**Table 2** & **Figure 8**). Overall, Crusty's carbon utilization is similar to that of *E. viscosium* and *E. limosus* (Carr et al., 2022). However, two carbon sources that Crusty is capable of using that *E. viscosium* and *E. limosus* cannot use are D-saccharose and D-raffinose, and carbon sources that Crusty cannot use that the others can are L-arabinose, erythritol, D-trehalose, and potassium 2-ketoglutarate (**Figure 8**). Interestingly, we again see the presence of a difference in coloration with the growth of Crusty on N-acetyl glucosamine, making a reddish pigment. We were also able to confirm Crusty's ability to produce DHN melanin with the esculin ferric citrate assay presenting a dark coloration (**Figure 8**)

Nitrogen Utilization of Crusty

To investigate nitrogen source utilization of Crusty, we used MN media (**Table 1**) and dropped out the nitrate to add in our various nitrogen sources for testing Crusty's ability to grow on them. According to the XTT assay and visual confirmation of growth, peptone remains Crusty's preferred source of nitrogen, with urea and serine as close second preferable sources (**Figure 9**). Proline, glutamate, and aspartate were all similar in

usage and the next preferred nitrogen source, followed by nitrate. Interestingly, the absence of a source seemed to promote more growth than did either glycine or ammonia (**Figure 9**).

UV-resistance of Crusty

Since Crusty's colony morphology is drastically dark in color due to melanin deposition in its cell wall, we believed that it would be resistant to high amounts of UV exposure. Performing a serial dilution of Crusty before exposing the cells to the 245nm UV-C light allowed us to ensure that cells were not protected from their 3D clumping nature. In the 0x UV-exposed plate, it seemed that much of the original amount of growth from the control plate was able to grow, accounting for 32% survival by pixel area (**Figure 10**). However, when diluting down to 10x it was obvious that much less of the cells survived with only 8.5% of the control's area being represented in the UV-exposed plate (**Figure 10**). Finally, on the 100x diluted plate, only 5.4% of the control area was able to grow after UV exposure (**Figure 10**). Considering, *S. cerevisiae* and *E. dermatitidis* are unable to grow at this length of UV-C exposure, Crusty can be considered resistant to UV-C.

Metal Tolerance of Crusty

Polyextremotolerant fungi are well known for their metal resistance, particularly due to melanin's metal chelating abilities (Cordero & Casadevall, 2017; Gadd & de Rome, 1988; Hong & Simon, 2007). Therefore, we wanted to determine how resistant Crusty was to various metal species; treatment results were binned based on their inhibition size: none, medium, and high. Crusty showed no zone of clearing when exposed to 1M $FeSO_4$ or 2M $LiCl_2$ (**Figure 11** & **Table 3**). Crusty was moderately

resistant to 1.5M $CuCl_2$, 470 mM $AgNO_3$, and $CoCl_2$ with a 1.4 cm, 2.8 cm, and 3 cm zones of clearing respectively (**Figure 11** & **Table 3**). Crusty showed the lowest resistance to 10mM $CdSO_4$ and 1.5M $NiCl_2$ with 4.5 cm and 4.7 zone of clearing respectively (**Figure 11** & **Table 3**).

Temperature Growth Range of Crusty

To determine the growth range and optimal growth temperature of Crusty we grew Crusty in a 10x serial dilution at five different temperatures from 4 °C to 42 °C. Crusty was capable of slow growth at 4 °C. The optimal growth temperature of Crusty was 23 °C, which showed extensive growth of Crusty at all dilutions (**Figure 12**). Interestingly, at 28 °C Pinky was able to outgrow Crusty making the dilutions above 0x all Pinky colonies with the 0x showing some Crusty colonies with Pinky covering them. Both 37 °C and 42 °C did not promote the growth of Crusty, even though Crusty only remained at those temperatures for 48 hours. Returning Crusty to room temperature after incubation at the higher temperatures did not restore growth, thereby suggesting that exposure to 37 °C and 42 °C might be lethal (**Figure 12**).

Experiments to Decipher the Relationship Between Crusty and its Methylobacterium spp. Symbionts

Determination of Endosymbiosis via 16S rDNA Amplification Post-chloramine-T Treatment

Once it was apparent that Crusty had *Methylobacterium* spp. present in its culture, even when they were not forming colonies on a plate, we wanted to determine if the bacteria were inside the fungal cells or not. A method that has been used by previous

studies to determine fungal-bacterial endosymbiosis is cell surface sterilization using the Chloramine-T method (Mondo et al., 2012). This is meant to ensure that the only bacteria that DNA is extracted from and therefore 16S rDNA is amplified from, is inside of the fungal cell wall.

We performed this method on Crusty and *S. cerevisiae* as a negative control. When the 16S rDNA region extracted from Crusty prior to Chloramine-T treatment is amplified we see a distinct band, which indicates bacterial presence (**Figure 13**). After Chloramine-T treatment, the 16S rDNA band is still present in Crusty, which indicates the presence of bacteria inside its cell wall. This 16S rDNA band is not present in *S. cerevisiae* which is not known to have a bacterial endosymbiont, and the 16S rDNA band is present for the Light Pinky positive control (**Figure 13**).

Confocal Microscopy to Observe Bacterial Presence in Fungus

Additional evidence of bacterial endosymbiosis was obtained by performing a bacterial live-dead stain along with a fungal cell wall stain on Crusty. This method was used in another fungal-bacterial endosymbiont study by Partida-Martinez & Hertweck to observe the presence of live bacterial cells within hyphae of Rhizopus (Partida-Martinez & Hertweck, 2005). Replication of their method with the addition of calcofluor white for chitin staining of the fungal cell wall allowed us to observe the relative location of bacteria within Crusty within the same x-axis but this method is unable to resolve a z-axis resolution.

When Crusty cells are stained with PI (red), SYTO9 (green), and calcofluor white (blue) we can see that all three stains will stain parts of the cell (**Figure 14**). The calcofluor white stains only the fungal cell wall, PI stains likely dead bacterial cells, and

the SYTO9 stains where presumably live bacterial cells reside. This combination of stains was also performed on the Pinky cells alone, which showed that calcofluor did not stain any cells, and also that not all bacterial cells were capable of being stained with either bacterial stain (**Figure 14**). Additionally, it was obvious that either the bacterial stains were not able to penetrate every fungal cell or that not every fungal cell contained bacteria, because not all fungal cells showed the fluorescence of the bacterial stains (green or red) (**Figure 14**).

Antibiotics to Treat Crusty of its Methylobacterium Co-occurring Bacteria

In order to create a control strain of Crusty, we attempted to remove its *Methylobacterium* symbionts by using antibiotic exposure. Before we could start with exposing Crusty to antibiotics, we first had to determine which antibiotic would be best to test against Pinky. We performed the Kirby-Bauer antibiotic disk diffusion test using multiple antibiotics individually on a lawn on Pinky (Bauer et al., 1959). The antibiotic that showed the largest zone of clearing was Tetracycline 100 mg/mL (**Figure 15**). However, Tetracycline is only bacteriostatic not bactericidal, meaning it would theoretically not kill and remove Pinky from Crusty but only stop it from growing. The second-best antibiotic that is also bactericidal was Gentamycin 10 mg/mL (**Figure 15**). We decided to use Gentamycin and Tetracycline moving forward in attempting to clear Crusty of its Pinky symbionts.

Gentamycin treatment of Crusty, Pinky, and S. cerevisiae

Using the bactericidal Gentamycin on Crusty as a means of removing its Pinky symbionts did not remove the bacteria. Instead, Crusty was incapable of growth in the presence of this antibiotic. This led us to determine if Gentamycin was capable of killing

fungal cells in addition to bacterial cells. Using the XTT assay we tested Gentamycin on Crusty, Pinky, and *S. cerevisiae* to determine if Gentamycin was capable of killing fungal cells and therefore killing Crusty as well, or if it was just killing bacterial cells which, in turn resulted in the inhibition of growth of Crusty. After all three microbial species were grown up in the presence of Gentamycin, only Crusty and Pinky were unable to grow in the presence of Gentamycin. *S. cerevisiae* was capable of growing in Gentamycin's presence indicating that Gentamycin is not an antifungal (**Figure 15**).

Testing Fungal and Bacterial Ability to Grow in the Presence of Tetracycline

Continuing to test antibiotics on Crusty for both the goal of obtaining a bacterial-free culture and now determining how dependent Crusty is on this bacterial presence, we decided to use the more effective bacteriostatic antibiotic Tetracycline. Since it is a bacteriostatic, tetracycline would not be able to entirely kill Pinky but would prevent its growth and therefore stop it from performing metabolic functions that would potentially be essential for its symbiosis with Crusty. We decided to first test Crusty grown in increasing amounts of Tetracycline and then determined the area of growth on plates with and without Tetracycline to observe how Crusty's growth changes when Pinky's growth is halted.

When Crusty is grown in increasing amounts of Tetracycline there is a decrease in its ability to grow compared to the carrier 70% ethanol (**Figure 17**). Growing Crusty in 1 μL/mL of Tetracycline all the way up to 4 μL/mL of Tetracycline provides the same amount of growth repression when it is grown on Tetracycline plates, continuing the blocking of Pinky's growth (**Figure 17**). However, when the same cultures are plated out onto media that does not have Tetracycline added, a dose-dependent response is seen,

where the more Tetracycline Crusty was exposed to, the less growth is observed (**Figure 17**). Additionally, no bacteria-free Crusty colonies were able to be recovered from exposure to Tetracycline, even after many attempts.

To ensure that this observation was once again related only to Tetracycline's effect on the bacteria and not a potential effect on the fungus, we performed the same experiment with *S. cerevisiae* alone and in co-culture with Pinky. This time we chose to use the highest dosage of Tetracycline at 4 μL/mL. When *S. cerevisiae* alone is grown in the presence of Tetracycline its growth actually increases likely due to the presence of the ethanol carrier, indicating no antifungal properties of Tetracycline (**Figure 18**). Additionally, when *S. cerevisiae* is co-cultured with Pinky, there is not a very high decrease in growth (**Figure 18**).

When comparing the growth inhibition of Crusty, Pinky, and *S. cerevisiae* with and without Tetracycline, we decided to compare the percentage of pixel area between the controls and the 4 μL/mL Tetracycline treatments, due to the differential nature of the colony heights and therefore cell layers unaccounted for by surface area between the three species. When comparing these microbes' percentage of growth when grown in 4 μL/mL of Tetracycline compared with the ethanol carrier control, Crusty experienced the most drastic decrease in growth, where only 31% of cells were able to grow in the presence of Tetracycline compared to the control growth (**Figure 19**). Pinky experienced the second least growth at 35% compared to its control, and *S. cerevisiae* in co-culture with Pinky only had 81% growth compared to its control (**Figure 19**). This difference in cell area is very apparent when observing the plates themselves, where the *S. cerevisiae* control plates looks almost identical to the 4 μL/mL of Tetracycline plate, whereas both

the Crusty and Pinky plates show a large decrease in colonies on the Tetracycline plates compared to their controls (**Figure 20**).

Microbial Interaction Experiments

Tri-culture Experiments in Carbonless BBM to Observe Nutrient Acquisition from C. sorokiniana to Crusty

Our larger question in the isolation and identification of multiple polyextremotolerant fungi has been to determine if they can undergo lichen-like interactions with photosynthetic algae and nitrogen-fixing bacteria. When this experiment began, we did not know if the *Methylobacterium* spp. harbored by Crusty contained nitrogen-fixing metabolism or not. However, we assumed that they would, based on their phylogenetic relationship with Rhizobiales and other nitrogen fixing *Methylobacterium* spp. Therefore, we thought that the Crusty-Pinky symbiosis would be the more successful fungus to try in attempting a lichen-like co-culture (or tri-culture) with the algae *C. sorokiniana*, in addition to the well-known production of growth hormones by *Methylobacterium* spp. which would likely assist in this tri-culture. The algae *C. sorokiniana* was also chosen due to its phylogenetic relationship to lichen forming Trebouxioid algae, and convenience due to its availability in our stock collection. We performed a tri-culture, and respective mono- and co-cultures for controls, of Crusty, Pinky, and *C. sorokiniana* UTEX 1230 in BBM with no carbon source and performed the XTT assay to observe if Crusty had increased active metabolism (the direct measurement of the XTT assay) with only an algae's secretion of sugar as a potential source of carbon after 27 days.

Tri-culture of Crusty with Pinky and *C. sorokiniana* did not result in increased metabolism, compared to Crusty without any added microbes (**Figure 21**). Additionally, Crusty grown in the presence of *C. sorokiniana* only (with its presumed Pinky endosymbiont) also did not have increased metabolism compared to Crusty without any added microbes (**Figure 21**). The only conditions that did increase the active metabolism of Crusty was when 10 μL instead of 100 μL of Pinky was externally added to the tri-culture (**Figure 21**). Most notably, Crusty was capable of active metabolism in a carbonless medium without a photosynthetic microbe present, only relying on itself and Pinky, which was not initially thought to provide a carbon source to Crusty (**Figure 21**).

Crusty-Pinky +/- Carbon, Nitrogen, Light

Due to the interesting observations seen in the tri-culture experiment, where Crusty was capable of active metabolism in a carbonless environment, we decided to re-test the Crusty-Pinky symbiosis against multiple media drop-out conditions. We grew Crusty-Pinky in BBM media that either did or did not contain mannitol as a carbon source or nitrate as a nitrogen source. All conditions were either exposed to a 12-hour light/dark cycle or kept permanently in the dark (n=3, 3 biological replicates). This experiment was done to determine whether the Crusty-Pinky symbiosis was capable of active metabolism in the absence of essential carbon and nitrogen sources, and whether light induced active metabolism in these conditions. If either or both organisms were capable of active metabolism without any external carbon or nitrogen source, then it is likely that Pinky could be producing a carbon or nitrogen source for Crusty, or that Pinky is engaging in anoxygenic photosynthesis.

When Crusty-Pinky was grown up in BBM with no carbon, no nitrogen, and no light, the XTT assay showed that active metabolism decreased from day 7 to day 14 (**Figure 22**). However, the CFU assay for these same conditions showed on day 7 a pure culture of Crusty with no Pinky escaping the Crusty cells, but on day 14 there was a mixed culture of Crusty and Pinky colonies (**Figure 23**). Interestingly, when light is introduced to the no nitrogen and no carbon conditions (-N -C), there is a significant increase in active metabolism from day 7 to day 14 (**Figure 22**). Although, this does not reflect an increase in cellular growth as seen in the CFU assay. The CFU plates for Day 7 and 14 of the no nitrogen, no carbon, plus light contained the same colony number as the no light plates (**Figure 23**). This trend of an increase in active metabolism with the addition of light to the various conditions tested, is seen in every other condition tested (+N, +C, +N +C), and is statistically significant with $p < 0.05$ (n=3) in all except the +N +C conditions (**Figure 22**).

CFU plates of each condition show a rough ratio of Crusty to "escaped" Pinky that would be reflective in the XTT assay performed. Interestingly, addition of carbon leads to the retention of Pinky on day 7 whether there is light exposure or not (**Figure 23**), and on day 14 only very few Pinky colonies can be seen in the no light but added carbon condition (**Figure 23**). However, when light exposure is present, Pinky is capable of being released in the carbon conditions on day 14 (**Figure 23**). The rest of the CFU plates whether light, carbon, and/or nitrogen are present show a mixture of Crusty and Pinky colonies on all plates (**Figure 23**).

Overlay of Algae over Methylobacterium spp. Spots

The reason for why Pinky is associated with Crusty is still largely unknown. However, *Methylobacterium* spp. are known to produce plant phytohormones (Koenig et al., 2002; Tani et al., 2012). Therefore, to determine if Light Pinky and Dark Pinky were capable of growth stimulation of algae, we decided to observe how the individual Pinky's would interact with the algae *C. sorokiniana*. All *Methylobacterium* isolates and the combination of Light and Dark Pinky were spotted onto MEA, which is a medium that they all readily grow on. Then, we overlayed either 0x, 10x, 100x, or 1000x diluted *C. sorokiniana* in 0.5% agar BBM. This allowed us to observe how the bacteria on the spots would affect the algae directly above them.

Growth stimulation of *C. sorokiniana* when overlayed on top of Pinky (both Light Pinky and Dark Pinky) at every dilution seemed minor (**Figure 24**). There was only a slight growth increase directly over the bacterial spots, but the algae grew in an even coating across the plates. However, when Light Pinky and Dark Pinky were spotted individually, both were capable of stimulating algae growth directly above their spots (**Figure 24**). Light Pinky was more capable of enhancing the growth of the algae than Dark Pinky because there was more algal growth on the algae that was directly touching the spots over Light Pinky than over Dark Pinky. Interestingly, both Dark Pinky and Light Pinky also show a slight zone of inhibition at the highest concentration of *C. sorokiniana* (0x). The area directly around the middle dot surrounded by the other eight dots is paler for both plates (**Figure 24**). Directly over the dots still shows growth enhancement, as there is also growth enhancement over each of the dilutions for Light and Dark Pinky. Additionally, both Light Pinky and Dark Pinky seem to enhance colony formation of *C. sorokiniana* versus planktonic growth when compared to their

combination (Pinky) or the other *Methylobacterium* spp. P3, on the other hand, had a complete zone of inhibition, clearing out any algal growth especially on the 10x diluted sample (**Figure 24**). In the 0x sample, it appears that there is some growth stimulation on the corner bacterial dots though. However, the zone of inhibition becomes larger as the algal concentration decreases to where there is almost no algal growth in the 1000x sample (**Figure 24**).

Discussion

Crusty is a Novel Polyextremotolerant Fungi

In this study, we have described a novel polyextremotolerant fungal species that appears to harbor endosymbiotic bacteria. The morphological group of polyextremotolerant fungi is not historically a widely studied group of fungi, yet active research into this group has recently increased which will likely lead to the discovery and characterization of new polyextremotolerant fungi in the near future. . Crusty is likely a member of the genus *Neophaeococcomyces* based on the current ITS sequences and phylogenetic analyses performed. However, documentation of this genus is limited to sequences in the NCBI database, with no full publications of experiments on members of the genus itself, and only the initial descriptions required for novel species identification (Crous et al., 2015; Moreno-Rico et al., 2014; Réblová et al., 2016). With this detailed description and experimentation of the novel species Crusty we expect to gain additional knowledge into this cryptic genus.

Mimicking the Biological Soil Crust Symbiosis with Crusty, Pinky, and C. sorokiniana

Biological soil crusts are vastly complex biofilms, containing millions of different taxa with a range of ecological relevance (Belnap et al., 2001; Belnap & Lange, 2003). Therefore, studying them for their microbial interactions can be quite difficult, as microbial interactions in any microbiome are very complex. In an attempt to simplify this complex consortium, we whittled this down to what we believe to be some of the most important niches within a biological soil crust: a nitrogen source provider, a carbon source provider, and a structural biomass adherence and/or provision of abiotic stress tolerance (melanin). The first two niches are metabolically essential, in that there is no external source of nitrogen or carbon for the biological soil crust biofilm (Belnap, 2002; Belnap & Büdel, 2016; Li et al., 2012). Both niches are largely held in the beginning by cyanobacteria, particularly *Microcoleus* spp. (Belnap, 2003), then algal and nitrogen-fixing bacteria participate in those roles during the later stages of biological soil crust development (Bowker et al., 2002; Lan et al., 2012). Since we had a fungus with symbiotic bacteria that we believed at the time to have nitrogen assimilating capabilities and an alga of the family Trebouxiophyceae, a common lichen photobiont (Ahmadjian, 1982; Kroken & Taylor, 2000; Triebel & Dagmar, 1992), we decided that these would be our best candidates for attempting a simulated biological soil crust symbiosis experiment, the tri-culture experiment.

The algae *C. sorokiniana* was chosen initially because it belongs to one of the most extensive lichen photobiont groups Trebouxiophyceae. However, we did not know at the time that *C. sorokiniana* does not perform the same metabolic functions that its lichenized Trebouxioid relatives have, mainly the production and secretion of polyols, particularly ribitol, as a carbon source (Richardson & Smith, 1968; Richardson et al.,

1967). Instead, *C. sorokiniana* and other *Chlorella* species do not secrete any polyols (Gustavs et al., 2011), they only produce and excrete glucose and maltose (Fischer et al., 1989; Kessler et al., 1991). While these are still carbon sources that can be used by any microbes in its vicinity, they may not be a good analogue for the algal portion of the biological soil crust symbiosis that we had hoped to mimic. Mainly, glucose as a carbon source induces carbon catabolite repression, which is a major metabolic and transcriptional regulator for many other "non-ideal" nutrient metabolite processes such as nitrogen metabolism (Dowzer & Kelly, 1991; Nair & Sarma, 2021; Portnoy et al., 2011; Ries et al., 2016). The reason we did not see a distinct increase in the growth of Crusty when co-cultured or tri-cultured with *C. sorokiniana*, may have been because of this distinct metabolic and therefore interactive difference.

We observed an increase in growth in one of the tri-culture flasks containing 10 µL of added external Pinky with 100 µL of *C. sorokiniana* and Crusty individually. These conditions had the highest increase in active metabolism across the tri-cultures, including higher metabolism than cultures inoculated with all three microbes in equal amounts. An explanation for this, could lie in the bacterial component. *Methylobacterium* spp. are known to produce plant phytohormones, which increase the growth of the plants in exchange for methanol which is released from plant stomata (Kutschera, 2007; Trotsenko et al., 2001). The *Methylobacterium* produce multiple types of these compounds, mainly cytokinins and indole acetic acid (Ivanova et al., 2001; Koenig et al., 2002; Meena et al., 2012), which have been shown to increase the growth of algae (Khasin et al., 2018) and increase fungal growth (Fu et al., 2015; Kulkarni et al., 2013; Sun et al., 2014). These phytohormones are shown to have dose-dependent response in these systems, only

stimulating growth at low levels, with higher levels causing growth repression (Kulkarni et al., 2013; Sun et al., 2014) . It could be that when Pinky was added at $1/10^{th}$ of the ratio of the algal and fungal components to the tri-culture system, it did not exceed the amount of hormone production for growth promotion. Additionally, less bacterial initial inoculum possibly prevented the bacteria from scavenging more of the glucose carbon source from Crusty.

We were able to confirm that both Light Pinky and Dark Pinky have growth promoting capabilities with the *C. sorokiniana* plate overlay experiments, the growth of *C. sorokiniana* was greatly increased directly over the spots of bacteria that were grown on MEA. This did not occur with our other *Methylobacterium* sp. isolate P3, which was isolated from North Antelope Valley Creek in Lincoln, NE. It indicated that P3 is a potential antagonist against algal growth; as algae could be competition in water ecosystems as opposed to in a biological soil crust where they would be the main source of carbon. Which specific growth hormones our *Methylobacterium* spp. are producing were not identified though. It will be something we will look into in the future. The importance of Pinky's ability (and possibly Crusty's) (Fu et al., 2015; Hoffman et al., 2013) to produce growth-stimulating hormones will be a topic of future study as we continue to dissect the interactions involved in biological soil crust symbioses.

Crusty has Methylobacterium spp. Symbionts Which are Likely Endosymbionts

Confirmation of Crusty's bacterial symbionts Light Pinky and Dark Pinky have been shown through multiple experimental means. We have replicated multiple forms of fungal-bacterial endosymbiont confirming methodologies to ensure that our hypothesis of these *Methylobacterium* spp. symbiotically interacting with Crusty are accurate. For one,

it seems so far that we cannot optimally grow Crusty without an actively growing Pinky. When antibiotics which kill or halt the growth of Pinky were used on Crusty, it also halted the growth of Crusty while not halting the growth of *S. cerevisiae* at the same dosage. This observation was seen in the usage of both Tetracycline and Gentamycin for all three organisms.

We replicated the bacterial live-dead staining implemented by Partida-Martinez & Hertweck to show bacterial presence within the cell wall of Crusty (2005). This result, however, can easily be contested even in the original publication, as SYTO9, the "live stain" portion is meant to stain nucleic acids. Since fungi's nuclei and mitochondria also contain nucleic acids, it cannot be confirmed that the nucleic acids being stained are bacterial in origin. This was later acknowledged by ThermoFisher on their website after the study was performed ("SYTO™ 9 Green Fluorescent Nucleic Acid Stain,"). However, unless the nucleic acids of Crusty are spread out across the entire cell instead of in the nucleus, what we observed in these images is still likely bacterial or mitochondrial in origin. Optimally, we would like to perform immunogold labeling TEM on Crusty to confirm the presence of Pinky inside of the fungal cells. Unfortunately, this is a lengthy and expensive process and was not feasible at the time.

To molecularly determine if Pinky was an endosymbiont of Crusty or if Pinky was on the outside of the cell wall, we reproduced methods by Mondo et al., utilizing a cell surface sterilization technique to ensure only DNA that is inside of the fungal cell wall was being extracted and amplified (Mondo et al., 2012). This Chloramine-T treatment resulted in 16S rDNA amplification after treatment of Crusty's cells, which

strongly indicates that the bacterial DNA and therefore the bacteria were inside the fungal cell wall and endosymbiotic.

Results collected from the +/- carbon, nitrogen, light experiment, and the addition of antibiotics experiment, tested Crusty's ability to interact with Pinky. If Crusty was unable to interact with Pinky, then the differences observed between the conditions in these two experiments would presumably be non-significant. However, both experiments showed that there is a significant difference in active metabolism when light is exposed to the Crusty-Pinky symbiosis in the absence of vital nutrients ($p < 0.05$, $n=3$), and that Crusty is significantly stunted in its growth in the presence of antibiotics that also stop the growth of Pinky ($p < 0.01$, $n=3$). Therefore, we can reject the null hypothesis that there are no interactions between Crusty and Pinky; however, with confidence we cannot completely confirm the hypothesis that Pinky is Crusty's endosymbiont, only that some form of interaction is occurring.

The results displayed here show that Crusty is capable of at least bacterial symbiosis if not full endosymbiosis, which has not previously been described within polyextremotolerant fungi. While other fungal groups have been identified to have endosymbiotic bacteria (Lumini et al., 2007; Mondo et al., 2012; Partida-Martinez & Hertweck, 2005), none has yet been found in the Chaetothyriales or Dothidiales where polyextremotolerant fungi reside. Further research will need to be performed on these fungi to determine if others also harbor bacterial symbionts, if symbiosis is specific to *Methylobacterium* spp., or if Crusty is a unique outlier. However, multiple other polyextremotolerant fungi in my collection also harbor *Methylobacterium* associates, and a quick 16S rDNA amplification revealed many other fungi in my collection with

positive amplification (data not shown). Indicating that Crusty is likely not the only polyextremotolerant fungus to have a *Methylobacterium* symbiont.

Interactions of Crusty with its Methylobacterium Symbionts

We showed here that Crusty is capable of engaging in direct interactions with its bacterial symbionts, resulting in morphological changes of Crusty, increased active metabolism in nutrient-deplete conditions, and restricted fungal growth with simultaneous bacterial growth restriction in the presence of antibiotics. These observations are crucial for further understanding how the microbes in biological soil crusts are interacting for survival, and how rudimentary biofilms evolved into developing close interactions such as those seen in lichens. Additionally, specific interactions that are shown to be occurring between Crusty and its *Methylobacterium* symbionts seem to align well with other bacterial-eukaryotic symbioses.

Unique cell morphologies of the Crusty-Pinky symbiosis resemble distinct plant-bacterial and fungal-nematode interactive cell morphogenesis, particularly the root nodules that form in legume-Rhizobium symbioses (Cullimore et al., 2001; Esseling et al., 2003, 2004) and the fungal loop traps found in *Arthrobotrys oligospora* to trap nematodes (Niu & Zhang, 2011; Vidal-Diez de Ulzurrun & Hsueh, 2018). Similar morphologies in Crusty would indicate that these curved cells form in order to inoculate a fungal cell with the bacterial symbiont. Cell directionality in fungi that is not straight polar growth is generally caused by a form of chemotropism, luring the cells to grow in a specific direction that is perceived as beneficial chemical to the cell (Clark-Cotton et al., 2022; Harris, 2006; Yu et al., 2021). It has also been shown that some *Methylobacterium* spp. are capable of soybean root nodulation, implying that a similar cellular

morphogenesis could be performed for fungi as well (Jourand et al., 2004; Sy et al., 2001). Without a Crusty cured of Pinky, testing this hypothesis for chemotropism and re-endosymbiosis caused by the bacteria will be difficult. However, the similarities indicates that similar mechanisms involving aforementioned symbioses and cell morphogenesis may be occurring within Crusty.

Metabolic interactions between Crusty and Pinky were of particular interest while attempting to decipher their symbiosis. We were expecting that the *Methylobacterium* spp. would contain the capabilities to perform nitrogen fixation, which is common amongst Rhizobiales (Carvalho et al., 2010). However, neither Light Pinky nor Dark Pinky contains the essential genes required for any of the three forms of nitrogen fixation (Bellenger et al., 2020; Chatterjee et al., 1997; Joerger et al., 1988). In annotating the nitrogen-fixation genes we did find the genes essential for production of bacteriochlorophyll, which are indicative of aerobic anoxygenic photosynthesis, which are evolutionarily related to the nitrogen fixing genes to the point of significant homologous protein sequences between the two separate systems (Fujita & Bauer, 2000). Other *Methylobacterium* spp. have been shown to contain genes for aerobic anoxygenic photosynthesis as well and are implied to be able to perform this function, but no direct measurement of photosynthesis has been performed (Atamna-Ismaeel et al., 2012; Zervas et al., 2019).

Results from our Crusty-Pinky culture grown in the presence or absence of light, and with or without a source of carbon or nitrogen, showed a significant increase in active metabolism when the cells were exposed to light even in the absence of carbon or nitrogen. These results indicate that a form of light-dependent metabolism must be

occurring. Currently, our only known source of light-dependent metabolism in this system would be the *Methylobacterium*'s aerobic anoxygenic photosynthesis. However, it has been previously noted that bacteriochlorophyll is easily degraded when exposed to even fluorescent lights (Raser et al., 1992), which is what was used in this experiment.

If these *Methylobacterium* spp. are actually capable of performing anoxygenic photosynthesis, they are most likely to be using the bacteriochlorophyll *a* or *b* found in the *Rhodobacter* spp. (Permentier et al., 2001; Sauer et al., 1966). These bacteriochlorophylls are unique in that they absorb light at a much higher wavelength than their green relatives; they absorb light in the red to near infrared part of the spectrum (700-850 nm), a range which includes wavelengths above that which melanin has been shown to absorb (Meredith & Sarna, 2006; Tran et al., 2006). This means that when the *Methylobacterium* cells are within the melanized fungal cell wall, the melanin is not capable of blocking the wavelengths of light required for bacteriochlorophyll excitation. It has also been shown that UV light can disrupt bacteriochlorophyll *a* completely (Raser et al., 1992), giving credence to the protective inner sanctum of the melanized fungal cell.

This combination of melanin blocking UV light but allowing near infrared light, allows the *Methylobacterium* to perform aerobic anoxygenic photosynthesis while being constantly exposed to extreme UV light, if they are inside of the melanized fungal cell wall. It has also been shown, that biological soil crust growth significantly increased when grown under the exposure of only red and near infrared light (Tang et al., 2018). This light exposure type specifically enhanced for the growth of aerobic anoxygenic photosynthetic bacteria, with *Methylobacterium* amongst one of the most abundant genera, and an increase in fungal taxa (Tang et al., 2018). The UV blocking capabilities

of melanin overlapping with the near infrared requiring *Methylobacterium*, could be the basis for the Crusty-Pinky endosymbiosis, but it will require more direct experiments for confirmation.

Why is a Polyextremotolerant Fungi Harboring a Growth-Stimulating Bacteria, and How It can Help the Greater Biological Soil Crust Consortium

Ascertaining the reason for the Crusty-Pinky symbiosis is still under investigation. Whether this attempt at a simplified version of a biological soil crust was successful or not is also being analyzed. Although we still believe the essential niches for a biological soil crust remain the same (nitrogen producer, carbon producer, and biological scaffolding and/or abiotic resistance inducer), we cannot confirm that we were able to represent all three niches in the overall scheme of these experiments. For one, we can confirm that neither Light Pinky nor Dark Pinky contain the ability to perform nitrogen fixation. However, we do believe that these *Methylobacterium* spp. are performing aerobic anoxygenic bacterial photosynthesis due to the increase in active metabolism only in the presence of a light source, with the absence of vital carbon and nitrogen sources. Additionally, we have shown that Light and Dark Pinky are capable of growth stimulation of algae, which in itself could be an essential niche we had not anticipated, especially when the optimal growth periods of biological soil crusts are particularly short each year (Belnap et al., 2001; Belnap & Eldridge, 2001; Harper & Marble, 1988; Johansen, 1993; Raggio et al., 2017).

Growth stimulation of algae, cyanobacteria, and fungi, caused by *Methylobacterium*, could coincide with the specific conditions that allow for active microbial growth within the biological soil crust, increasing what could be a much slower

process otherwise. We showed that in specific circumstances the bacteria will leave the confides of the fungal cells, with the most important abiotic factor influencing this escape being light availability. Since biological soil crusts are most active during the wet seasons (Harper & Marble, 1988; Miralles et al., 2012; Swenson et al., 2018), it could be that these conditions also allow Pinky to leave the fungal cells and release growth promoting hormones into the microbial biofilm. When conditions become inhospitable again, such as a lack of light in the winter months of Canada, this would reduce photosynthesis and therefore reduce the external carbon pool. Under these conditions, the *Methylobacterium* would either need to re-enter the fungus through a yet unknown mechanism that we have only observed via Crusty's chemotropic curved cell morphology. Alternatively, there could be a maintained population of *Methylobacterium* inside of the fungal cells, which can be maintained internally to be released again when conditions improve.

If these *Methylobacterium* spp. are able to freely leave and enter the fungal cells during certain conditions/times of year, they could be surviving inside of the fungal cells by performing anoxygenic photosynthesis inside the fungi during the winter months while being free-living heterotrophic bacteria (with growth stimulating abilities) during the summer months. This would allow them the flexibility of optimizing these harsh conditions for their benefit, and their subsequent survival allows for production of growth-promoting hormones which in turn benefit the entire biological soil crust community. This ecological niche which is only possible through the melanized cell wall of Crusty and other polyextremotolerant fungi, could be an important niche in allowing the entire biological soil crust to more rapidly grow during the short optimal windows of growth conditions. Without this ecological niche, it is possible that the biological crust

consortium would not be as effective in taking advantage of the short growth windows, and therefore not be as successful of a biofilm overall. Further tests will need to be performed to determine how vital the production of auxins and cytokinins are on the biological soil crust, and if the Crusty-Pinky endosymbiosis is the keystone niche for phytohormone production.

Acknowledgements

We would like to acknowledge Tania Kurbessoian for her contribution to this manuscript in producing the ITS phylogenetic tree for Crusty and its relatives. We would also like to acknowledge Nancy M. Nguyen, who performed the algal overlay experiments as an undergraduate researcher in the Riekhof lab here at UNL.

References

Abarenkov, K., Nilsson, R. H., Larsson, K.-H., Alexander, I. J., Eberhardt, U., Erland, S., . . . ljalg, U. (2010). The UNITE database for molecular identification of fungi – recent updates and future perspectives. *The New Phytologist*, *186*(2), 281-285.

Afgan, E., Baker, D., Batut, B., van den Beek, M., Bouvier, D., Čech, M., . . . Blankenberg, D. (2018). The Galaxy platform for accessible, reproducible and collaborative biomedical analyses: 2018 update. *Nucleic Acids Research*, *46*(W1), W537-W544. https://doi.org/10.1093/nar/gky379

Ahmadjian, V. (1982). Algal/fungal symbioses. *Progress in phycological research*.

Antachopoulos, C., Meletiadis, J., Roilides, E., Sein, T., & Walsh, T. J. (2006). Rapid susceptibility testing of medically important zygomycetes by XTT assay. *J Clin Microbiol*, *44*(2), 553-560. https://doi.org/10.1128/JCM.44.2.553-560.2006

Atamna-Ismaeel, N., Finkel, O., Glaser, F., Von Mering, C., Vorholt, J. A., Koblížek, M., . . . Béjà, O. (2012). Bacterial anoxygenic photosynthesis on plant leaf surfaces. *Environmental Microbiology Reports*, *4*(2), 209-216. https://doi.org/10.1111/j.1758-2229.2011.00323.x

Bastías, D. A., Johnson, L. J., & Card, S. D. (2020). Symbiotic bacteria of plant-associated fungi: friends or foes? *Current Opinion in Plant Biology*, *56*, 1-8. https://doi.org/https://doi.org/10.1016/j.pbi.2019.10.010

Bates, S. T., Reddy, G. S., & Garcia-Pichel, F. (2006). Exophiala crusticola anam. nov.(affinity Herpotrichiellaceae), a novel black yeast from biological soil crusts in the Western United States. *International journal of systematic and evolutionary microbiology*, *56*(11), 2697-2702.

Bauer, A. W., PERRY, D. M., & KIRBY, W. M. (1959). Single-disk antibiotic-sensitivity testing of staphylococci: An analysis of technique and results. *AMA archives of internal medicine*, *104*(2), 208-216.

Bellenger, J., Darnajoux, R., Zhang, X., & Kraepiel, A. (2020). Biological nitrogen fixation by alternative nitrogenases in terrestrial ecosystems: a review. *Biogeochemistry*, *149*(1), 53-73.

Belnap, J. (2002). Nitrogen fixation in biological soil crusts from southeast Utah, USA. *Biology and fertility of soils*, *35*(2), 128-135.

Belnap, J. (2003). The world at your feet: desert biological soil crusts. *Frontiers in Ecology and the Environment*, *1*(4), 181-189.

Belnap, J., & Büdel, B. (2016). Biological soil crusts as soil stabilizers. In *Biological soil crusts: an organizing principle in drylands* (pp. 305-320). Springer.

Belnap, J., Büdel, B., & Lange, O. L. (2001). Biological soil crusts: characteristics and distribution. In *Biological soil crusts: structure, function, and management* (pp. 3-30). Springer.

Belnap, J., & Eldridge, D. (2001). Disturbance and recovery of biological soil crusts. In *Biological soil crusts: structure, function, and management* (pp. 363-383). Springer.

Belnap, J., & Lange, O. L. (2001). *Biological soil crusts: structure, function, and management* (Vol. 150). Springer.

Belnap, J., & Lange, O. L. (2003). *Biological soil crusts: structure, function, and management* (Vol. 150). Springer.

Belnap, J., Phillips, S. L., & Miller, M. E. (2004). Response of desert biological soil crusts to alterations in precipitation frequency. *Oecologia*, *141*(2), 306-316. https://doi.org/10.1007/s00442-003-1438-6

Bengtsson-Palme, J., Ryberg, M., Hartmann, M., Branco, S., Wang, Z., Godhe, A., . . . de Sousa, F. (2013). Improved software detection and extraction of ITS1 and ITS2 from ribosomal ITS sequences of fungi and other eukaryotes for analysis of environmental sequencing data. Methods Ecol Evol. 2013; 4 (10): 914–9. In.

Berridge, M. V., Herst, P. M., & Tan, A. S. (2005). Tetrazolium dyes as tools in cell biology: new insights into their cellular reduction. *Biotechnol Annu Rev*, *11*, 127-152. https://doi.org/10.1016/S1387-2656(05)11004-7

Bianciotto, V., Lumini, E., Lanfranco, L., Minerdi, D., Bonfante, P., & Perotto, S. (2000). Detection and identification of bacterial endosymbionts in arbuscular mycorrhizal fungi belonging to the family Gigasporaceae. *Appl Environ Microbiol*, *66*(10), 4503-4509. https://doi.org/10.1128/AEM.66.10.4503-4509.2000

Birkeland, S., Gustafsson, A. L. S., Brysting, A. K., Brochmann, C., & Nowak, M. D. (2020). Multiple genetic trajectories to extreme abiotic stress adaptation in Arctic Brassicaceae. *Molecular biology and evolution*, *37*(7), 2052-2068.

Bonfante, P. (2003). Plants, Mycorrhizal Fungi and Endobacteria: a Dialog Among Cells and Genomes. *The Biological Bulletin*, *204*(2), 215-220. https://doi.org/10.2307/1543562

Boulc'h, P.-N., Caullireau, E., Faucher, E., Gouerou, M., Guérin, A., Miray, R., & Couée, I. (2020). Abiotic stress signalling in extremophile land plants. *Journal of Experimental Botany*, *71*(19), 5771-5785.

Bowker, M. A., Reed, S., Belnap, J., & Phillips, S. (2002). Temporal variation in community composition, pigmentation, and Fv/Fm of desert cyanobacterial soil crusts. *Microbial Ecology*, 13-25.

Büttner, H., Niehs, S. P., Vandelannoote, K., Cseresnyés, Z., Dose, B., Richter, I., . . . Hertweck, C. (2021). Bacterial endosymbionts protect beneficial soil fungus from nematode attack. *Proc Natl Acad Sci U S A*, *118*(37). https://doi.org/10.1073/pnas.2110669118

Camacho, C., Coulouris, G., Avagyan, V., Ma, N., Papadopoulos, J., Bealer, K., & Madden, T. L. (2009). BLAST+: architecture and applications. *BMC Bioinformatics*, *10*(1), 421. https://doi.org/10.1186/1471-2105-10-421

Cardinale, M., Puglia, A. M., & Grube, M. (2006). Molecular analysis of lichen-associated bacterial communities. *FEMS Microbiol Ecol*, *57*(3), 484-495. https://doi.org/10.1111/j.1574-6941.2006.00133.x

Cardinale, M., Vieira de Castro, J., Müller, H., Berg, G., & Grube, M. (2008). In situ analysis of the bacterial community associated with the reindeer lichen Cladonia arbuscula reveals predominance of Alphaproteobacteria. *FEMS Microbiol Ecol*, *66*(1), 63-71. https://doi.org/10.1111/j.1574-6941.2008.00546.x

Carr, E. C., Barton, Q., Grambo, S., Sullivan, M., Renfro, C. M., Kuo, A., . . . Harris, S. D. (2022). Deciphering the potential niche of two novel black yeast fungi from a biological soil crust based on their genomes, phenotypes, and melanin regulation. *bioRxiv*, 2021.2012.2003.471027. https://doi.org/10.1101/2021.12.03.471027

Carvalho, F. M., Souza, R. C., Barcellos, F. G., Hungria, M., & Vasconcelos, A. T. R. (2010). Genomic and evolutionary comparisons of diazotrophic and pathogenic bacteria of the order Rhizobiales. *BMC microbiology*, *10*(1), 1-15.

Chatterjee, R., Allen, R. M., Ludden, P. W., & Shah, V. K. (1997). In vitro synthesis of the iron-molybdenum cofactor and maturation of the nif-encoded apodinitrogenase. Effect of substitution of VNFH for NIFH. *J Biol Chem*, *272*(34), 21604-21608. https://doi.org/10.1074/jbc.272.34.21604

Chistoserdova, L., Chen, S. W., Lapidus, A., & Lidstrom, M. E. (2003). Methylotrophy in Methylobacterium extorquens AM1 from a genomic point of view. *J Bacteriol*, *185*(10), 2980-2987. https://doi.org/10.1128/JB.185.10.2980-2987.2003

Clark-Cotton, M. R., Jacobs, K. C., & Lew, D. J. (2022). Chemotropism and Cell-Cell Fusion in Fungi. *Microbiol Mol Biol Rev*, *86*(1), e0016521. https://doi.org/10.1128/mmbr.00165-21

Cock, P. J. A., Chilton, J. M., Grüning, B., Johnson, J. E., & Soranzo, N. (2015). NCBI BLAST+ integrated into Galaxy. *GigaScience*, *4*(1), s13742-13015-10080-13747. https://doi.org/10.1186/s13742-015-0080-7

Connon, R. (2007). Culturing of Chlorella vulgaris-Standard Operating Procedure, SOP on how to prepare Bold's Basal Medium (BBM). In: University of Reading.

Cordero, R. J., & Casadevall, A. (2017). Functions of fungal melanin beyond virulence. *Fungal Biology Reviews*, *31*(2), 99-112.

Crous, P. W., Wingfield, M. J., Le Roux, J. J., Richardson, D. M., Strasberg, D., Shivas, R. G., . . . Sharma, R. (2015). Fungal Planet description sheets: 371–399. *Persoonia-Molecular Phylogeny and Evolution of Fungi*, *35*(1), 264-327.

Csotonyi, J. T., Swiderski, J., Stackebrandt, E., & Yurkov, V. (2010). A new environment for aerobic anoxygenic phototrophic bacteria: biological soil crusts. *Environmental Microbiology Reports*, *2*(5), 651-656.

Cullimore, J. V., Ranjeva, R., & Bono, J.-J. (2001). Perception of lipo-chitooligosaccharidic Nod factors in legumes. *Trends in plant science*, *6*(1), 24-30.

Dowzer, C. E., & Kelly, J. M. (1991). Analysis of the creA gene, a regulator of carbon catabolite repression in Aspergillus nidulans. *Mol Cell Biol*, *11*(11), 5701-5709.

Edberg, S., Chaskes, S., Alture-Werber, E., & Singer, J. (1980). Esculin-based medium for isolation and identification of Cryptococcus neoformans. *Journal of Clinical Microbiology*, *12*(3), 332-335.

Edberg, S. C., Pittman, S., & Singer, J. (1977). Esculin hydrolysis by Enterobacteriaceae. *Journal of Clinical Microbiology*, *6*(2), 111-116.

Edgar, R. C. (2004). MUSCLE: a multiple sequence alignment method with reduced time and space complexity. *BMC Bioinformatics*, *5*, 113. https://doi.org/10.1186/1471-2105-5-113

Erlacher, A., Cernava, T., Cardinale, M., Soh, J., Sensen, C. W., Grube, M., & Berg, G. (2015). Rhizobiales as functional and endosymbiontic members in the lichen symbiosis of Lobaria pulmonaria L. *Frontiers in microbiology*, *6*, 53.

Esseling, J. J., Lhuissier, F. G., & Emons, A. M. C. (2003). Nod factor-induced root hair curling: continuous polar growth towards the point of nod factor application. *Plant physiology*, *132*(4), 1982-1988.

Esseling, J. J., Lhuissier, F. G., & Emons, A. M. C. (2004). A nonsymbiotic root hair tip growth phenotype in NORK-mutated legumes: implications for nodulation factor–induced signaling and formation of a multifaceted root hair pocket for bacteria. *The Plant Cell*, *16*(4), 933-944.

Evans, R., & Johansen, J. (1999). Microbiotic crusts and ecosystem processes. *Critical reviews in plant sciences*, *18*(2), 183-225.

Fischer, A., Meindl, D., & Loos, E. (1989). Glucose excretion by the symbiotic Chlorella of Spongilla fluviatilis. *Planta*, *179*(2), 251-256.

Frases, S., Salazar, A., Dadachova, E., & Casadevall, A. (2007). Cryptococcus neoformans can utilize the bacterial melanin precursor homogentisic acid for fungal melanogenesis. *Applied and environmental microbiology*, *73*(2), 615-621.

Fu, S.-F., Wei, J.-Y., Chen, H.-W., Liu, Y.-Y., Lu, H.-Y., & Chou, J.-Y. (2015). Indole-3-acetic acid: A widespread physiological code in interactions of fungi with other organisms. *Plant signaling & behavior*, *10*(8), e1048052.

Fujita, Y., & Bauer, C. E. (2000). Reconstitution of Light-independent Protochlorophyllide Reductase from Purified Bchl and BchN-BchB Subunits. *Journal of Biological Chemistry*, *275*(31), 23583-23588. https://doi.org/10.1074/jbc.m002904200

Gadd, G. M., & de Rome, L. (1988). Biosorption of copper by fungal melanin. *Applied microbiology and biotechnology*, *29*(6), 610-617.

Gao, Q., & Garcia-Pichel, F. (2011). Microbial ultraviolet sunscreens. *Nature Reviews Microbiology*, *9*(11), 791-802. https://doi.org/10.1038/nrmicro2649

Gorbushina, A. A. (2007). Life on the rocks. *Environmental microbiology*, *9*(7), 1613-1631.

Gorbushina, A. A., Andreas, B., & Schulte, A. (2005). Microcolonial rock inhabiting fungi and lichen photobionts: evidence for mutualistic interactions. *Mycological Research*, *109*(11), 1288-1296.

Gostinčar, C., Grube, M., De Hoog, S., Zalar, P., & Gunde-Cimerman, N. (2009). Extremotolerance in fungi: evolution on the edge. *FEMS microbiology ecology*, *71*(1), 2-11.

Gostinčar, C., Muggia, L., & Grube, M. (2012). Polyextremotolerant black fungi: oligotrophism, adaptive potential, and a link to lichen symbioses. *Frontiers in Microbiology*, *3*, 390.

Grube, M., Cardinale, M., de Castro, J. V., Müller, H., & Berg, G. (2009). Species-specific structural and functional diversity of bacterial communities in lichen symbioses. *ISME J*, *3*(9), 1105-1115. https://doi.org/10.1038/ismej.2009.63

Grube, M., Muggia, L., & Gostinčar, C. (2013). Niches and adaptations of polyextremotolerant black fungi. In *Polyextremophiles* (pp. 551-566). Springer.

Gustavs, L., Görs, M., & Karsten, U. (2011). POLYOL PATTERNS IN BIOFILM-FORMING AEROTERRESTRIAL GREEN ALGAE (TREBOUXIOPHYCEAE, CHLOROPHYTA) 1. *Journal of phycology*, *47*(3), 533-537.

Harper, K. T., & Marble, J. R. (1988). A role for nonvascular plants in management of arid and semiarid rangelands. In *Vegetation science applications for rangeland analysis and management* (pp. 135-169). Springer.

Harris, S. D. (2006). Cell polarity in filamentous fungi: shaping the mold. *Int Rev Cytol*, *251*, 41-77. https://doi.org/10.1016/S0074-7696(06)51002-2

Hiraishi, A., Furuhata, K., Matsumoto, A., Koike, K. A., Fukuyama, M., & Tabuchi, K. (1995). Phenotypic and genetic diversity of chlorine-resistant Methylobacterium strains isolated from various environments. *Appl Environ Microbiol*, *61*(6), 2099-2107. https://doi.org/10.1128/aem.61.6.2099-2107.1995

Hodkinson, B. P., & Lutzoni, F. (2009). A microbiotic survey of lichen-associated bacteria reveals a new lineage from the Rhizobiales. *Symbiosis*, *49*(3), 163-180.

Hoffman, M. T., Gunatilaka, M. K., Wijeratne, K., Gunatilaka, L., & Arnold, A. E. (2013). Endohyphal bacterium enhances production of indole-3-acetic acid by a foliar fungal endophyte. *PLoS One*, *8*(9), e73132.

Hong, L., & Simon, J. D. (2007). Current understanding of the binding sites, capacity, affinity, and biological significance of metals in melanin. *J Phys Chem B*, *111*(28), 7938-7947. https://doi.org/10.1021/jp071439h

Ivanova, E., Doronina, N., & Trotsenko, Y. A. (2001). Aerobic methylobacteria are capable of synthesizing auxins. *Microbiology*, *70*(4), 392-397.

Ivanova, E. G., Doronina, N. V., Shepeliakovskaia, A. O., Laman, A. G., Brovko, F. A., & Trotsenko, I. A. (2000). [Facultative and obligate aerobic methylobacteria synthesize cytokinins]. *Mikrobiologiia*, *69*(6), 764-769.

Izumi, H., Anderson, I. C., Alexander, I. J., Killham, K., & Moore, E. R. B. (2006). Endobacteria in some ectomycorrhiza of Scots pine (Pinus sylvestris). *FEMS Microbiology Ecology*, *56*(1), 34-43. https://doi.org/10.1111/j.1574-6941.2005.00048.x

Jiang, L., An, D., Wang, X., Zhang, K., Li, G., Lang, L., . . . Jiang, Y. (2020). Methylobacterium planium sp. nov., isolated from a lichen sample. *Arch Microbiol*, *202*(7), 1709-1715. https://doi.org/10.1007/s00203-020-01881-4

Joerger, R. D., Bishop, P. E., & Evans, H. J. (1988). Bacterial alternative nitrogen fixation systems. *CRC Critical reviews in microbiology*, *16*(1), 1-14.

Johansen, J. R. (1993). Cryptogamic crusts of semiarid and arid lands of North America. *Journal of phycology*, *29*(2), 140-147.

Jourand, P., Giraud, E., Béna, G., Sy, A., Willems, A., Gillis, M., . . . de Lajudie, P. (2004). Methylobacterium nodulans sp. nov., for a group of aerobic, facultatively methylotrophic, legume root-nodule-forming and nitrogen-fixing bacteria. *Int J Syst Evol Microbiol*, *54*(Pt 6), 2269-2273. https://doi.org/10.1099/ijs.0.02902-0

Kessler, E., Kauer, G., & Rahat, M. (1991). Excretion of sugars by Chlorella species capable and incapable of symbiosis with Hydra viridis. *Botanica acta*, *104*(1), 58-63.

Khasin, M., Cahoon, R. R., Nickerson, K. W., & Riekhof, W. R. (2018). Molecular machinery of auxin synthesis, secretion, and perception in the unicellular chlorophyte alga Chlorella sorokiniana UTEX 1230. *PloS one*, *13*(12), e0205227.

Kobayashi, D. Y., & Crouch, J. A. (2009). Bacterial/Fungal Interactions: From Pathogens to Mutualistic Endosymbionts. *Annual Review of Phytopathology*, *47*(1), 63-82. https://doi.org/10.1146/annurev-phyto-080508-081729

Koenig, R. L., Morris, R. O., & Polacco, J. C. (2002). tRNA is the source of low-level trans-zeatin production in Methylobacterium spp. *J Bacteriol*, *184*(7), 1832-1842. https://doi.org/10.1128/JB.184.7.1832-1842.2002

Kroken, S., & Taylor, J. W. (2000). Phylogenetic species, reproductive mode, and specificity of the green alga Trebouxia forming lichens with the fungal genus Letharia. *Bryologist*, 645-660.

Kulkarni, G. B., Sanjeevkumar, S., Kirankumar, B., Santoshkumar, M., & Karegoudar, T. B. (2013). Indole-3-acetic acid biosynthesis in Fusarium delphinoides strain GPK,

a causal agent of Wilt in Chickpea. *Appl Biochem Biotechnol*, *169*(4), 1292-1305. https://doi.org/10.1007/s12010-012-0037-6

Kutschera, U. (2007). Plant-associated methylobacteria as co-evolved phytosymbionts: a hypothesis. *Plant signaling & behavior*, *2*(2), 74-78.

Lan, S., Wu, L., Zhang, D., & Hu, C. (2012). Successional stages of biological soil crusts and their microstructure variability in Shapotou region (China). *Environmental Earth Sciences*, *65*(1), 77-88.

Lanfear, R., Calcott, B., Kainer, D., Mayer, C., & Stamatakis, A. (2014). Selecting optimal partitioning schemes for phylogenomic datasets. *BMC Evol Biol*, *14*, 82. https://doi.org/10.1186/1471-2148-14-82

Lange, O. L., Belnap, J., Reichenberger, H., & Meyer, A. (1997). Photosynthesis of green algal soil crust lichens from arid lands in southern Utah, USA: role of water content on light and temperature responses of CO2 exchange. *Flora*, *192*(1), 1-15. https://doi.org/10.1016/s0367-2530(17)30749-1

Li, X., Zhang, P., Su, Y., & Jia, R. (2012). Carbon fixation by biological soil crusts following revegetation of sand dunes in arid desert regions of China: a four-year field study. *Catena*, *97*, 119-126.

Lumini, E., Bianciotto, V., Jargeat, P., Novero, M., Salvioli, A., Faccio, A., . . . Bonfante, P. (2007). Presymbiotic growth and sporal morphology are affected in the arbuscular mycorrhizal fungus Gigaspora margarita cured of its endobacteria. *Cell Microbiol*, *9*(7), 1716-1729. https://doi.org/10.1111/j.1462-5822.2007.00907.x

Madhaiyan, M., Alex, T. H. H., Ngoh, S. T., Prithiviraj, B., & Ji, L. (2015). Leaf-residing Methylobacterium species fix nitrogen and promote biomass and seed production

in Jatropha curcas. *Biotechnology for Biofuels*, *8*(1). https://doi.org/10.1186/s13068-015-0404-y

Madigan, M. T. (1995). Microbiology of Nitrogen Fixation by Anoxygenic Photosynthetic Bacteria. In R. E. Blankenship, M. T. Madigan, & C. E. Bauer (Eds.), *Anoxygenic Photosynthetic Bacteria* (pp. 915-928). Springer Netherlands. https://doi.org/10.1007/0-306-47954-0_42

Maier, S., Muggia, L., Kuske, C. R., & Grube, M. (2016). Bacteria and non-lichenized fungi within biological soil crusts. In *Biological Soil Crusts: An Organizing Principle in Drylands* (pp. 81-100). Springer.

McFarland, J. (1907). The nephelometer: an instrument for estimating the number of bacteria in suspensions used for calculating the opsonic index and for vaccines. *Journal of the American Medical Association*, *49*(14), 1176-1178.

Meena, K. K., Kumar, M., Kalyuzhnaya, M. G., Yandigeri, M. S., Singh, D. P., Saxena, A. K., & Arora, D. K. (2012). Epiphytic pink-pigmented methylotrophic bacteria enhance germination and seedling growth of wheat (Triticum aestivum) by producing phytohormone. *Antonie Van Leeuwenhoek*, *101*(4), 777-786.

Meredith, P., & Sarna, T. (2006). The physical and chemical properties of eumelanin. *Pigment Cell Research*, *19*(6), 572-594. https://doi.org/10.1111/j.1600-0749.2006.00345.x

Minh, B. Q., Schmidt, H. A., Chernomor, O., Schrempf, D., Woodhams, M. D., von Haeseler, A., & Lanfear, R. (2020). IQ-TREE 2: New Models and Efficient Methods for Phylogenetic Inference in the Genomic Era. *Mol Biol Evol*, *37*(5), 1530-1534. https://doi.org/10.1093/molbev/msaa015

Miralles, I., Domingo, F., García-Campos, E., Trasar-Cepeda, C., Leirós, M. C., & Gil-Sotres, F. (2012). Biological and microbial activity in biological soil crusts from the Tabernas desert, a sub-arid zone in SE Spain. *Soil Biology and Biochemistry*, *55*, 113-121.

Mitchison-Field, L. M. Y., Vargas-Muñiz, J. M., Stormo, B. M., Vogt, E. J. D., Van Dierdonck, S., Pelletier, J. F., . . . Gladfelter, A. S. (2019). Unconventional Cell Division Cycles from Marine-Derived Yeasts. *Current Biology*, *29*(20), 3439-3456.e3435. https://doi.org/10.1016/j.cub.2019.08.050

Molina, L., & Molina, M. (1986). Absolute absorption cross sections of ozone in the 185- to 350-nm wavelength range. *Journal of Geophysical Research: Atmospheres*, *91*(D13), 14501-14508.

Mondo, S. J., Toomer, K. H., Morton, J. B., Lekberg, Y., & Pawlowska, T. E. (2012). Evolutionary stability in a 400-million-year-old heritable facultative mutualism. *Evolution*, *66*(8), 2564-2576. https://doi.org/10.1111/j.1558-5646.2012.01611.x

Moreno-Rico, O., Groenewald, J. Z., & Crous, P. W. (2014). Foliicolous fungi from Arctostaphylos pungens in Mexico. *IMA Fungus*, *5*(1), 7-15. https://doi.org/10.5598/imafungus.2014.05.01.02

Moss, B. J., Kim, Y., Nandakumar, M. P., & Marten, M. R. (2008). Quantifying metabolic activity of filamentous fungi using a colorimetric XTT assay. *Biotechnol Prog*, *24*(3), 780-783. https://doi.org/10.1021/bp070334t

Muggia, L., Gueidan, C., Knudsen, K., Perlmutter, G., & Grube, M. (2013). The Lichen Connections of Black Fungi. *Mycopathologia*, *175*(5-6), 523-535. https://doi.org/10.1007/s11046-012-9598-8

Nair, A., & Sarma, S. J. (2021). The impact of carbon and nitrogen catabolite repression in microorganisms. *Microbiological Research*, *251*, 126831.

Niu, X.-M., & Zhang, K.-Q. (2011). Arthrobotrys oligospora: a model organism for understanding the interaction between fungi and nematodes. *Mycology*, *2*(2), 59-78.

Pakvaz, S., & Soltani, J. (2016). Endohyphal bacteria from fungal endophytes of the Mediterranean cypress (Cupressus sempervirens) exhibit in vitro bioactivity. *Forest Pathology*, *46*(6), 569-581.

Partida-Martinez, L. P., & Hertweck, C. (2005). Pathogenic fungus harbours endosymbiotic bacteria for toxin production. *Nature*, *437*(7060), 884-888. https://doi.org/10.1038/nature03997

Permentier, H. P., Neerken, S., Overmann, J., & Amesz, J. (2001). A Bacteriochlorophyll a Antenna Complex from Purple Bacteria Absorbing at 963 nm[,]. *Biochemistry*, *40*(18), 5573-5578. https://doi.org/10.1021/bi0024308

Portnoy, T., Margeot, A., Linke, R., Atanasova, L., Fekete, E., Sándor, E., . . . Kubicek, C. P. (2011). The CRE1 carbon catabolite repressor of the fungus Trichoderma reesei: a master regulator of carbon assimilation. *BMC Genomics*, *12*, 269. https://doi.org/10.1186/1471-2164-12-269

Raggio, J., Allan Green, T. G., Sancho, L. G., Pintado, A., Colesie, C., Weber, B., & Büdel, B. (2017). Metabolic activity duration can be effectively predicted from macroclimatic data for biological soil crust habitats across Europe. *Geoderma*, *306*, 10-17. https://doi.org/10.1016/j.geoderma.2017.07.001

Raja, P., Uma, S., & Sundaram, S. (2006). Non-nodulating pink-pigmented facultative Methylobacterium sp. with a functional nifH gene. *World Journal of Microbiology and Biotechnology*, *22*(12), 1381-1384. https://doi.org/10.1007/s11274-006-9199-0

Raser, L., Thomas, L., Kim, J.-H., Cotton, T., & Uphaus, R. (1992). Factors determining stability of bacteriochlorophyll monolayers. *Thin solid films*, *210*, 753-755.

Richardson, D., & Smith, D. (1968). Lichen physiology: IX. Carbohydrate movement from the Trebouxia symbiont of Xanthoria aureola to the fungus. *New Phytologist*, *67*(1), 61-68.

Richardson, D., Smith, D., & Lewis, D. (1967). Carbohydrate movement between the symbionts of lichens. *Nature*, *214*(5091), 879-882.

Ries, L. N., Beattie, S. R., Espeso, E. A., Cramer, R. A., & Goldman, G. H. (2016). Diverse Regulation of the CreA Carbon Catabolite Repressor in Aspergillus nidulans. *Genetics*, *203*(1), 335-352. https://doi.org/10.1534/genetics.116.187872

Ruiz-Herrera, J., León-Ramírez, C., Vera-Nuñez, A., Sánchez-Arreguín, A., Ruiz-Medrano, R., Salgado-Lugo, H., . . . Peña-Cabriales, J. J. (2015). A novel intracellular nitrogen-fixing symbiosis made by *Ustilago maydis* and *Bacillus spp.* *New Phytologist*, *207*(3), 769-777. https://doi.org/10.1111/nph.13359

Réblová, M., Hubka, V., Thureborn, O., Lundberg, J., Sallstedt, T., Wedin, M., & Ivarsson, M. (2016). From the Tunnels into the Treetops: New Lineages of Black Yeasts from Biofilm in the Stockholm Metro System and Their Relatives among Ant-Associated Fungi in the Chaetothyriales. *PLoS One*, *11*(10), e0163396. https://doi.org/10.1371/journal.pone.0163396

Sauer, K., Smith, J. R. L., & Schultz, A. J. (1966). The Dimerization of Chlorophyll a, Chlorophyll b, and Bacteriochlorophyll in Solution1. *Journal of the American Chemical Society*, *88*(12), 2681-2688.

Schreier, W. J., Gilch, P., & Zinth, W. (2015). Early events of DNA photodamage. *Annual review of physical chemistry*, *66*, 497-519.

Seemann, T. (2014). Prokka: rapid prokaryotic genome annotation. *Bioinformatics*, *30*(14), 2068-2069. https://doi.org/10.1093/bioinformatics/btu153

Shaffer, J. P., U'Ren, J. M., Gallery, R. E., Baltrus, D. A., & Arnold, A. E. (2017). An endohyphal bacterium (Chitinophaga, Bacteroidetes) alters carbon source use by Fusarium keratoplasticum (F. solani species complex, Nectriaceae). *Frontiers in microbiology*, *8*, 350.

Silva-Dias, A., Miranda, I. M., Branco, J., Monteiro-Soares, M., Pina-Vaz, C., & Rodrigues, A. G. (2015). Adhesion, biofilm formation, cell surface hydrophobicity, and antifungal planktonic susceptibility: relationship among Candida spp. *Front Microbiol*, *6*, 205. https://doi.org/10.3389/fmicb.2015.00205

Steenwyk, J. L., Buida, T. J., Li, Y., Shen, X. X., & Rokas, A. (2020). ClipKIT: A multiple sequence alignment trimming software for accurate phylogenomic inference. *PLoS Biol*, *18*(12), e3001007. https://doi.org/10.1371/journal.pbio.3001007

Sterflinger, K. (2006). Black yeasts and meristematic fungi: ecology, diversity and identification. In *Biodiversity and ecophysiology of yeasts* (pp. 501-514). Springer.

Steven, B., Gallegos-Graves, L. V., Belnap, J., & Kuske, C. R. (2013). Dryland soil microbial communities display spatial biogeographic patterns associated with soil depth and soil parent material. *FEMS microbiology ecology*, *86*(1), 101-113.

Sun, P.-F., Fang, W.-T., Shin, L.-Y., Wei, J.-Y., Fu, S.-F., & Chou, J.-Y. (2014). Indole-3-acetic acid-producing yeasts in the phyllosphere of the carnivorous plant Drosera indica L. *PloS one*, *9*(12), e114196.

Swenson, T. L., Karaoz, U., Swenson, J. M., Bowen, B. P., & Northen, T. R. (2018). Linking soil biology and chemistry in biological soil crust using isolate exometabolomics. *Nature Communications*, *9*(1). https://doi.org/10.1038/s41467-017-02356-9

Sy, A., Giraud, E., Jourand, P., Garcia, N., Willems, A., de Lajudie, P., . . . Dreyfus, B. (2001). Methylotrophic Methylobacterium bacteria nodulate and fix nitrogen in symbiosis with legumes. *J Bacteriol*, *183*(1), 214-220. https://doi.org/10.1128/JB.183.1.214-220.2001

SYTO™ 9 Green Fluorescent Nucleic Acid Stain. In. ThermoFisher Scientific: Invitrogen.

Tang, K., Jia, L., Yuan, B., Yang, S., Li, H., Meng, J., . . . Feng, F. (2018). Aerobic anoxygenic phototrophic bacteria promote the development of biological soil crusts. *Frontiers in microbiology*, 2715.

Tani, A., Sahin, N., Matsuyama, Y., Enomoto, T., Nishimura, N., Yokota, A., & Kimbara, K. (2012). High-throughput identification and screening of novel Methylobacterium species using whole-cell MALDI-TOF/MS analysis. *PLoS One*, *7*(7), e40784.

Teixeira, M. M., Moreno, L. F., Stielow, B. J., Muszewska, A., Hainaut, M., Gonzaga, L., . . . de Hoog, G. S. (2017). Exploring the genomic diversity of black yeasts and relatives (Chaetothyriales, Ascomycota). *Studies in mycology*, *86*, 1-28. https://doi.org/https://doi.org/10.1016/j.simyco.2017.01.001

Tesei, D., Tafer, H., Poyntner, C., Piñar, G., Lopandic, K., & Sterflinger, K. (2017). Draft Genome Sequences of the Black Rock Fungus Knufia petricola and Its Spontaneous Nonmelanized Mutant. *Genome Announc*, *5*(44). https://doi.org/10.1128/genomeA.01242-17

Tran, M. L., Powell, B. J., & Meredith, P. (2006). Chemical and Structural Disorder in Eumelanins: A Possible Explanation for Broadband Absorbance. *Biophysical Journal*, *90*(3), 743-752. https://doi.org/10.1529/biophysj.105.069096

Triebel, G. R., & Dagmar. (1992). *The Inter-lecanoralean Associations*. Schweizerbart Science Publishers.

Trotsenko, Y. A., Ivanova, E., & Doronina, N. (2001). Aerobic methylotrophic bacteria as phytosymbionts. *Microbiology*, *70*(6), 623-632.

Turner, S., Pryer, K. M., Miao, V. P. W., & Palmer, J. D. (1999). Investigating Deep Phylogenetic Relationships among Cyanobacteria and Plastids by Small Subunit rRNA Sequence Analysis. *The Journal of Eukaryotic Microbiology*, *46*(4), 327-338. https://doi.org/10.1111/j.1550-7408.1999.tb04612.x

Vidal-Diez de Ulzurrun, G., & Hsueh, Y. P. (2018). Predator-prey interactions of nematode-trapping fungi and nematodes: both sides of the coin. *Appl Microbiol Biotechnol*, *102*(9), 3939-3949. https://doi.org/10.1007/s00253-018-8897-5

Weber, S. (2005). Light-driven enzymatic catalysis of DNA repair: a review of recent biophysical studies on photolyase. *Biochimica et Biophysica Acta (BBA)-Bioenergetics*, *1707*(1), 1-23.

White, T. J., Bruns, T., Lee, S., & Taylor, J. (1990). 38 - AMPLIFICATION AND DIRECT SEQUENCING OF FUNGAL RIBOSOMAL RNA GENES FOR PHYLOGENETICS. In M. A. Innis, D. H. Gelfand, J. J. Sninsky, & T. J. White (Eds.), *PCR Protocols* (pp. 315-322). Academic Press. https://doi.org/https://doi.org/10.1016/B978-0-12-372180-8.50042-1

Wick, R. R., Judd, L. M., Gorrie, C. L., & Holt, K. E. (2017). Unicycler: resolving bacterial genome assemblies from short and long sequencing reads. *PLoS computational biology*, *13*(6), e1005595.

Yu, X., Hu, X., Pop, M., Wernet, N., Kirschhöfer, F., Brenner-Weiß, G., . . . Fischer, R. (2021). Fatal attraction of Caenorhabditis elegans to predatory fungi through 6-methyl-salicylic acid. *Nat Commun*, *12*(1), 5462. https://doi.org/10.1038/s41467-021-25535-1

Zervas, A., Zeng, Y., Madsen, A. M., & Hansen, L. H. (2019). Genomics of Aerobic Photoheterotrophs in Wheat Phyllosphere Reveals Divergent Evolutionary Patterns of Photosynthetic Genes in Methylobacterium spp. *Genome Biology and Evolution*, *11*(10), 2895-2908. https://doi.org/10.1093/gbe/evz204

Figures and Tables

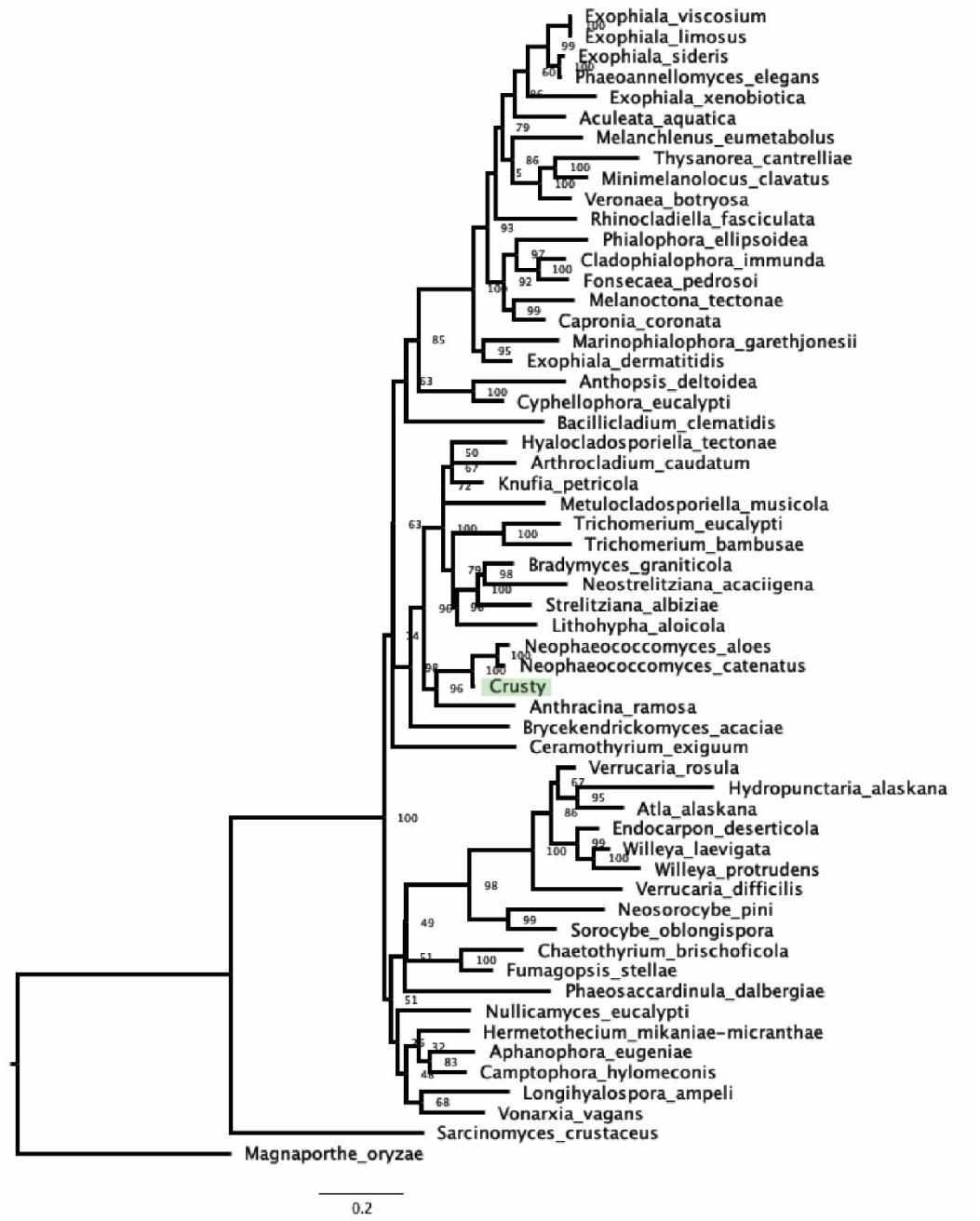

Figure 1: Maximum likelihood phylogenetic tree of Chaetothyriales using ITS sequences and 1000 bootstraps. The phylogenetic location of Crusty (green) within Chaetothyriales can be seen as closely related to *Neophaeococcomyces*, with a high confidence of a 96% bootstrap value. *Magnaporthe oryzae* was used at the outgroup.

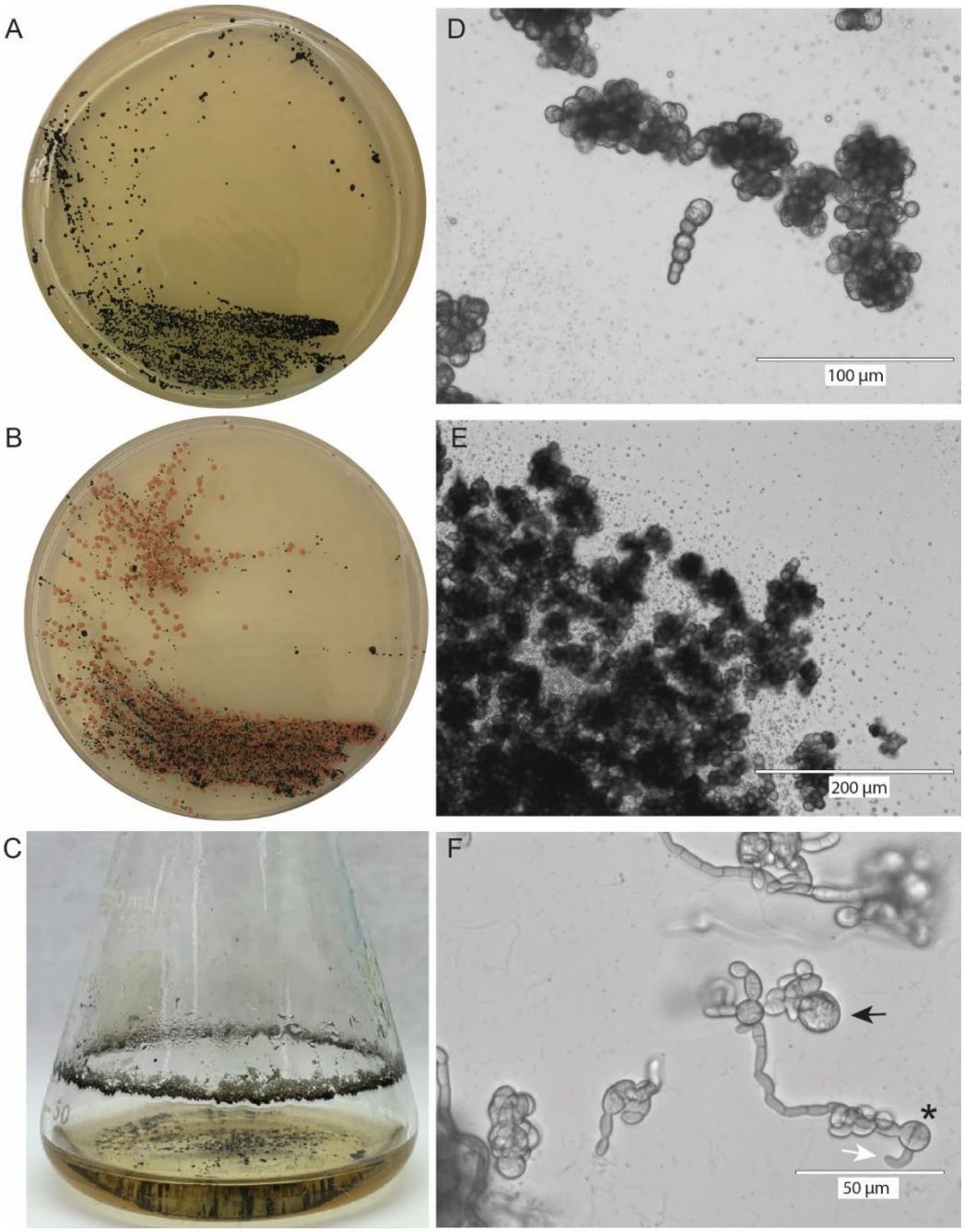

Figure 2: A) Colony morphology of Crusty grown on MEA + 10 mg/mL Tetracycline. Colonies are black, small, and no bacterial growth is present. B) Colony morphology of Crusty and Pinky when Crusty is grown from freezer stocks on MEA without antibiotics. Pinky colonies are able to grow as a result of the lack of antibiotics, due to burst cells from frozen stock. C) Liquid growth of Crusty in MEA. Crusty forms extensive biofilms at the air-liquid interface, that which forms distinct honeycomb-like patterns. In the liquid itself, Crusty does not grow planktonically but stays in its clumped morphology. D & E) Crusty cell morphology when grown on a plate of MEA. Perfectly round cells form, and high amounts of melanin are observed. E) Lipid droplets come out of large clumps of Crusty when the coverslip is placed over the cells. F) Crusty grown in BBM for 20 days showed unique morphologies: black arrows are large round cells; asterisks are multi-septated meristematic cells; white arrows are curved cells.

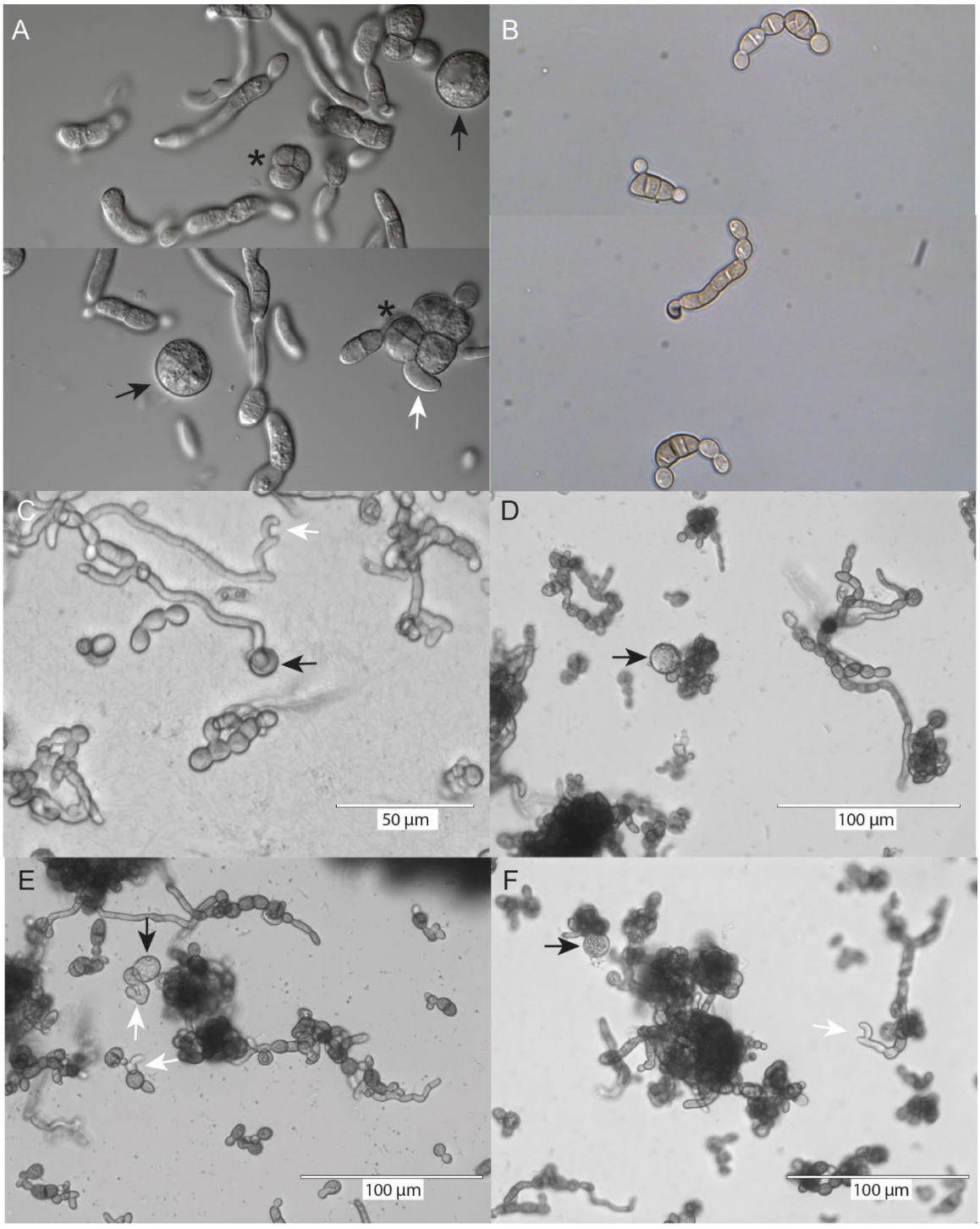

Figure 3: Various cell morphologies of Crusty cells. A & B) Crusty grown up in liquid MEA for 6 days. B) C) Crusty was grown up in BBM plus mannitol with a 12 hour light/dark cycle for 6 days. D, E, & F) Crusty was grown in BBM with no nitrate and added mannitol with a 12 hour light/dark cycle for D & F) 10 days and E) 17 days. White arrows point to curved cells; black arrow indicates large circular cells, possibly chalmydospores; asterisks indicate possible meristematic cell morphologies.

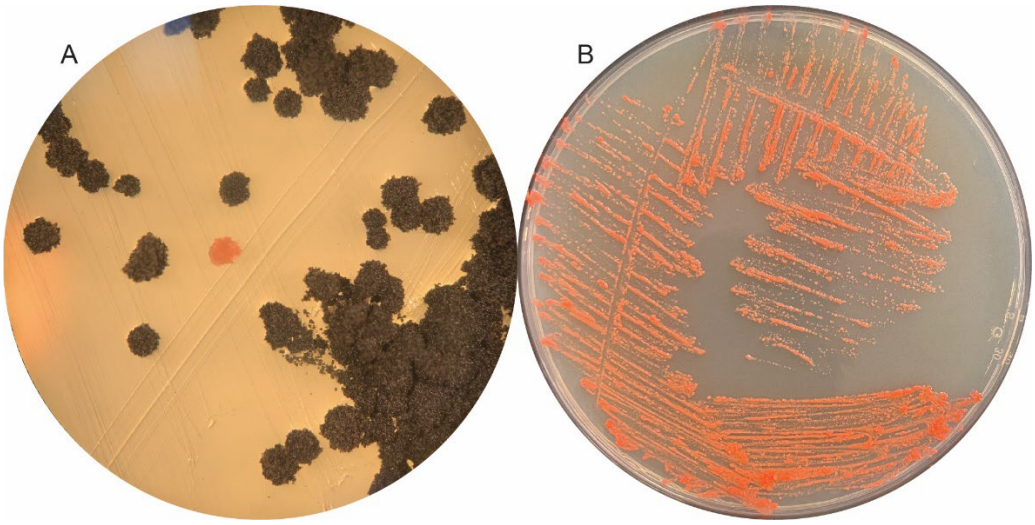

Figure 4: A) First instance of a pink albino colony of Crusty forming spontaneously on an MEA plate. B) Pure culture of the albino pink Crusty grown on MEA.

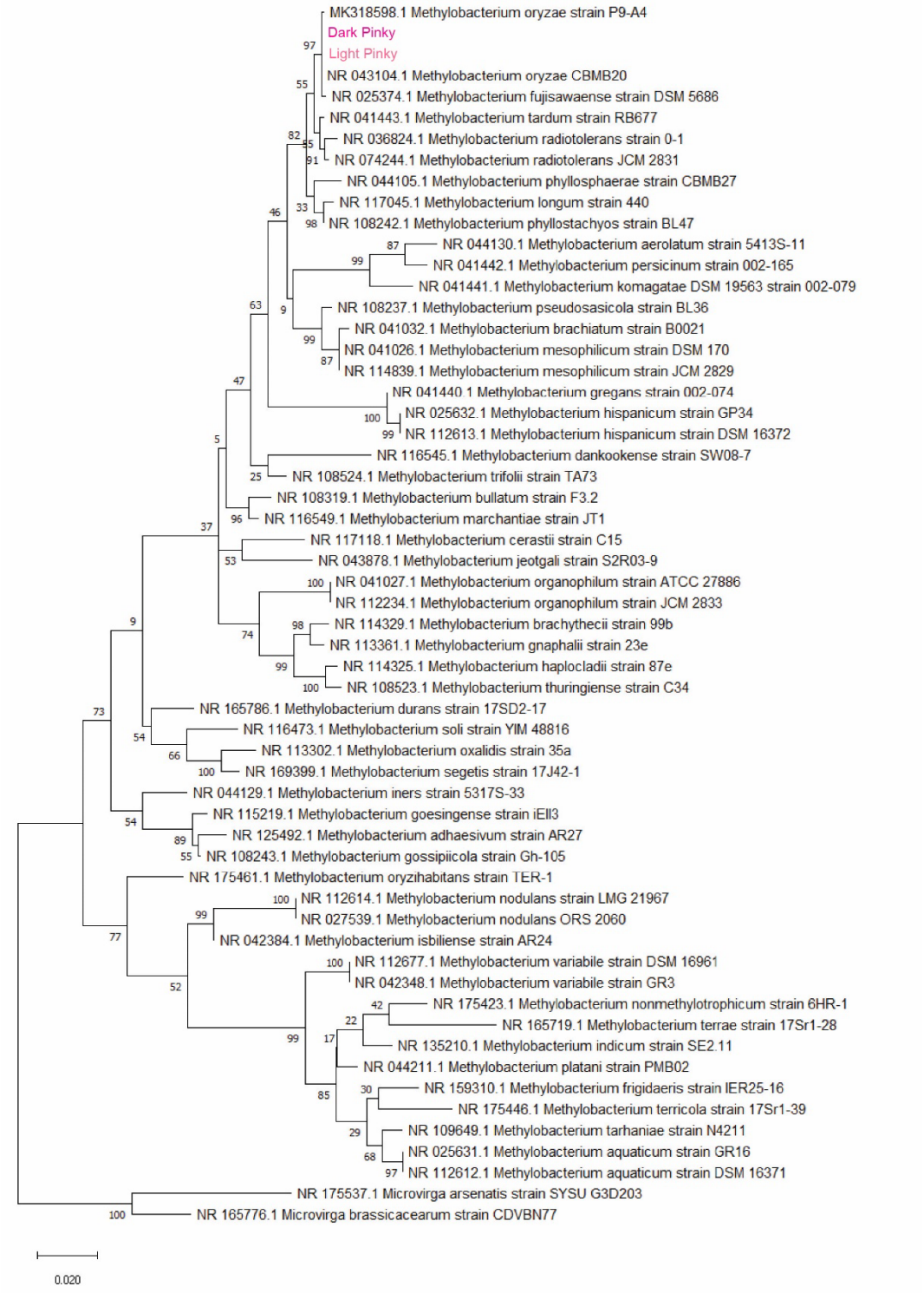

Figure 5: Maximum likelihood phylogenetic tree of the 16S rDNA region of *Methylobacterium* spp. with 1000 bootstraps. Values at nodes represent bootstrap values (%) of the nodes. Phylogenetic analyses confirm that Light Pinky and Dark Pinky are *M. oryzae*, but also closely related to *M. fujisawaense,* confounding the species name. *Microvirgra* species were used as the outgroup.

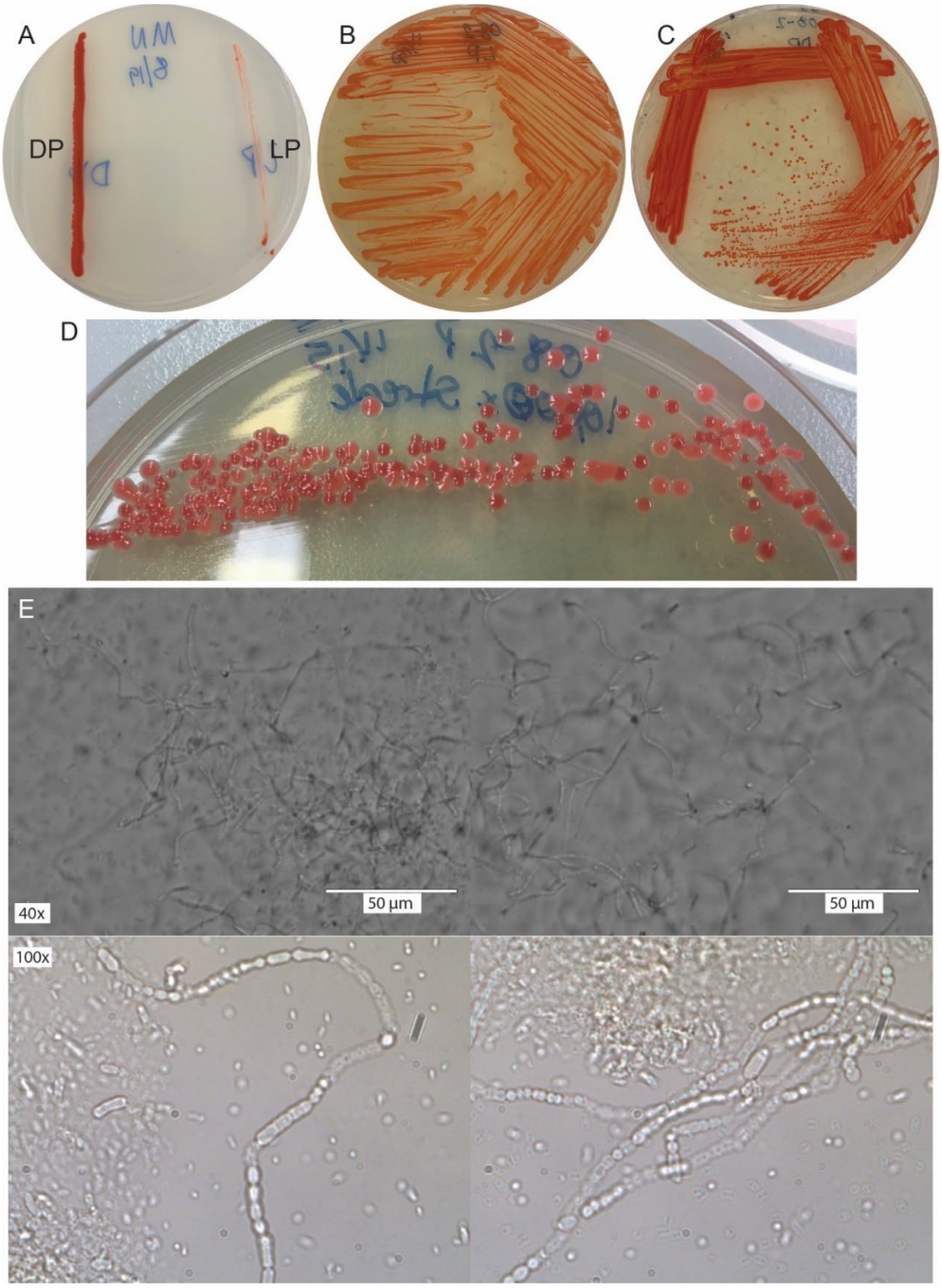

Figure 6: A) Dark Pinky (DP) and Light Pinky (LP) plated out on MN media together. On MN media it is obvious their color distinction, and the reduced growth by Light Pinky. B) Light Pinky grown on MEA. C) Dark Pinky grown on MEA. D) Colony morphologies of Light Pinky and Dark Pinky when growing out a 1000x diluted stock of their combined form Pinky, also shows their distinct color differences. E) Pinky control grown in BBM for 22 days, filamentation occurs.

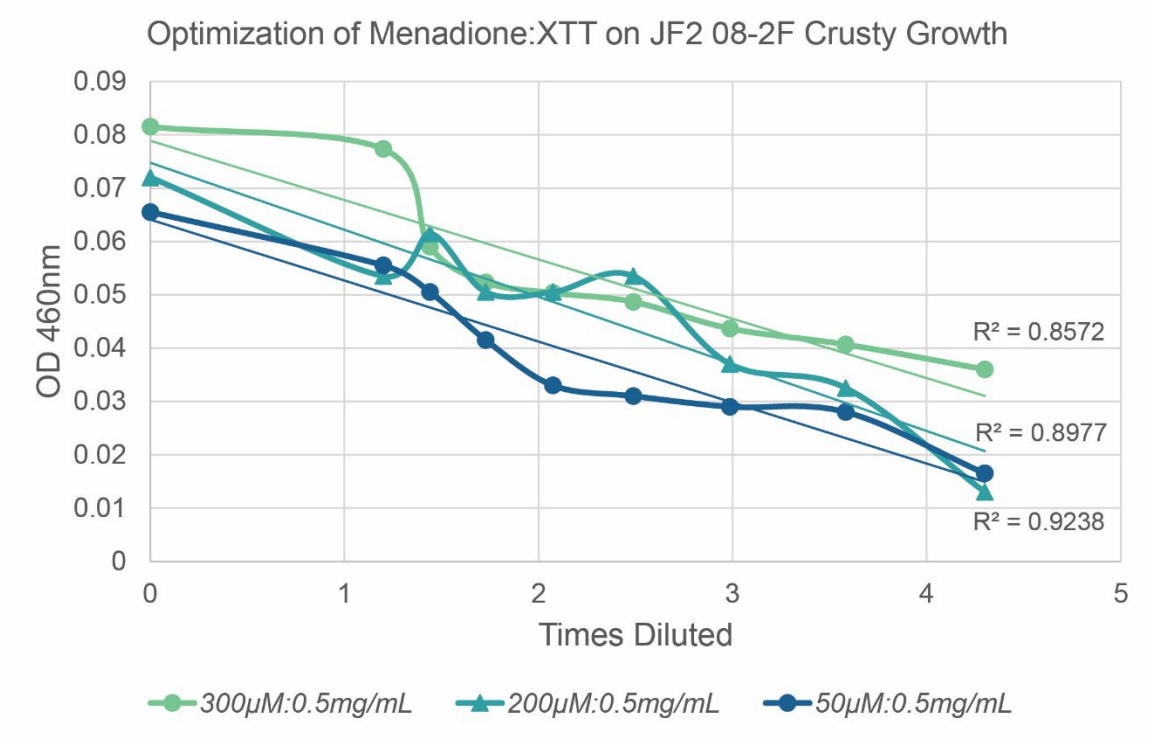

Figure 7: Optimization of the XTT assay used for multiple experiments. Specific amounts of Menadione to XTT were analyzed to determine which combination would most accurately represent the cell amount. The combination that had the highest R^2 value would be the most accurate, which is shown here to be the 50 µM:0.5 mg/mL (menadione:XTT) combination at 0.9238.

Figure 8: C32 strip results for Crusty. Darker wells indicate more growth which indicates more preference, except for ESC which is a chemical reaction not growth.

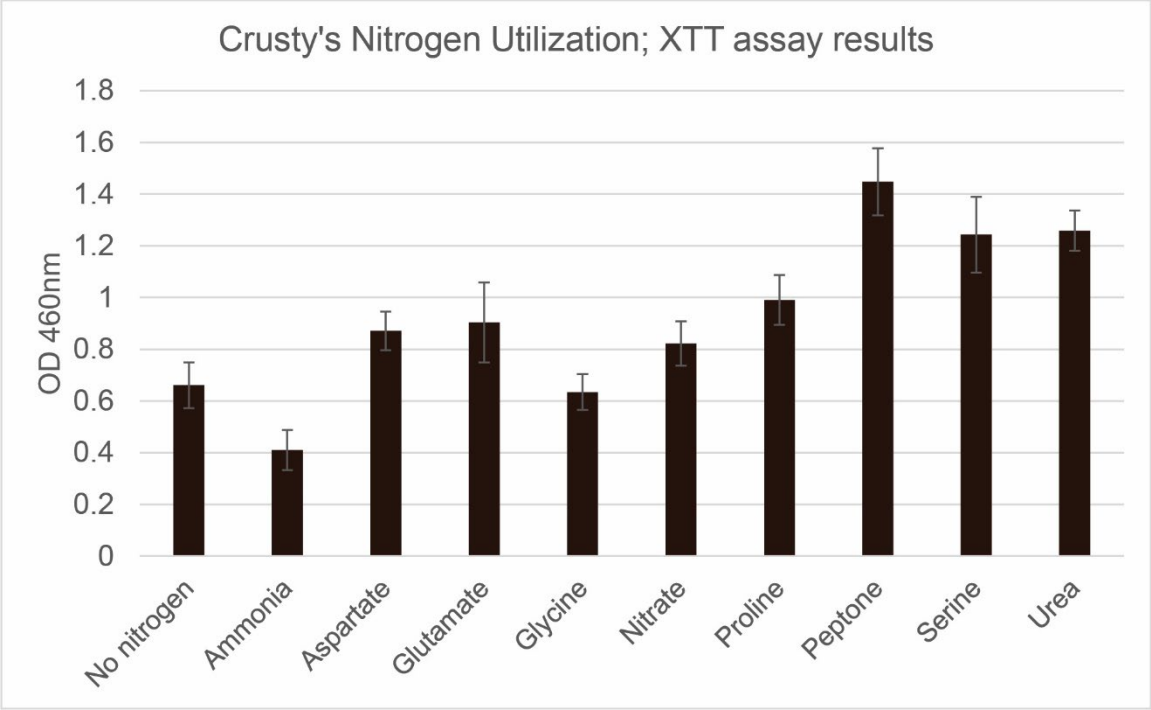

Figure 9: Crusty's Nitrogen utilization after 10 days of growth, with XTT live growth assay. Peptone showed the highest growth amount, and Ammonia showed the lowest growth amount, oddly lower than no nitrogen source. (n=6, 6 biological replicates)

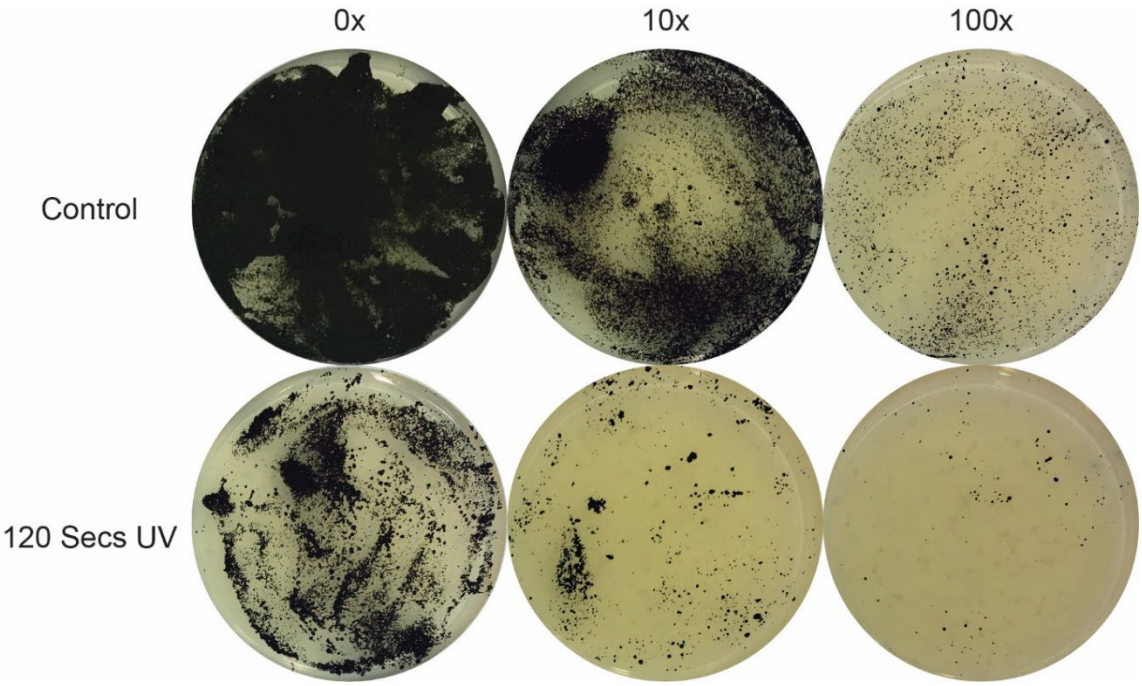

Figure 10: UV resistance of Crusty. Serial dilution of Crusty was performed with 10x intervals, to prevent cells from covering each other and creating an artificially inflated resistance appearance. Control plates had no UV exposure, and UV plates had 120 seconds of 245 nm UV light exposure. As the dilution factor goes up, the amount of cells that survive the UV exposure decrease indicating a coverage protection in the 0x conditions. (n=3, 3 biological replicates)

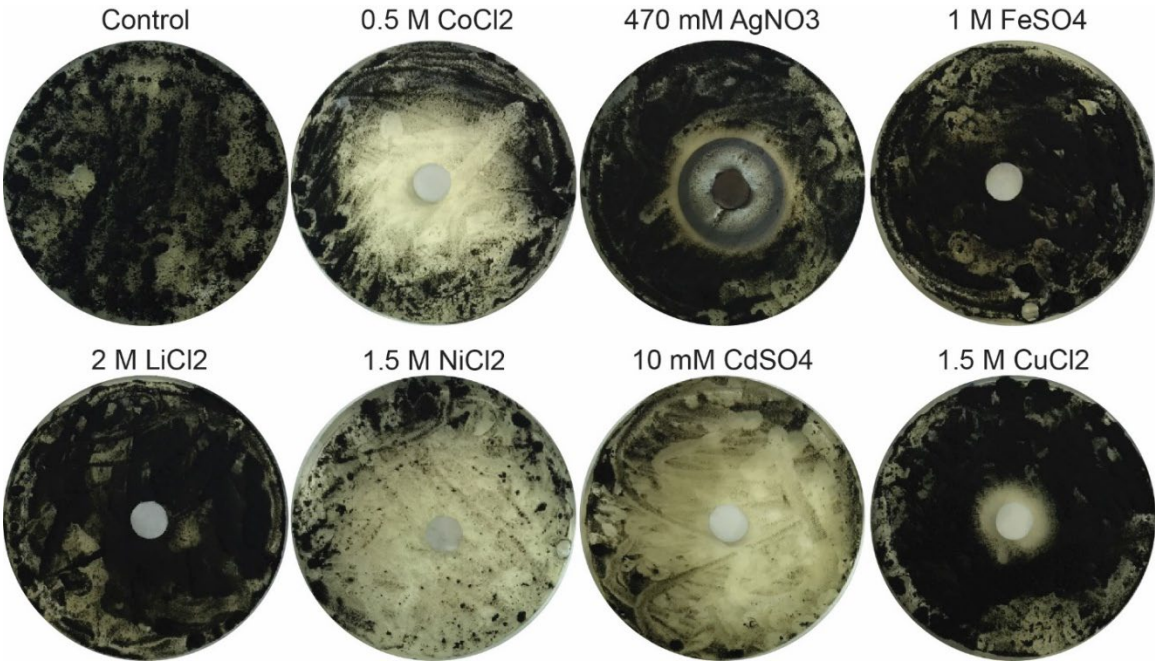

Figure 11: Metal tolerance of Crusty to various metals. In order of most tolerable to least Crusty can completely tolerate FeSO4 and LiCl2 with no zone of clearing, CuCl2 with a 1.4 cm zone of clearing, AgNO3 with a 2.8 cm zone of clearing, CdSO4 with a 4.5 cm zone of clearing, and NiCl2 with a 4.7 cm zone of clearing.

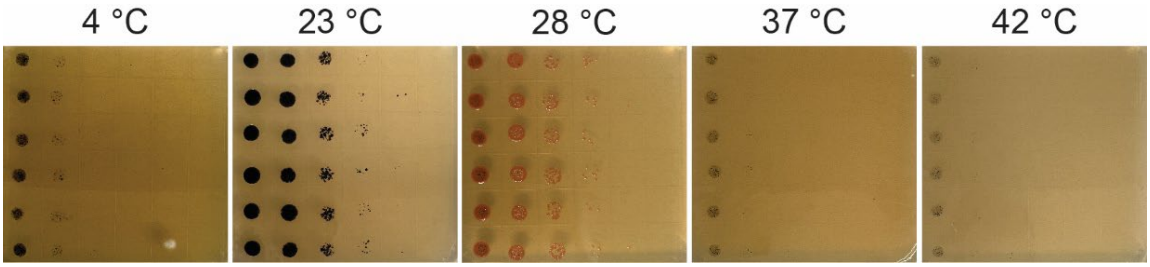

Figure 12: Temperature growth range of Crusty grown on solid media. Serial dilution with a 10x dilution was performed to observe the ability to grow in varying concentrations, and plates were grown for 10 days. Crusty seems to prefer 23 °C for growing but is capable of growing at temperatures as low as 4 °C. Crusty was unable to grow at 37 °C or above, and was killed with 48 hours of exposure at 37 °C or higher.

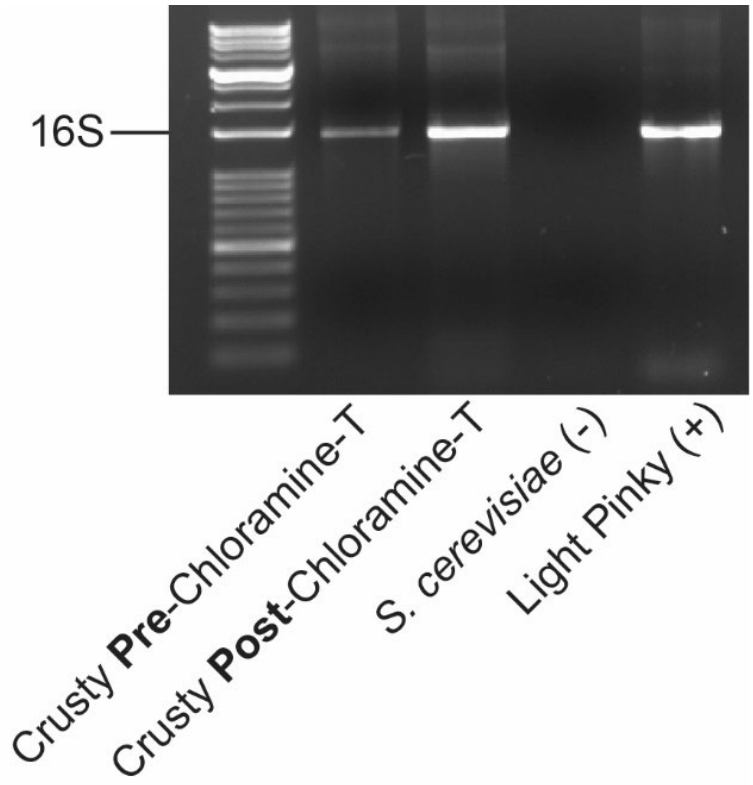

Figure 13: Electrophoresis gel of the PCR amplified 16S region of bacterial DNA. Crusty that was surface sterilized before 16S amplification showed a clear 16S bacterial DNA band, indicating bacterial presence inside of the cells. There was no 16S amplification for the fungus *S. cerevisiae*. There was 16S amplification for the positive control Light Pinky bacteria, and for the non-surface sterilized Crusty.

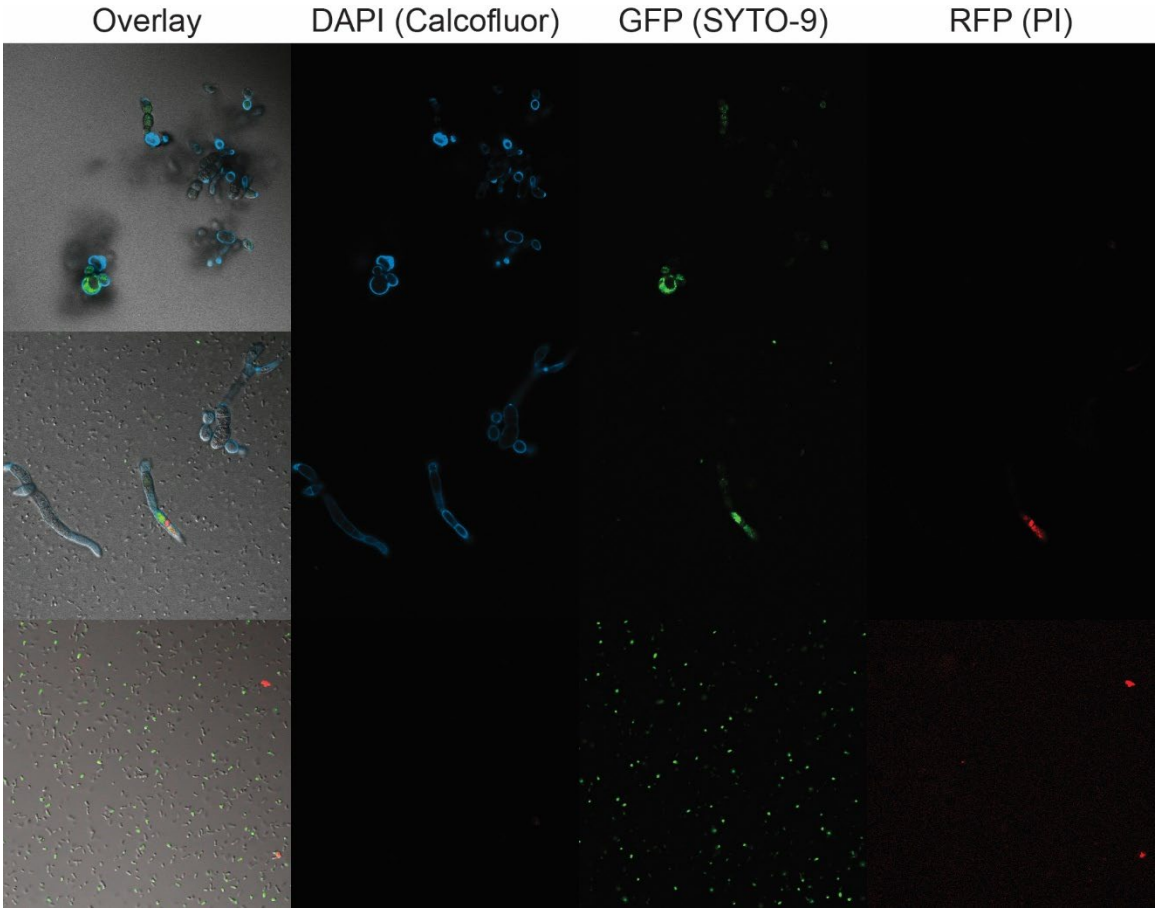

Figure 14: Confocal microscopy of Crusty and Pinky with fluorescent stains. Calcofluor (blue) staining of chitin was done to observe the fungal cell wall which can be seen in the images containing fungi. SYTO9 (green) and PI (red) staining was done to observe the presence of bacteria. SYTO9 was able to stain structures inside of the fungal cells, as was PI. Some bacterial cells were able to be stained with SYTO9 and PI outside of the fungal cells as well.

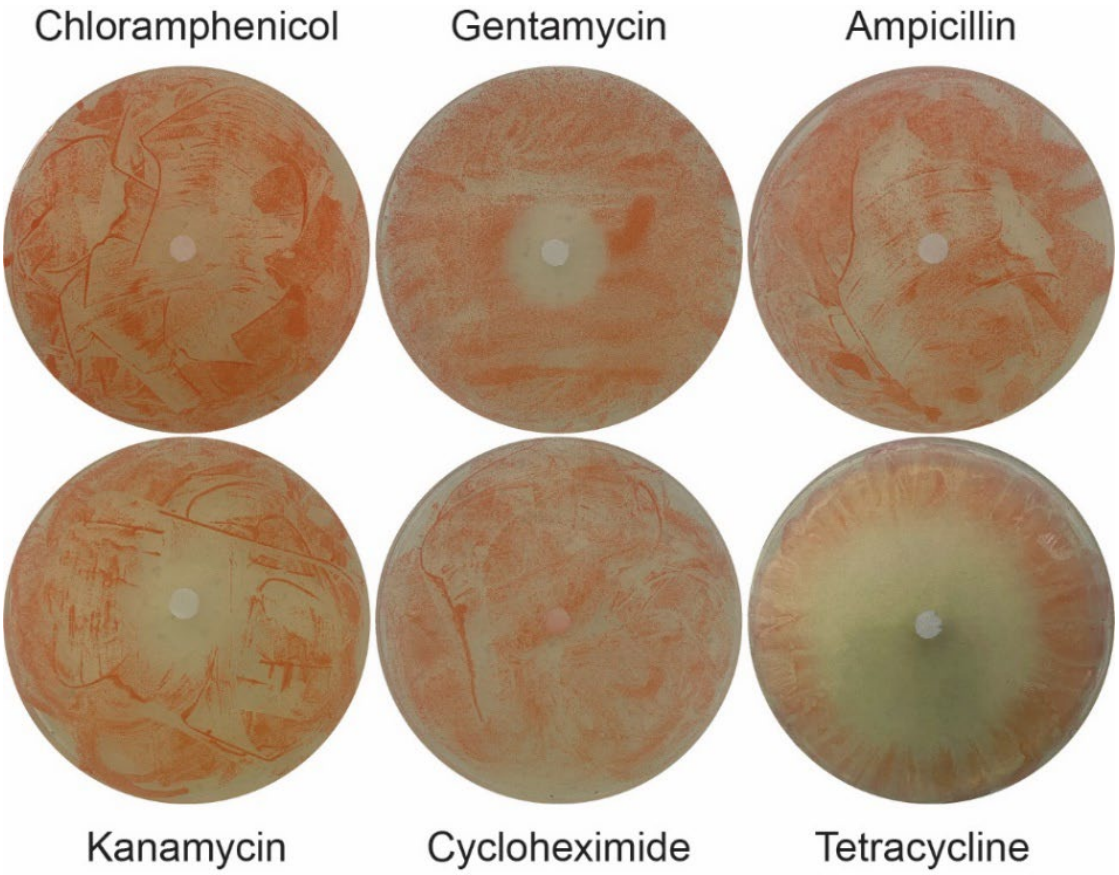

Figure 15: Antibiotic disk test on Pinky to determine best antibiotic to use. Tetracycline showed the largest zone of clearing out of all of the antibiotics, followed by Kanamycin, and Gentamycin. Chloamphenicol, Ampicillin, and Cycloheximide did not create a zone of clearing for Pinky. (n=3, 3 biological replicates)

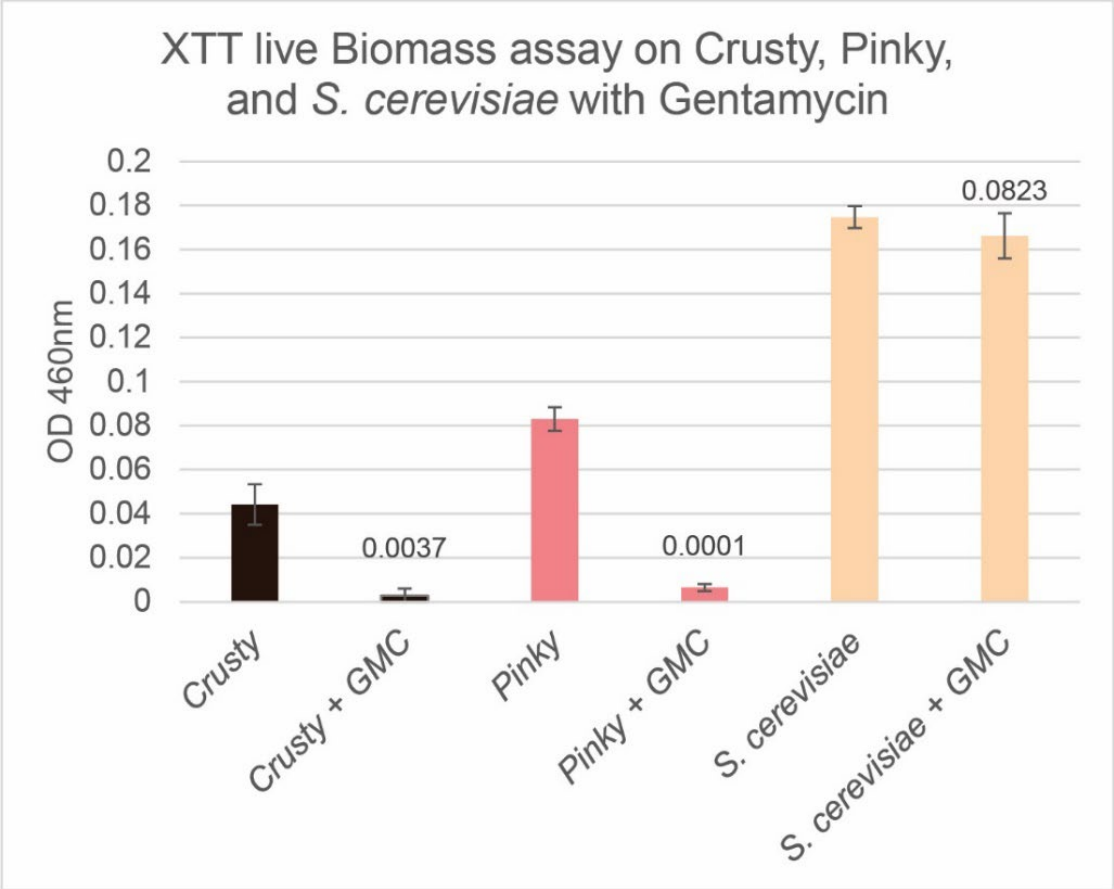

Figure 16: Gentamycin treatment of Crusty, Pinky, and *S. cerevisiae* in liquid culture, with XTT assay live cell confirmation. Crusty and Pinky were both incapable of growth in the presence of Gentamycin, both with p-values less than .01. However, *S. cerevisiae* was capable of growth in the presence of Gentamycin, and the cells exposed to Gentamycin did not have a p-value less than 0.05 compared to the control. (n=3, 3 biological replicates)

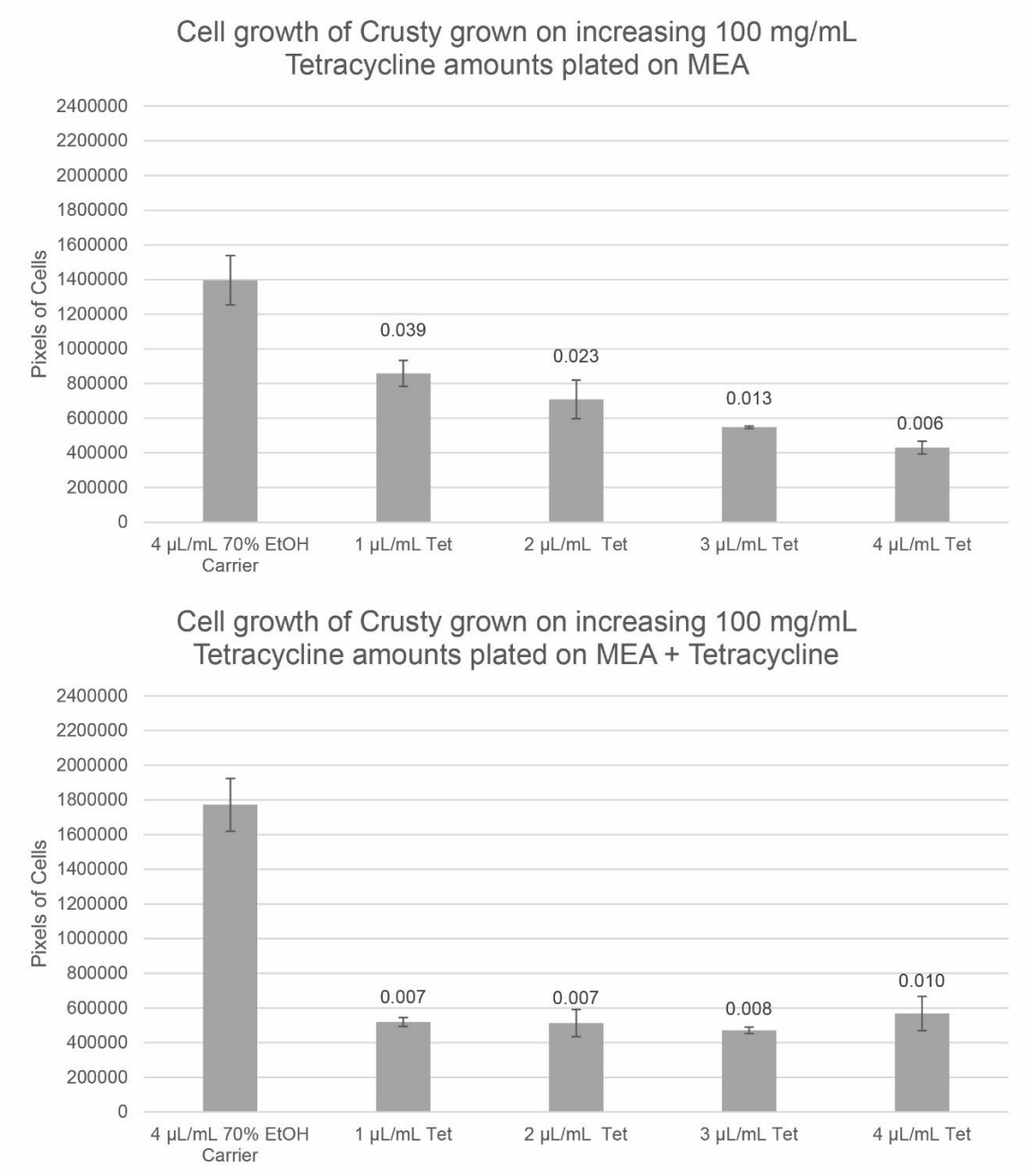

Figure 17: Growth of Crusty on solid media in area of pixels, after various amounts of Tetracycline treatment. After Tetracycline treatment, Crusty that was grown on solid media without Tetracycline added showed an increase in survivability that correlated with a decrease in the Tetracycline treatment, with 4 µL/mL Tetracycline having the least growth p-value 0.006. However, when Tetracycline was added to the solid media that Crusty was grown on after Tetracycline treatment, Crusty had similarly decreased growth at all previous exposure concentrations, and all treatments were significantly different ($p < 0.01$, n=3, 3 biological replicates).

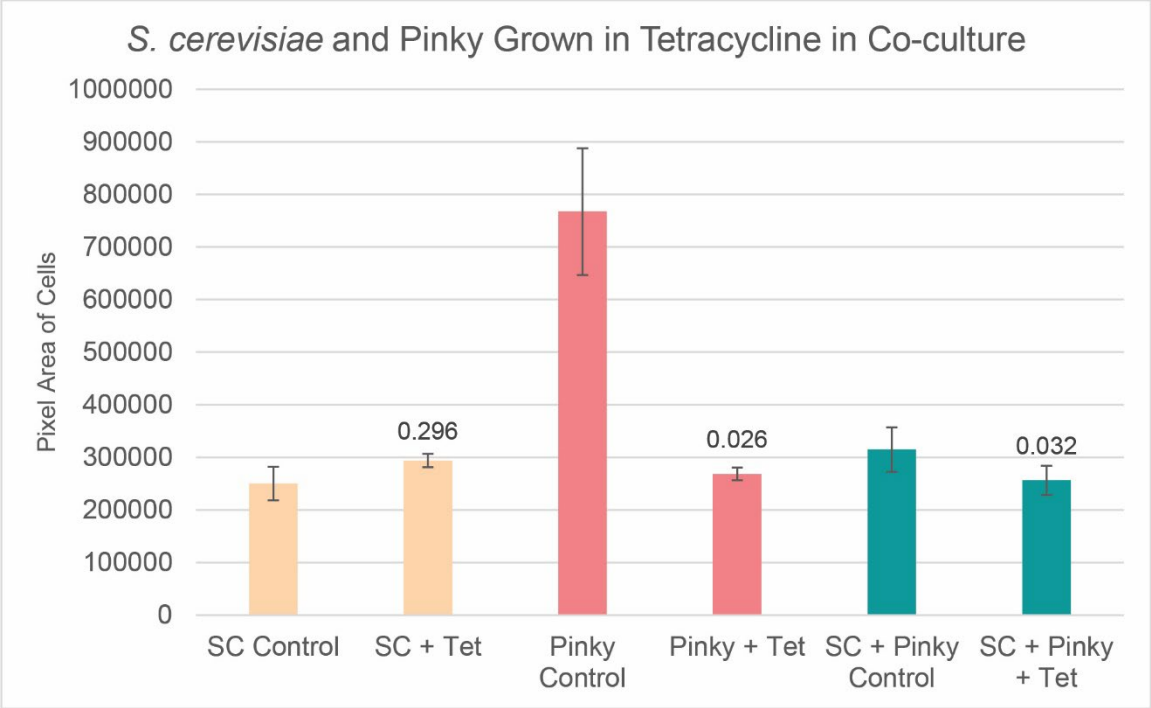

Figure 18: Growth of *S. cerevisiae*, Pinky, and their co-culture after being in the presence of 4 µL/mL of Tetracycline. *S. cerevisiae* had no significant change with the exposure to Tetracycline. Pinky had a significant decrease in growth when exposed to Tetracycline, $p < 0.05$, n=3, 3 biological replicates. Co-culture of *S. cerevisiae* and Pinky had a significant decrease in growth $p < 0.05$, n=3, 3 biological replicates.

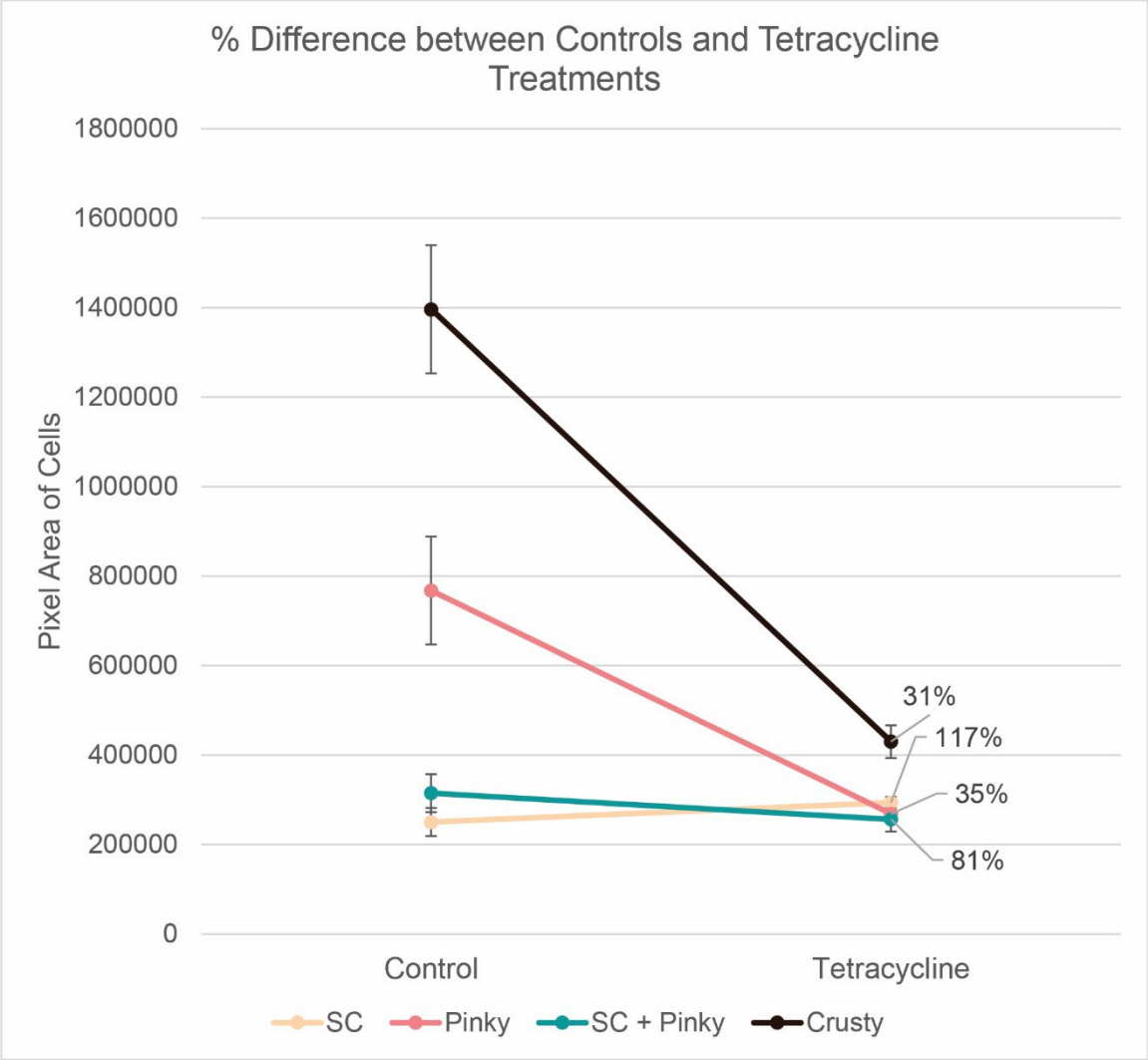

Figure 19: Percent difference between the Pixel area of *S. cerevisiae*, Pinky, Crusty, and the co-culture of Pinky and *S. cerevisiae* grown with and without 4 µL/mL of Tetracycline. Only 31% of control Crusty was able to grow compared to growth in the Presence of Tetracycline. 117% of S. cerevisiae was able to growth in the presence of Tetracycline compared to its control growth. Pinky had a similar growth decrease as Crusty, in that only 35% of the original growth amount was seen in the presence of Tetracycline. Finally, 81% of cellular growth was seen in the S. cerevisiae-Pinky co-culture in the presence of Tetracycline compared to the control.

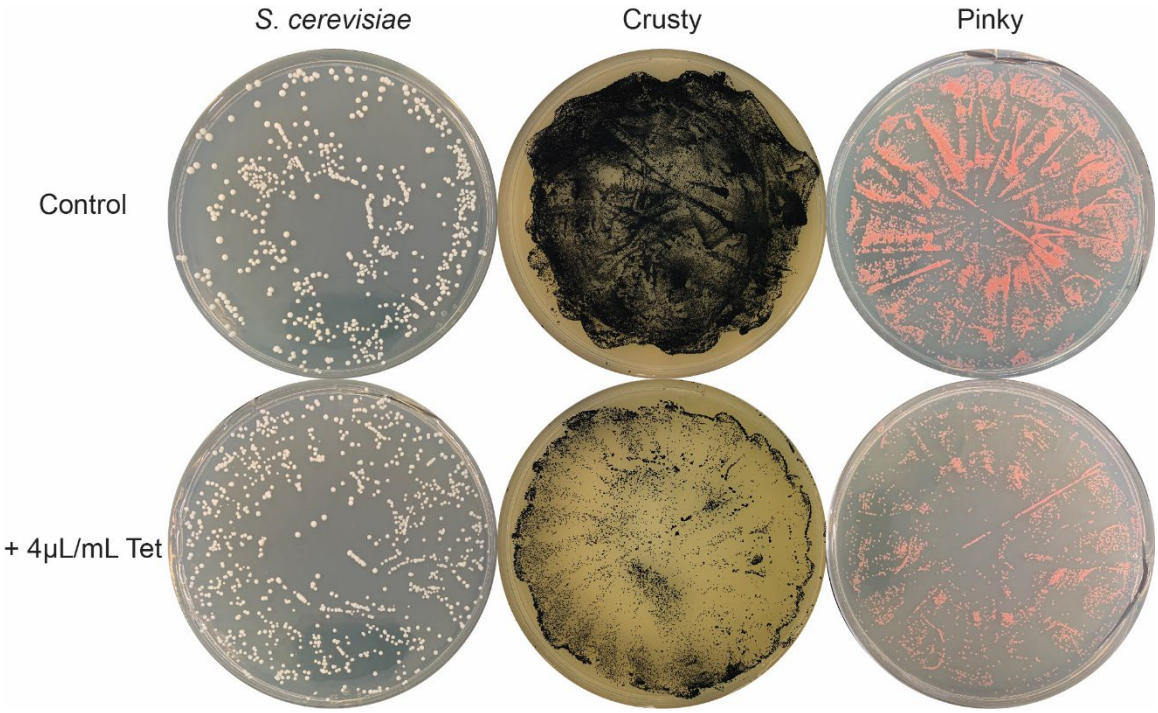

Figure 20: Representatives of the CFU plates used to determine pixel area of *S. cerevisiae*, Crusty, and Pinky control and after 4 µL/mL Tetracycline exposure. The difference in area covered in cells on the control plates for Crusty and Pinky compared to the 4 µL/mL of Tetracycline plates shows a great decrease in survivability or growth.

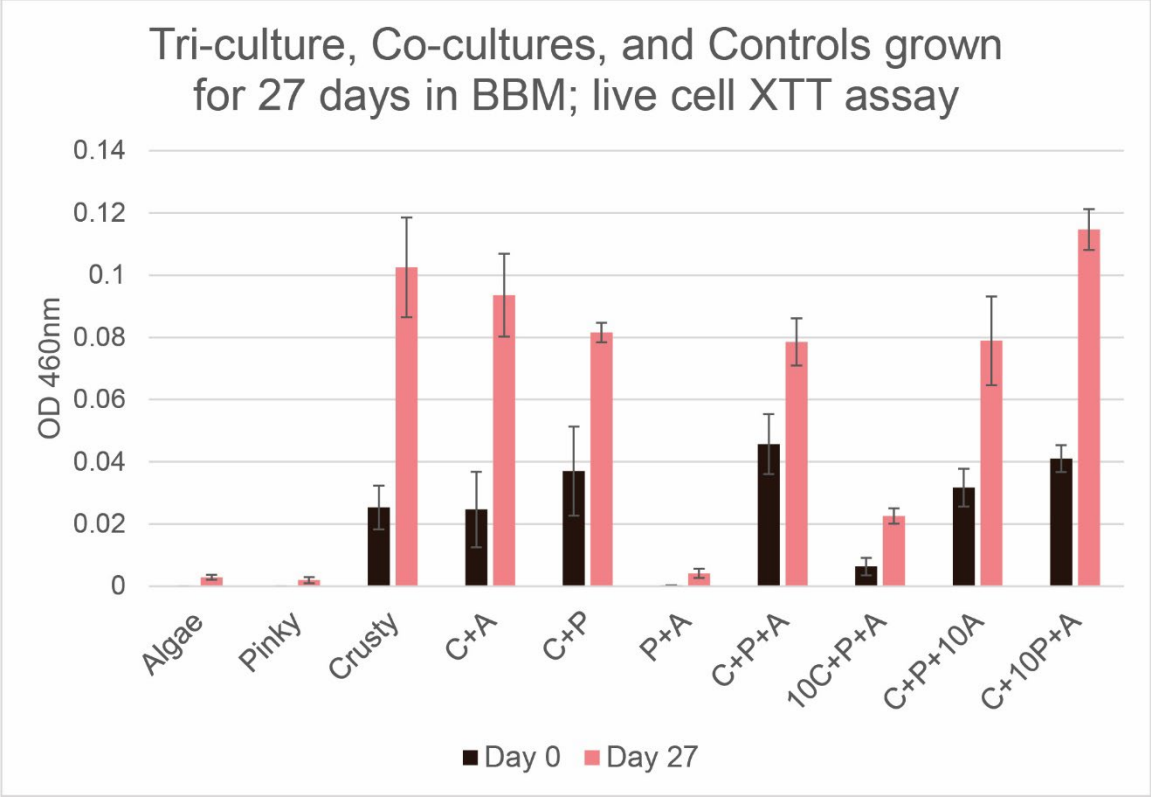

Figure 21: XTT live cell assay OD showing fungal cell growth. All microbes were added to the flask in 100 µL amounts, except the conditions that have 10 before their letter which indicates only 10 µL of that microbe was added. The Algae (*C. sorokiniana*) and Pinky were unable to be properly detected via the XTT assay, which was optimized for Crusty. Crusty growth in BBM without added external microbes had the second highest growth amount after Crusty + 10 µL of Pinky + Algae, but the difference between these is not significant. None of the other conditions showed a significant increase or decrease in growth of Crusty, except when $1/10^{th}$ the volume of Crusty was added initially (10C+P+A). (n=3, 3 biological replicates)

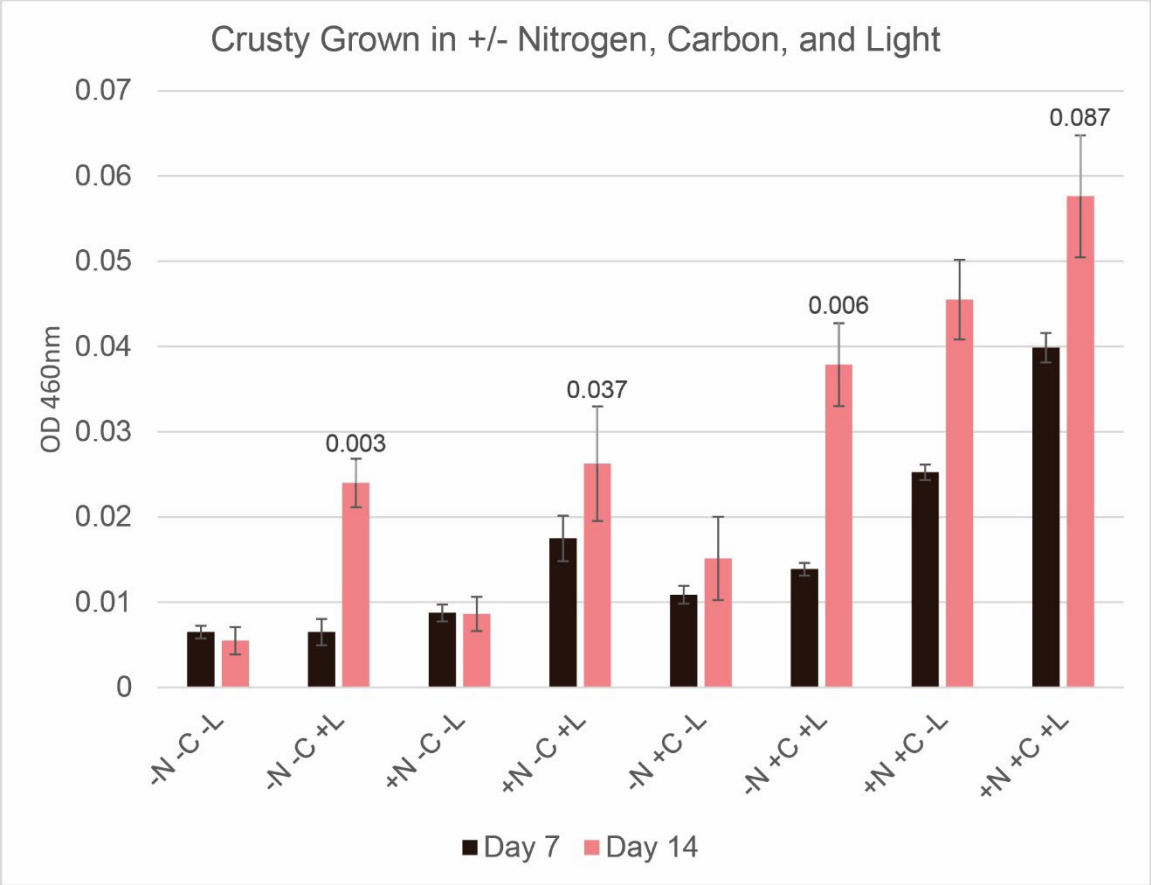

Figure 22: XTT assay results of Crusty growth in BBM with and without the addition of a carbon source, and nitrogen source, and 12 hours of light per day. Crusty was capable of growth without a carbon source or a nitrogen source, as long as it had 12 hours of light per day, $p = 0.003$. When an external nitrogen source was added growth did not increase if light was not available, but growth significantly increased when light was available compared to no light, $p = 0.037$. When a carbon source was added growth was capable even without light, but was much higher with light present, $p = 0.006$. When all nutrients were provided, growth was capable even without light, but with added light growth was not significantly higher than without light, $p = 0.087$. (n=3. 3 biological replicates)

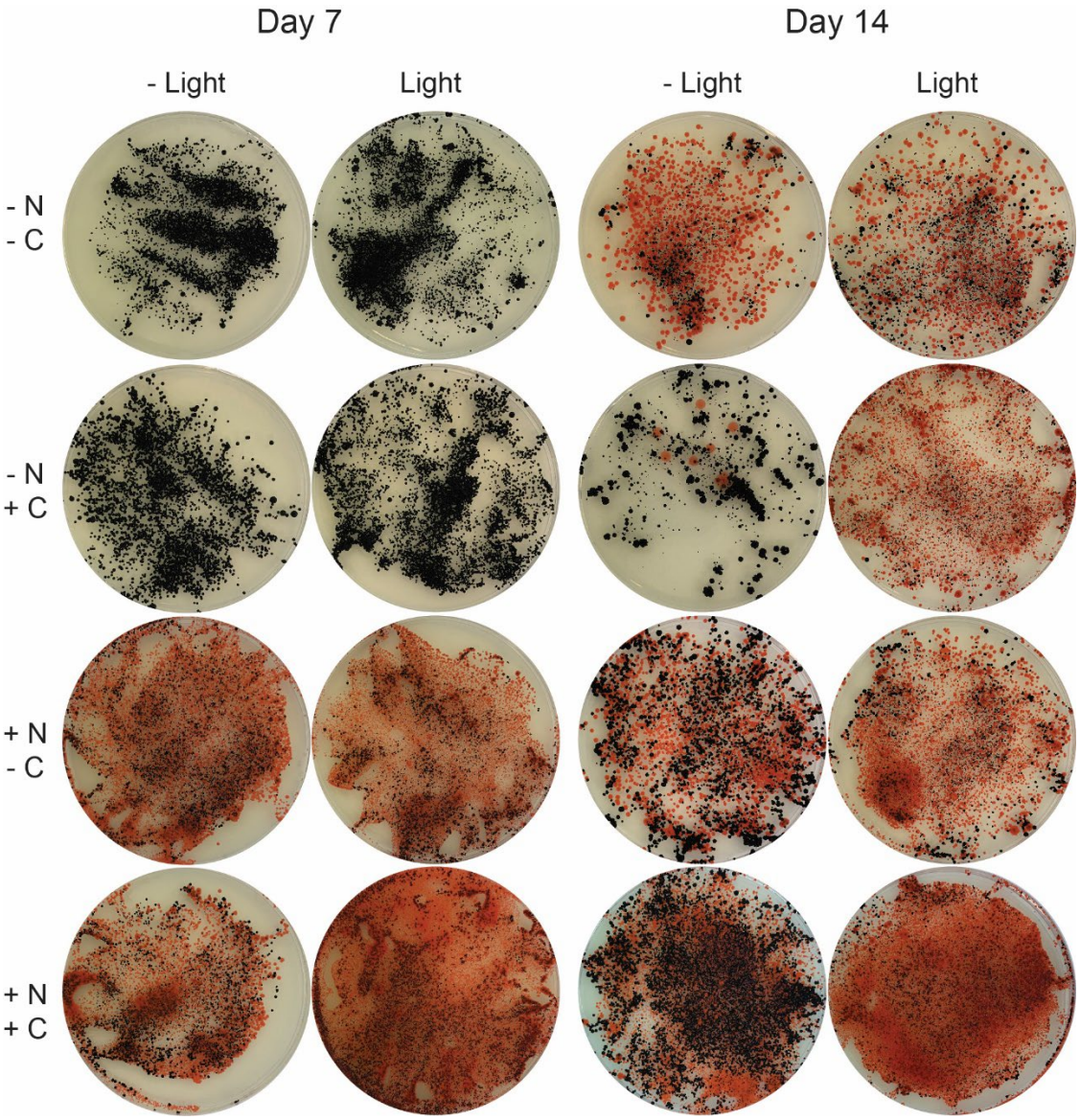

Figure 23: CFU plates of Crusty growth with and without carbon, nitrogen, and light at day 7 and day 14. On day 7 Crusty grown without a nitrogen source prevented Pinky from coming out of its cells, with or without light. However, when a nitrogen source was present, Pinky was able to escape Crusty by day 7. On day 14 only the no nitrogen, added carbon, no light had limited Pinky release from Crusty cells. All other conditions allowed Pinky to leave the cells. Although, if light was not present the amount of Pinky colonies seen outside of Crusty were much less than if light was present.

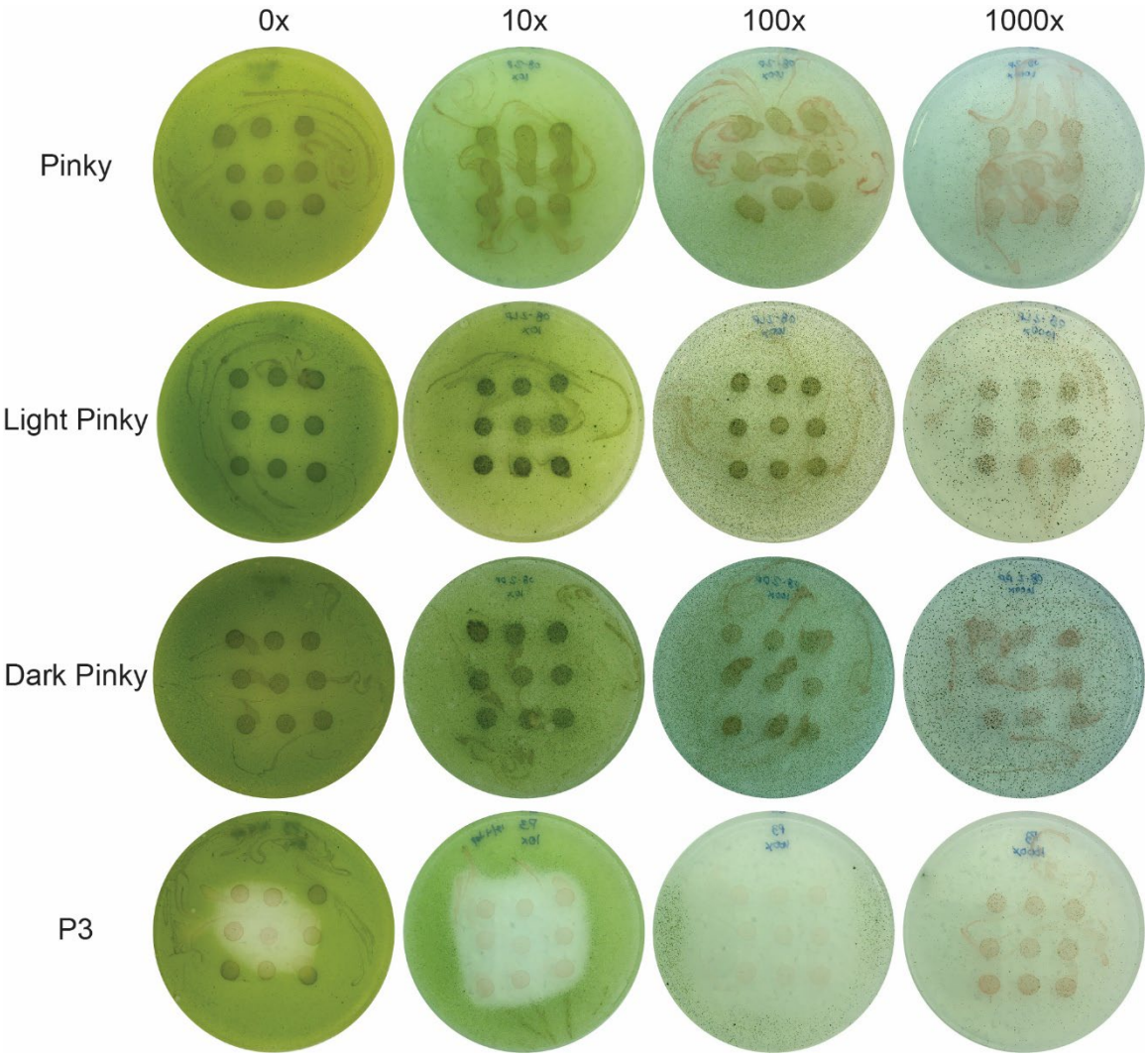

Figure 24: *C. sorokiniana* overlay on top of bacterial spots to determine in-direct growth promotion of algae from bacteria. Pinky, the combination of both Light Pinky and Dark Pinky, showed a slight growth increase of the algae that were directly on top of the bacterial spots. Light Pinky and Dark Pinky both showed very robust increase in algal growth at all dilutions of the algae. Additionally, they seemed to enhance the colony-forming nature of the algae, as it formed spots on the agar instead of a lawn. They also showed some slight growth decreasing ability in the 0x algae growth in the area directly around where the bacterial spots were placed. P3 on the other hand showed complete zones of inhibition, directly killing or repressing the growth of the algae that were in the vicinity of its colonies. (n=3, 3 biological replicates)

Table 1: Media compositions of media used in this study.

Media Name	**Acronym**	**Composition (L^{-1})**
Malt Extract Agar	MEA	20 g Dextrose 20 g Malt Extract 2 g Peptone 15 g Agar
Minimal	MN	10 g Dextrose 50 mL 20x Nitrate salts 1 mL Hutner's Trace Elements
Minimal + Vitamins	MNV	10 g Dextrose 50 mL 20x Nitrate salts 1 mL Hutner's Trace Elements 1 mL Vitamin Mix to MN
Yeast Extract Peptone Dextrose	YPD	20 g Dextrose 20 g Peptone 10 g Yeast Extract 20 g Agar
Bold's basal medium	BBM	(Connon, 2007)
Additives	**Volume/L**	**Composition**
20X Nitrate Salts/MN salts	50 mL	120 g $NaNO_3$ (remove for "MN salts") 10.4 g KCl 10.4 g $MgSO_4$-$7H_2O$ 30.4 g KH_2PO_4
Hutner's Trace Elements	1 mL	2.2 g $ZnSO_4$-$7H_2O$ 1.1 g H_3BO_3 0.5 g $MnCl_2$-$4H_2O$ 0.5 g $FeSO_4$-$7H_2O$ 0.17 g $CoCL_2$-$6H_2O$ 0.16 g $CuSO_4$-$5H_2O$ 0.15 g Na_2MoO_4-$2H_2O$ 5 g EDTA (Disodium) 100 mL ddH_2O
Vitamin Mix	1 mL	10 mg biotin 10 mg pyridoxin 10 mg thiamine 10 mg riboflavin 10 mg p-aminobenzoic acid (PABA) 10 mg nicotinic acid 100 mL ddH_2O

Table 2: Carbon Utilization of Crusty. (n=3, 3 biological replicates)

Carbon Source		*# 1*	*# 2*	*# 3*	*Average*	*Score*
D-galactose	GAL	4	4	4	4	+
D-sorbitol	SOR	5	4	5	4.7	+
Actidione (cycloheximide)	ACT	3	4	4	3.7	+
D-xylose	XYL	3	3	4	3.3	V
D-saccharose (sucrose)	SAC	5	5	5	5	+
D-ribose	RIB	2	3	1	2	V
N-acetyl-glucosamine	NAG	5	5	5	5	+
Glycerol	GLY	4	4	5	4.3	+
Lactic acid	LAT	2	2	2	2	V
L-rhamnose	RHA	3	4	4	3.7	+
L-arabinose	ARA	2	2	1	1.7	-
palatinose	PLE	3	4	4	3.7	+
D-cellobiose	CEL	5	5	5	5	+
Erythritol	ERY	2	1	1	1.3	-
D-raffinose	RAF	5	5	5	5	+
D-melibiose	MEL	4	3	3	3.3	V
D-maltose	MAL	2	2	2	2	V
sodium glucuronate	GRT	3	3	3	3	V
D-trehalose	TRE	2	1	1	1.3	-
D-melezitose	MLZ	5	5	5	5	+
potassium 2-ketogluconate	2KG	4	4	3	3.7	+
potassium gluconate	GNT	2	2	1	1.7	-
methyl-aD-glucopyranoside	MDG	2	1	1	1.3	-
levulinic acid (leuvulinate)	LVT	2	2	2	2	V
D-mannitol	MAN	4	4	5	4.3	+
D-glucose	GLU	5	5	5	5	+
D-lactose	LAC	1	1	1	1	-
L-sorbose	SBE	4	4	4	4	+
Inositol	INO	4	4	4	4	+
glucosamine	GLN	1	1	1	1	-
no substrate	No	1	1	1	1	-
Esculin ferric citrate	ESC	+	+	+	+	+

Table 3: Average zone of clearing for all metals tested on Crusty. (n=3, 3 biological replicates)

Metal	Zone of clearing (cm)
0.5 M $CoCl_2$	3.0
470 mM $AgNO_3$	2.8
1 M $FeSO_4$	0.0
2 M $LiCl_2$	0.0
1.5 M $CuCl_2$	1.4
1.5 M $NiCl_2$	4.7
10 mM $CdSO_4$	4.5

Table 4: BLASTp results of all bch genes against the Dark Pinky genome. All proteins sequences were originally obtained from *Rhodobacter capsulatus,* except *bchN* came from *Methylobacter extorquens* and *bchB* came from *Cereibacter sphaeroides*

Protein	Percent identical matches	Percent positive matches	E-value	Dark Pinky Protein Sequence
bchB	66.544	77.94	0	MQLTLWTYEGPPHIGAMRVATAMSGLHYVLHAPQGDTYADLLFTMIERRDA RPPVTYTTFRAQDLGRDTAELFKEAVAAAHARFQPQAMIVGASCTAELIQDD PGGLAKALNLPIPVIPLELPAYQKKENWGASETFYRLVRALAGPPAPRPAREP GRRPLCNILGPTALGFRHRDDLIEIRRLLDSLGIAVNIVAPLGASPADLGRLGD ADFNVVLYPETARSAAEYLKKSFGQPFTQTLPIGVGGTRRFVAEVAEIAGIDP APVLDGPGSRLPWYSRSVDSTYLTAKRVFVFGDATHAIGIARVAARELGFTV VGLGTYSREFAREVRAEAAEHGIEALITDDYLDVEAAIRAAAPELVLGTQMER HVAKRLGIPCAVISAPVHVQDFPARYAPQMGFEGANVLFDTLVHPLMMGLEE HLLGMFREDPEFHDGVGPSHLGGKSFGTPADGALEAGERAPADTPPTL--APV PIMLDRPVATA----------WSPEAEKELRKIPFFVRGKARSNTETFARERHLPLITIE TLYDAKAHYGR
bchC	59.744	70.93	1.5E-117	MDALAVILENPEHLSVQRLALTPPGDADAVVAISWSGISTGTERLLWSGRMPP FPGMGYPLVPGYESVGTVIEAGADTSVRVGQTVYVPGARCF-GSVRGLFGGA ASHLVAPAARLVPVDASLGDRACLLALAATAYRALGGIRPGATPLIVGHGVL GRLLARLTLAAGAEP-TVWETDPARATGDHGYAVVAPDADPRRDYATITDVS GNAAGLDDLIARLAPGGEIVLAGFYEAPLSFAFPPAFMREARIRISAEFRPEDT AAVTTLIEGGRLSLDGLITHRLPAGRAQDAYRTAFADPACLKMILDWRDA

bchD	45.406	59.19	6.7E-103	PWTDAHRAARLLAADPHGLGGAVVRAPPGPERERWLETLRAALPSGTPWRR LPPGIGDDSLLGGLDLAATLAAGRPIARAGLLAEADGGIVVVPMAERLPAGTA SRLAAALDAGTAVDRPARFGLILLDEG-EADETVAEALADRLAFRIDLNGL----- -------AEPPPAEPEPVSDAPEPDPVGSLCALAEAFGIASLRGPILAVRVARALA--- GDGPIGRAEIVAAGRLVLAPRATRLPAPEEPRPETAEAPPADAPQEQPRAETTD PSAAETPDDVVLEAVRAAIPPNLLDQLLAG-GRRLTAAKSGRVGQAAAARTG RPVGCRRGDPRRG-RLDLLATLRTAAPWQALRRTGEETRRIV-VRRDDLRIRIL KQRTETTTVFCVDASGSAALERLAEAKGAVELLLAEAYVRRDRVALVAFRGT GAELVLPPTRSLTRAKRGLSGLPGGGGTPLAAGIDAAVAVALGVRRGGSRPAI VLLTDGRANVARSGEGGRARAGAEALQAARTLRAAGLAALVVDTGTRGED AR-AVADAMGARYLKLPRAEAGQLSAAVRAAL
bchE	25.376	40.65	5.31E-21	MRTLFLQAPTFDGFDGGAGSRYQAKREIKSFWYPTWLAQPAALVPNS-----KLI DAPPHNIKLPEIVAQANDF--DLVVLHTSVPSFKSDVKTIEALKAANPKLIAGLI GAKVAVDAAGAMAQAPVVDFCARNEFDFTVKEVAEGVP-------MSEIKGLSY RDANGVVVHNEDREIMTDMDQLPFVTSVYKRDLEMEKYFIGYLKHPYISF---- ---YSGRGCKSRCTFCLWPQTVGGHTYRTRSVAHVIEEIKYCLKEFPQTKEFFFD DDTFTDNLPRAEEIARELGKLG----VTWSCNAKAN---VPRETLKVLKENGLRLL LVGYESGNQTILHNIKKGMRVEVAEKFTKDCHDLGIAIHGTFILGLPGETKETI QETIAFAKRINPHTIQVSLAAPYPGTFLYKQAVENGWLDIENAELVDENGVQ- VAPLHYPH-LSHTEIFTSVEEFYKKFYFR
bchF	62.112	73.91	9.29E-58	PEDRPARPLYTPAERRRRDSSPWTLVQGVLAPLQFAIFLISLVLVLRTLATGAG QFAAEISVVVKTLALYAIMVTGSIWEKAVFGRWLFAPAFFWEDVVSMLVLAL HTAYLAALITGALSGQALLLLALAAYATYVVNAGQFLMKLRAARLEGTGSR APRL
bchG	54.671	69.9	7.5E-105	ATPAPSAVIELLKPLTWFAPMWAFACGVISSGQPASGQWPVIAAGVLLAGPLV CATSQAANDWFDRHVDAINEPNRPIPSGRIPGRWGLYLALGWTLLSLVVAAA LGPWILGAALFGLVLAWIYSAPPVRLKRNGWWGNAAVALCYEGLPWFTGAA VM---AAALPDRRVLLVALLYAAGAHGIMTLNDFKSVEGDRRMGLLSLPVQM GSQRAARFACLVMALPQVAVIALLVGWERYWHAGLVAALLAGQAALMVRF LENPRERAIWYNGTGTTLYVLGMLVSAFALR

bchH	53.976	69.8	0	TAARPPIR-----VVIVTLDNHLASAVERARLRLRSEMPGLVLGFHAAAEWETDP ATLEACRADIAQADIVLSAMLFMDEHVRAILPALAARREACDAMIGCMSAGD VVKTTRLGRFDMSGTKRSALDFLKKLRGK--PGQQGNAGRQMALVRKLPKIL RFIPGSAQDVRAYFLTLQYWLAGSDENVAALVRFLVHRYAAGERAAWRDGP AAPAPLDYPETGLYHPRLPGRIGADPSRLPRRADATGRVGLLVMRSYVLAGN TAHYDGVIAALEAKGLDVVPAFASGLDNRPAVDSFFMRDGRACIDALVSLTG FSLVGGPAYNDAASAEAMLARLDVPYLAAQALEFQTLEQWEAGERGLSPVE ATMMVAIPELDGATAPMVFGGRSAASGS----------DNSRDMRVHPERAARLA ERVERLVSLRRTEKAERRLAVVLFNFPPNAGATGTAAFLSVYASLRNTLKGL AADGYTV-DVPESVDALRAAILEGNAKRYGTQANVHARIPAEDHLRRETYLA EIETQWGPSPGRHQTNGAEIFVLGAQFGNVFVGVQPAFGYEGDPMRLLFERG FAPTHAFSAFYRYLREDFSADAVLHFGTHGALEFMPGKQTGLSEACWPERLIG ALPNVYLYAANNPSEGTLAKRRSAATLVSYLTPSLAAAGLYRGLIDLKSSME RWRGLDLEAGTERESLARMIQDQGAALDLVAAEPAWTGDLGARVGALWSA VQELEQTLIPHGLHVVGAGTPEVERVDLLLALAESAHGVSPERAGIEALVAGH GVEAALTASGLSADETSRAAFASLAETDRLLARDHEVPALLRALDGRFVPPV AGGDLLRNPAILPTGRNLHGFDPYRLPSAFAVADGARQVARILERFAADGKPC PESVALVLWGTDNLKSEGGPIAQALALIGAAPRFDGYGRLSGAELIPLETLGRP RIDAVVTLSGIFRDLLPLQTKLLAEASYLAATA-DEPLEQNFVRKHALAIQAEQ GCDLETAALRVFSNAEGAYGANVNHLVDSGSWDDDAELCETFSRRKSFAYG RTGRPAPQRALMQAVLASVDMAYQNLDSVEVGVTSVDHYFDGLGGMGRAV ARAK-GEAVPIYISDQTRGEGRVRSLEEQVALETRTRMLNPKWYEGLLGHGY EGVRQIETHLTNTVGWSATANAVQPWIYERITETYVLDPAMRERMAALNPTA SAKVAQRLIEAHRRGFWTPNAEMRDALDRAEEELEDRLEGV
bchI	62.745	74.51	3.8E-145	LHPPISGSSPRGEERSQSQNPVPTFPFSAIVGQDEMRQALLIAAVDPSVGGVLV FGDRGTGKSTAIRALAALLPPMRAVAGCPYNCDPDSPAAS-CPHCAEGVPRKS HKTPVPVVDLPLGATEDRVVGTLDLERALGAGVKAFEPGLLARANRGFLYID EVNLLEDHLVDLLLDVAASGVNTVEREGLSLRHPARFVLVGSGNPEEGELRP QLLDRFGLACEVVTPKDIPTRIAVVRARDAYERDPEGFCAARARDEAAIRKRL LLARERLPSVTVPDAALERAARLCLTLGTDGLRGELTLMRTARALAALDGAG AVTDDHLRRIAPAALRHRLRRNPLDESGSTARVERALAEMF

bchM	51.77	67.26	6.06E-65	ASYDARRGELTTYFDRTAVEAWSRLTS-DAPVSRIRATVRAGRDAMRATLLS WLPADMTGLRLLDAGCGTGALSVEAAHRGAEVVAIDVSPTLIGLAQERLPAI AGAGRIDFRVGDMLDPGLGRFDHVVAMDSLIHYRAADIARALAALGARTDG SVLFTVAPRTALLTVMHAAGKFFPRSDRSPAIVPVTEGGLRRRMTSETALDAF TWARSHRINSGFYLSNAV
bchN	83.051	88.86	0	GIDLHQEQGQRAVFCGLTGIVWLHRKIQDAFFLVVGSRTCAHLIQSAAGVMIF AEPRFATAIIDERDLAGIADANEELDRVVTRLIERRPDIKLLFLVGSCPSEVIKL DLSRAAQRLSGRLAP-VRVLNYSGSGIETTFTQGEDACLAALVPDLPREVETA APSLLVVGALADVVEDQFLRIFAAMGIGDVRFLPARRADTMPAVGRNTRYLL AQPFLADTARALEERGARRLPAPFPLGAEGTTGWLRAAAEAFGVAEAVFDRA TAPGRTRAETALAPHREKLAGKRVFFFPDSQLEVPLARFLARELGADLVEVGT PYLHRAHLAAEIELLPQGTRVTEGQSLDDQMDRCRAARPDLTVCGLGLANPL EAEGLSTKWSIELLFTPVQGYEQAGDLAELFVRPLRRRALLEV
bchP	56.349	69.31	6.6E-141	DLARAGHAVLLLDKPGRIKPCGGAIPPRLIRDFAIPDALLVAKIRSARMVAPSG KAVDMPVGEGFVGMVDREHFDPWLRARAEEAGADLRDAAYDRITRPDDGV PLVHFTTGTGADLARHAVRARLVIGADGACSPVGRAEVPGHAKMRQVFAYH EILRVPEAGTPGAEAVEATRCDVYYQGRHSPDFYSWIFPHGDTLSIGTGSARK GFSLRSSIRALRAATGLDHAETVRREGAPLPLKPLKRWDNGRDVLLAGDAAG VVAPASGEGIYYAMLGGRLSAEAAAAFLRTGDARALAGARKAFMKLHGRVF WILGMMQWVWYRSDGLRERFVSICRDKDVQQLTWDSYMNKELVRAKPAA HARIFFKDLAHLFRWVSP
bchX	75.776	84.16	2.9E-159	AQLRAEAAVEPD-PVATSPAKKETQIIAIYGKGGIGKSFTLANLSYMMAQQGK KVLLIGCDPKSDTTSLLFGGKACPTIIETSTKKKLAGEAVAIGDVCFKRDGVYA MELGGPEVGRGCGGRGIIHGFELLEKLGFHEWGFDFVLLDFLGDVVCGGFGL PIARDMCQKVIVVGSNDLQSLYVANNVCSAVEYFRKLGGNVGVGGLVINKD DGTGEAQAFADAAGIPVLASIPADDDIRRKSANYEIIGRPESRWGSLFSDLAAN VADAAPHRPTPLTQDGLLGLFSSDVTGRDVVLVPATHEDMCGVAHVSKPSLE VVYDEV

bchY	70.996	82.47	0	GCHAGKDAMRAAAEAAGLSDTLAQLRSDYPQGPHDQPQSMCPAFGSLRVGL RMRRTATILSGSACCVYGLTFTSHFYGARRSVGYVPFNSETLVTGKLFEDIRE AVYATAKPEDYDAVVVINLCVPTASGVPLRLLPKEIDGVRVIGIDVPGFGVPT HAEAKDVLAGAMLKVARAEAEQGPVAAPRGGRSERPSVALLGEVFPADPVV IASLLEPLGLAAGPVVPTREWRELYAALDCAAVAAIHPFYTASIREFEAAGRPI VGSAPVGVDGTADWLDRIGEACAVPRAIVEAAKNRILPGIRGALAAMPIKGRI TLSGYEGSELLVARLLVESGAEVPYVGTACPRTPWSESDRAWLEARGTQVQY RASLEDDLYALDTLKPDLAIGTTPVVQRAKERGTPALYFTNLISARPLMGAAG AGSLATVINAALGNKARFDAMRDFFEGVGTGYAAGVWQEVPQ
bchZ	71.154	79.91	0	MLILDHDRAGGYWGAVYVFTAIKGLQVVIDGPVGCENLPVTSVLHYTDALPP HELPIVVTGLAEEELGRHGTEGAMKRAHATLDPGQPSVVVTGSIAEMIGGGV TPEGTGLQRFLPRTIDEDQWQAADRAMRWLWQEYGAKKFAKKGIPARPERK PGERPRVNLIGPAYGTFNMPSDLAEIRRLVEGIGAEVNLTFPLGSHLADVPKLV NADANICLYREFGRLLCEDLERPYLQAPIGILSTTKFLRSLGAILGLDPEPFIERE RHTTIKPVWDLWRSVTQDFFGTASFGIVATETYARGVRHFLEDEMGLPCHFA FGRSAGLKPDNDAVRAAIAAKPPLVLFGSFNERMYLAEC----GARATYVPASF PGAIIRRHTGTPFMGYAGATYLVQEICNALFDTLFHILPLARDMDKVEATPAR LHRELPWDEAARQALDSLVEAQPVLARISAAKRLRDAAERAARD

CONCLUSIONS

Throughout this dissertation, our goal was to show that polyextremotolerant fungi of Chaetothyriales are capable of transient interactions with microbes in their environment. We hypothesized that the non-lichenized microbes of the biological soil crust are engaged in transient interactions, such as exchange of nutrients and abiotic resistance factors, similar to that of lichens. Here, we have presented the first whole genome sequenced and fully characterized fungi isolated from biological soil crusts, which are polyextremotolerant fungi. Although fungi have been identified within the biological soil crust community for some time, only one other study has successfully isolated fungi from a biological soil crust which at the time could only be identified with ITS sequencing (Bates et al., 2006). However, with our efforts we have been able to genome sequence and characterize multiple fungi isolated from this community allowing us to further determine their ecological roles within the biological soil crust, providing us novel insights into polyextremotolerant fungi and the biological soil crust consortium.

Fully characterized polyextremotolerant fungi are currently limited to only a few taxa, particularly the medically relevant *Exophiala dermatitidis* and *E. oligosperma,* along with environmental isolate *Knufia petricola* (Nai et al., 2013). However, the newly whole genome sequenced and characterized *E. viscosium* and *E. limosus* have provided us with many new fungal characteristics which will be beneficial not only to fungal biology, but to industrial purposes as well. *E. viscosium* and *E. limosus*' main feature is their excessive amount of melanin production and secretion. While other fungi may have been noted to secrete dark substances, very few have been measured for how much melanin they secrete, or undergone confirmation that the dark material secreted is in fact

melanin (Butler et al., 2009). However, the capability of these fungi to secrete melanin will allow future researchers to obtain melanin from cellular supernatant, allowing continual growth of cells and thereby reducing the need to extract melanin directly from the cells.

Additional knowledge of the melanin production pathways of *E. viscosium* and *E. limosus* has provided us with important biochemical pathways that can be used for production of high-value beachhead molecules. Most polyextremotolerant fungi are characterized by their ability to make 1,8-DHN melanin (Sterflinger, 2006), but recently it has been shown that some have genetic mechanisms to produce other forms of melanin such as L-DOPA melanin or Tyrosine melanin (Teixeira et al., 2017). Since *E. viscosium* and *E. limosus* are shown to have the genes for all three types of fungal melanin production, they can therefore be genetically manipulated to turn off 1,8-DHN melanin production and presumably shunt that carbon into production of L-tyrosine and downstream high-value molecules. It will also be biologically relevant to determine the regulation of melanin production in these species at the transcriptional level, to establish if they are able to produce these alternative melanins during certain environmental conditions.

With these melanin-production anomalies, we have also observed extreme UV resistance in our new fungal strains. All polyextremotolerant fungi studied here have shown to be resistant to UV-C light. Although, this is not currently a biologically relevant light source on Earth, as UV-C is completely blocked by the ozone layer. However, this result demonstrates the extreme UV resistance of fully melanized fungi, which is the main characteristic of polyextremotolerant fungi. Additionally, while the ozone layer is

currently protecting the Earth's surface from UV-C, it is slowly being worn away by human intervention, which will eventually allow UV-C to penetrate down to the Earth's surface (Van Der Leun, 2004). Fungi with melanized cellular structures will be better adapted to withstand higher levels of UV light that we are gradually being exposed to on Earth. Additionally, these fungi could be beneficial to future plans of colonizing planets without ozone layers. The utilization of fungi for assistance of terraforming planets and other extra-terra structures is already being studied (De Vera et al., 2019).

The most unique aspect of some of these fungi that we have studied has been their cell morphologies, and their possible link to bacterial endosymbiosis. In particular, Crusty has shown quite a breadth of cell morphologies which are not seen in either *E. viscosium* or *E. limosus.* Most pointedly, Crusty showed many curved cellular structures which are not typical of hyphal growth unless stimulated to turn by chemotaxis of some sort (Clark-Cotton et al., 2022). Many fungi are capable of moving their cell polarity in response to an external stimulus, but in this instance, we aren't entirely sure what the stimulus exactly is. Our reigning theory is based on the bacterial-root symbioses in which a bacterium will induce the curling of a root hair to form a nodule around the bacterium creating an anaerobic pocket for nitrogen fixation. We believe a similar mechanism might be occurring here with Crusty cells as the "root hair" and the *Methylobacterium* Pinky producing the external stimulus that induces nodulation, by analogy to its Rhizobiales relatives. This is an attractive hypothesis for the acquisition of Pinky as an endosymbiont. Though details regarding the nature of the signaling process and the beneficial effects of this symbiosis will be of interest for future studies of these interactions.

Novel cellular processes discovered in these taxa have revealed potential niches that polyextremotolerant fungi could have within the biological soil crust. First and foremost, these melanized fungi are likely contributing to UV-resistance of the crust itself, whether that be in the secreted melanin or just in the cells creating latices of UV protection. Other microbes within the crust are known to have sunscreen-like compounds, but not all organisms are capable of producing them (Gao & Garcia-Pichel, 2011). Therefore, these melanized fungi are likely to be protecting other exposed microbes using their cell wall or secreted melanin. Additionally, we have shown that some polyextremotolerant fungi have bacterial associations. While we focused primarily on the Crusty-Pinky symbiosis, we also performed a sample-wide 16S amplification analysis of the other Jackman Flats fungi that resulted in seven out of sixteen fungal samples with 16S bands. Two of those fungi have also been identified as capable of harboring specifically *Methylobacterium* spp. through 16S verification, culturing, and sequencing means. The *Methylobacterium* spp. that Crusty is harboring was able to increase the growth of the microbes in its surroundings. If these other fungi and their bacterial associations are doing the same, and are as widespread as this quick analysis implies, then polyextremotolerant fungi's bacterial associations may be essential in increasing the rate of microbial growth during the short windows of optimal conditions for metabolic activity of the biological soil crust consortium. These two niches alone are seemingly quite important to the survival and success of the entire biological soil crust consortium, without which might their ability to be as successful as they are would likely be reduced.

With the results presented here, we were able to answer additional broader questions that have been speculated by the scientific community as well.

Polyextremotolerant fungi are definitively found within biological soil crusts. With only one other culture-based identification study (Bates et al., 2006) and one DDGE study (Bates et al., 2010) asking the same question previously, we are able to support these claims with modern methods presenting the first whole genome sequenced and characterized fungi isolated from biological soil crusts. This adds to the range of ecosystems in which polyextremotolerant fungi have been found, contributing to both their ubiquitous nature and preference for nutrient-deplete ecosystems. Additionally, we have shown that polyextremotolerant fungi are engaging in microbial interactions with other microbes. Although we were unable to confirm fungal-algal interactions with our available algal species, we can definitively confirm that our fungi are interacting with bacteria in their environment in a positive mutualistic manner. These were two big questions that, until these studies were performed, did not have concrete answers.

Polyextremotolerant fungi are an untapped mine of new insights into fungal ecology, biological processes, and genetic regulation of cellular processes. New species described here have shown many novel features of polyextremotolerant fungi, some of which have been theorized but not shown, and others completely novel. We have been able to determine biological capabilities of these fungi due to extensive experimental and observational efforts. Obtaining fully annotated genome sequences of *E. viscosium* and *E. limosus* allowed us to explore even more avenues of biological intrigue that we were unable to think of with other nonsequenced fungi. Soon we will be inundated with sequenced polyextremotolerant fungal isolates, which hopefully this thesis has laid the groundwork to make characterization of these future polyextremotolerant fungi, and all difficult to work with fungi, easier. Our next steps are to dive deeper into the interactions

of these fungi with the proper algal species also isolated from the same sites, the *Methylobacterium* spp. we have already, and possibly cyanobacteria to confirm some of these hypotheses of fungal-microbial interactions.

References

Bates, S. T., Garcia-Pichel, F., & Nash III, T. (2010). Fungal components of biological soil crusts: insights from culture-dependent and culture-independent studies. *Bibliotheca Lichenologica*, *105*, 197-210.

Bates, S. T., Reddy, G. S., & Garcia-Pichel, F. (2006). Exophiala crusticola anam. nov.(affinity Herpotrichiellaceae), a novel black yeast from biological soil crusts in the Western United States. *International journal of systematic and evolutionary microbiology*, *56*(11), 2697-2702.

Butler, M. J., Gardiner, R. B., & Day, A. W. (2009). Melanin synthesis by Sclerotinia sclerotiorum. *Mycologia*, *101*(3), 296-304.

Clark-Cotton, M. R., Jacobs, K. C., & Lew, D. J. (2022). Chemotropism and Cell-Cell Fusion in Fungi. *Microbiol Mol Biol Rev*, *86*(1), e0016521. https://doi.org/10.1128/mmbr.00165-21

De Vera, J.-P., Alawi, M., Backhaus, T., Baqué, M., Billi, D., Böttger, U., . . . Zucconi, L. (2019). Limits of Life and the Habitability of Mars: The ESA Space Experiment BIOMEX on the ISS. *Astrobiology*, *19*(2), 145-157. https://doi.org/10.1089/ast.2018.1897

Gao, Q., & Garcia-Pichel, F. (2011). Microbial ultraviolet sunscreens. *Nature Reviews Microbiology*, *9*(11), 791-802. https://doi.org/10.1038/nrmicro2649

Nai, C., Wong, H. Y., Pannenbecker, A., Broughton, W. J., Benoit, I., de Vries, R. P., . . . Gorbushina, A. A. (2013). Nutritional physiology of a rock-inhabiting, model microcolonial fungus from an ancestral lineage of the Chaetothyriales

(Ascomycetes). *Fungal Genetics and Biology*, *56*, 54-66. https://doi.org/https://doi.org/10.1016/j.fgb.2013.04.001

Sterflinger, K. (2006). Black yeasts and meristematic fungi: ecology, diversity and identification. In *Biodiversity and ecophysiology of yeasts* (pp. 501-514). Springer.

Teixeira, M. M., Moreno, L. F., Stielow, B. J., Muszewska, A., Hainaut, M., Gonzaga, L., . . . de Hoog, G. S. (2017). Exploring the genomic diversity of black yeasts and relatives (Chaetothyriales, Ascomycota). *Studies in mycology*, *86*, 1-28. https://doi.org/https://doi.org/10.1016/j.simyco.2017.01.001

Van Der Leun, J. C. (2004). The ozone layer. *Photodermatology, Photoimmunology and Photomedicine*, *20*(4), 159-162. https://doi.org/10.1111/j.1600-0781.2004.00091.x